INFORMATION TO USERS

This manuscript has been reproduced from the microfilm master. UMI films the text directly from the original or copy submitted. Thus, some thesis and dissertation copies are in typewriter face, while others may be from any type of computer printer.

The quality of this reproduction is dependent upon the quality of the copy submitted. Broken or indistinct print, colored or poor quality illustrations and photographs, print bleedthrough, substandard margins, and improper alignment can adversely affect reproduction.

In the unlikely event that the author did not send UMI a complete manuscript and there are missing pages, these will be noted. Also, if unauthorized copyright material had to be removed, a note will indicate the deletion.

Oversize materials (e.g., maps, drawings, charts) are reproduced by sectioning the original, beginning at the upper left-hand corner and continuing from left to right in equal sections with small overlaps.

ProQuest Information and Learning
300 North Zeeb Road, Ann Arbor, MI 48106-1346 USA
800-521-0600

Alterations in Cardiac Excitation Contraction Coupling in Ventricular Myocytes From Aging Hearts and Myocytes From Hearts That Overexpress Beta Adrenergic Receptors

by

Scott A. Grandy

Submitted in partial fulfillment of the requirements for the degree of Doctorate of Philosophy

at

Dalhousie University
Halifax, Nova Scotia

April, 2005

DALHOUSIE UNIVERSITY

To comply with the Canadian Privacy Act the National Library of Canada has requested that the following pages be removed from this copy of the thesis:

Preliminary Pages
- Examiners Signature Page (pii)
- Dalhousie Library Copyright Agreement (piii)

Appendices
- Copyright Releases (if applicable)

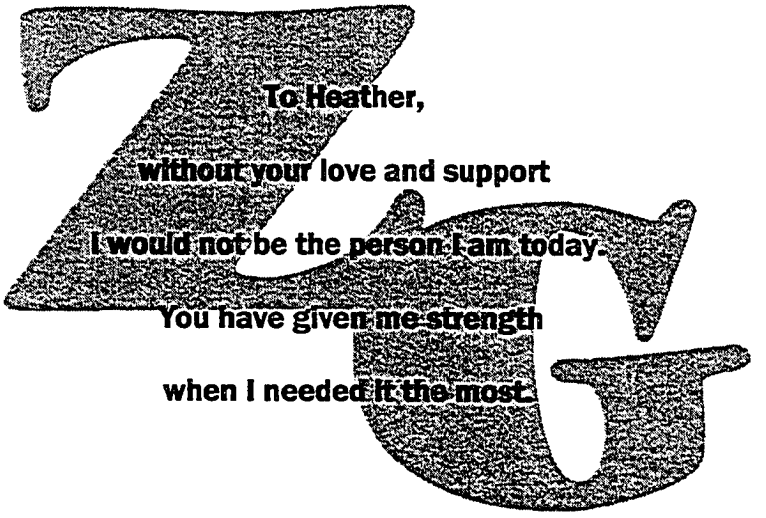
To Heather,
without your love and support
I would not be the person I am today.
You have given me strength
when I needed it the most.

Table of Contents

LIST OF FIGURES

LIST OF TABLES

ABSTRACT

Cardiac excitation contraction (EC) coupling is the process whereby the depolarization of the sarcolemma results in a transient increase in intracellular Ca^{2+} and ultimately cardiac contraction. Several studies have suggested that cardiac contractile function is altered with advancing age. In aged ventricular myocytes, contraction and Ca^{2+} transient amplitudes are reasonably well preserved at rest, but the effects of aging on L-type Ca^{2+} current ($I_{Ca\text{-}L}$) are unclear. Furthermore, the relationship between contraction and $I_{Ca\text{-}L}$ in aging heart has not been examined. Therefore, the first objective of this study was to simultaneously measure amplitudes of contraction and $I_{Ca\text{-}L}$ in voltage clamped young adult and aged murine ventricular myocytes at physiological temperatures to determine the effects of aging on EC coupling. Results showed that contraction amplitudes, $I_{Ca\text{-}L}$ amplitudes and Ca^{2+} transient amplitudes were significantly reduced in aged myocytes paced at 2 Hz. However, the gain of CICR, which is the amount of calcium released from the sarcoplasmic reticulum (SR) per nA of $I_{Ca\text{-}L}$, was similar in young adult and aged myocytes. This suggests that the relationship between $I_{Ca\text{-}L}$ and contraction was not altered in aged myocytes. The present study also found that SR Ca^{2+} stores were similar in young adult and aged myocytes. This suggests changes in SR Ca^{2+} load are not responsible for the reduction in SR Ca^{2+} release in aged myocytes. Thus, decreased SR Ca^{2+} release in aged myocytes is likely attributable to the reduction in Ca^{2+} trigger. Therefore, reductions in $I_{Ca\text{-}L}$ and SR Ca^{2+} release result in the reduction of contraction amplitudes in aged myocytes. These findings suggest that EC coupling is altered in aged myocytes and that these alterations may decrease contractile function in the aged heart. One method that could be used to enhance cardiac contractility in aging heart is to increase the number of β-adrenergic receptors (βARs) in the heart. This would increase the number of receptors for circulating catecholamines and possibly increase contractile function. In fact, previous studies have shown that, in field-stimulated cardiac myocytes that overexpress β_2ARs (TG4), contraction amplitudes are increased compared to wild-type (WT) myocytes. However, EC coupling has not been investigated in cardiac myocytes that overexpress β_2ARs. Therefore, the second objective of this study was to characterize the relationship between $I_{Ca\text{-}L}$, SR Ca^{2+} release and contraction in TG4 myocytes at physiological temperatures. Results showed that contraction amplitudes were significantly greater in field-stimulated TG4 myocytes than in WT myocytes. However, contraction amplitudes were similar in voltage clamped WT and TG4 myocytes, despite a significant reduction in the magnitude of $I_{Ca\text{-}L}$ in TG4 myocytes. Peak Ca^{2+} transient amplitudes also were similar in voltage clamped WT and TG4 myocytes. Since peak contraction and Ca^{2+} transient amplitudes were maintained despite a reduction in $I_{Ca\text{-}L}$, this suggests that the gain of CICR was increased in TG4 myocytes. Furthermore, SR Ca^{2+} stores were significantly increased in TG4 myocytes. Thus, it is possible that the increased gain of CICR in TG4 myocytes is attributable, in part, to increased SR Ca^{2+} load. Together, these results suggest that contraction amplitude is maintained in TG4 myocytes by an increase in the gain of CICR. Thus, contraction amplitudes are maintained in TG4 myocytes despite a reduction in $I_{Ca\text{-}L}$, which suggests that EC coupling is altered in TG4 myocytes. It is possible that increasing the number of βARs in aged myocytes may help maintain contractile function in aging heart.

LIST OF ABBREVIATIONS

$[\ ]_i$	intracellular concentration
°C	degrees Celsius
µg	microgram
µl	microliter
µm	micrometer
µM	micromolar
AC	adenylate cyclase
AKAP	A-kinase anchoring protein
ANOVA	analysis of variance
AM	acetoxymethyl
AP	action potential
ATP	adenosine triphosphate
Ba^{2+}	barium
βAR	beta–adrenergic receptor
bp	base pair
Ca^{2+}	calcium
CaM Kinase	Ca^{2+}-calmodulin dependent protein kinase
cAMP	adenosine-3'5'-cyclic-monophosphate
Cd^{2+}	cadmium
CICR	calcium-induced calcium release
cm	centimeter
DHP	dihydropyridine
DMSO	dimethyl sulphoxide
dSEVC	discontinuous single electrode voltage clamp
EC coupling	excitation-contraction coupling
EGTA	ethylene glycol-bis(β-aminoethyl ether)N,N,N',N'-tetraacetic acid
FKBP	FK506 binding protein
g	gram
G_i	inhibitory G-protein
G_s	stimulatory G-protein
HEPES	10 N-(2-hydroxyethyl) piperazine-N'-(2-ethanesulfonic acid)
Hz	hertz
ICI	β_2AR inverse agonist ICI 118, 551
$I_{Ca\text{-}L}$	L-type calcium current
$I_{Ca\text{-}T}$	T-type calcium current
I_{K1}	inward rectifier potassium current
I_{Kr}	delayed rectifier potassium current
I_{to}	transient outward potassium current
K^+	potassium
KCl	potassium chloride
KDa	kilodalton
kg	kilogram
kHz	kilohertz
mΩ	megaOhm

M	molar
mg	milligram
min	minute
Mg^{2+}	magnesium
MHC	myosin heavy chain
ml	milliliter
mm	millimeter
mM	millimolar
ms	millisecond
mV	millivolts
nA	nanoampere
Na^{+}	sodium
NCX	sodium-calcium exchange
Ni^{2+}	nickel
nm	nanometer
pA	picoampere
PCR	polymerase chain reaction
pF	picofarad
PKA	protein kinase A
PKC	protein kinase C
PLB	phospholamban
PTX	pertussis toxin
RyR	ryanodine receptor
SERCA	sarcoplasmic-endoplasmic reticulum Ca^{2+}-ATPase
SNS	sympathetic nervous system
SR	sarcoplasmic reticulum
TBE	tris borate EDTA
TG4	transgenic mice overexpressing human cardiac β_2ARs
TnC	troponin C
TnI	troponin I
TnT	troponin T
t-tubule	transverse-tubule
V	volts
V_{cmd}	command potential
V_m	membrane potential
V_{PC}	post-conditioning potential
UV	ultra violet
WT	wild-type

ACKNOWLEDGEMENTS

Foremost, I would like to thank my supervisor Dr. Susan Howlett for her continuous support throughout my many years as a graduate student. I would also like to thank Dr. Howlett for fostering my interest in aging and giving me the opportunity to experience basic research. Her advice and guidance has helped to improve my research skills and prepare me for my future in research.

I would like to thank Dr. Greg Ferrier for his advice, guidance and his many contributions to my projects. Also, my thanks go out to Dr. Eileen Denovan-Wright for all her help with the genotyping of the transgenic animals. I never knew molecular biology could be so much fun, when it works.

A special thanks goes out to the Peter Nicholl and Cindy Mapplebeck. Without your help I am sure I would have blown something up or burned something down. I was going to say broke something, but I know I did that on several occasions. I would also like to thank Steve Foster and Dr. Zhu for their help and for listening to my banter while working on the fluorescence rig. I would also like to thank the office staff, Luisa Vaughan, Sandi Leaf and Janet Murphy for their help and answering all my questions over the years. Finally, to all my friends not mentioned here, thank you for the laughs and adding some fun and/or mischief to every day.

Finally, I would like to thank the Canadian Institutes of Health Research and the Heart and Stroke Foundation of Canada for their financial support during my Ph.D.

PUBLICATIONS

The following are papers and abstracts based on my Ph.D. research that have been published:

Grandy, SA, Denovan-Wright, EM, Ferrier, GR and Howlett, SE. 2004. Overexpression of human β_2-adrenergic receptors increases gain of excitation-contraction coupling in mouse ventricular myocytes. *Am J Physiol Heart Circ Physiol* 287: H1029-1038.

Grandy SA, Mueller EE, Ferrier GR and Howlett SE. 2004. The role of beta-2 adrenergic receptor signaling in the regulation of cardiac contraction. *Recent Res Devel Physiol* 2: 1-19.

Grandy S, Ferrier G and Howlett S. (2005). Contraction amplitude is not decreased in ventricular myocytes from aged mice, despite a reduction in L-type Ca^{2+} current. *Biophysical Journal* 88: 138a

Grandy S, Ferrier G and Howlett S. (2004). The relationships between contraction amplitudes, membrane potential and $I_{Ca\text{-}L}$ vary dramatically in cardiac myocytes from young and old mice. *Biophysical Journal* 86: 64a.

Grandy, S., Denovan-Wright, E., Ferrier, G. and Howlett, S. (2003). Contraction amplitude in TG4 mice is maintained, despite decreased $I_{Ca\text{-}L}$. *Biophysical Journal*, 84(2): 430a.

Mueller, E., **Grandy, S.**, Ferrier, G. and Howlett, S. (2003). Basal contraction is enhanced in ventricular myocytes from mice over-expressing β-adrenergic kinase (βARK). *Biophysical Journal*, 84(2): 434a.

Grandy, S., Ferrier, G. and Howlett, S. (2002). Mechanisms of excitation-contraction (EC) coupling in mouse ventricular myocytes overexpressing β_2-adrenergic receptors. *Biophysical Journal*, 82(1): 67a.

INTRODUCTION

The Cardiovascular System

Approximately 8 million Canadians suffer from some form of cardiovascular disease, and it is estimated that one third of all annual deaths can be attributed to heart disease (Heart and Stroke Foundation of Canada, 2003). The high incidence of cardiovascular disease has generated intense interest in the function of the heart in health and in disease states.

Interest in the cardiovascular system and the diseases that affect it has existed for thousands of years. One of the earliest documented references to the cardiovascular system comes from the ancient Egyptians. Writings from the *Papyrus Ebers* (1553-1550 BC) indicate that the early Egyptians knew the heart was connected to all parts of the body by blood vessels (Van Praagh, 1983). However, ancient Egyptians did not differentiate between arteries or veins. They believed that all the blood vessels served a single purpose, to transport blood, tears, urine and sperm around the body (http://en.wikipedia.org). The Greek philosopher Aristotle (384-322 BC), provided a more in depth characterization of the heart and blood vessels in the 4th century BC (Van Praagh, 1983). Aristotle described the heart as a three-chambered organ that was connected to the lungs. Aristotle also identified the 'Great Blood-vessel', which originated from the largest cavity of the heart, and he identified the aorta, which originated from the cavity located in the middle of the heart. The importance of this finding was that the 'Great Blood-vessel' is actually the superior vena cava, which makes this the first known reference to a vein (Van Praagh, 1983).

The Greek physician Galen (130-201 AD) further advanced the understanding of the cardiovascular system during the 2nd century AD. He proposed that veins were connected to the right side of the heart and that arteries were attached to the left side of the heart (Rothschuh, 1973). Galen was also the first to describe the contractile function of the heart (Rothschuh, 1973). He believed that the heart enlarged to attract useful contents and then contracted to expel unwanted contents (Rothschuh, 1973). However, it was not until the 17th century that an English physician, William Harvey (1578-1657), clearly defined the role of the cardiovascular system. Harvey established that the primary role of the heart was to propel blood through the blood vessels to the various tissues of the body (Rothschuh, 1973). He determined that blood left the heart via the aorta, traveled the arterial system to the organs and tissues and returned to the heart via the veins. Based on his experiments, he concluded that blood was constantly driven in a circle by the contraction of the heart (Rothschuh, 1973).

Clear descriptions of abnormal heart function also have been recorded for many centuries. As early as the 12th century, the daughter of Alexius I (1081-1118), ruler of the Byzantine Empire, provided the first clear description of heart failure. She noted that her father's heart was inflamed and that his condition worsened on a daily basis. She described her father as being in a weakened state, with difficulty breathing. She also noted that there was significant swelling in the lower extremities (Lutz, 1988). Also in the 12th century, Avenozar wrote a text called *Altheisir* in which he classified heart diseases. For example, one disease state documented in his text was heart palpitations (AstraZeneca, 2000). Thus, interest in the heart has existed for thousands of years and

continues today in an effort to understand how the heart functions in normal and diseased states.

Recent studies have shown that aging is an important risk factor for the development of cardiovascular disease (Heart and Stroke Foundation of Canada, 2003). In addition, advanced age is considered to be the most significant risk factor for the development of heart failure (Peeters et al., 2002). In fact, 85% of all patients with heart failure are over the age of 65 (Fitchett & Rockwood, 2002). One of the hallmark characteristics of heart failure is a reduction in myocardial contractility (Sjaastad et al., 2003; Wehrens & Marks, 2004). Interestingly, cardiac contractility also is affected by biological aging in the absence of overt cardiovascular disease (Besse et al., 1993; Capasso et al., 1983). Studies have shown that contraction is relatively well preserved at rest in the aged heart, but force production is compromised during exercise in the aging heart (Fraticelli et al., 1989; Lim et al., 2000). However, the mechanisms underlying depressed contractile function in the aged heart are not clearly understood. Therefore, a major goal of this thesis is to investigate and compare cardiac contraction and the cellular mechanisms that underlie contraction in ventricular myocytes from young and aged hearts.

Changes in cardiovascular function during aging and disease result in increased morbidity and disability in the aging population (Lye & Donnellan, 2000). One method to decrease the incidence of disability would be to enhance cardiac contractility. Cardiac contraction is modulated by the sympathetic nervous system which releases catecholamines. Catecholamines activate cardiac beta-adrenergic receptors (βAR), which results in an increase in the force of cardiac contraction (Dzimiri, 1999; Post et al., 1999).

Therefore, increasing the number cardiac βARs could serve as a therapeutic strategy to augment cardiac contraction in aging and diseased hearts. Several βAR overexpression models have been created to determine the effects of βAR overexpression on cardiac contraction (Engelhardt et al., 1999; Liggett et al., 2000; Milano et al., 1994; Shah et al., 2000). These studies have shown that overexpression of one subtype of βARs, β_2ARs, results in enhanced cardiac contractile function (Xiao et al., 1999; Zhang et al., 2000; Zhou et al., 1999a; Zhou et al., 1999b). However, the cellular mechanisms that underlie the increase in contractile function in cells that overexpress β_2ARs are not clearly understood. Therefore, the second major goal of this thesis is to investigate the mechanisms by which cardiac contractile function is augmented in ventricular myocytes isolated from a murine model of β_2AR overexpression.

Excitation contraction coupling

Cardiac contraction is initiated by a transient rise in intracellular free Ca^{2+} in cardiac muscle cells. Excitation of the cardiac cell membrane by an action potential leads to a small influx of Ca^{2+} via membrane bound Ca^{2+} channels. Ca^{2+} influx triggers the release of a much larger amount of Ca^{2+} from an internal storage compartment, known as the sarcoplasmic reticulum (SR). Ca^{2+} is released from the SR through SR Ca^{2+} release channels. Ca^{2+} is then either taken back up into the SR or removed from the cell. This results in a transient increase in intracellular Ca^{2+}, which is known as the Ca^{2+} transient. Intracellular Ca^{2+} interacts with contractile proteins to initiate contraction of the myocyte (Bers, 2002). The process whereby excitation of the myocyte membrane leads to SR Ca^{2+} release and contraction is known as excitation contraction (EC) coupling. This

process, along with the cellular structures involved in EC coupling, will be discussed in the following sections.

Cellular structures involved in EC coupling

The sarcolemma

The cardiac cell membrane, or sarcolemma, provides a physical barrier between the inside of the cell and the extracellular space. Within the sarcolemma there are tunnel-like invaginations known as t-tubules, whose membrane is continuous with the sarcolemma. The t-tubules enter the myocyte perpendicular to the SR. The space between the SR membrane and the sarcolemma is approximately 15 nm and is called either the *fuzzy space* or the diadic cleft (Langer & Peskoff, 1996; Lederer et al., 1990). The diadic cleft is critical for EC coupling as it contains sarcolemmal Ca^{2+} channels and SR Ca^{2+} release channels (Figure 1) (Bers, 2001; Brette & Orchard, 2003). The t-tubules form a network that aids in the propagation of cardiac action potentials into the cell. This ensures that cellular structures deep within the cell are activated at the same time as structures in close proximity to the sarcolemma. This leads to the simultaneous release of SR Ca^{2+} stores and results in a synchronous contraction (Brette & Orchard, 2003). Therefore, the sarcolemma plays a key role in EC coupling by linking cardiac excitation to cardiac contraction.

Cardiac Ca^{2+} Channels

Contraction of cardiac muscle requires both extracellular and intracellular Ca^{2+}. Extracellular Ca^{2+} can enter the cell via sarcolemmal Ca^{2+} channels. There are two types

Figure 1: Schematic model of the diadic cleft.

The t-tubule is located in close proximity to the sarcoplasmic reticulum (SR). The space separating these two structures is approximately 15 nm wide and is known as the diadic cleft. L-type Ca^{2+} channels and Na^{+}-Ca^{2+} exchangers are located within the t-tubule. SR Ca^{2+} release channels, also known as ryanodine receptors, are located on the SR facing the L-type Ca^{2+} channels. The close proximity of the t-tubule and the SR allows the interaction of L-type Ca^{2+} channels and ryanodine receptors.

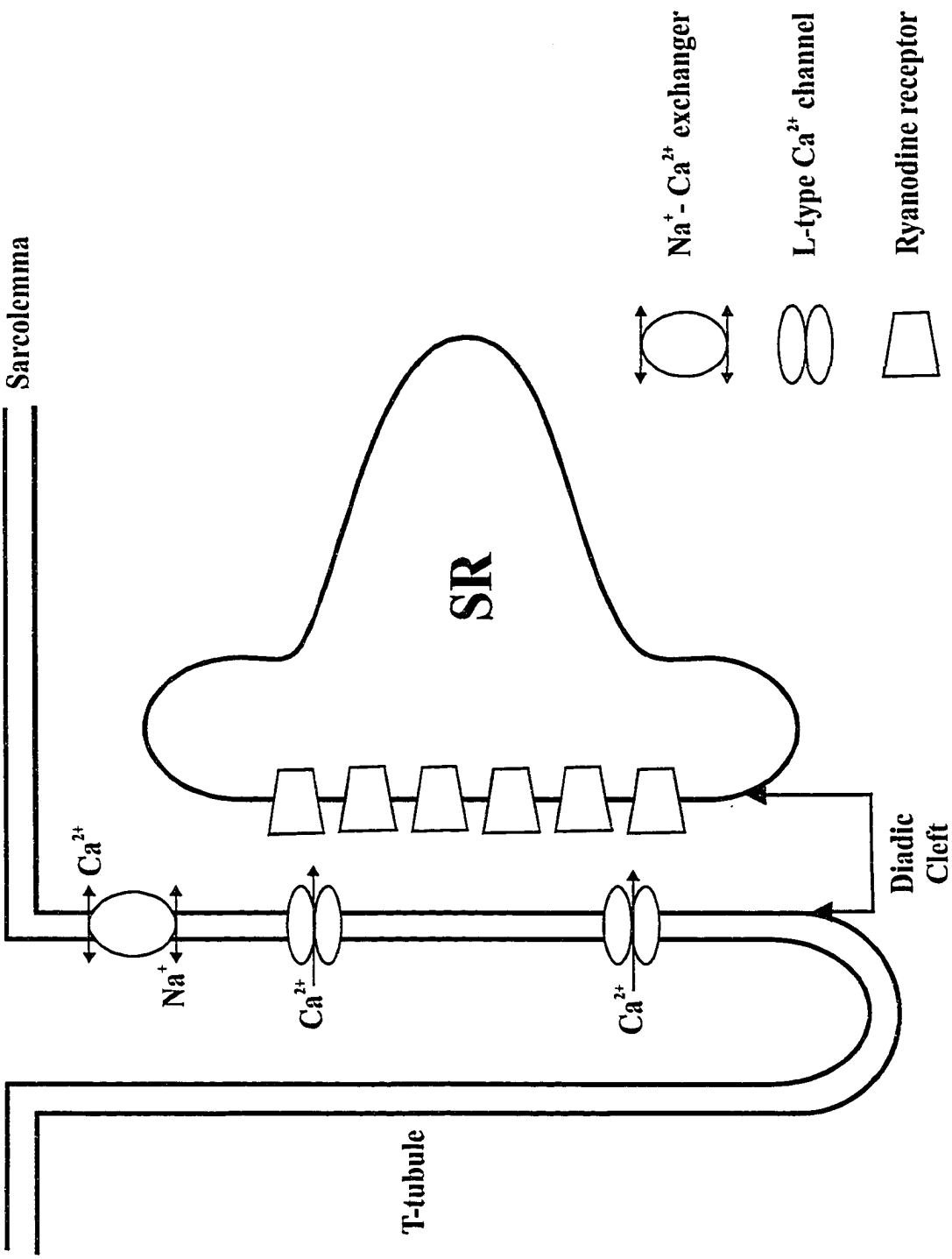
Sarcolemma
Ca2+
Na+
Ca2+
Ca2+
SR
Diadic Cleft
T-tubule
Na+ - Ca2+ exchanger
L-type Ca2+ channel
Ryanodine receptor

Figure 1

of sarcolemmal Ca^{2+} channels in the heart, L-type Ca^{2+} channels and T-type Ca^{2+} channels (Bers, 2001). The structure and function of these two channels is slightly different, but both facilitate the movement of extracellular Ca^{2+} across the sarcolemma and into the cytosol. In the following section, the structure and function of L-type and T-type Ca^{2+} channels will be discussed.

L-type Ca^{2+} channels are prominent in all cardiac tissues and are the predominant Ca^{2+} channel in ventricular myocytes. The L-type Ca^{2+} channel is composed of four distinct subunits: α_{1c}, α_2, β, and δ subunits (Bers & Perez-Reyes, 1999; Mikami et al., 1989). The α_{1c} subunit consists of four homologous domains, each of which has 6 transmembrane spanning regions (Bers & Perez-Reyes, 1999). Located within the α_{1c} subunit is the ion conducting pore of the channel. In addition, the α_{1c} subunit contains phosphorylation sites for protein kinase A (PKA) and protein kinase C (PKC) as well as ligand binding sites (Bers, 2001). Furthermore, the α_{1c} subunit has the ability to conduct Ca^{2+} current when isolated from the other subunits (Perez-Reyes et al., 1989). However, coexpression of the β subunit with the α_{1c} subunit, increases the magnitude of L-type Ca^{2+} current ($I_{Ca\text{-}L}$) and accelerates the activation and inactivation kinetics of $I_{Ca\text{-}L}$ (Perez-Reyes et al., 1992). This evidence suggests that the functional properties of L-type Ca^{2+} channels reside in the α_{1c} subunit, but that both α_{1c} and β subunits are required for the channel to function effectively.

In comparison to L-type Ca^{2+} channels, relatively little is known about T-type Ca^{2+} channels. Electrophysiological recordings of T-type Ca^{2+} current ($I_{Ca\text{-}T}$) have been used to identify cardiac tissue containing T-type Ca^{2+} channels. $I_{Ca\text{-}T}$ is present in atrial cells (Bean, 1985) and in Purkinje fibers (Hirano et al., 1989), but is either very small or

absent in ventricular myocytes (Mitra & Morad, 1986; Yuan et al., 1996). This differs from L-type Ca^{2+} channels, which are prominent in all cardiac tissues (Bers, 2001). In addition, molecular cloning has helped identify the molecular structure of the T-type Ca^{2+} channel. To date, three T-type Ca^{2+} channel α subunit isoforms have been cloned: α_{1G}, α_{1H} and α_{1I}. However, only α_{1G} and α_{1H} subunit mRNAs are expressed in cardiac tissue (Cribbs et al., 1998; Perez-Reyes et al., 1998). Furthermore, both the α_{1G} and α_{1H} subunits have the ability to conduct Ca^{2+} current (Cribbs et al., 1998; Perez-Reyes et al., 1998). Therefore, it appears that the α subunit is the functional subunit of the T-type Ca^{2+} channel.

L-type Ca^{2+} channels and T-type Ca^{2+} channels can be differentiated based on differences in voltage dependence, duration of channel openings and channel conductance. Ca^{2+} channels are activated by membrane depolarization. T-type Ca^{2+} channels are activated at approximately –60 mV and L-type Ca^{2+} channels are activated at approximately –30 mV (Bers, 2001; Page et al., 2002). Peak Ca^{2+} current is observed at -30 mV and 0 mV for $I_{Ca\text{-}T}$ and $I_{Ca\text{-}L}$, respectively (Langer, 1997). The inactivation of T-type Ca^{2+} channels is voltage dependent, whereas inactivation of L-type Ca^{2+} channels is dependent on both voltage and intracellular Ca^{2+} concentration (Hadley & Hume, 1987; Lee et al., 1985). Furthermore, L-type channels have long lasting openings and relatively large conductance whereas T-type channels have a tiny conductance and exhibit transient openings (Bers, 2001). Interestingly, L- and T-type Ca^{2+} channels also can be differentiated pharmacologically. L-type channels can be blocked by 1,4 dihydropyridines (DHPs), whereas T-type channels are relatively insensitive to DHP blockade (Bers, 2001; Langer, 1997). However, T-type Ca^{2+} channels are more

susceptible to blockade by Ni^{2+} than L-type Ca^{2+} channels (Hirano et al., 1989). In summary, although L- and T-type Ca^{2+} channels both allow Ca^{2+} influx into the myocyte, these channels differ substantially. These differences suggest that each type of Ca^{2+} channel may serve a different purpose in the heart.

Ca^{2+} currents mediated by $I_{Ca\text{-}L}$ and $I_{Ca\text{-}T}$ are involved in several cardiac processes. In atrial cells and Purkinje fibers, $I_{Ca\text{-}T}$ is thought to contribute inward current which is important in depolarization of pacemaker cells (Bers, 2001). Blockade of $I_{Ca\text{-}T}$ results in the slowing of pacemaker activity (Hagiwara et al., 1988; Wu & Lipsius, 1990). Thus, $I_{Ca\text{-}T}$ has the ability to modulate pacemaker activity in certain cardiac cell types. In contrast, $I_{Ca\text{-}L}$ modulates the plateau phase of the action potential in ventricular myocytes and is a determinant of action potential duration (Bers, 2001; Langer, 1997). $I_{Ca\text{-}L}$ also is a determinant of SR Ca^{2+} load (Trafford et al., 2001). For example, an increase in $I_{Ca\text{-}L}$ increases Ca^{2+} entry into the cell and thereby increases SR Ca^{2+} content (Trafford et al., 2001). Finally, the activation of $I_{Ca\text{-}L}$ results in an increase in intracellular Ca^{2+}. The increase in intracellular Ca^{2+} is greater than the amount of Ca^{2+} that enters via the L-type Ca^{2+} channel (Bers, 2001). This suggests that $I_{Ca\text{-}L}$ may be involved in initiation of SR Ca^{2+} release. This theory will be discussed in a later section of the introduction.

Sarcoplasmic Reticulum

The SR is an essential component of the EC coupling process. The SR is a membrane bounded intracellular compartment, which is the primary storage site for intracellular Ca^{2+}. The SR is composed of longitudinal SR and terminal SR (Meissner, 2004). Each SR segment consists of longitudinal SR with a terminal cisternae region on

each end (Page et al., 2002). The terminal cisternae are in close proximity to the t-tubule (Page et al., 2002) and contain SR Ca^{2+} release channels. This region is the primary site of SR Ca^{2+} release (Winegrad, 1965). The longitudinal SR surrounds the myofibrils and contains Ca^{2+} ATPase pumps. The SR Ca^{2+} ATPase is responsible for sequestration of Ca^{2+} after it has been released into the cytosol (Meissner, 1975; Meissner, 2004). Together the SR Ca^{2+} release channels and SR Ca^{2+} pumps function to regulate intracellular Ca^{2+} in the cardiac myocyte. The structure and function of the SR Ca^{2+} release channels and the SR Ca^{2+} ATPase will be discussed in the following sections.

Ryanodine Receptors

For cardiac contraction to occur, Ca^{2+} must be released from the SR into the cytosol where it can interact with myofilaments. Ca^{2+} is released from the SR via Ca^{2+} release channels. These channels were first identified as SR projections called 'feet' that extended from the terminal cisternae of the SR into the diadic cleft (Franzini-Armstrong, 1970). The neutral plant alkaloid, ryanodine, has been used to demonstrate that the 'foot' projections in the terminal cisternae are ryanodine receptors (Inui et al., 1987a; Inui et al., 1987b; Lai et al., 1988). Thus far, three ryanodine receptor subtypes have been identified: RyR1 in skeletal muscle, RyR2 in cardiac tissue and RyR3 in brain tissue (Bers, 2001). A separate gene codes for each receptor subtype, but there is approximately 70% sequence similarity between all three genes (Bers, 2001; Meissner, 2004). RyRs are homotetrameric complexes that consist of four 560 kDa RyR subunits in tight association with four 12-kDa FK506 binding protein subunits (FKBP) (Meissner, 2004). The RyR subunits are transmembrane spanning domains and are believed to form

the Ca^{2+} release channel (Meissner, 2004; Rapundalo, 1998). The cytoplasmic portion of the RyR, which appears to be the 'foot' structure that projects into the diadic cleft, contains the binding sites for FKBPs as well as calmodulin (Meissner, 2004). The function of the FKBPs is to stabilize RyR gating (Kaftan et al., 1996) and to mechanically link groups of RyRs (Marx et al., 1998). Since the number of RyRs is greater than the number of L-type Ca^{2+} channels (Bers & Stiffel, 1993), it is believed that the physical coupling between adjacent RyRs facilitates cooperative gating when one RyR is activated (Marx et al., 1998). Thus, the influx of Ca^{2+} through a single L-type channel should activate more than one RyR.

Cardiac RyRs are regulated by Ca^{2+}, ATP and Mg (Bers, 2001; Meissner, 2004). RyRs can be activated by sub-micromolar Ca^{2+} concentrations and maximal activation occurs in the presence of 100 μm Ca^{2+} (Bers, 2001; Meissner & Henderson, 1987; Rousseau & Meissner, 1989). ATP also activates RyRs, but only if the channel has been partially activated by Ca^{2+} (Bers, 2001). In contrast, in the absence of ATP, Mg blocks RyR activation by competing with Ca^{2+} for high-affinity activation sites as well as for low affinity inactivation sites (Meissner, 2004). Cellular Mg and ATP form an MgATP complex. During steady-state conditions, the ability of the MgATP complex to inhibit RyR function is modest compared to the ability of free Mg to inhibit RyR function (Meissner, 2004). However, since ATP and Mg concentrations do not change rapidly during EC coupling it is unlikely that changes in ATP and Mg affect RyR activation during cardiac contraction (Bers, 2001). RyRs also contain phosphorylation sites for Ca^{2+}/calmodulin dependent kinase II and cAMP-dependent PKA (Bers & Perez-Reyes, 1999; Vildivia et al., 1997; Witcher et al., 1991). However, it is not yet clear how

phosphorylation of these sites affects RyR function (Meissner, 2004). Therefore, during EC coupling, RyR function is primarily regulated by intracellular Ca^{2+} and not by Mg or ATP.

SR Ca^{2+} ATPase pump

Following activation of contraction, the cardiac myocyte must relax before another contraction can be initiated. Relaxation depends upon the inactivation of RyRs and the removal of cytosolic Ca^{2+} (Bers, 2001). Ca^{2+} is removed from the cytosol by reuptake into the SR or by removal from the cell across the sarcolemma. Cytosolic Ca^{2+} moves into the SR via the SR Ca^{2+} pump, whereas the sarcolemmal Ca^{2+} pump and the Na^{+}-Ca^{2+} exchanger remove Ca^{2+} from the cell. Removal of cytosolic Ca^{2+} results in termination of the Ca^{2+}-dependent activation of the myofilaments (Frank et al., 2003).

The SR Ca^{2+} ATPase is responsible for resequesteration of approximately 70-80% of the Ca^{2+} present in the cytosol. SR Ca^{2+} pumps are encoded by the gene, SERCA2 (Brandl et al., 1987; Brandl et al., 1986), and are primarily located in the longitudinal SR (Meissner, 1975). The pump contains a channel required for the translocation of Ca^{2+} across the SR membrane as well as binding sites for Ca^{2+} and ATP (Bers, 2001; Page et al., 2002). When Ca^{2+} and ATP bind to the Ca^{2+} pump, ATP is consumed and phosphorylation alters the structure of the channel so that Ca^{2+} cannot be released back into the cytosol. At the same time, the affinity of the binding site for Ca^{2+} is reduced, which allows the Ca^{2+} to move from the SR Ca^{2+} ATPase channel into the SR (Bers, 2001). The SR Ca^{2+} pump can transport two Ca^{2+} ions at the expense of one molecule of ATP (Reddy et al., 1982). The reuptake of Ca^{2+} into the SR via the SR Ca^{2+} pump results

in relaxation of the myocyte and ensures that there is adequate SR Ca^{2+} for the next contraction.

SR Ca^{2+} pump activity is primarily regulated by the phosphoprotein phospholamban (PLB) (Frank et al., 2003). The association of PLB with the SR Ca^{2+} pump inhibits pump function by decreasing Ca^{2+} transport and ATPase activity (Hicks et al., 1979; Inui et al., 1986; Tada et al., 1982). Phosphorylation of PLB by cAMP-dependent PKA (Kirchberger et al., 1974; Simmerman et al., 1986; Tada et al., 1974) and Ca^{2+}/calmodulin-dependent protein kinase II (Kranias, 1985; Simmerman et al., 1986) removes inhibition of SERCA2 and increases the affinity of the SR pump for Ca^{2+} (Bers, 2001; Kranias, 1985). Furthermore, endogenous catecholamines act on βARs to activate the cAMP-dependent PKA pathway and increase phosphorylation of PLB (Brittsan & Kranias, 2000; Koss & Kranias, 1996). This leads to an increase in SR Ca^{2+} uptake, which enhances the rate of relaxation. Therefore, PLB plays an important role in regulation of the rate of cardiac relaxation.

Myofilaments and Contractile proteins

Contraction of the cardiac myocyte is achieved by the interaction of cardiac myofilaments. The myofilaments occupy 45-60% of the volume of a cardiac myocyte (Bers, 2001; Page et al., 2002) and are arranged in structural units called sarcomeres. Sarcomeres are repeating units of structure that run the longitudinal axis of the myocyte (Page et al., 2002). The sarcomere is bounded by a Z-line on each end, with thick and thin filaments running longitudinally between the two Z-lines. The sarcomere is organized so that the thick and thin filaments alternate. The thin filaments are anchored

to the Z-line and extend into the sarcomere, whereas the thick filaments are longitudinally centered (Bers, 2001; Langer, 1997). This creates an overlap between the two filaments and allows them to interact with one another.

Cardiac contraction results from the interaction between the thick and thin filaments. The thin filaments are composed of two actin filaments and a tropomyosin filament (Bers, 2001; Langer, 1997). Troponin complexes are attached at regular intervals to the tropomyosin filament. Troponin T, troponin C and troponin I subunits make up the troponin complex. Troponin T is the tropomyosin binding unit (TnT), troponin C (TnC) binds Ca^{2+} and troponin I (TnI) is the inhibitory subunit (Bers, 2001). Together, the troponin complex regulates cross-bridge formation and thus force development (Langer, 1997). The thick filaments are composed of approximately 300 myosin molecules. Each myosin molecule consists of a globular head and a tail region. The tails form the thick axis of the myosin filament, whereas the globular heads overlap the actin filaments. Furthermore, the myosin heads have actin binding sites and ATPase activity (Bers, 2001; Langer, 1997). It is the interaction between the myosin head and the actin filament that results in shortening of the sarcomere and cardiac contraction.

Contraction of the myocyte is dependent on an increase in intracellular Ca^{2+}. When Ca^{2+} binds to troponin C, a conformational change occurs in the troponin-tropomyosin complex, which reveals the myosin binding site on the actin filament (Bers, 2001). This results in the myosin head binding to the actin filament, which is known as cross-bridge formation. The thin filament then slides past the adjacent thick filament using energy from the hydrolysis of ATP. This results in shortening of the sarcomere and production of force. Relaxation occurs primarily as a result of a decrease in intracellular

Ca^{2+} concentration. As intracellular Ca^{2+} levels decline, Ca^{2+} dissociates from troponin C and the troponin-tropomyosin complex blocks the myosin binding site. This results in inhibition of the actin-myosin complex and force cannot be produced (Bers, 2001; Langer, 1997).

Triggers for EC coupling

Cardiac contraction is initiated by excitation of the cell membrane by an action potential (AP). This depolarization activates several mechanisms that trigger the release of SR Ca^{2+}, which leads to a rise in intracellular Ca^{2+} and ultimately cardiac contraction. A number of mechanisms can activate SR Ca^{2+} release and these mechanisms will be discussed in the following section.

Action Potentials in Ventricular Myocytes

The cardiac AP is responsible for the depolarization of the cell membrane, which initiates contraction. The AP is a membrane potential waveform that is produced by the coordinated interaction of numerous ion channels and transporters (Bers, 2001). Since ion channels are distributed heterogeneously within the heart, the morphology of the AP varies markedly between different regions of the heart (Langer, 1997). The type and distribution of cardiac ion channels also differs between species, which accounts for differences in AP morphology observed between species. In general, the action potential begins with the upstroke, which depolarizes the cell and is followed by repolarization of the cell. For example, in rabbit ventricular myocytes, the AP begins with the upstroke (phase 0), which is carried predominantly by Na^{+} current. Next, Ca^{2+}-independent and

Ca^{2+}-dependent transient outward K^+ currents are activated, which results in early rapid repolarization (phase 1). Phase 1 repolarization is followed by a slow repolarization phase, known as phase 2. During this phase, delayed rectifier K^+ currents are activated and L-type Ca^{2+} current inactivates. The final phase of the AP is called the late rapid repolarization phase or phase 3. During phase 3, the delayed rectifier (I_{Kr}) and the inward rectifier (I_{K1}) currents increase rapidly which increases the rate of repolarization (Langer, 1997). It should be noted that age and pathology can alter the AP waveform potential greatly. These changes in AP configuration have a major impact on cardiac contraction and will be discussed in later sections.

Ca^{2+} Induced Ca^{2+} Release

The process whereby a small influx of extracellular Ca^{2+} triggers a much larger release of Ca^{2+} from the SR is known as Ca^{2+} induced Ca^{2+} releases (CICR). CICR was first identified in skeletal muscle fibers (Endo et al., 1970) and later identified in cardiac myocytes (Fabiato & Fabiato, 1973). CICR was initially examined in cardiac myocytes where the sarcolemma had been removed by chemical or mechanical means (Fabiato, 1985a, 1985b, 1985c). Skinned cardiac myocytes are used so that free Ca^{2+} concentrations surrounding the SR can be changed rapidly. For example, in skinned cells the Ca^{2+} concentration outside the SR can be changed in approximately 1 ms as opposed to 4-5 ms in intact cells (Fabiato, 1985a). This approach was used by Fabiato to explore factors that control SR Ca^{2+} release in cardiac myocytes (Fabiato, 1983; Fabiato, 1985a, 1985b, 1985c; Fabiato & Fabiato, 1975, 1979).

In skinned cardiac myocytes, Ca^{2+} current was simulated by the rapid application Ca^{2+}, which resulted in SR Ca^{2+} release (Fabiato, 1983; Fabiato, 1985a, 1985b, 1985c; Fabiato & Fabiato, 1977, 1978). Interestingly, the amount of SR Ca^{2+} release is dependent on trigger Ca^{2+}concentration (Fabiato, 1983; Fabiato, 1985c). In fact, SR Ca^{2+} release increases with increasing trigger Ca^{2+} concentrations up to an optimum level (Bers, 2001). However, when trigger Ca^{2+} concentration exceeds the optimum, SR Ca^{2+} release is inhibited. Furthermore, SR Ca^{2+} release decreases as the concentration of the trigger Ca^{2+} decreases (Fabiato, 1985c). These findings suggest that the activation of CICR is dependent on trigger Ca^{2+} concentration (Fabiato, 1985c). It also suggests that SR Ca^{2+} release is graded by the magnitude of the Ca^{2+} trigger.

CICR has been extensively characterized in intact cardiac myocytes (Nabauer et al., 1989; Nabauer & Morad, 1990; Niggli & Lederer, 1990). In intact cardiac myocytes, brief photolysis of photolabile chelated Ca^{2+} induces contraction (Nabauer & Morad, 1990; Niggli & Lederer, 1990). However, photolytically released Ca^{2+} is unable to generate a significant contraction when SR Ca^{2+} stores are depleted or when SR Ca^{2+} release channels are blocked (Nabauer & Morad, 1990; Valdeolmillos et al., 1989). This suggests that SR Ca^{2+} release, not the influx of extracellular Ca^{2+}, activates contractions in cardiac myocytes.

In skeletal muscle, intramembrane charge movement is associated with SR Ca^{2+} release (Melzer, 1986). Therefore, it was suggested that charge movement may play a role in SR Ca^{2+} release in cardiac myocytes. Nabauer et al. (1989) showed that Ca^{2+} current triggers SR Ca^{2+} release in cardiac myocytes. When Ca^{2+} concentration is reduced to submicromolar levels, the Ca^{2+} channel carries sodium current (Nabauer et al.,

1989). However, Na^+ current is unable to trigger SR Ca^{2+} release (Nabauer et al., 1989). Ba^{2+} also moves through the Ca^{2+} channel and supports intramembrane charge movement. However, when cells bathed in a Ba^{2+} solution are depolarized, there is no subsequent SR Ca^{2+} release (Nabauer et al., 1989). Together these findings suggest that SR Ca^{2+} release does not depend on charge movement across the sarcolemma (Nabauer et al., 1989). Therefore, the influx of extracellular Ca^{2+} appears to be the primary trigger for SR Ca^{2+} release in cardiac myocytes.

L-type Ca^{2+} channels are the predominant Ca^{2+} channel in the heart and act to transport extracellular Ca^{2+} into the myocyte (Bers & Perez-Reyes, 1999). Therefore, it was hypothesized that L-type Ca^{2+} channels were involved in the process of CICR. Indeed, studies have shown that $I_{Ca\text{-}L}$ can trigger SR Ca^{2+} release in cardiac myocytes (Bers, 2001; Beuckelmann & Wier, 1988; Nabauer et al., 1989; Niggli & Lederer, 1990). Studies also have shown that the magnitudes of Ca^{2+} transients and contractions are proportional to the magnitude of $I_{Ca\text{-}L}$ (Beuckelmann & Wier, 1988). In addition, the voltage dependence of $I_{Ca\text{-}L}$ and Ca^{2+} transients are very similar in cardiac myocytes (Beuckelmann & Wier, 1988; Callewaert et al., 1988; Cannell et al., 1987; London & Krueger, 1986). Specifically, as membrane potential increases from –30 to 0 mV, the magnitudes of $I_{Ca\text{-}L}$ and Ca^{2+} transients increase. In contrast, at more positive potentials, the magnitudes of $I_{Ca\text{-}L}$ and Ca^{2+} transients decline in parallel (Callewaert et al., 1988). In general, these findings suggest that $I_{Ca\text{-}L}$ is the primary trigger for CICR in cardiac myocytes.

Extracellular Ca^{2+} also can enter the cell via T-type Ca^{2+} channels. Several studies have suggested that $I_{Ca\text{-}T}$ also may act as a trigger for CICR (Sipido et al., 1998;

Zhou & January, 1998). In fact, $I_{Ca\text{-}T}$ can trigger SR Ca^{2+} release and initiate contractions (Sipido et al., 1998; Zhou & January, 1998). However, the amount of Ca^{2+} released from the SR by $I_{Ca\text{-}T}$ is modest compared to SR Ca^{2+} release triggered by $I_{Ca\text{-}L}$ (Sipido et al., 1998; Zhou & January, 1998). Furthermore, the onset of Ca^{2+} release and the kinetics of release are slower when $I_{Ca\text{-}T}$ is the trigger (Sipido et al., 1998; Zhou & January, 1998). In addition, when $I_{Ca\text{-}T}$ triggers contraction there is a longer delay to the onset of contraction, contraction amplitude is smaller, time-to-peak contraction is increased and the time required for relaxation is increased compared to contractions triggered by $I_{Ca\text{-}L}$ (Zhou & January, 1998). Overall, it appears that $I_{Ca\text{-}T}$ is a less efficient trigger for SR Ca^{2+} release than $I_{Ca\text{-}L}$ (Sipido et al., 1998; Zhou & January, 1998). Therefore, it is unlikely that $I_{Ca\text{-}T}$ plays a major role in triggering CICR.

The Na^{+}-Ca^{2+} exchanger (NCX) also may act as a trigger for SR Ca^{2+} release under certain conditions. Although the primary function of the NCX is to remove Ca^{2+} from the cytosol, several groups have shown that, under certain conditions, NCX can operate in reverse mode to transport Ca^{2+} into the cell (Bers et al., 1988; Leblanc & Hume, 1990; Wasserstrom & Vites, 1996). At very positive membrane potentials and in the absence of $I_{Ca\text{-}L}$, Ca^{2+} influx via NCX can trigger SR Ca^{2+} release and initiate contraction (Baartscheer et al., 1996; Levi et al., 1994; Wasserstrom & Vites, 1996). When SR Ca^{2+} release is triggered by NCX, the amount of Ca^{2+} release is markedly lower than when $I_{Ca\text{-}L}$ is the trigger (Sipido et al., 1997). Therefore, it appears that the NCX is not a significant trigger for SR Ca^{2+} release under physiological conditions (Sham et al., 1992; Sipido et al., 1995).

In summary, extracellular Ca^{2+} can enter the cardiac myocyte via L-type or T-type Ca^{2+} channels and via the NCX operating in reverse mode. Ca^{2+} entry via all three routes has the ability to trigger the release of SR Ca^{2+} (Levi et al., 1994; Sham et al., 1995; Sipido et al., 1998). However, based on current evidence, it appears that $I_{Ca\text{-}L}$ is the primary trigger for CICR under physiological conditions.

As previously stated, CICR is the process whereby a small influx of Ca^{2+} triggers a larger release of Ca^{2+} from the SR. Interestingly, CICR is an intrinsically positive feedback system, which suggests that Ca^{2+} release may become regenerative (Stern & Lakatta, 1992). This means that, as more Ca^{2+} is released, additional RyRs are activated and this process should continue until all the RyRs have been activated and contraction is maximal (Stern & Lakatta, 1992). However, SR Ca^{2+} release is graded by the magnitude of $I_{Ca\text{-}L}$ (Cannell et al., 1994; Lopez-Lopez et al., 1994). This paradox can be explained by a concept known as local control theory. Local control theory suggests that adjacent L-type Ca^{2+} channels, and not a general increase in the concentration of cytosolic Ca^{2+}, control RyR activation (Cannell et al., 1995; Lopez-Lopez et al., 1995; Santana et al., 1996). It has been proposed that a single L-type Ca^{2+} channel can activate a cluster of RyRs (Stern, 1992). This grouping of channels is considered to be a single release unit. Therefore, the greater the magnitude of $I_{Ca\text{-}L}$, the more release units are activated, which results in a larger Ca^{2+} transient and contraction. Local control theory has been used to explain why $I_{Ca\text{-}L}$, Ca^{2+} transients and contraction display similar bell-shaped voltage dependence (Stern, 1992).

Evidence in support of local control theory comes from experimental observations of elementary Ca^{2+} release events called Ca^{2+} sparks. Ca^{2+} sparks have been identified by

laser scanning confocal microscopy in myocytes loaded with the Ca^{2+} sensitive dye fluo-3 (Cheng et al., 1993). Sparks are localized events (Cheng et al., 1993) that occur randomly and at low frequencies in the resting myocyte (Bers, 2001). It is believed that a single release unit produces a single Ca^{2+} spark (Bers, 2001). However, activation of $I_{Ca\text{-}L}$ results in the activation of a large number of release units, which results in the synchronous production of several thousand sparks, whose summation forms the Ca^{2+} transient (Bers, 2001). It is believed that both the physical distance between release units and the high concentration of Ca^{2+} required to activate an individual unit prevent one release unit from activating another. Therefore, only Ca^{2+} influx via an adjacent L-type Ca^{2+} channel can activate a release unit. Furthermore, as the membrane potential becomes more positive, the driving force for Ca^{2+} influx declines, which decreases the magnitude of $I_{Ca\text{-}L}$ (Cannell et al., 1994; Lopez-Lopez et al., 1994). Therefore, the number of L-type channels that generate sufficient current to activate release units decreases and the Ca^{2+} transient declines. The result is a decrease in the amplitude of contraction at positive potentials.

Since SR Ca^{2+} release is graded by $I_{Ca\text{-}L}$, the question arises as to what is the amplification factor for CICR. This amplification factor is referred to as gain and can be calculated by dividing SR Ca^{2+} release by the trigger $I_{Ca\text{-}L}$ (Bers, 2001). In rat ventricular myocytes, gain has been estimated as 16 (Wier et al., 1994), whereas in rabbit ventricular myocytes, gain is approximately 3-8 (Shannon et al., 2000). Changes in either $I_{Ca\text{-}L}$ amplitude and/or SR Ca^{2+} release will affect gain. Therefore, gain of CICR can be compared under different conditions to determine the efficiency of EC coupling.

High Gain CICR

In contrast to conventional CICR, several studies have reported that Ca^{2+} transients and contractions are not always proportional to the magnitude of $I_{Ca\text{-}L}$ (Ferrier & Howlett, 1995; Ferrier et al., 1998; Howlett et al., 1998). When ventricular myocytes are depolarized from physiological potentials at physiological temperatures (37°C), the contraction-voltage relations are sigmoidal, whereas the current-voltage relations are bell shaped. This demonstrates that contractions initiated from physiological membrane potentials are not proportional to the amplitude of $I_{Ca\text{-}L}$ (Ferrier & Howlett, 1995; Ferrier et al., 1998; Howlett et al., 1998). The lack of dependence on the magnitude of $I_{Ca\text{-}L}$ suggests that the gain of CICR is high under these conditions, since a large amount of Ca^{2+} is released from the SR in response to a small amount of Ca^{2+} influx. Responses initiated under these conditions are thought to be initiated by a form of high-gain CICR (Xiong et al., 2004).

High-gain CICR can be distinguished from traditional CICR with pharmacological agents. When $I_{Ca\text{-}L}$ is blocked by Ni^{2+} or Cd^{2+}, contractions and Ca^{2+} transients generated by high-gain CICR are not inhibited (Ferrier et al., 2000; Hobai et al., 1997). In addition, inhibition of Ca^{2+} entry via the NCX has no effect on Ca^{2+} transients and contractions produced by high-gain CICR (Ferrier & Howlett, 1995; Ferrier et al., 2000). It also has been demonstrated that high-gain CICR is dependent on phosphorylation via the adenylyl cyclase-PKA pathway and/or the Ca^{2+}-calmodulin kinase dependent pathway (Ferrier & Howlett, 2001). When ventricular myocytes are dialyzed with patch pipettes filled with K^{+}-based solutions, high-gain CICR is inhibited (Hobai et al., 1997: Zhu & Ferrier, 2000). However, high-gain CICR can be restored

with the addition of either 8-bromo-cAMP or calmodulin to the pipette solution (Hobai et al., 1997; Zhu & Ferrier, 2000). These results suggest that cell dialysis disrupts phosphorylation pathways required by high-gain CICR (Ferrier & Howlett, 2001). Interestingly, even though high-gain CICR is not dependent on $I_{Ca\text{-}L}$, it still requires extracellular Ca^{2+} to function (Ferrier & Howlett, 1995). Further exploration has shown that the amount of external Ca^{2+} required to activate high-gain CICR is minimal (50 μM) (Ferrier & Howlett, 1995). This suggests that high-gain CICR employs a microscopic Ca^{2+} current to trigger SR Ca^{2+} release and generate contraction (Ferrier et al., 2004). Overall, it appears the gain of CICR may increase under physiological conditions.

Aging: cardiac performance and EC coupling

Cardiac aging is a nonspecific term that refers to physiological changes that occur within the heart over the entire life span of an individual (Lakatta & Yin, 1982). Early in life, these changes are part of normal development and maturation. Developmental changes tend to be beneficial to the individual. However, the changes that occur during senescence can compromise cardiac function (Besse et al., 1993; Capasso et al., 1983; Lakatta & Sollot, 2002). In addition, aging is a risk factor for the development of cardiovascular disease (Heart and Stroke Foundation of Canada, 2003) and is a significant risk factor for the development of heart failure (Peeters et al., 2002). Since it is estimated that one in five Canadians will be 65 years of age or older by the year 2026 (Canada, 2002), cardiovascular disease and cardiac dysfunction represent a growing health problem in the aging population. In order to treat this growing health problem it is necessary to understand changes in cardiac structure and function that underlie disease.

However, this is difficult since changes in cardiac physiology in the elderly may be the result of advancing age and/or pathology. Therefore, it is necessary to study the effects of age on cardiac structure and function in the absence of disease. This will help identify age-related changes in the heart that may predispose the aging heart towards the development of disease.

Age related changes in cardiac structure and function

Alterations in cardiac structure and function occur with advancing age (Lakatta & Sollot, 2002). These alterations include changes in left ventricular wall thickness, changes in diastolic filling rate and changes in the responsiveness of the heart to sympathetic stimulation (Lakatta & Sollot, 2002). These changes have been extensively studied in both human and animal models of aging. The following sections will review what is known about age-related changes in cardiac structure and function.

Significant changes in the structure of the heart are thought to occur as a result of aging. One large population study suggests that left ventricular weight increases with increasing age (Dannenberg et al., 1989). However, the population sampled for this study included both healthy and diseased individuals. Interestingly, when patients with cardiovascular disease are removed from consideration, it appears that left ventricular weight does not increase in senescent adults (Dannenberg et al., 1989; Kitzman et al., 1988; Olivetti et al., 1991). Other studies have examined the effects of aging on ventricular wall thickness. These studies have shown that, in clinically healthy patients, left ventricular wall thickness increases with age (Ganau et al., 1995; Kitzman et al., 1988) without an increase in left ventricular weight (Ganau et al., 1995). Together, these

results suggest that, despite increases in left ventricular wall thickness in healthy aged individuals, left ventricular weight does not increase with aging.

Increases in left ventricular wall thickness in the aging heart are partially attributable to age and pathology related increases in the connective tissue (collagen, fibronectin) content in the extracellular matrix (Lakatta & Sollot, 2002). In addition, an increase in either the number or the size of ventricular myocytes also may contribute to the increase in ventricular wall thickness in the aged heart. With advancing age, the total number of ventricular myocytes does not increase (Lakatta & Sollot, 2002), but declines by 35% by the seventh decade (Oxenham & Sharpe, 2003). Therefore, an increase in the number of ventricular myocytes cannot account for increases in ventricular wall thickness in aging. In fact, it would be expected that ventricular wall thickness would decrease in aging as the number of ventricular myocytes declines. However, in the aged heart, increases in cell length, cell membrane area (Fraticelli et al., 1989; Lim et al., 2000; Liu et al., 2000) and cell volume (Fraticelli et al., 1989; Oxenham & Sharpe, 2003) have been observed in surviving ventricular myocytes. This indicates that ventricular myocytes in the aged heart are much larger than myocytes from younger adult hearts. It is believed the increase in myocyte size may be a mechanism to compensate for the loss of ventricular myocytes associated with aging (Oxenham & Sharpe, 2003). It should be noted that sarcomere length does not change with aging (Fraticelli et al., 1989; Lim et al., 2000), which suggests that cell length increases by the addition of sarcomeres. Overall, left ventricular wall thickness increases as a result of an increase in ventricular myocyte size and not an increase in the number of myocytes. The compensatory change in

ventricular myocyte size helps to maintain and/or increase ventricular wall thickness, despite an overall reduction in the number of ventricular myocytes.

Interestingly, despite changes in cardiac structure, age appears to have little effect on human left ventricular systolic function at rest (Chen et al., 1998; Morley & Reese, 1989). The values for left ventricular ejection fraction, cardiac output and stroke volume in senescent subjects at rest are similar to those from adult subjects (Morley & Reese, 1989; Oxenham & Sharpe, 2003). However, it appears that cardiac function at rest is maintained as a result of age-related compensatory changes in the heart. For example, increases in left ventricular wall thickness help to compensate for increases in left ventricular wall tension that occur with advancing age (Lakatta & Sollot, 2002). Also, cardiac contraction is prolonged in the aged heart, which helps maintain ejection fraction (Lakatta & Sollot, 2002). Unfortunately, these compensatory adaptations make it difficult to determine the precise effects of age on human cardiac function.

Many studies of aging also have used senescent animals, where senescence is the point at which 50% colony mortality occurs (Lakatta & Sollot, 2002). In senescent mice, left ventricular contractile function is significantly depressed (Yang et al., 1999). Stroke volume, cardiac output, ejection fraction and the maximum derivative of the change in systolic pressure over time also decline in aging mice (Yang et al., 1999). Furthermore, ejection fraction, fractional shortening and circumferential fiber shortening are reduced in resting aged rats in comparison to young rats (Boluyt et al., 2004). These changes significantly decrease left ventricular systolic function at rest in aged animals (Boluyt et al., 2004; Pacher et al., 2004).

Diastolic function also is affected by advancing age. Specifically, left ventricular diastolic function decreases with increasing age in both humans and in animal models of aging (Boluyt et al., 2004; Hees et al., 2004; Pacher et al., 2004). In the aged human heart, overall diastolic filling is altered as a result of a decrease in the early diastolic filling rate and an increase in the late diastolic filling rate (Gardin et al., 1998; Kitzman et al., 1991; Oxenham & Sharpe, 2003). Similarly, late diastolic filling rate also increases in the aging mouse heart (Boluyt et al., 2004). Changes in the early diastolic filling rate may be attributable to a decrease in ventricular compliance, which increases left ventricular stiffness. In addition, isovolumic relaxation rate also increases in both the aged human and animal hearts. Increases in the isovolumic relaxation rate may also contribute to the altered filling rate in aging (Boluyt et al., 2004; Hees et al., 2004; Oxenham & Sharpe, 2003). Together, these age-related changes prevent the left ventricle from filling properly during early diastole. Interestingly, the increase in late diastolic filling rate overcompensates for the reduction in the early diastolic filling rate. This results in a slight increase in left ventricular end diastolic volume in the aging heart (Lakatta & Sollot, 2002). Therefore, the compensatory changes in the late diastolic filling rate help to minimize the effects of aging on diastolic function at rest.

Overall, age-related changes in the heart appear to have relatively little impact on cardiovascular function in the older adult at rest. However, when peripheral demand increases, such as during aerobic activity, alterations in the systolic and diastolic function of the aging heart become more pronounced. This results in impaired cardiac function and intolerance to demanding activities (e.g. exercise).

During exercise, ejection fraction can increase by up to 30% in a healthy individual (Fleg et al., 1995). Ejection fraction represents an index that can be used to evaluate left ventricular systolic function (Najjar et al., 2004). Interestingly, the ability to increase ejection fraction during exercise is compromised in aged individuals, when compared to young individuals (Fleg et al., 1995; Najjar et al., 2004). It is believed that this inability to increase ejection fraction during exercise results from reduced intrinsic myocardial contractility and reduced responsiveness of the aging heart to βAR stimulation (Lakatta & Sollot, 2002). Thus, these findings suggest that systolic function is compromised in older adults during periods of increased cardiac demand.

Changes in diastolic function also have been observed in the elderly during exercise (Lakatta & Sollot, 2002; Levy et al., 1993; Schulman et al., 1992). During high intensity exercise, the rate of diastolic filling cannot be separated into early and late diastolic filling rates and is referred to as the peak diastolic filling rate. In contrast, during low intensity exercise, both early and late diastolic filling rates can be observed (Levy et al., 1993). Numerous studies have reported that peak diastolic filling rate is decreased in elderly subjects during high intensity exercise (Levy et al., 1993; Schulman et al., 1992). Similarly, both the early and late diastolic filling rates decrease in aged individuals during low intensity exercise (Levy et al., 1993; Oxenham & Sharpe, 2003). A reduction in the rate of diastolic filling could result in inadequate filling of the ventricles and the inability to maintain stroke volume during exercise (Vanoverschelde et al., 1993). Interestingly, the duration of the diastolic filling period is increased during exercise in elderly individuals (Levy et al., 1993). It is possible the increased duration of

diastolic filling in aging acts as a compensatory mechanism, which helps to reduce the impact of the reduction in rate of diastolic filling.

In summary, both systolic and diastolic function are compromised during exercise in the aged heart. Diastolic function is reduced at rest in the aged heart, but the effects of aging on systolic function remain unclear. Changes in diastolic function at rest and during exercise may be attributable to age-related reductions the rates of diastolic filling. Changes in cardiac responsiveness to sympathetic innervation likely contribute to contractile dysfunction observed during systole in the aging heart. However, age-related changes in EC coupling also are thought to be involved in contractile dysfunction in aging. This topic will be discussed in the next section.

Effects of aging on EC coupling

In the aging heart, contractile function is impaired during exercise (Najjar et al., 2004). In the absence of disease, age–related changes in the responsiveness of the heart to sympathetic stimulation may partially explain the change in contractile function. However, age also has deleterious effects on EC coupling in cardiac myocytes. Some studies have shown that biological aging is associated with an increase in action potential duration, an increase in contraction duration and an increase in the rate of relaxation of cardiac myocytes (Lakatta & Sollot, 2002). In addition, the responsiveness of cardiac myocytes to βAR stimulation is blunted in aged animals (Lakatta & Sollot, 2002). In animal models of aging, alterations in EC coupling and the modulation of contraction by the sympathetic nervous system contribute to the decreased systolic and diastolic function in senescent heart (Boluyt et al., 2004; Lakatta & Sollot, 2002; Yang et al., 1999). The

specific changes that underlie alterations in cardiac function in senescent heart will be explored in the following section.

Cardiac EC coupling is initiated by excitation of the sarcolemma by an action potential (Lakatta & Sollot, 2002). However, biological aging leads to alterations in the cardiac action potential, which might contribute to contractile dysfunction in aging heart. Numerous studies have demonstrated that both the early and late repolarization phases of the cardiac action potential are prolonged in senescent rat and sheep myocytes (Capasso et al., 1983; Dibb et al., 2004; Liu et al., 2000; Walker et al., 1993; Wei et al., 1984). Interestingly, studies have shown the duration of the action potential is largely dependent on transient outward K^+ currents (Kukushkin et al., 1983; Saxon & Safronova, 1982). Therefore, the increase in action potential duration observed in aged myocytes may be the result of alterations in repolarizing potassium currents.

Transient outward K^+ current (I_{to}) is the major determinant of cardiac repolarization in rat ventricular myocytes (Liu et al., 2000; Walker et al., 1993). Several studies have investigated whether a reduction in I_{to} is involved in the prolongation of repolarization in senescent rat cardiac myocytes (Liu et al., 2000; Walker et al., 1993). Walker et al. (1993) showed that peak I_{to} density was smaller in senescent rat myocytes. In contrast, Liu et al. (2000) demonstrated that peak I_{to} density was significantly increased in aged rat myocytes. The differences in I_{to} density between studies may be the result of differences in cellular preparations. In the study by Walker et al. (1993), rat myocytes were freshly isolated, whereas the studies conducted by Liu et al. (2000) used cultured rat myocytes.

Changes in I_{to} density could occur as a result of changes in the structure of I_{to} channels or alterations in the number of I_{to} channels. A reduction in I_{to} density should decrease the rate of repolarization and thereby increase action potential duration. In contrast, increased I_{to} density should increase the rate of depolarization and decrease action potential duration. However, action potential duration is prolonged in aged rat ventricular myocytes (Liu et al., 2000; Walker et al., 1993), which is compatible with a decrease in I_{to} in aging. To determine if the structure or function of the K^+ channel changes with aging, the activation and inactivation properties of I_{to} also have been examined in aged cardiac myocytes. Walker et al. (1993) showed the voltage dependence of activation and inactivation of I_{to} were similar in young and aged rat myocytes. This suggests the structure and function of the K^+ channel does not change with advancing age (Walker et al., 1993). Overall, these findings suggest that aging does not alter the properties of the I_{to} channel, but may affect the density of I_{to} (Walker et al., 1993). Therefore, a reduction in I_{to} channels may contribute to an increase in action potential duration in senescent cardiac myocytes.

The rate of cardiac repolarization also is determined in part by the rate of $I_{Ca\text{-}L}$ inactivation (Langer, 1997). The time course of $I_{Ca\text{-}L}$ inactivation in rat ventricular myocytes has been measured by fitting the time course of $I_{Ca\text{-}L}$ with a two-exponential function (Liu et al., 2000; Walker et al., 1993). Several studies have shown that the rate of the fast component of inactivation is significantly decreased in aging myocytes compared to cells from young hearts (Liu et al., 2000; Walker et al., 1993). In addition, the rate of inactivation of the slow component of $I_{Ca\text{-}L}$ is decreased in senescent myocytes (Walker et al., 1993), although this has not been observed in all studies (Liu et al., 2000).

In summary, age-related slowing of $I_{Ca\text{-}L}$ inactivation occurs and may contribute to prolongation of action potential duration in aged myocytes.

$I_{Ca\text{-}L}$ is the primary trigger for SR Ca^{2+} release and contraction. Thus, a number of studies also have investigated whether aging affects peak $I_{Ca\text{-}L}$ density. Studies have shown that peak $I_{Ca\text{-}L}$ density is larger in aged sheep myocytes in comparison to young cells (Dibb et al., 2004). In contrast, Walker et al. (Walker et al., 1993) found that the density of $I_{Ca\text{-}L}$ was similar in young and aged rat myocytes. Other studies have reported that peak $I_{Ca\text{-}L}$ density is actually decreased in aged myocytes (Isenberg et al., 2003; Liu et al., 2000). These findings are in agreement with results of receptor binding studies which showed that the number of cardiac L-type Ca^{2+} channels decreases in aged hearts (Howlett & Nicholl, 1992). However, there is little agreement on whether the magnitude of $I_{Ca\text{-}L}$ is altered in aging heart.

Aged ventricular myocytes also have been studied to determine the effects of biological aging on cardiac contraction. These studies indicate that contraction amplitudes are reduced and time courses of contraction are prolonged in aging myocytes, at least in field-stimulated myocytes paced at rapid rates (Fraticelli et al., 1989; Lim et al., 2000). In ventricular myocytes paced at low to moderate stimulation frequencies (0.4 to 4 Hz), there is no difference in peak contraction amplitude between young and aged myocytes (Fraticelli et al., 1989; Lim et al., 2000). However, at higher simulation frequencies contraction amplitudes are smaller in aged myocytes in comparison to young myocytes (Lim et al., 2000). In addition, the time required to reach peak contraction and the overall duration of contraction increase in aged myocytes (Fraticelli et al., 1989). The time required for myocyte relaxation also is significantly prolonged in aged myocytes

when paced at rapid stimulation rates (Lim et al., 2000). However, when cells are paced at slower rates, relaxation times are similar in young and aged myocytes (Fraticelli et al., 1989; Lim et al., 2000). Overall, these findings suggest that contractile function is maintained at resting heart rates, but that ability to respond to an increase in cardiac demand is impaired in aged myocytes.

In cardiac myocytes, contraction is dependent on SR Ca^{2+} release (Bers, 2001). Therefore, changes in SR Ca^{2+} release and reuptake could account, at least in part, for changes in contraction amplitudes and time courses in aged myocytes (Fraticelli et al., 1989; Lim et al., 2000). Changes in Ca^{2+} transient amplitudes with aging are dependent on stimulation frequency in aging mouse ventricular myocytes (Isenberg et al., 2003; Lim et al., 2000). At high stimulation frequencies, Ca^{2+} transient amplitudes are reduced in aged myocytes compared to young cells, whereas at low stimulation frequencies Ca^{2+} transient amplitudes are similar in young and aged myocytes (Isenberg et al., 2003; Lim et al., 2000). In addition, the time to peak Ca^{2+} transient amplitude is increased (Isenberg et al., 2003) and the rate of Ca^{2+} transient decay is prolonged in aged myocytes compared to young cells when myocytes are paced at rapid rates (Isenberg et al., 2003; Lim et al., 2000). In contrast, Dibb et al. (2004) showed that Ca^{2+} transient amplitudes were increased and the rate of decay was faster in aged myocytes in comparison to young controls (Dibb et al., 2004). Of note, Dibb et al. (2004) studied sheep ventricular myocytes, whereas experiments by Lim et al. (2000) and Isenberg et al. (2003) studied mouse ventricular myocytes. Therefore, it is possible that the differences in results reflect differences between species. In summary, Ca^{2+} transient amplitudes do not increase at higher rates of stimulation in aged myocytes. This suggests that SR Ca^{2+}

release does not increase at higher stimulation rates in aged myocytes. The lack of an increase in SR Ca^{2+} release could explain the reduction in the magnitude of contractions in aged myocytes at higher stimulation frequencies.

In cardiac myocytes, relaxation depends upon the removal of cytosolic Ca^{2+}. Cytosolic Ca^{2+} can be transported back into the SR via the SR Ca^{2+} ATPase or it can be removed from the cell via the sarcolemmal Ca^{2+} ATPase and the NCX (Bers, 2001). The reduction in the rate of Ca^{2+} transient decay in aged myocytes suggests that aging somehow alters the reuptake or removal of intracellular Ca^{2+} after contraction. Indeed, studies have shown that the mRNA for SR CaATPase is decreased in the aged myocyte (Besse et al., 1993; Schmidt et al., 2000). The activity of SR Ca^{2+} pump also is decreased in aging myocytes. In fact, one study has shown phosphorylation of SR Ca^{2+} ATPase by CaM kinase II is reduced by 25-40 % in aged myocytes (Xu & Narayanan, 1998). Furthermore, PLB protein levels are increased in aged myocytes (Lim et al., 1999), which also would decrease SR Ca^{2+} ATPase activity. A reduction in SR Ca^{2+} ATPase density as well as a decrease in SR Ca^{2+} ATPase activity would decrease the rate at which intracellular Ca^{2+} is taken up into the SR in the aging myocyte. In addition, NCX mRNA also is reduced in aged myocytes (Lim et al., 1999). This suggests that removal of intracellular Ca^{2+} via the NCX also may be decreased in aging cardiac myocytes. Together, a reduction in SR Ca^{2+} reuptake and a decrease in Ca^{2+} removal via the NCX would prolong the Ca^{2+} transient and result in prolongation of the cardiac contraction.

SR Ca^{2+} release and contraction amplitudes are graded by the magnitude of $I_{Ca\text{-}L}$ in cardiac myocytes. Therefore, any age-related changes in $I_{Ca\text{-}L}$ should affect Ca^{2+} transient and contraction amplitudes. Interestingly, in field-stimulation studies, aging has

little effect on contraction and Ca^{2+} transient amplitudes in cardiac myocytes stimulated at low to moderate rates. This suggests that the magnitude of $I_{Ca\text{-}L}$ does not differ between young and aged cardiac myocytes. However, studies have shown that $I_{Ca\text{-}L}$ is increased, decreased or unchanged in aged cardiac myocytes. Interestingly, no study has examined the effects of aging on $I_{Ca\text{-}L}$ and contraction simultaneously in the same cell. Furthermore, the relationship between $I_{Ca\text{-}L}$ and Ca^{2+} transients in aging also is not clear. For example, a previous study has reported that when $I_{Ca\text{-}L}$ is reduced in aged myocytes, there is no corresponding reduction in the Ca^{2+} transient amplitude (Isenberg et al., 2003). This suggests that SR Ca^{2+} content might increase in aging although this has not been examined. Based on the preceding evidence, it is not clear whether aging affects the relationship between $I_{Ca\text{-}L}$, SR Ca^{2+} release and contraction. To determine whether aging affects cardiac EC coupling, $I_{Ca\text{-}L}$, SR Ca^{2+} release and contraction should be examined simultaneously under physiological conditions.

Beta- adrenergic receptor signaling

Overview of cardiac βAR signaling

In cardiac myocytes, EC coupling can be modulated by the sympathetic nervous system (SNS). This is done through the release of catecholamines, which act on cardiac beta-adrenergic receptors (βAR) (Dzimiri, 1999; Xiao, 2001). βARs are integral membrane proteins and members of the G-protein coupled superfamily (Dzimiri, 1999; Xiao, 2001). Stimulation of βARs by catecholamines leads to the activation of G-proteins, which interact with downstream proteins and second messengers (Xiao, 2001).

This results in an increase in contraction amplitude and an increase in the rate of relaxation in cardiac myocytes.

To date, four distinct βAR subtypes (β_1-β_4AR) have been identified in human cardiac tissue (Bristow et al., 1990; Dzimiri, 1999). β_1ARs represent approximately 70-80% of the βAR population in the heart (Dzimiri, 1999) and signal via stimulatory G-proteins (G_s). The binding of an agonist to β_1ARs leads to the activation of G_s, which stimulates adenylate cyclase (AC) and increases the synthesis of cAMP. This leads to the activation of PKA, which can phosphorylate a number of intracellular targets involved in EC coupling such as L-type Ca^{2+} channels, SR Ca^{2+} release channels, phospholamban and troponin (Dzimiri, 1999; Post et al., 1999). The overall result of phosphorylation of these targets is a positive inotropic response. This response is characterized by enhanced cardiac contraction, an increase in the rate of cardiac relaxation and an increase in heart rate (Dzimiri, 1999; Post et al., 1999).

More recently, cardiac βAR research has focused on investigations of the function of the β_2AR signaling pathway. β_2ARs represent approximately 20-30% of the cardiac βAR population (Dzimiri, 1999). Unlike β_1ARs, β_2ARs interact with G_s as well as an inhibitory G-protein (G_i) (Xiao, 2001). Activation of the β_2AR-G_s pathway results in positive inotropic responses which are similar to those produced by β_1AR stimulation (Dzimiri, 1999; Gille et al., 1985; Kaumann & Lemoine, 1987; Kaumann et al., 1982). In contrast, activation of the β_2AR-G_i pathway results in inhibition of AC activity, which prevents an increase in the synthesis of intracellular cAMP (Dzimiri, 1999). However, the function of the β_2AR-G_i signaling pathway remains unclear at this time.

In aging and in some disease states, the responsiveness of cardiac myocytes to β_2AR signaling is reduced (Lakatta & Sollot, 2002; Post et al., 1999). This results in decreased contractile function (Lakatta & Sollot, 2002; Post et al., 1999). In theory, it may be possible to overcome this deficit and augment cardiac contraction by increasing the number of βARs in the heart. However, overexpression of β_1ARs in the heart leads to the onset of cardiac pathology at an early age (Engelhardt et al., 1999). Mice overexpressing β_1ARs develop progressive heart failure which leads to a 35% reduction in contractile function by 35 weeks of age (Engelhardt et al., 1999). In contrast, low level overexpression of cardiac β_2ARs augments contraction without the development of pathology (Liggett et al., 2000; Shah et al., 2000). Therefore, several β_2AR overexpression models have been created to determine the effects of β_2AR overexpression on EC coupling in cardiac myocytes. This section will review β_2AR signaling and examine effects of β_2AR overexpression on EC coupling.

β_2-adrenergic receptor signaling in ventricular tissue

Radioligand binding studies conducted during the 1980's established that β_2ARs exist in both atrial and ventricular tissue (Brodde et al., 1983; Heitz, Schwartz & Velly, 1983; Robberecht et al., 1983; Stiles et al., 1983; Wilson & Lincoln, 1984). In both types of cardiac tissue, circulating catecholamines bind to β_2ARs and activate a signaling cascade that results in a positive inotropic response (Kaumann & Lemoine, 1987; Kaumann et al., 1985; Kaumann & Lobnig, 1986; Xiao & Lakatta, 1993). However, it is not clear whether the β_2AR signaling cascade is similar to the β_1AR signaling pathway.

It is well established that β_1AR stimulation activates the cAMP-PKA pathway, which results in a positive inotropic response (Steinberg, 2000; Xiao, 2001). Since β_1ARs and β_2ARs produce similar inotropic effects and show 50% homology (Dzimiri, 1999; Xiao et al., 1999), it is plausible that they both utilize the same signaling pathway. To determine whether β_2ARs signal via a cAMP-dependent pathway, the effects of β_2AR stimulation on cAMP levels, PKA activity and protein phosphorylation have been investigated in ventricular myocytes (Kuschel et al., 1999; Xiao et al., 1994; Zhou et al., 1997). Activation of both β_1ARs and β_2ARs increases total cellular cAMP (Xiao et al., 1994). However, the location of cAMP production, the rate of production and the overall level of cAMP differ depending on whether β_1ARs or β_2ARs are activated. When β_2ARs are activated, the rate of cAMP production is reduced in comparison to rate cAMP production mediated by the activation of β_1ARs (Xiao et al., 1994). Specifically, the total cAMP concentration produced by β_2AR stimulation is 50% less in comparison to the β_1AR-mediated increases in cAMP concentration (Xiao et al., 1994). It is likely that differences in the rate and overall levels of cAMP production are the result of differences in β_1AR and β_2AR receptor density. In the ventricles, β_1ARs outnumber β_2ARs by approximately 3:1 (Dzimiri, 1999; Sathyamangla et al., 2001). Therefore, β_1ARs may activate more AC, which will result in a rapid increase in cAMP levels and greater total cAMP levels. Overall, these results demonstrate that β_2AR activation can increase cAMP production in ventricular myocytes.

The ability of β_2AR stimulation to induce cAMP production does not, by itself, demonstrate the dependence of β_2AR signaling on a cAMP-dependent pathway. For example, activation of the β_1AR cAMP-dependent pathway by an agonist increases

intracellular cAMP concentration with corresponding increases in contraction amplitude. When contraction amplitude and cAMP concentration are plotted against agonist concentration, the concentration-response curves for twitch amplitude and intracellular cAMP concentration are almost identical (Xiao et al., 1994). Therefore, if β_2ARs signal via a cAMP-dependent pathway, then contractions induced by β_2AR activation should be proportional to cAMP levels. Interestingly, activation of β_2ARs leads to a moderate increase in overall cAMP levels as well as an increase in Ca^{2+} transient amplitudes and twitch amplitudes (Xiao et al., 1994). However, moderate increases in total intracellular cAMP concentration have little effect on Ca^{2+} transient amplitude and twitch amplitude. In fact, Ca^{2+} transient and twitch amplitudes do not increase until maximal cAMP production occurs (Xiao et al., 1994). This suggests that β_2AR may signal via a cAMP-independent pathway.

In theory, if β_2ARs utilize a cAMP-independent pathway then inhibition of PKA should not affect β_2AR-mediated responses. To test this hypothesis, inhibitory cAMP analogs, which block the interaction between cAMP and PKA by competing for native cAMP binding sites on regulatory subunits of PKA, were applied to the cell in conjunction with β_2AR agonists (Adamson et al., 2000; Zhou et al., 1997). Interestingly, inhibitory cAMP analogs antagonize the effects of β_2AR stimulation on Ca^{2+} transients and twitch amplitudes (Adamson et al., 2000; Kuschel et al., 1999; Zhou et al., 1997). This suggests that, although there is not a direct relationship between β_2ARs and cAMP, PKA is necessary for β_2AR signaling. Another explanation for the above results is that β_2ARs may utilize more than one signaling pathway.

The role of PKA in β_2AR signaling also has been investigated. In several studies, the activation of β_2ARs increases cytosolic PKA activity in ventricular myocytes (Bartel et al., 2003; Kuschel et al., 1999). In another study, β_2AR stimulation had no effect on PKA activity in ventricular myocytes (Kuschel et al., 1999). However, in the presence of PKA-blocking agents such as H-89 and protein kinase peptide inhibitor, β_2AR stimulation is unable to increase contraction or L-type Ca^{2+} current in ventricular myocytes (Kuschel et al., 1999; Skeberdis & Fischmeister, 1997). Thus, these results suggest that PKA is required in the β_2AR signaling pathway.

Overall, these findings show that β_2AR stimulation produces positive inotropic effects in ventricular tissue (Kuschel et al., 1999; Xiao et al., 1994; Zhou et al., 1997). In addition, both cAMP and PKA are required for β_2AR signaling to occur. However, the relationship between β_2AR-mediated inotropic responses and cAMP levels is quite different from the relationship between β_1AR-mediated response and cAMP levels. This suggests that β_2ARs and β_1ARs use different signaling pathways. An alternate possibility is that β_2ARs utilize more than one signaling pathway, where one subset of β_2ARs induce increases in intracellular cAMP and the other subset does not. The overall effect would be a positive inotropic response, but cAMP concentration would be less than that produced by β_1AR activation.

$\underline{\beta_2\text{ARs couple to pertussis toxin-sensitive } G_i}$

It is generally agreed that cardiac β_1ARs and β_2ARs interact with G_s to produce positive inotropic responses (Xiao et al., 1994; Xiao, 2001; Zhou et al., 1997). However, a major difference between β_1ARs and β_2ARs is the relationship that exists between

intracellular cAMP and contraction amplitude. Unlike β_1ARs, stimulation of β_2ARs produces an increase in cardiac contraction that is not proportional to intracellular cAMP levels (Xiao et al., 1994). This suggests that β_2ARs may interact with more than one G-protein (Xiao et al., 1995). If β_2ARs interact with G_i, this could explain the observed differences in cAMP levels produced by β_1AR and β_2AR activation.

To determine if β_2ARs interact with G_i, pertussis toxin (PTX), which disrupts G_i signaling (Gong et al., 2000; Xiao, 2001), was used in conjunction with β_2AR agonists. Experiments showed that PTX potentiated the effects of β_2AR stimulation, which suggests that β_2AR signaling involves a PTX-sensitive G protein (Xiao et al., 1994). Furthermore, pretreatment of murine ventricular myocytes with PTX augments the positive inotropic effect of β_2AR stimulation (Gong et al., 2000; Xiao et al., 1999; Xiao et al., 1995; Zhou et al., 1997). Together, these results strongly suggest that β_2ARs interact with a PTX-sensitive G_i-protein. They also suggest that G_i has an inhibitory effect on EC coupling, since blockade of G_i increases the positive inotropic response produced by β_2AR stimulation.

To confirm the interaction of G_i with β_2ARs, G-protein activation by β_2AR agonists was measured with photoaffinity labeling (Xiao et al., 1999). Exposure of ventricular myocytes to β_2AR agonists increases G_i labeling (Xiao et al., 1999). However, G_i labeling does not increase when β_2AR agonists are applied in conjunction with the β_2AR inverse agonist ICI 118, 551 (ICI) (Xiao et al., 1999). Furthermore, inhibition of β_1ARs has no effect on β_2AR agonist-induced G_i labeling (Xiao et al.,

1999). Overall, these findings confirm that, unlike β_1ARs, β_2ARs can interact with G_i. However, the function of β_2AR-G_i signaling in the cardiac myocyte remains unclear.

β_2AR signaling theories

The activation of β_1- and β_2ARs by catecholamines and βAR agonists results in positive inotropic responses (Gille et al., 1985; Kaumann & Lemoine, 1987; Kaumann et al., 1982). However, unlike β_1AR stimulation which increases the rate of cardiac relaxation (Xiao et al., 1995; Xiao & Lakatta, 1993), β_2AR stimulation has little, if any, effect on cardiac relaxation (Xiao et al., 1994). One theory as to why β_2ARs are able to modulate cardiac contraction but not cardiac relaxation is that β_2AR signaling is localized within sarcolemmal invaginations, known as caveolae. This localization prevents the phosphorylation of intracellular targets, such as phospholamban, which are required to speed relaxation. Two different theories have been proposed to explain the compartmentalization of β_2AR signaling. Each will be discussed in the following sections.

Compartmentalization of β_2AR signaling: The involvement of G_i

Cell-attached patch clamp techniques have been used to investigate the compartmentalization of β_2AR signaling. This technique separates the membrane inside the bore of the patch pipette from the membrane outside the pipette. Stimulation of cells outside the pipette (remote stimulation) has no effect on Ca^{2+} channel activity or availability inside the patch. On the other hand, stimulation of β_2ARs inside the patch (local stimulation) increases both Ca^{2+} channel activity and availability within the patch,

but not at the remote location (Chen-Izu et al., 2000). In addition, application of a β_2AR agonist to one end of a cardiac myocyte has little stimulatory effect at the other end of the cell (Jurevicius & Fischmeister, 1996; Skeberdis & Fischmeister, 1997). In contrast to β_2AR agonists, both remote and local application of β_1AR agonists increases Ca^{2+} channel activity and availability within the patch (Chen-Izu et al., 2000). This suggests that β_2AR signaling is localized to the immediate area surrounding the activated receptor. Therefore, it is unlikely that β_2AR signaling could induce phosphorylation of intracellular targets involved in cardiac relaxation.

The mechanism underlying the localization of β_2AR signaling in not clear, but it has been suggested that G_i-proteins may be involved (Daaka et al., 1997; Xiao et al., 1999; Xiao et al., 1995). As described above, cell-attached patch clamp experiments show that remote activation of β_2ARs has no effect on Ca^{2+} channel activity within the patch (Chen-Izu et al., 2000). However, when myocytes are pretreated with PTX to uncouple G_i from β_2ARs, remote β_2AR stimulation increases Ca^{2+} channel activity within the patch (Chen-Izu et al., 2000). Furthermore, in the presence of PTX, β_2AR stimulation increases the phosphorylation of PLB and enhances relaxation in cardiac myocytes (Kuschel et al., 1999). Together, these results suggest that the interaction of β_2ARs with a PTX sensitive G_i protein is responsible for localization of β_2AR signaling.

Compartmentalization of β_2AR signaling: The involvement of caveolae

The sarcolemma contains flask shaped invaginations known as caveolae (Levin & Page, 1980). Caveolae have a distinct lipid and protein composition (Okamoto et al., 1998; Shaul & Anderson, 1998; Steinberg & Brunton, 2001) and contain L-type Ca^{2+}

channels, G-proteins (G_s and G_i), AC, PKA and A-kinase anchoring proteins (AKAP) (Lohn et al., 2000; Rybin et al., 2000; Schwencke et al., 1999; Steinberg & Brunton, 2001). Furthermore, β_2AR have been shown to reside exclusively in caveolae (Rybin et al., 2000; Schwencke et al., 1999; Xiang et al., 2002). It is believed that caveolae act to arrange β_2ARs and various signaling molecules into localized signaling complexes (Okamoto et al., 1998; Ostrom et al., 2000; Shaul & Anderson, 1998). It also is thought that these signaling complexes are anchored within the caveolae (Steinberg & Brunton, 2001). Therefore, it is possible that caveolae are involved with the compartmentalization of βAR signaling (Okamoto et al., 1998).

Experiments have examined the role of caveolae in cardiac β_2AR signaling by disrupting caveolae with cholesterol-binding drugs. Stimulation of β_2ARs results in a much larger increase in intracellular cAMP levels in cells with disrupted caveolae than in cells with intact caveolae (Rybin et al., 2000). This suggests that the disruption of caveolae removes some type of inhibitory mechanism that modulates intracellular cAMP levels. Furthermore, studies that have examined spontaneous beating in cardiac myocytes have shown that caveolae have an inhibitory effect on β_2AR signaling (Devic et al., 2001; Xiang et al., 2002). It is believed that the protein caveolin, a structural component of caveolae, may negatively regulate the activation of G-proteins (Steinberg & Brunton, 2001). Therefore, caveolae could dampen the β_2AR signal and prevent phosphorylation of targets outside the immediate area of the caveolae, which could result in signal localization.

In summary, β_2AR signaling appears to be localized in cardiac myocytes. The evidence clearly shows that both caveolae and G_i-proteins are involved in β_2AR signal

localization. However, it is not clear whether G_i and caveolae act in conjunction or independently. Therefore, the exact nature of β_2AR-G_i signaling remains to be fully clarified.

β_2AR overexpression in the heart

Several studies have shown that cardiac βAR density is decreased in aging and diseased hearts (Lakatta & Sollot, 2002; Milano et al., 1994). As a result, the aging and diseased hearts are less responsive to circulating catecholamines released by the SNS. Thus, the ability of the SNS to modulate heart rate, force of cardiac contraction and rate of cardiac relaxation is reduced. It is possible that increasing the number of βARs in aging and diseased hearts may help restore and/or augment cardiac contraction.

Transgenic Models

Transgenic animal models that overexpress either β_1ARs or β_2ARs in heart (Engelhardt et al., 1999; Liggett et al., 2000; Milano et al., 1994; Shah et al., 2000) have been created to investigate the effects of βAR overexpression on EC coupling. The overexpression of either β_1ARs or β_2ARs in the heart leads to an increase in cardiac contractility (Engelhardt et al., 1999; Liggett et al., 2000; Milano et al., 1994). However, low levels of β_1AR overexpression also lead to the development of cardiac pathology and mortality at an early age (Engelhardt et al., 1999). In contrast, there is no evidence of disease in transgenic animals that overexpress β_2AR at low levels (Shah et al., 2000). Therefore, a β_2AR overexpression model has been used to investigate possible therapeutic effects of βAR augmentation on cardiac function.

Several different transgenic models that overexpress human β_2ARs in mouse ventricular myocytes have been developed (Liggett et al., 2000; Milano et al., 1994; Shah et al., 2000). Different methods can be used to vary the degree of β_2AR overexpression and to localize overexpression to specific tissues, such as cardiac tissue (Liggett et al., 2000; Milano et al., 1994; Shah et al., 2000). For example, the coding sequence for the human β_2AR can be attached to the alpha myosin heavy chain promoter to form the transgene construct (Liggett et al., 2000; Milano et al., 1994). This construct produces a transgenic mouse model that displays cardiac specific overexpression of β_2ARs, with no increase β_2ARs in other organs or tissues (Milano et al., 1994).

Overexpression of human β_2ARs in mouse cardiac tissue results in phenotypic changes that appear to be receptor-density dependent (Liggett et al., 2000; Milano et al., 1994). In animals with high levels of β_2AR overexpression (350 times), there is an increase in heart weight, enlargement of the ventricles and impairment of ventricular function. These changes also are accompanied by increased cardiac fibrosis and myocyte hypertrophy (Liggett et al., 2000). It also should be noted that early mortality is observed in mice with high levels of β_2AR overexpression (Liggett et al., 2000). In contrast, there is no change in physical phenotype in animals with low levels of β_2AR overexpression, nor is there any impairment of ventricular function (Liggett et al., 2000). In fact, fractional shortening is significantly enhanced with a 60 to 200 times greater overexpression of β_2ARs in comparison to control animals. However, no change in contraction is observed in animals with a 350 times overexpression of β_2ARs (Liggett et al., 2000). Overall, these results suggest that low levels of β_2AR overexpression may

improve cardiac function, whereas high levels of overexpression may adversely affect cardiac function.

Hemodynamic function also is altered by the overexpression of β_2ARs. In animals overexpressing a moderate level of β_2ARs (10-200 fold), the maximum first derivative of left ventricular pressure is significantly increased (Liggett et al., 2000; Maurice et al., 1994; Rockman et al., 1996; Shah et al., 2000), left ventricular relaxation time is decreased and heart rate is increased (Liggett et al., 2000; Milano et al., 1994). However, β_2AR overexpression does not affect left ventricular end diastolic pressure or aortic pressure (Milano et al., 1994). In a model of heart failure, a 30-fold overexpression of β_2ARs improves the maximum first derivative of left ventricular pressure (Dorn et al., 1999). This suggests that β_2AR overexpression could be used to augment contractile function in aged and diseased hearts.

The effects of β_2AR overexpression on EC coupling in ventricular myocytes

The effects of β_2AR overexpression on EC coupling have been examined in isolated murine ventricular myocytes with a 200 times overexpression of β_2ARs (TG4 mice). In field-stimulated myocytes, contraction amplitudes are significantly greater in myocytes overexpressing β_2ARs in comparison to control myocytes (Xiao et al., 1999; Zhang et al., 2000; Zhou et al., 1999a; Zhou et al., 1999b). Interestingly, these increases in contraction amplitude occurred in the absence of a β_2AR agonist. In contrast, other studies have found that contraction amplitudes are similar in wild-type myocytes (WT) and in myocytes overexpressing β_2ARs (Gong et al., 2000; Heubach et al., 1999). The reasons for these different observations are not clear. However, studies that report an

increase in contraction amplitude in TG4 myocytes were conducted at room temperature, whereas studies that observed no difference in contraction amplitude between TG4 and WT myocytes were conducted at 32°C. This suggests that contraction amplitude may not be increased in TG4 myocytes at physiological temperatures.

In vitro studies have revealed that increases in contraction amplitudes in TG4 myocytes also are accompanied by increases in AC activity and cAMP levels (Liggett et al., 2000; Milano et al., 1994; Zhang et al., 2000; Zhou et al., 1999a). Interestingly, increases in AC activity and cAMP levels occur in the absence of a β_2AR agonist (Bond et al., 1995; Liggett et al., 2000; Milano et al., 1994; Rockman et al., 1996; Zhang et al., 2000; Zhou et al., 1999a). One explanation for the increase in second messengers may be that β_2ARs are active in TG4 myocytes, despite the absence of a βAR agonist.

To determine the mechanism(s) underlying the increased contraction amplitudes observed in myocytes that overexpress β_2ARs, further experiments were conducted with the nonselective competitive βAR antagonist, alprenolol, or the β_2AR inverse agonist, ICI. Since alprenolol displaces endogenous catecholamines from βAR receptors, it was expected that it would block the increase in contraction and reduce AC activity. However, alprenolol has no effect on either contraction or AC activity in mice overexpressing cardiac β_2ARs (Milano et al., 1994). However, the β_2AR inverse agonist ICI, which shifts the receptor from the active to inactive conformation, clearly reduced both contraction amplitudes and AC activity in TG4 ventricular myocytes (Milano et al., 1994). This suggests that, unlike the native murine β_2ARs, the overexpressed human β_2ARs are constitutively active. Other studies also have suggested that non-native β_2ARs possess constitutive activity (Gurdal et al., 1997; Samama et al., 1997; Xiao, 2001; Zhou

et al., 1999a; Zhou et al., 2000). For example, Zhou et al. (1999) showed that contraction amplitudes and intracellular cAMP concentrations were increased in TG4 ventricular myocytes in the absence of a βAR agonist. However, the increases in contraction amplitude and intracellular cAMP concentration were abolished in the presence of ICI. Therefore, it is believed that constitutive activity of the human β_2ARs is responsible for increased contraction amplitude and increased AC activity in TG4 ventricular myocytes.

As previously mentioned, contraction and Ca^{2+} transient amplitudes are graded by trigger $I_{Ca\text{-}L}$ (Callewaert et al., 1988; London & Krueger, 1986). Therefore, since contraction amplitudes are increased in TG4 myocytes, it would be expected that the magnitude of $I_{Ca\text{-}L}$ also might be increased in TG4 cells. However, some studies suggest that the magnitude of $I_{Ca\text{-}L}$ is similar in WT myocytes and myocytes overexpressing β_2ARs (Zhou et al., 1999a; Zhou et al., 1999b). Other studies have demonstrated that $I_{Ca\text{-}L}$ is reduced in TG4 myocytes in comparison to WT myocytes (Heubach et al., 1999; Liggett et al., 2000). These findings suggest that the overexpression of β_2ARs may alter the relationship between contraction amplitude and $I_{Ca\text{-}L}$. However, the relationship between contraction and $I_{Ca\text{-}L}$ can only be inferred from previous studies, since contraction and $I_{Ca\text{-}L}$ were examined separately with either field-stimulation (contraction) or voltage-clamp ($I_{Ca\text{-}L}$) protocols.

Increases in contraction amplitudes without corresponding increases in $I_{Ca\text{-}L}$ in TG4 ventricular myocytes could be explained by an increase in the gain (Ca^{2+} transient/$I_{Ca\text{-}L}$) of CICR. In TG4 myocytes, Ca^{2+} transient amplitudes are increased even though there is no corresponding increase in $I_{Ca\text{-}L}$ (Zhou et al., 1999a; Zhou et al., 1999b). These findings support the idea that the gain of CICR is increased in TG4 myocytes.

Increases in SR Ca^{2+} release could be attributable to increased SR Ca^{2+} load and/or an increase in the sensitivity of SR Ca^{2+} release channels. Interestingly, SR Ca^{2+} stores are similar in TG4 and WT myocytes (Zhou et al., 1999b). This suggests that SR Ca^{2+} load does not modulate Ca^{2+} transient amplitudes in TG4 myocytes. However, the incidence, frequency and amplitudes of elementary Ca^{2+} release events, known as Ca^{2+} sparks, are increased in TG4 myocytes (Grandy et al., 2004; Zhou et al., 1999b). Furthermore, the spatial width of Ca^{2+} sparks is increased in TG4 myocytes (Zhou et al., 1999b). Since the sensitization of SR Ca^{2+} release channels can be represented by an increase in the frequency of Ca^{2+} sparks (Viatchenko-Karpinski & Gyorke, 2001), it is possible that the sensitivity of SR Ca^{2+} release channels is increased in TG4 myocytes. Overall, these results suggest that SR Ca^{2+} release is not affected by changes in SR Ca^{2+} stores in TG4 myocytes, but may be increased as a result of changes in SR Ca^{2+} release channel sensitivity. Furthermore, an increase in the sensitivity SR Ca^{2+} release channels may result in greater SR Ca^{2+} release for a given $I_{Ca\text{-}L}$. Thus, the gain of CICR is increased. Of note, the preceding experiments were conducted at room temperature, which is important because several groups have shown that temperature markedly affects SR Ca^{2+} stores, Ca^{2+} transients and Ca^{2+} sparks (Ferrier et al., 2003; Puglisi et al., 1996). Therefore, it is possible that Ca^{2+} cycling in TG4 myocytes at physiological temperatures is substantially different than that described at room temperature.

Overall, it appears that overexpression of β_2ARs in mouse ventricular myocytes results in increased contraction amplitudes in field-stimulated myocytes and an increase in the incidence, frequency and amplitude of Ca^{2+} sparks. However, the effect of β_2AR overexpression on $I_{Ca\text{-}L}$ remains unclear. Furthermore, since contraction, $I_{Ca\text{-}L}$ and Ca^{2+}

transients were examined in separate cells under different experimental conditions, the relationship between the three can only be inferred. In addition, previous studies were conducted at room temperature. As contraction, $I_{Ca\text{-}L}$ and Ca^{2+} cycling are affected by temperature (Ferrier et al., 2003; Puglisi et al., 1996; Puglisi et al., 1999), it is unclear whether changes in EC coupling observed at room temperature also will be present at physiological temperature. Therefore, to evaluate the effects of β_2AR overexpression on EC coupling, contraction, $I_{Ca\text{-}L}$ and Ca^{2+} transients should be studied simultaneously at physiological temperature under the same experimental conditions.

Hypotheses and Objectives

Part I

In cardiac myocytes, amplitudes of Ca^{2+} transients and contraction are graded by the magnitude of $I_{Ca\text{-}L}$. Previous studies have shown that contractile function is relatively well preserved at rest in aged myocytes, but the effects of aging on $I_{Ca\text{-}L}$ are unclear. It has been reported that the density of L-type Ca^{2+} channels decreases with advancing age. If the number of L-type Ca^{2+} channels is reduced in aged myocytes, it would be expected that the magnitude of $I_{Ca\text{-}L}$ would be reduced, which could lead to a decrease in Ca^{2+} transient amplitudes, which would disrupt contractile function. Previous studies also have shown that when cells are stimulated at high frequencies to simulate exercise, contractile function is markedly impaired in aged myocytes. This suggests that contractile dysfunction in aging will be exacerbated at rapid heart rates. The major hypothesis investigated in part I of this thesis is that age-related abnormalities in cardiac

EC coupling disrupt cardiac contractile function, especially when cells are paced at rapid rates.

The objectives for the first part of the current study are:

1) To compare amplitudes of contraction and $I_{Ca\text{-}L}$ in voltage-clamped ventricular myocytes at physiological temperatures in young adult and aged myocytes.
2) To compare Ca^{2+} transients and SR Ca^{2+} content in young adult and aged ventricular myocytes under conditions identical to those used to evaluate contraction and $I_{Ca\text{-}L}$.
3) To determine whether the effects of aging on components of EC coupling are exacerbated at rapid stimulation rates.

Part II

Studies have shown that contraction amplitude and Ca^{2+} transients are increased in field-stimulated cardiac myocytes from TG4 mice examined at 22°C. Other studies have reported that contraction amplitudes are similar in field-stimulated TG4 and WT myocytes examined at 32°C. In cardiac muscle, Ca^{2+} transients and contraction are graded by the magnitude of $I_{Ca\text{-}L}$. Interestingly, studies have shown that $I_{Ca\text{-}L}$ is unchanged or decreased in TG4 myocytes in comparison to WT myocytes. This suggests that the relationship between $I_{Ca\text{-}L}$ and contraction may be altered in TG4 myocytes. However, $I_{Ca\text{-}L}$ was examined with voltage clamp protocols, whereas contractions were measured separately with field-stimulation techniques. Since these studies were not conducted in the same cells or under the same experimental conditions, it is not clear how

overexpression of β_2ARs affects the relationship between $I_{Ca\text{-}L}$ and contraction in TG4 myocytes.

Since contraction amplitude is increased in TG4 myocytes without a corresponding increase in $I_{Ca\text{-}L}$ the major hypothesis investigated in part II of this thesis is: overexpression of β_2ARs increases the gain of CICR in TG4 myocytes, which results in increased contraction amplitude.

The objectives for the second part of the study are:

1) To compare amplitudes of contraction in field-stimulated TG4 and WT myocytes at physiological temperature.
2) To measure contraction and $I_{Ca\text{-}L}$ simultaneously in voltage-clamped ventricular myocytes.
3) To assess SR Ca^{2+} content and Ca^{2+} transients under conditions identical to those used to evaluate contraction and $I_{Ca\text{-}L}$.
4) To determine whether abnormalities in EC coupling in TG4 myocytes are abolished by the β_2AR inverse agonist ICI 118, 551

MATERIALS AND METHODS

Animals

All experiments were conducted on ventricular myocytes isolated from mouse hearts. A number of experiments used CD-1® mice that were supplied by Charles River (St. Constant, Quebec). Other experiments utilized transgenic mice that had a cardiac specific overexpression of human β_2ARs (Milano et al., 1994). A mouse colony was established in the Dalhousie University Animal Care facility to supply the mice for these experiments. Two breeding pairs were used to establish the transgenic mouse colony and were named A1 and A2. Each breeding pair was made up of a wild-type female (B6SJLF1/J) and transgenic male (B6SJL-TgN(Wtbeta2)4Wjk) supplied by Jackson Laboratories (Bar Harbour, Maine). Litters were born approximately every 21 to 28 days. Mouse pups were weaned and sexed 21 days after birth and housed by sex (male or female). New breeding pairs were derived from the available offspring every 6 to 8 months. Breeding pairs were made up of unrelated male and female mice to prevent interbreeding. In addition, new wild-type breeding stock was introduced on a yearly basis. For example, wild-type females (B6SJLF1/J) were ordered from Jackson Laboratories and then paired with transgenic males from the colony to create new breeding pairs. Approximately 30% of each litter was transgenic animals.

All experiments were performed in accordance with the Canadian Council on Animal Care guidelines (CCAC Guide to the Care and Use of Experimental Animals, Ottawa, ON; Vol. 1, 2nd edition, 1993; Vol. 2, 1984) and were approved by the Dalhousie University Committee on Animal Care. Animals were housed in the Dalhousie

University Animal Care facility and were kept on a 12 hour day night cycle. Food and water were freely available at all times.

Genotyping

Mice were genotyped to identify those mice that expressed the human β_2AR transgene. This process consisted of three phases: 1) Tissue collection and DNA isolation, 2) amplification of the DNA with the polymerase chain reaction; and 3) gel electrophoresis to visualize the transgene.

Tissue collection and DNA Isolation

The first step in the genotyping process was to acquire a sample of mouse tissue from which DNA could be isolated. Mouse tissue samples were taken from the ear with a 1 mm circular ear punch (Roboz Surgical Instrument Co., Inc., Gaithersburg, MD). Ear tissue was removed from the ear punch and placed in a 1.5 ml eppendorf tube. This tissue was stored in 90 µl ear punch digestion buffer (Table 1) at 4°C until the DNA could be isolated. The surgical ear punch was rinsed in either alcohol or DNA-Away (Molecular BioProducts, San Diego, CA) to solubilize any remaining DNA. Next, the ear punch was placed in a glass bead sterilizer (FST 250, Fine Science Tools, North Vancouver, BC) after each ear punch to destroy any contaminants and to decrease the risk of infection. The ear punch was then rinsed and cooled in sterile 0.9% saline (Abbott Laboratories, Montreal, QC) before the next ear punch was completed.

To digest the ear tissue, 10 µl of Proteinase K (Promega Corporation, Madison, WI) were added to the ear punch digestion buffer containing the tissue sample. The samples were vortexed and then placed in a dry bath incubator (Fisher Scientific, Nepean,

Table 1: Composition of ear punch digestion buffer.

Compound	Concentration (mM)
Tween-20	0.5%
Tris-HCl pH 8.0	11.1
EDTA (ethylenediaminetetraacetic acid)	5.5
NaCl	55.5

ON) for 5 to 8 hours to allow tissue digestion to occur. Samples were vortexed frequently during this time period to aid the digestion process. Once the tissue was digested, DNA was isolated from the ear tissue with a REDExtract-N-Amp Blood PCR Kit (XNAB, Sigma Chemical Co., St. Louis, MO). This kit contained "lyse buffer", "neutralize buffer" and Extract-N-Amp Blood PCR ready mix. To isolate the DNA, 10 µl of digested tissue was added to 20 µl of "lyse buffer" in a 0.5 ml eppendorf tube and vortexed. These samples were incubated at room temperature for 5 minutes before 180 µl of "neutralize buffer" was added to the mixture to stop lysis. The samples were vortexed one final time to complete the DNA isolation procedure. Isolated DNA was stored at 4°C until use.

Polymerase Chain Reaction Amplification

The polymerase chain reaction (PCR) was used to amplify both control mouse DNA sequence and the human β_2AR transgene. The PCR protocol used was a modified version of the protocol obtained from the Jackson laboratories website (www.jax.org/jaxmice/micetech). This protocol has two different reactions, each designed to amplify a specific DNA sequence. The first reaction, reaction A, was designed to amplify the 200 base pair (bp) DNA fragment from the mouse wild-type allele. Reaction B was designed to amplify the 1200 bp transgene encoding the human β_2AR transgene. Each reaction contained specific primers and the Extract-N-Amp Blood PCR ready mix (buffer, salts, dNTPs, *Taq* polymerase and loading dye). The reagents used for reactions A and B are found in Table 2 and Table 3 respectively. The primers used for reaction A (015 and 016) and reaction B (379 and 380) were purchased from

Table 2: Composition of PCR reaction A.

Compound	µl per tube
Extract-N-Amp Blood PCR ready mix	5.00
10 µM primer 015	0.25
10 µM primer 016	0.25
Distilled water	0.50

Table 3: Composition of PCR reaction B.

Compound	µl per tube
Extract-N-Amp Blood PCR ready mix	5.00
10 µM primer 379	0.50
10 µM primer 380	0.50
Distilled water	0.00

Sigma-Genosys (The Woodlands, TX) and their composition is described in Table 4. For each sample, it was necessary to determine if the mouse wild-type allele and/or the transgene was present. Therefore, two PCR tubes were prepared for each DNA sample. The first PCR tube was loaded with 6 µl of reaction A buffer and 4 µl of DNA and the second PCR tube was loaded with 6 µl of reaction B buffer and 4 µl of the same DNA sample. In addition, 6 µl of reaction A and B were each loaded with 4 µl of deionized water instead of DNA. This was done as a control, to determine if any DNA contamination had occurred. Since the water did not contain any DNA, there should be no DNA to amplify and therefore no visible bands on the gel. The PCR tubes were placed in a PCR Express Thermal Cycler (Hybaid Ltd., Ashford, Middlesex, UK). Identical PCR cycling conditions were used to amplify reactions A and B as shown in Table 5. Amplified DNA samples were kept at 4°C until used for gel electrophoresis.

Gel Electrophoresis

Amplified DNA samples containing loading dye were loaded on agarose gels for gel electrophoresis. This procedure was used to separate DNA fragments according to size. These experiments used 1.2% agarose gels with 0.5 mM tris borate EDTA (TBE) buffer (Table 6) and ethidium bromide. Gels were prepared and run in a mid-horizontal electrophoresis system (Model FB-SB-710, Fisher Scientific, Mississauga, ON). The gel chamber was filled with 0.5 M TBE buffer to cover the gel prior to loading the PCR amplicons. The first lane of each row was loaded with 3 µl of a 100 bp DNA ladder (MBI Fermentas; Burlington, ON). The DNA ladder was used to estimate the size of DNA fragments in subsequent lanes. All other lanes were loaded with 8 µl of the PCR

Table 4: Oligonucleotide sequences for PCR amplification of DNA from WT and TG4 mice.

Primer	BP Sequence
015	5'- CAA Atg TTg CTT gTC Tgg Tg –3'
016	5'- gTC AgT CgA CAC AgT TT –3'
379	5'- CTC CCC CAT AAg AgT TTg AgT Cg –3'
380	5'- gAg TAg CCA CAT TTC CCA TAg gCC TTC –3'

Table 5: Cycling conditions for reactions A and B for WT and TG4 DNA.

Step	Temperature	Time	Note
1	94°C	1.5 min	
2	94°C	30 sec	
3	60°C	30 sec	
4	72°C	2 min	Repeat steps 2-4, 20 cycles
5	94°C	30 sec	
6	60°C	30 sec*	*-0.5°C per cycle
7	72°C	2 min	Repeat steps 5-7, 17 cycles
8	72°C	2 min	
9	10°C	Holding Step	

Table 6: Composition of 0.5 M TBE buffer.

Compound	Concentration (mM)
TRISMA (tris hydroxylmethyl aminomethane) base	45
EDTA	1
Boric Acid	45
Ethidium Bromide	0.0025%

product from reactions A or B. Typically, PCR amplicons from reaction A were loaded in one row, while the corresponding PCR amplicons from reaction B were loaded in an adjacent row. An EC105 power supply (EC Apparatus Corporation) was used to produce electrical current to move the DNA molecules through the gel. At the negative electrode (bottom of the gel) the current repels DNA molecules, whereas the current at the positive electrode (top of the gel) attracts DNA molecules. This combination of electrical repulsion and attraction moves DNA molecules through the gel. For the purpose of these experiments, gels were run at 80 mV for approximately 1 hour or until the visible bands approached the edge of the gel. The gel was then removed from the electrophoresis system and placed in the compact darkroom of a Gel Doc EQ System (Bio-Rad Laboratories, Hercules, CA). A UV transilluminator (Bio-Rad Laboratories, Hercules, CA) was used to visualize the DNA bands. The gel was then photographed with a CCD camera and the Gel-Doc EQ system software (Bio-Rad Laboratories, Hercules, CA). A representative gel is illustrated in figure 2.

Ventricular Myocyte Isolation

Experiments were conducted on cardiac myocytes isolated from both male and female animals. The ages of these animals ranged from 3 to 26 months, depending, on the experiments being conducted. This is described in more detail in the results section.

Mouse body weight was measured to the nearest 0.01 g to determine the proper anesthetic dosage. Mice were then anesthetized with sodium pentobarbital (200-300 mg/kg, i.p.) 5 minutes prior to opening the chest cavity. The sodium pentobarbital was

Figure 2: Identification of mice carrying the human β_2 adrenergic receptor gene. Genotype was determined based on bands created on an agarose gel during gel electrophoresis. The location of the band is dependent on DNA fragment size, which can be determined by comparison with a DNA ladder. The human β_2AR gene was approximately 1200 bp. The internal mouse control band was approximately 200 bp. Of note, in several experiments reaction A and reaction B were combined in a single PCR tube. The PCR product could then be separated on an agarose gel to identify both the transgene and the internal mouse control gene.

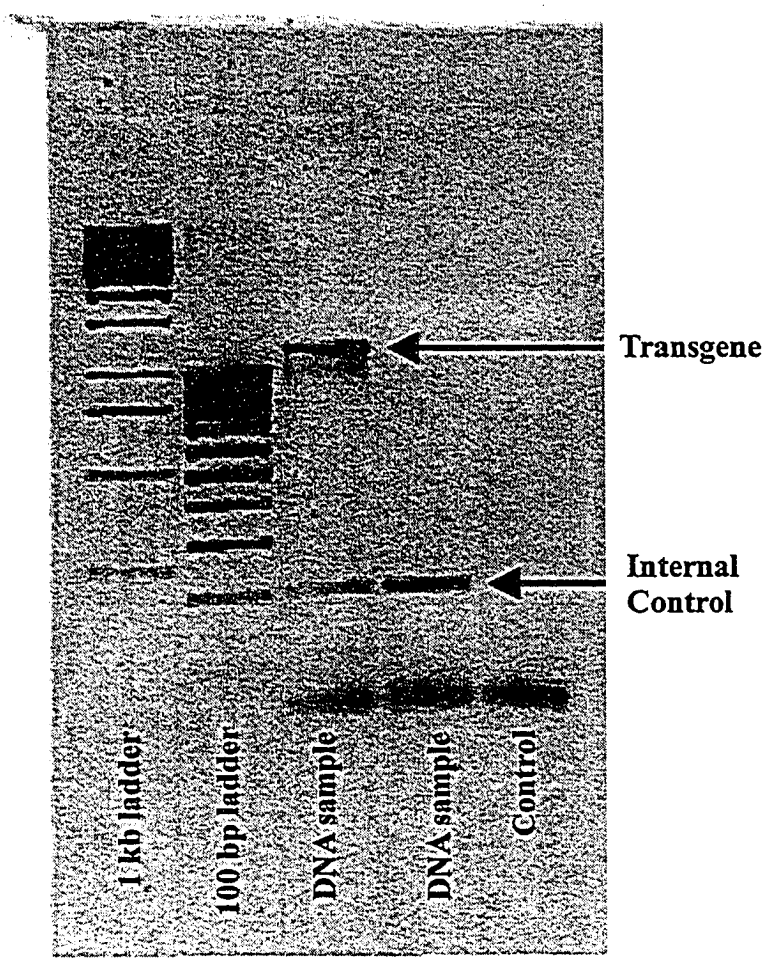
Transgene
Internal Control
1 kb ladder
100 bp ladder
DNA sample
DNA sample
Control

Figure 2

coinjected with heparin (100 U) to decrease blood coagulation. Prior to opening the chest cavity, animals were checked for responses to physical stimuli (pinching a paw and/or touching the eye) to ensure that the animals were well anesthetized. If the animals responded to the physical stimuli they were given an additional injection of sodium pentobarbital. Next, the soft tissue covering the thoracic cavity and the ventral portion of the rib cage were reflected to expose the heart. The aorta was then cut, cannulated *in situ* and immediately perfused retrogradely with oxygenated (100% O_2; Praxair Canada Inc.; 37°C) Ca^{2+}-free solution (Table 7). The heart was then removed from the chest cavity and the excess fat and tissue was trimmed. Hearts were perfused at a rate of 2 ml/min with a peristaltic pump (Cole-Parmer Instruments Co., Chicago IL). The temperature of the perfusate was maintained at 37°C with a circulating water bath (Haake Model L, Fisher Scientific, Berlin, Germany). The heart was then perfused for an additional 10 minutes with Ca^{2+} free solution containing collagenase (24 mg/30 ml, 244 U/mg, Worthington), dispase II (0.33 mg/30 ml, Boehringer-Mannheim) and trypsin (1 mg/30 ml, Sigma) supplemented with 50 μM Ca^{2+}.

Perfusion pressure was monitored with a pressure gauge (Dresser Measurement, Mississauga, ON). A drop in perfusion pressure to negligible levels (near 0 psi) typically occurred after approximately 8 to 10 minutes. At this time perfusion was terminated. The ventricles were minced in a high K^+ buffer (Table 8). The cells were then allowed to settle to the bottom of the dish and the high K^+ buffer was removed and was replaced with fresh high K^+ buffer. This process was then repeated a second time to remove cellular debris and the enzymes used to digest the tissue.

Table 7: Composition of Ca^{2+}-free myocyte isolation solution.

Compound	Concentration (mM)
NaCl	130
KCl	5
HEPES	25
NaH_2PO_4	0.33
$MgCl_2$	1
Glucose	20
Na-pyruvate	3
Lactic acid	1

pH 7.4 with NaOH

Table 8: High K^+ buffer solution for storage of ventricular myocytes.

Compound	Concentration (mM)
KOH	90
Glutamic acid	50
KCl	30
KH_2PO_4	30
Taurine	20
HEPES	10
Glucose	10
$MgSO_4$	3
EGTA	0.5

pH 7.4 with KOH

In some experiments weights of the ventricles and the lungs were obtained. Wet ventricle weight was measured by cutting the ventricles into a small beaker containing high K^+ buffer. The beaker containing the ventricles was weighed and weight was recorded to the nearest 0.0001 g. After the heart was removed from the chest cavity the lung tissue was removed, placed on a piece of sterile gauze and transferred to a small weigh boat. The wet lung tissue was then weighed and the weight was recorded to the nearest 0.0001 g. The weigh boat containing the lung tissue was then placed in a sealed container and the lung tissue was allowed to dry for 60 days at room temperature. The tissue was then removed from the container and weighed to obtain dry lung weight. Dry lung weight was recorded to the nearest 0.0001 g. Lung fluid was calculated by subtracting dry lung weight from wet lung weight.

Experimental Setup

Isolated myocytes were placed in a 0.75 ml chamber on the stage of an inverted microscope (Model INT-2, Olympus Optical Co., Ltd., Tokoyo Japan or Nikon Eclipse TE 200, Nikon Canada Inc., Mississauga, ON). The experimental chamber (Figure 3) was custom made from plexiglass and a glass coverslip was used for the bottom of the chamber. The chamber had both inflow and outflow channels to maintain a constant flow of extracellular solution. The temperature of the superfusion solution was maintained at 37°C with a circulating water system. The water was circulated with an immersion-circulating pump and heater (Polystat Immersion Circulator, Cole-Parmer Instrument Company, Vernon Hills, IL). The cells were allowed to adhere to the bottom of the chamber for 15 to 20 minutes before initiating superfusion with buffer solution. Cells

Figure 3: Experimental setup.

Isolated myocytes were placed in an experimental chamber, as shown, and continuously superfused with extracellular solution. The myocyte in the figure has been impaled with a high-resistance microelectrode. The electrode was mounted in an electrode holder which was inserted into the headstage (A1). The circuit was grounded with a silver, silver chlorided wire. The silver chloride wire was placed in a well of KCl. The well was connected to the experimental chamber with an agar bridge. In single-electrode voltage clamp experiments, membrane voltage (V_M) was measured and compared to command voltage (V_{cmd}) with an amplifier (A2). When V_M differed from V_{cmd}, current was injected into the cell until V_M returned to V_{cmd}.

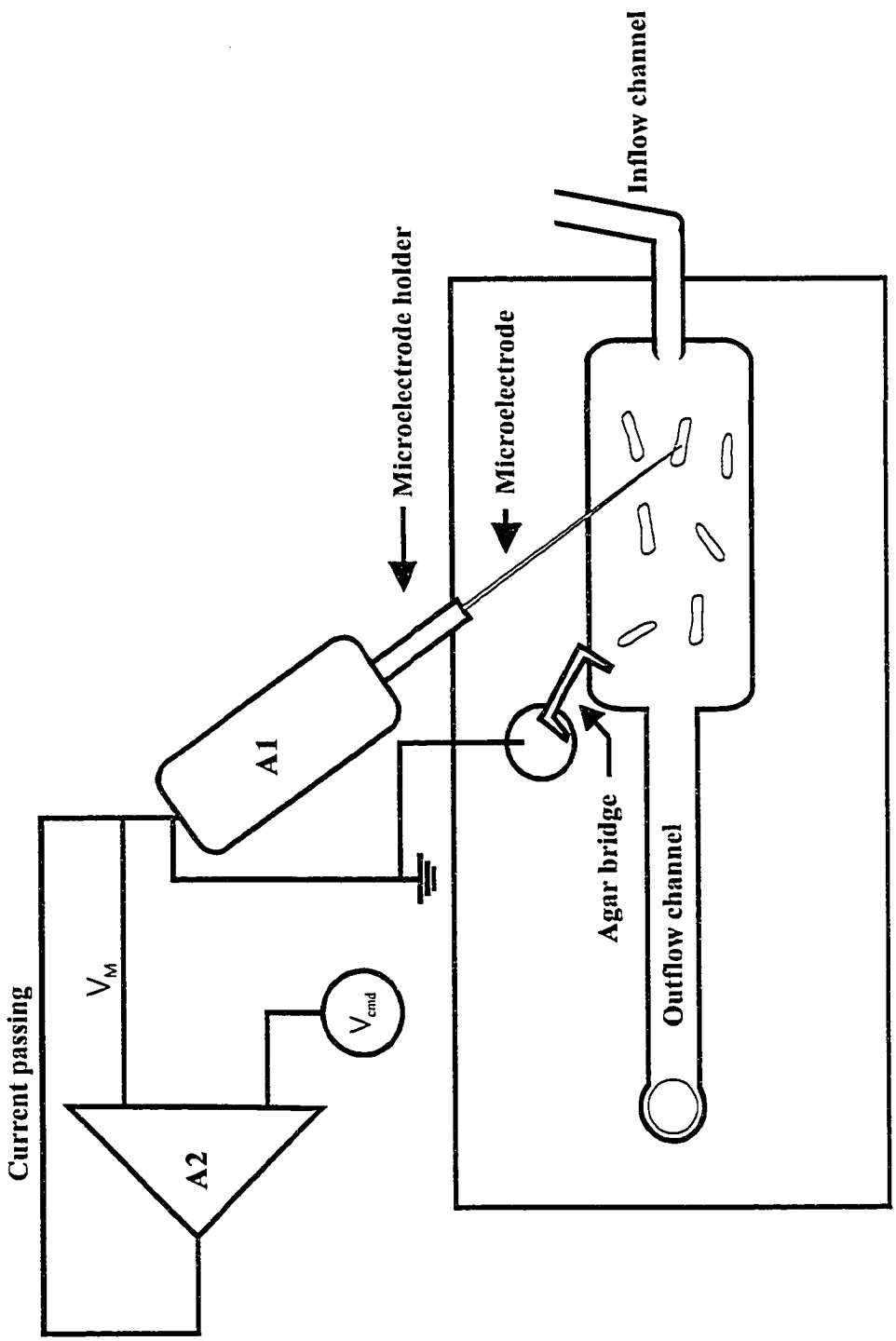
Inflow channel
Microelectrode holder
Microelectrode
A1
Agar bridge
Outflow channel
Current passing
V_M
V_{cmd}
A2

Figure 3

were superfused at approximately 3 ml/min with a buffer solution that was delivered by either gravity feed or by a peristaltic pump (Gilson Model M312, Villiers, France). Cells were superfused with either HEPES-buffered solution (Table 9) or a Tyrode's buffer (Table 10). In all voltage clamp experiments, HEPES-buffered solution was supplemented with 4 mM 4-aminopyridine to block transient outward current and 0.3 mM lidocaine to inward Na^+ current. In some experiments HEPES-buffered solution was supplemented $5x10^{-7}$ M ICI 118, 551 (ICI), a β_2AR inverse agonist. ICI has a high affinity for the inactive receptor, which decreases the number of spontaneously active receptors (Bond et al., 1995). Only those cells that were rod shaped and had clear, visible striations and intact membranes were used in experiments.

Experimental Procedures

Voltage-Clamp Measurements

In most experiments, cells were voltage clamped to examine contractions and Ca^{2+} current simultaneously. In some voltage-clamp experiments Ca^{2+} transients were measured in conjunction with contraction and current. Cells were impaled with high-resistance microelectrodes (16-26 mΩ) to minimize cell dialysis and to prevent buffering of intracellular Ca^{2+}. Microelectrodes were made from borosilicate glass tubes (Sutter Instruments Co., Novato, CA). Microelectrodes had outer and inner diameters of 1.2 mm and 0.69 mm, respectively. New electrodes were made on each experimental day with a Flaming/Brown micropipette puller (Model P-87, Sutter Instruments Co., Novato, CA). Electrodes were filled with 2.7 M filtered KCl. A drop of KCl was placed in the blunt

Table 9: Composition of HEPES-buffered solution.

Compound	Concentration (mM)
NaCl	145
KCl	4
$MgCl_2$	1
HEPES	10
Glucose	10
$CaCl_2$	1
pH 7.4 with NaOH	

Table 10: Composition of Tyrode's Solution

Compound	Concentration (mM)
NaOH	129
KCl	5.4
NaH_2PO_4	0.9
$NaHCO_3$	20
Glucose	5.5
$MgSO_4$	0.5
$CaCl_2$	1
Bubbled with	95% O_2/ 5% CO_2
pH 7.4	

end of the electrode with a 30 gauge needle and the tapered end was allowed to fill by capillary action. Once the tip had filled, the remainder of the electrode was filled with KCl. The electrode was then inserted into a microelectrode holder. Two types of microelectrode holders were used during the course of experiments. One electrode holder had a silver, silver-chloride pellet (World Precision Instruments, Inc., Sarasota, FL) and was filled with 2.7 M KCl. The second electrode holder (Model HL-U, Axon Instruments, Union City, CA) contained a silver, silver chloride wire located in the center of the holder and was not filled with KCl. The tip of the sliver wire was chlorided with chloride bleach prior to use, to coat the electrode with silver and silver chloride. Electrode holders were inserted into the pin jack in the headstage of a microelectrode amplifier (Axoclamp 2A and Axoclamp 2B, Axon Instruments, Union City, CA). The headstage was connected to the main amplifier and provided the first stage of amplification. The headstage was mounted on a micromanipulator (Leitz Inc., Wetzlar, Germany) which allowed the microelectrode to be accurately positioned within the experimental chamber.

Next, the tip of the microelectrode was placed in solution in the experimental chamber and lowered to a position just above the cell. The junction potentials in the circuit were then zeroed with the input offset dial on the Axoclamp amplifier. The resistance of the electrode was then determined by passing 1 nA of current. According to Ohm's Law, voltage is equal to the product of current multiplied by resistance (V=IR). Therefore, an 18 mV potential was equivalent to a microelectrode resistance of 18 mΩ. The bridge balance was adjusted to equal the resistance of the electrode, to cancel the voltage drop across the electrode. This ensured that the voltage recorded represented the

potential difference across the membrane of the myocyte being studied. It was also necessary to optimize the electrode capacitance to ensure the amplifier could accurately control membrane voltage. This was done by placing the amplifier in discontinuous current clamp mode and injecting a 1 nA current through the microelectrode. The switching rate between current injection and membrane potential recording was set to approximately 5-8 kHz. The monitor waveform was observed on an oscilloscope (Kikusui Model COR5541U, Kikusui Electronic Corp., Japan) and was then optimized with the capacitance neutralization dial on the amplifier.

The recording circuit was grounded with a silver wire. Prior to use, the wire was chlorided with chloride bleach to coat the wire with silver and silver chloride. The silver chloride wire was placed in a well of 2.7 M KCl. This well was connected to the experimental chamber by means of an agar bridge. The agar bridge was a U-shaped piece of glass tubing that had been filled with a 1% agar solution in 2.7 M KCl. The agar limited the movement of small ions and thus minimized junction potentials when the extracellular solution was changed. Once the steps outlined above were completed, the amplifier was placed in bridge mode. The micromanipulator was used to lower the electrode until it penetrated the cell membrane. This was observed as a drop in membrane potential on the amplifier.

Many experiments conducted in this thesis used a technique called voltage clamp. In voltage clamp, membrane potential is measured and held constant at a specified potential by injecting current across the cell membrane with a voltage clamp amplifier. This technique can be used to investigate the processes affecting membrane conductance. These studies used a technique called discontinuous single electrode voltage clamp (dSEVC) to measure current in ventricular myocytes. In dSEVC mode, the

microelectrode is used to both measure changes in cell voltage and to inject current. Time-sharing techniques are used to prevent interaction between these two tasks. The amplifier controls membrane voltage by rapidly switching (5-8 kHz) between voltage recording and current injection modes. In dSEVC a sample-and-hold circuit samples membrane potential and holds that for the rest of the cycle. In current injection mode, when the amplifier detects a difference between measured voltage and command voltage, a current is applied to the cell that is proportional to the difference in voltage. As a result, the membrane voltage is clamped at the command voltage. After current injection, the amplifier switches to the voltage-recording mode and the current output from the amplifier is zero. The voltage recorded during this period decays passively towards the membrane potential. Thus, sufficient time must be allowed before a new sample of membrane potential can be taken. At the end of the voltage-recording period, a new membrane potential sample is taken and a new cycle begins. The output of the switching circuit was monitored on an oscilloscope throughout all experiments to monitor voltage-clamp quality.

Impaled myocytes were voltage clamped at a holding potential of –80 mV. Voltage clamp experiments were then conducted. Voltage protocols consisted of a series of conditioning pulses followed by activation steps to test potentials. The conditioning pulses were used to provide a consistent history of regular activity. The number, duration and frequency of the conditioning pulses used in these experiments was varied. These parameters are described in the appropriate results sections. The last conditioning pulse and the activation steps were separated by a step to a post conditioning potential (V_{PC}), as described in the results section. Details for the activation steps also are provided in the appropriate sections of the results. All experiments were conducted at 37°C.

All measures of current and voltage were initially acquired as analog signals. These signals were then converted to digital signals with a Labmaster A/D interface (TL1-125, Axon Instruments Inc.). After the analog-to-digital conversion, the signals were stored on a computer for later analysis.

Measurements of Intracellular Calcium Concentration

Intracellular Ca^{2+} concentrations were measured by whole cell photometry with the Ca^{2+}-sensitive fluorescent dye, fura-2. Fura-2 has several properties that make it useful for estimating $[Ca^{2+}]_i$. First, fura-2 is a ratiometric Ca^{2+} chelator that absorbs light differently when bound to Ca^{2+}. In the unbound form, fura-2 absorbs light maximally at approximately 380 nm. In contrast, when fura-2 is bound to Ca^{2+}, it absorbs light maximally at approximately 340 nm (Grynkiewicz et al., 1985). However, in both states the dye emits light at 510 nm. As fura-2 can be excited at both 340 nm and 380 nm, but only emits light at 510 nm it is considered a dual excitation, single emission dye. The ratio of the emission at each excitation wavelength (E_{340}/E_{380}) can be used to calculate the concentration of intracellular calcium ($[Ca^{2+}]_i$). One advantage of fura-2 is that alterations associated with unequal loading and photobleaching will affect light absorption at both 340 nm and 380 nm. Thus, changes such as photobleaching will not alter the E_{340}/E_{380} ratio. The acetoxymethyl (AM) ester of fura-2 was used to load cells since it passively diffuses across the cell membrane. In the cytosol, the ester group is removed by intracellular esterases, which traps fura-2 in the cell. This helps to maintain a high intracellular concentration of fura-2. In addition, fura-2 is unable to enter the SR (Sipido et al., 1995) and thus primarily reflects the cytosolic Ca^{2+} concentration. This makes fura-2 an excellent tool with which to measure Ca^{2+} transients.

Approximately 1 ml of murine ventricular myocytes was decanted from the high potassium storage solution into a 1.5 ml eppendorf tube. Cells were loaded with fura-2 AM (5 μM) and gently agitated. The cells were incubated in the dark for 15 minutes and then placed in the experimental chamber mounted on the stage of a Nikon Eclipse fluorescence microscope (Model TEG220, Mississauga, ON). Cells were allowed to adhere to the bottom of the chamber for 20 minutes in the dark. Then cells were superfused with a HEPES-buffered solution to remove any fura-2 not taken up by the cells.

Fluorescence experiments were conducted with a system for whole cell photometry from Photon Technology International (PTI, Brunswick, NJ). The main components of the photometry system are a PTI DeltaRam high-speed multiwavelength illuminator and a photometer (Model D-104, PTI, Brunswick, NJ). A xenon arc lamp located in the arc lamp housing of the illuminator is powered by the LPS-220 lamp power supply. This lamp produces the UV light required to excite the cells. The light passes through a bandpass filter that controls light intensity. Adjusting the slit width can change the bandpass. Therefore, light intensity can be increased or decreased by increasing or decreasing the slit width. The light from the illuminator is collected by a quartz fiber optic cable which transmits the light from the illuminator to the microscope. Collected photons pass through a variable aperture in the photometer. The amount of fluorescent light being collected can be adjusted with the variable aperture in the photometer. The size of the aperture was adjusted so the myocyte of interest filled the field of view. Myocytes were alternately excited at 340 nm and 380 nm and the emission at each wavelength was measured at 510 nm. The emitted light was collected by an oil

emmersion objective (40X Nikon, numerical aperture 1.3) and passed through a dichroic cube in the microscope. This cube split the light so that 80% was directed to the D-104 microscope photometer (PTI). The light was then detected by the Analog Photomultiplier Detection System (Model 814, PTI). The analog signal was then transmitted to a computer for visualization and storage via a computer interface (PTI). The other 20% of the light was directed to a closed circuit television camera used to measure unloaded cell shortening. The dichroic cube allows Ca^{2+} transients and cell shortening to be measured simultaneously.

The photometry system was calibrated for fura-2 experiments so that fluorescence ratios could be converted to Ca^{2+} concentrations. This was done with cell impermeant fura-2 and known concentrations of free Ca^{2+}. A 1.2 mM stock solution of cell impermeant fura-2 was made in deionized water. This stock was used to make the CaEGTA buffer (Table 11) and the EGTA buffer (Table 12). Each buffer was supplemented with 1 μM fura-2 and used to conduct a fura-2 titration. First, EGTA buffer was placed in the experimental chamber with no CaEGTA. An excitation scan was performed and saved. Next, a set volume of EGTA buffer was removed from the experimental chamber and replaced with an equal volume of CaEGTA buffer. This process of removing a set volume of solution from the experimental chamber and replacing it with an equal volume of CaEGTA was performed eight more times until the free Ca^{2+} concentration in the chamber was great enough to saturate fura-2. An excitation scan was performed after each serial exchange. The excitation scans for each concentration of Ca^{2+} were then analyzed. The peak fluorescence at 340 nm and 380 nm was measured for each scan. The ratio was then calculated by dividing E_{340} by E_{380}. Ca^{2+}

Table 11: Composition of CaEGTA buffer for Fura-2 Ca^{2+} measurement calibration.

Reagent	Concentration (mM)
KCl	100
EGTA	10
K-MOPS	10
$CaCl_2$	10
	pH 7.0

Table 12: Composition of EGTA buffer for Fura-2 Ca^{2+} measurement calibration.

Reagent	Concentration (mM)
KCl	100
EGTA	10
K-MOPS	10
	pH 7.0

concentrations and corresponding ratios were then entered into a lookup table and saved. This lookup table was used to convert fluorescence ratios to Ca^{2+} concentrations. A calibration curve prepared by plotting the E_{340}/E_{380} emission ratio as a function of Ca^{2+} concentration is shown in Figure 4.

Measurement of SR Ca^{2+} Stores

Caffeine has been shown activate SR Ca^{2+} release channels and cause the release of SR Ca^{2+} (Weber & Herz, 1968). Therefore, caffeine-induced Ca^{2+} transients were used to estimate of SR Ca^{2+} content. The following protocol was used to assess SR Ca^{2+} stores. Cells were activated repetitively by a series of conditioning pulses from –80 to 0 mV and then cells were repolarized to –60 mV. Caffeine was applied with a rapid solution switcher for 1 second, 500 milliseconds after repolarization to –60 mV. The rapid switcher is a computer controlled device that allows complete change of the solution surrounding the myocyte in less than 0.5 seconds while maintaining a solution temeperature of 37°C (Hobai et al., 1997). The caffeine solution used for these experiments contained zero Na^+ and zero Ca^{2+}, as described in Table 13. To balance the ions in the solution, NaCl was replaced with LiCl. Both Na^+ and Ca^{2+} were removed from the solution to prevent the loss of intracellular $[Ca^{2+}]_i$ through the Na^+/Ca^{2+} exchanger.

Measurement of Unloaded Cell Shortening

In field-stimulation and voltage-clamp experiments, cells were photographed with a closed-circuit television camera (Pulnix America, Model TM-640) and cell images were

Figure 4: Calibration curve for calculating intracellular Ca^{2+} concentration from E_{340}/E_{380} ratio.

A calibration curve was constructed by measuring E_{340}/E_{380} over a range of Ca^{2+} concentrations at pH 7.2. The Ca^{2+} solutions contained cell-impermeant fura-2. The curve shown is the average of two calibration experiments. This curve was used to convert E_{340}/E_{380} values to Ca^{2+} concentrations.

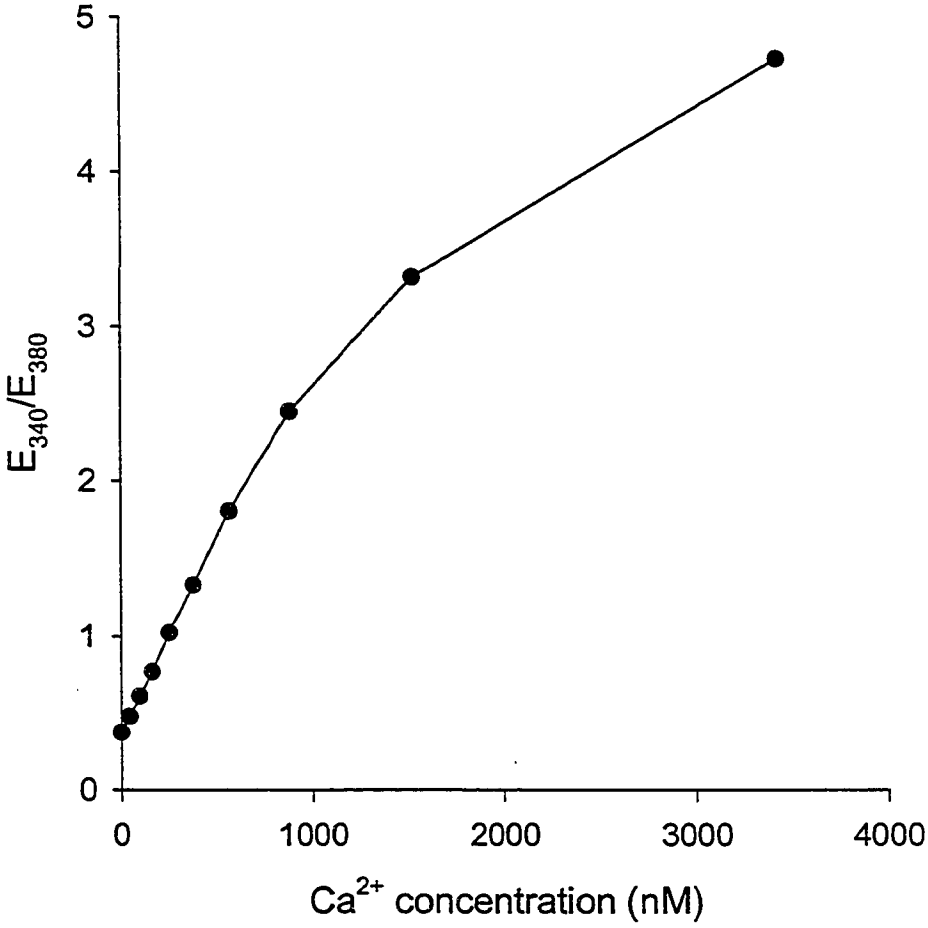

Figure 4

Table 13: Caffeine Solution Composition

Compound	Concentration (mM)
Caffeine	10
LiCl	140
KCl	4
Glucose	10
HEPES	5
$MgCl_2$	4
4-aminopyridine	2.5
Lidocaine	0.25

pH 7.4 with LiOH

displayed on a video monitor (Model OVM-12E12, Oriental Precision Co Ltd., Sung Nam City, Korea). Unloaded cell shortening was measured with a video edge detector (Model VED 103, Crescent Electronics, Sandy, UT) which sampled at 120 Hz. The analog contraction signal from the video edge detector was displayed on an oscilloscope (Kikusui Model COR5541U, Kikusui Electronic Corp., Japan) and was digitized with a Labmaster A/D interface so that it could be recorded on computer. In some experiments, the video edge detector tracked the movement of a single edge. In other experiments, the movement of both edges of the myocyte was tracked to allow the measurement of changes in cell length.

Field Stimulation

In several sets of experiments, field stimulation was used to initiate contractions in ventricular myocytes. Cells were stimulated with a pair of parallel platinum wires set approximately 1.5 cm apart. These wires were placed on the bottom of the experimental chamber and were connected to a Grass stimulator (Model 5D9B, Grass Medical Instruments, Quincy MA). The stimulator produced 100 V electrical pulses that were 3 ms in duration. These pulses resulted in the formation of an electrical field between the platinum wires. This electrical field triggered action potentials in myocytes located between the wires and activated contractions. Cells were stimulated at frequencies between 2 and 10 Hz. These contractions were recorded with a video edge detector as previously described.

Data Analysis

L-type Ca^{2+} current ($I_{Ca\text{-}L}$) was measured as the difference between peak inward current and a reference point at the end of the voltage step. $I_{Ca\text{-}L}$ was measured in nA. The Ca^{2+} channel blocker Cd^{2+} was used to validate measures of $I_{Ca\text{-}L}$. In these experiments, Cd^{2+} was applied with the rapid switcher for 3 seconds after the conditioning pulse train and during the test step (Figure 5-A). Test steps were made from –40 mV to 0 mV to activate transmembrane current. Current which remained in the presence of Cd^{2+} (Figure 5-C) was subtracted from the current recorded in the absence of Cd^{2+} (Figure 5-B) to obtain the Cd^{2+}-sensitive Ca^{2+} current (Figure 5-D). Next, mean peak Cd^{2+}-sensitive current was compared to mean peak Ca^{2+} current measured as the difference between peak inward current and a reference point at the end of the voltage step. There was no significant difference in the magnitudes of the Cd^{2+}-sensitive current and the peak Ca^{2+} current (Figure 6). Thus, measurement of the difference between peak inward current and a reference point at the end of the voltage step is a valid method for measuring the amplitude of $I_{Ca\text{-}L}$.

It is possible that ventricular myocytes differ in size between experimental and control animals. Thus, amplitudes of peak L-type Ca^{2+} current were normalized to cell membrane area to allow for accurate comparison between different experimental groups. Cell membrane area was estimated by measuring cell capacitance. Cell capacitance was estimated by integrating the area under the capacitive transient produced by a voltage step from –40 mV to –30 mV. Integration was accomplished with pClamp software (Calmpfit 8.1). Normalized L-type Ca^{2+} current is expressed as current density and represents the amount of L-type Ca^{2+} current (pA) per unit of membrane area (pF).

Figure 5: Measurements of $I_{Ca\text{-}L}$ reflect the Cd^{2+}-sensitive current in mouse ventricular myocytes.

A) Voltage-clamped cells were stimulated with a train of conditioning pulses delivered at 2 Hz prior to the test steps. Cells were held at a postconditioning potential of –65 mV. A step from –65 to –40 mV was used to inactivate Na^+ current and a step from –40 to 0 mV was used to activate inward current. Panel (B) illustrates a representative example of $I_{Ca\text{-}L}$ in a mouse ventricular myocyte. Panel (C) shows a representative example of a current recording in the presence of 100 μM Cd^{2+}. Cd^{2+} -sensitive current (C) was calculated by subtracting the current in the presence of Cd^{2+} from the current in the absence of Cd^{2+}. The Cd^{2+} sensitive current and $I_{Ca\text{-}L}$ appeared similar in mouse ventricular myocytes.

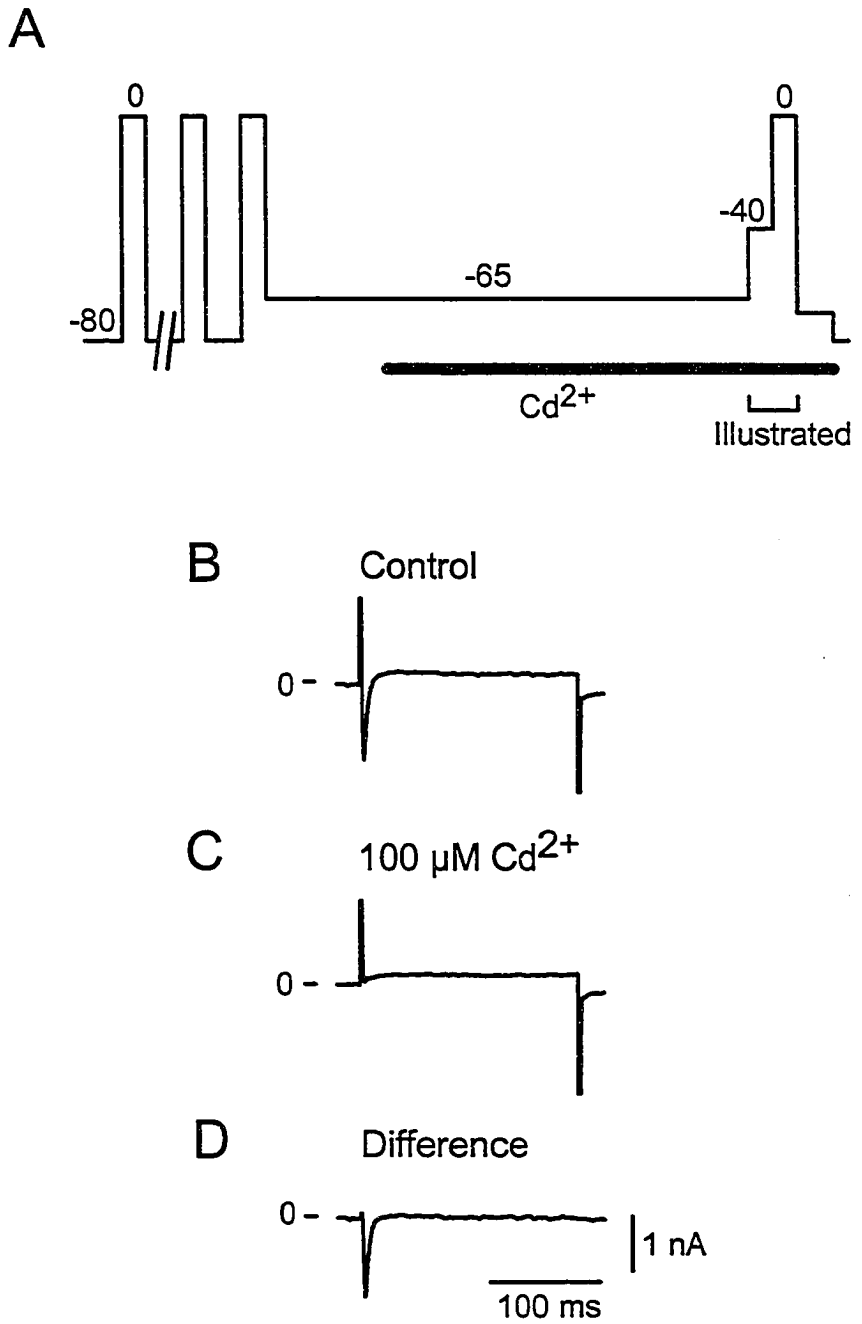
A
0
0
-40
-65
-80
Cd2+
Illustrated
B
Control
0
C
100 µM Cd2+
0
D
Difference
0
1 nA
100 ms

Figure 5

Figure 6: Mean peak Cd^{2+}-sensitive current was similar to mean peak $I_{Ca\text{-}L}$ measured as the difference between peak inward current and a reference point at the end of the voltage step.

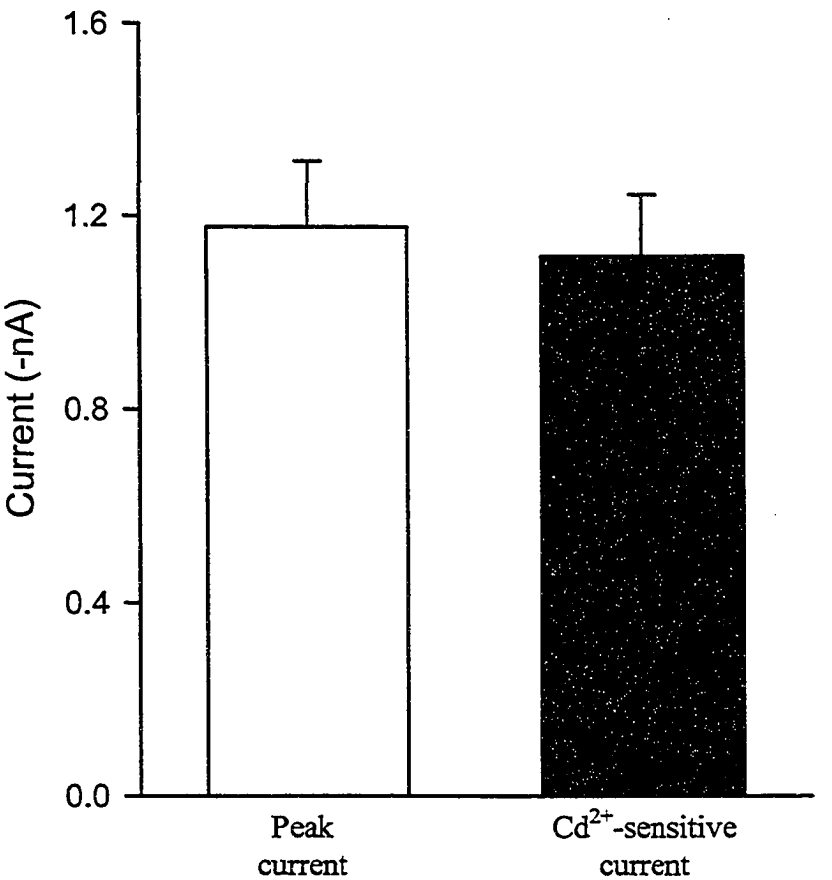

Figure 6

In some experiments the rate of $I_{Ca\text{-}L}$ inactivation also was calculated. Clampfit 8.1 (Axon Instruments, Union City, CA) was used to measure the inactivation of $I_{Ca\text{-}L}$. A single exponential function was fitted to the decay phase of the current recordings to calculate the time constant (tau) for $I_{Ca\text{-}L}$ inactivation. Tau represents the rate of $I_{Ca\text{-}L}$ inactivation.

In field-stimulation experiments, both edges of the cell were tracked. Accordingly, both diastolic and systolic cell length were measured. Peak cell shortening was calculated as the difference between systolic and diastolic length. In voltage clamp experiments, only one edge of the cell was tracked. Therefore, the period immediately preceding the onset of contraction served as the baseline for contraction measurements. Peak cell shortening was measured with respect to this baseline. Since maximum contraction amplitude could be affected by cell length, contractions were normalized to corresponding cell length and expressed as percent cell shortening. Time-to-peak contraction was measured as the time between initiation of contraction and maximal cell shortening. Time-to-half relaxation was measured as the time required for contraction amplitude to decrease by 50% of maximum.

Depolarization- and caffeine-induced Ca^{2+} transients were analyzed with Felix software (version 1.4, PTI). E_{340}/E_{380} fluorescence ratios were converted to Ca^{2+} concentrations with an *in vitro* calibration curve as described earlier (Figure 4). Both diastolic and systolic $[Ca^{2+}]_i$ were measured and Ca^{2+} transients were calculated as the difference between systolic and diastolic $[Ca^{2+}]_i$. Caffeine-induced Ca^{2+} transients were calculated with the same method, except that diastolic $[Ca^{2+}]_i$ was measured immediately prior to caffeine application.

Assessment of Physical and Behavioral Phenotype

In experiments on young and aging mice, physical and behavioral characteristics of the mice were assessed. The physical characteristics examined were palpebral (eyelid) position, overall degree of grooming and body posture. The behavioral characteristic examined was general locomotor activity.

Physical characteristic and behavioral assessment was conducted in the morning prior to the ventricular myocyte isolation procedure. The mouse was removed from its home cage and placed in a clean cage. This cage was taken back to the laboratory and placed in a quiet area. After 30 minutes, the physical characteristics of the mouse were scored. Palpebral condition was scored as either 1) wide/open or 2) flattened, swollen, squinty. Mice were then characterized as groomed or ungroomed. A mouse was considered groomed if the fur appeared smooth and clean, whereas the mouse was characterized as ungroomed if the fur appeared erected, scruffy and/or had patches of missing fur. Any wounds to the body, ears and/or tail also were noted at this time. Body posture was scored as 1) elongated (straight spine) or 2) closed (hunched or rounded spine). After the physical characteristics had been recorded, the locomotor activity of the mouse was assessed. The mouse was removed from the cage and placed in a clean 2 L beaker. The number of times the mouse touched the side of the beaker or jumped was recorded over a 2 minute period. Any time the mouse placed either one or both front paws on the side of the beaker was classified a touch. Of note, all four paws had to return to the bottom of the beaker prior to scoring another touch.

Statistical Analysis

Data are presented as means plus or minus the standard error of the mean (SEM). Differences between means were tested with either paired or unpaired t-tests. Differences between contraction-voltage and current-voltage relationships were analyzed with a two-way repeated measures analysis of variance (ANOVA). Behavioural data from young and aged mice were analyzed with a χ^2-test. Differences were considered significant when $p \leq 0.05$. All analyses were performed with SigmaStat 2.03 (Jandel) or SAS (SAS Canada, Toronto, ON). The value of "n" represents the number of myocytes sampled for each experiment. No more than 3 cells from one heart were included in any one data set.

Drugs and Chemicals

Lidocaine, EGTA, $MgCl_2$, HEPES buffer, 4-aminopyridine, ICI-118 551, and anhydrous DMSO were purchased from Sigma-Aldrich Canada (Oakville, ON). Caffeine was purchased from the Sigma Chemical Company (St. Louis, MO). All other chemicals for buffer solutions were purchased from BDH Inc. (Toronto, ON). Fura-2 AM and cell impermeant fura-2 were purchased from Molecular Probes (Eugene, OR). Proteinase K was purchased from Promega Corporation (Madison, WI). All drugs were dissolved in distilled water except fura-2 AM. A stock solution of fura-2 AM was created by dissolving 50 μg of fura-2 AM in 20 μl anhydrous DMSO.

RESULTS

1. Alterations in EC coupling in aged ventricular myocytes

Studies of the effects of aging on cardiac contraction have shown contractile function is impaired in aging, at least when cells are stimulated at rapid rates (Lakatta & Sollot, 2002). One explanation for a decrease in cardiac contraction in aging is that the magnitude of the trigger for contraction, $I_{Ca\text{-}L}$, is reduced in aging. However, it is not clear whether $I_{Ca\text{-}L}$ is altered in aging, as studies have reported that the magnitude of $I_{Ca\text{-}L}$ is either unchanged (Walker et al., 1993), increased (Dibb et al., 2004) or decreased (Isenberg et al., 2003; Liu et al., 2000) in aged ventricular myocytes. Furthermore, contraction and $I_{Ca\text{-}L}$ have been studied in separate cells under different experimental conditions. Thus, the relationship between $I_{Ca\text{-}L}$ and contraction has not been investigated in the aged myocyte. A major objective of this thesis was to evaluate $I_{Ca\text{-}L}$ and contraction in same cell to determine whether the relationship between $I_{Ca\text{-}L}$ and contraction was altered with advancing age.

The experiments described below compared components of EC coupling in ventricular myocytes from young adult and aged mice. However, in initial experiments physical and behavioral characteristics of young and aged mice were determined and compared to evaluate whether these characteristics differed between young adult and aged mice.

Mouse Characteristics

Several studies have shown that physical characteristics and behavioral patterns change with advancing age (de Boer et al., 2002; Shore, 1985; Trifunovic et al., 2004).

For example, physical activity is known to decrease with age, whereas body weight is known to increase (Ingram, 2000; Tou & Wade, 2002). Therefore, physical and behavioral characteristics of young adult and aged mice were compared to determine if these parameters were altered in aging. Age and body weight data were collected for all the young adult and aged mice used in the experiments discussed in section 1. Figure 7 shows that mean age (panel A) and mean body weight (panel B) were significantly greater in the aged mice compared to young adult mice. Next, observational studies were conducted to determine whether there were any physical and/or behavioral differences between young adult and aged mice. Figure 8 shows selected physical and behavioral characteristics in young adult and aged mice. Figure 8-A shows the incidence of palprebral closure was significantly greater in aged mice compared to young adult mice. In addition, approximately 50% of aged mice were classified as ungroomed, compared to 0% of young adult mice (Figure 8-B). Furthermore, approximately 30% of aged mice exhibited a closed (hunched) posture, whereas this posture was not observed in any of the young adult mice (Figure 8-C). The next set of experiments examined the effects of aging on physical activity. Young adult and aged mice were placed in a novel environment and the number of times the animal touched the side of the cage was recorded over a 2 minute period. Figure 8-D shows that the mean number of paw touches was not significantly different between young adult and aged mice. Thus, despite changes in physical appearance, activity levels were similar in young adult and aged animals. The next series of experiments was conducted to determine whether there was evidence of cardiac hypertrophy and/or pulmonary edema in aging mice. Ventricles from the hearts of young adult and aged mice were compared to determine if ventricular

Figure 7: Body weight was significantly increased in aged mice.

A) Aged mice were significantly older than young adult mice. **B)** Mean body weight was significantly greater in aged mice compared to young adult mice.

* Significantly different from young adult (n = 22 young adult mice and 21 aged mice).

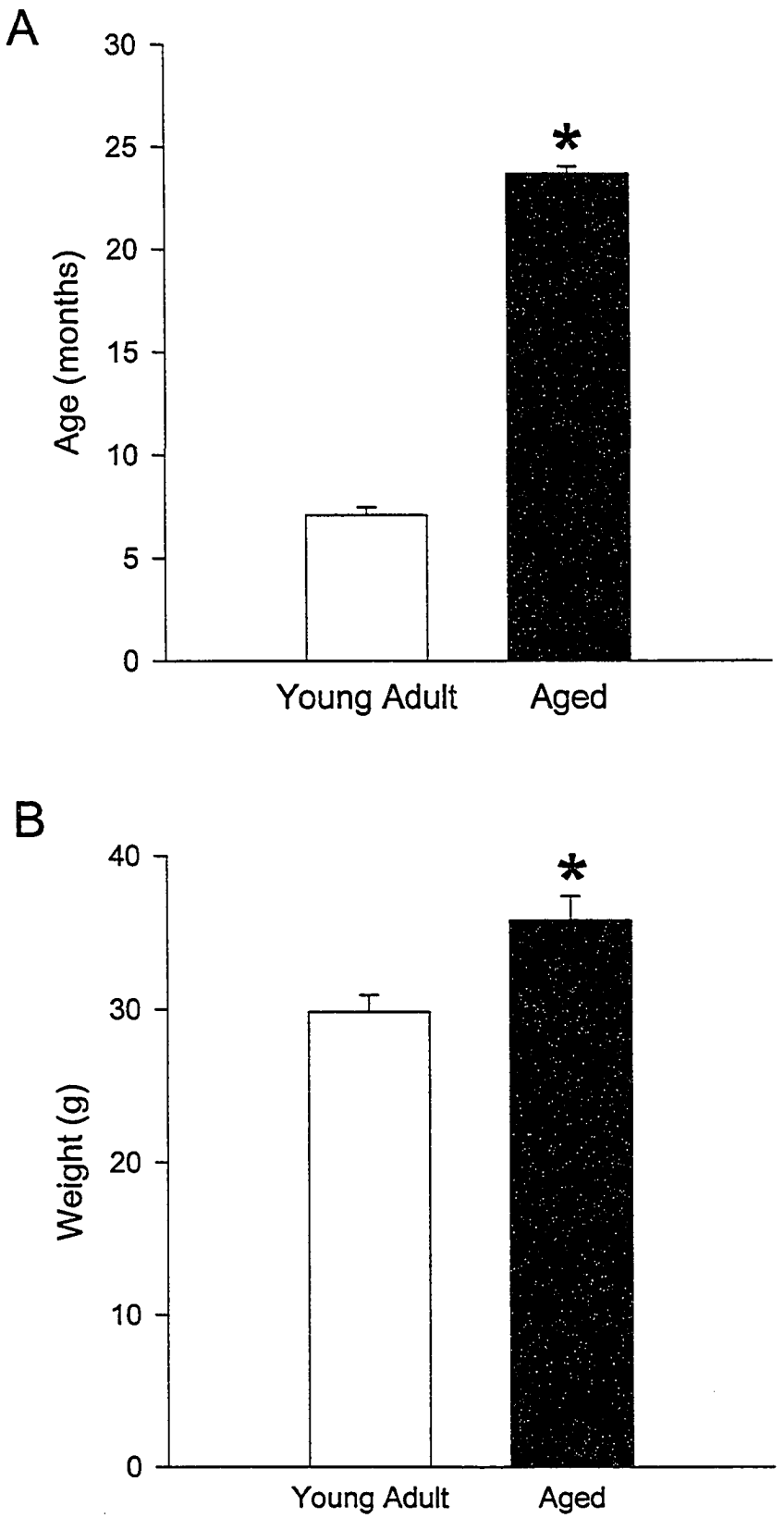
A
30
25
20
15
10
5
0
Age (months)
*
Young Adult
Aged
B
40
30
20
10
0
Weight (g)
*
Young Adult
Aged

Figure 7

Figure 8: Although there were physical differences between young and aged mice, physical activity levels were similar in the two groups.

A) Palpebral closure was significantly greater in aged mice compared to young adult mice. **B)** The number of ungroomed mice was significantly greater in the aged group compared to the young adult group. **C)** The incidence of closed posture was significantly greater in aged mice compared to young adult mice. **D)** Activity level, as indicated by number of paw touches, was not significantly different between young adult and aged mice. * Significantly different from young adult (n = 9-13 young adult mice and 13 aged mice).

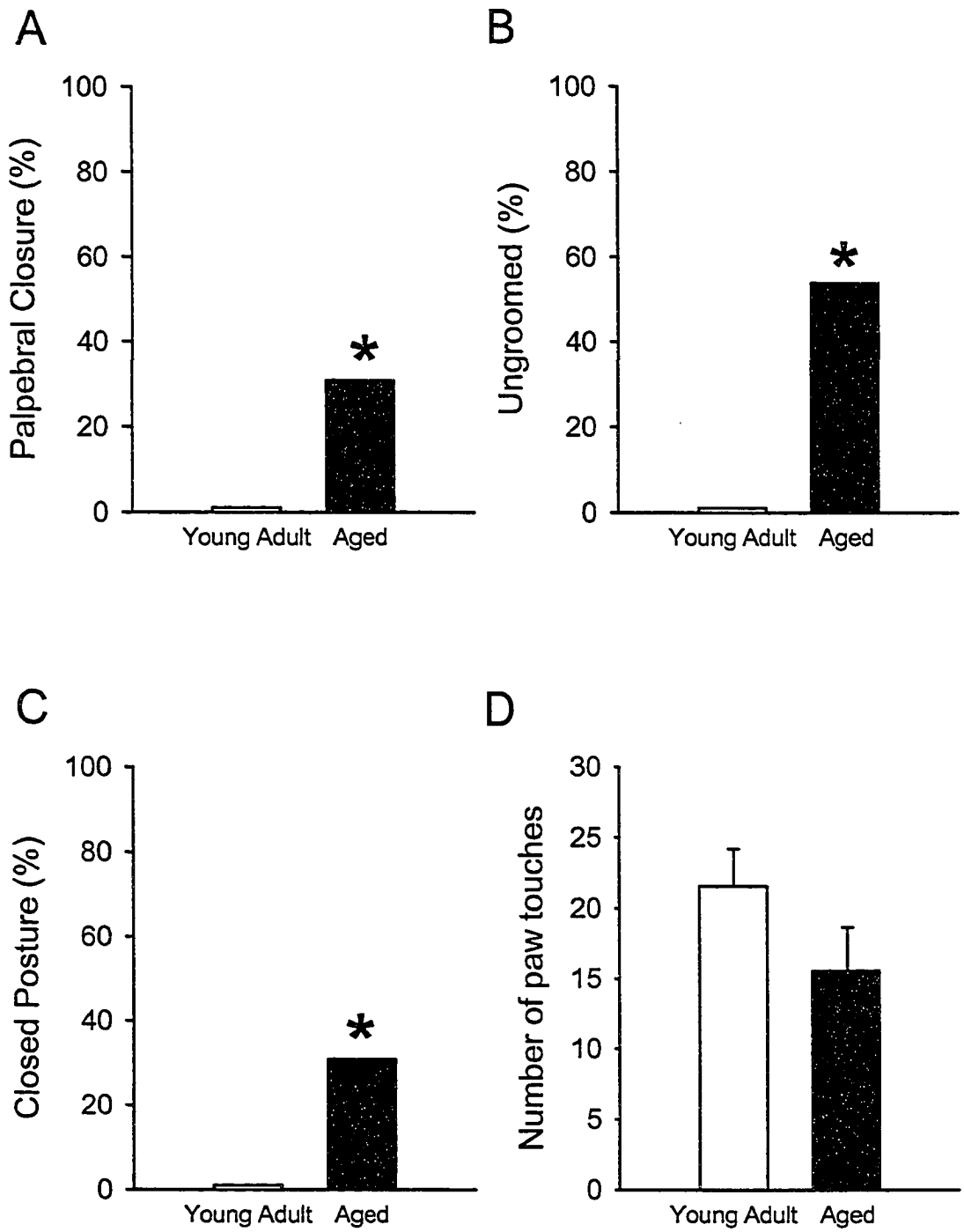
A
Palpebral Closure (%)
100
80
60
40
20
0
*
Young Adult
Aged
B
Ungroomed (%)
100
80
60
40
20
0
*
Young Adult
Aged
C
Closed Posture (%)
100
80
60
40
20
0
*
Young Adult
Aged
D
Number of paw touches
30
25
20
15
10
5
0
Young Adult
Aged

Figure 8

weight was increased in aged mice. Figure 9-A shows that ventricular wet weight was significantly greater in aged mice compared to young adult mice. To determine whether the increase in heart size was proportional to the increase in body weight in aged mice, ventricular weight was normalized to body weight. Figure 9-B shows that normalized ventricular weights were similar in young adult and aged mice. Thus, changes in ventricular weight in aged animals were most likely attributable to increased body weight. Next, lung weights and lung fluid were compared in young adult and aged mice to determine whether there was evidence of pulmonary edema in the aged group. Figure 10, panels A and B, shows that wet and dry lung weights were significantly greater in aged animals compared to young adult animals. Dry lung weights were subtracted from wet lung weights to calculate lung fluid. Figure 10-C shows that lung fluid was significantly increased in aged mice compared to young adult animals. Wet lung weight was then normalized to determine whether increased lung weight was the result of the increase in body weight. Figure 10-D shows that normalized wet lung weights were similar in young adult and aged animals. Thus, changes in lung weight in aged animals were proportional to the increased body weight.

This study has shown that ventricular weight increases in aged animals. However, the number of cardiac myocytes decreases with advancing age (Oxenham & Sharpe, 2003). Thus, increased myocyte size could contribute to the increase in ventricle

Figure 9: Ventricular weight to body weight ratios were similar in young adult and aged mice.

A) Mean ventricular weight was significantly increased in aged mice compared to young adult mice. **B)** Ventricular weight to body weight ratios were similar in young adult and aged mice. * Significantly different from young adult (n = 22 young adult mice and 21 aged mice).

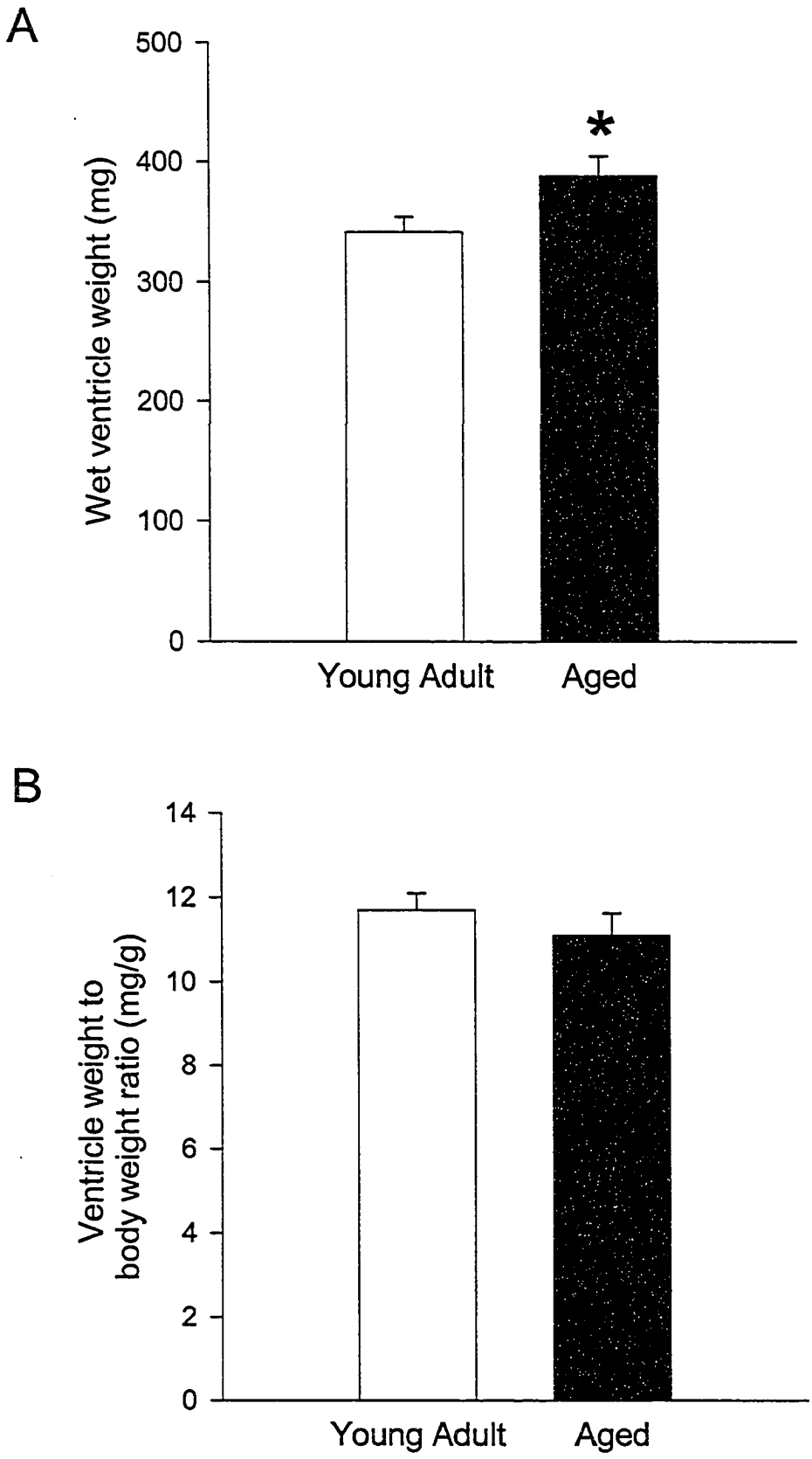
A
500
400
300
200
100
0
Wet ventricle weight (mg)
*
Young Adult
Aged
B
14
12
10
8
6
4
2
0
Ventricle weight to body weight ratio (mg/g)
Young Adult
Aged

Figure 9

Figure 10: Lung weight, normalized to body weight, was similar in young adult and aged mice.

Mean wet and dry lung weights were significantly greater in aged mice compared to young adult mice, panels **(A)** and **(B)**, respectively. **C)** Lung fluid was significantly greater in aged mice compared to young adult mice. **D)** Wet lung weights to body weight ratios were similar in young adult and aged mice. * Significantly different from young adult (n = 22 young adult mice and 21 aged mice).

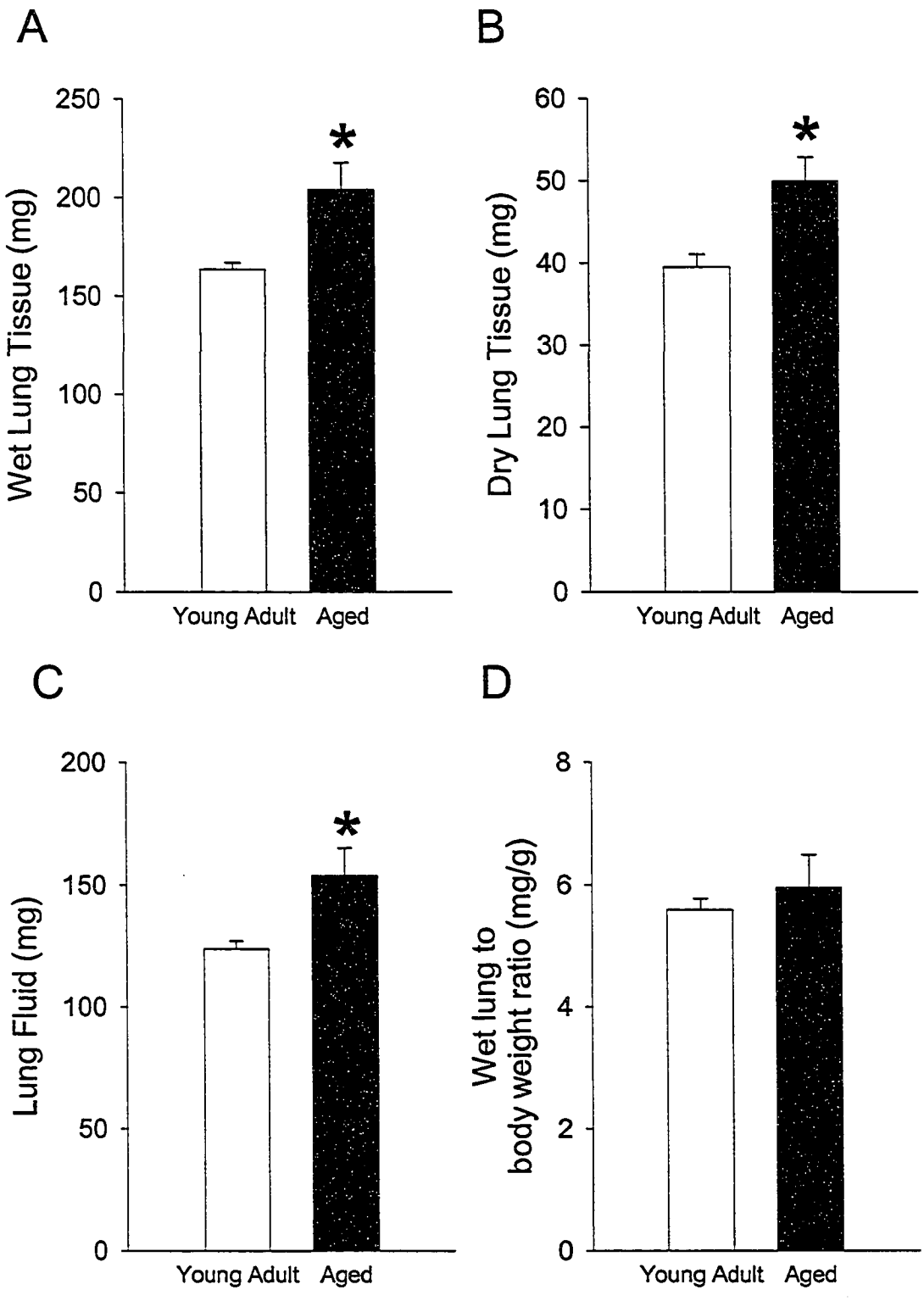
A
Wet Lung Tissue (mg)
250
200
150
100
50
0
*
Young Adult
Aged
B
Dry Lung Tissue (mg)
60
50
40
30
20
10
0
*
Young Adult
Aged
C
Lung Fluid (mg)
200
150
100
50
0
*
Young Adult
Aged
D
Wet lung to body weight ratio (mg/g)
8
6
4
2
0
Young Adult
Aged

Figure 10

weight in the aging heart. The next set of experiments compared ventricular myocyte size in young adult and aged animals. Figure 11-A shows that ventricular cell length was significantly increased in aged animals compared to young adult animals. In the next set of experiments, cells were impaled with a microelectrode and voltage clamped as described in the methods. Cell membrane area was estimated by calculating the capacitance of the cell. Figure 11-B shows that the cell capacitance of ventricular myocytes from aged mice was significantly greater compared to young adult mice, which suggests that membrane area is increased in aging. Thus, ventricular myocytes from aged mice were significantly larger than myocytes from young adults.

The relationship between $I_{Ca\text{-}L}$ and contraction in young adult and aged ventricular myocytes.

Next, the relationship between $I_{Ca\text{-}L}$ and contraction in young adult and aged myocytes was determined in voltage clamp experiments. The first series of experiments characterized and compared contractions and $I_{Ca\text{-}L}$ in voltage clamped young adult and aged myocytes. Figure 12 shows representative examples of contractions and $I_{Ca\text{-}L}$ recorded from young adult and aged ventricular myocytes. Figure 12-A shows the voltage protocol used to activate $I_{Ca\text{-}L}$ and contractions. A consistent activation history was obtained by stimulating cells with five 50 ms conditioning pulses delivered at a frequency of 2 Hz. Cells were held at a postconditioning potential of –40 mV and test steps were made to 0 mV. Representative contraction and current traces are shown in panels B and C, respectively. Figure 12-B shows that peak contraction amplitude was decreased in the aged myocyte (right panel) when compared to the young adult myocyte

Figure 11: Ventricular myocytes were significantly larger in aged mice compared to young adult mice.

A) Mean ventricular myocyte length was significantly increased in hearts from aged mice compared to hearts from young adult mice. B) The membrane area of ventricular myocytes isolated from aged hearts was significantly greater compared to myocytes from young adult hearts. Cell capacitance was used as an estimate of membrane area.

* Significantly different from young adult (n = 37 young adult mice and 36 aged mice).

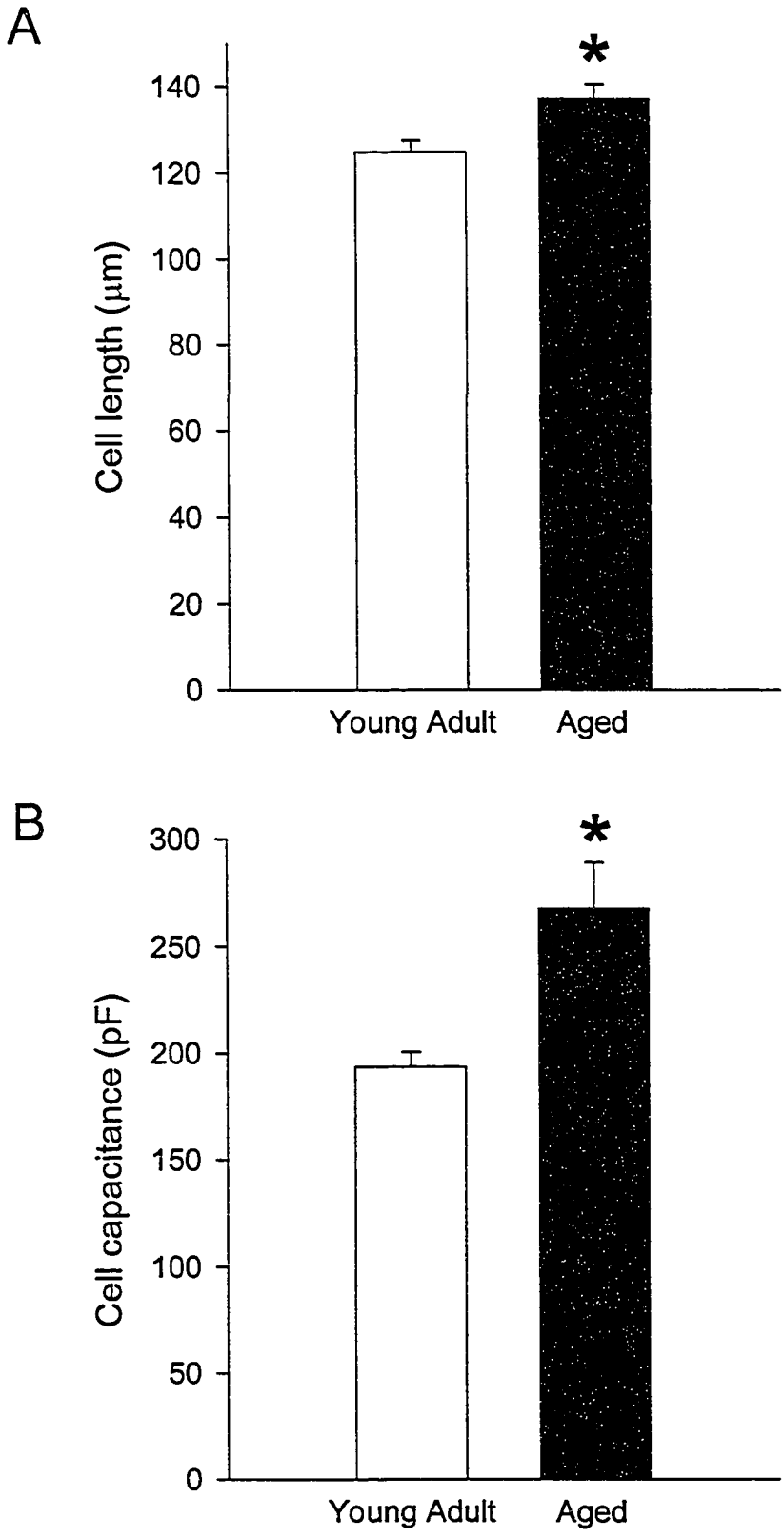
A
Cell length (μm)
140
120
100
80
60
40
20
0
*
Young Adult
Aged
B
Cell capacitance (pF)
300
250
200
150
100
50
0
*
Young Adult
Aged

Figure 11

Figure 12: Representative examples of contractions and $I_{Ca\text{-}L}$ recorded from a young adult and an aged ventricular myocyte.

A) Following 5 conditioning pulses administered at a frequency of 2 Hz, cells were depolarized from –40 to 0 mV to trigger $I_{Ca\text{-}L}$ and contraction. Representative contraction (B) and current (C) traces from young adult and aged myocytes. In the aged myocyte, contraction amplitude and peak magnitude of $I_{Ca\text{-}L}$ appeared smaller compared to the young adult cell.

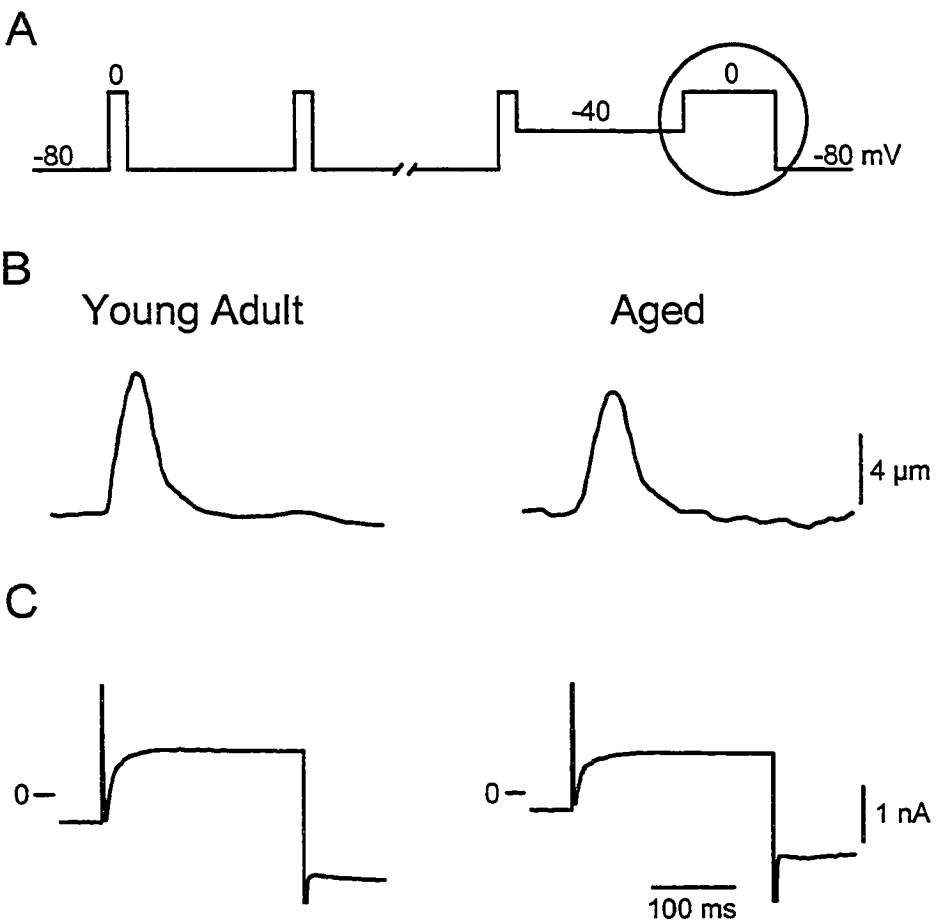

Figure 12

(left panel). Similarly, peak amplitude of $I_{Ca\text{-}L}$ was reduced in the aged myocyte (right panel) compared to the young adult myocyte (left panel) (Figure 12-C). Mean contraction and current data are shown in figure 13. Since aged myocytes were larger than young adult myocytes, contraction was normalized to resting cell length and $I_{Ca\text{-}L}$ was normalized to cell capacitance. In aged myocytes, peak contraction (panel A) and peak $I_{Ca\text{-}L}$ density (panel B) were significantly reduced compared to young adult myocytes. Thus, in voltage clamped ventricular myocytes, aging decreased magnitudes of $I_{Ca\text{-}L}$ and contraction.

The next series of experiments determined whether the time course of contraction differed between young adult and aged myocytes. Figure 14 shows mean time-to-peak and half-relaxation time for contractions initiated by voltage steps from –40 to 0 mV. Figure 14-A shows that the mean time-to-peak contraction was significantly prolonged in aged myocytes compared to young adult myocytes. In contrast, time-to-half relaxation was similar in young adult and aged myocytes (Figure 14-B).

The next part of this study determined whether the rate of $I_{Ca\text{-}L}$ inactivation was altered in aged myocytes compared to young adult myocytes. The time constant for $I_{Ca\text{-}L}$ inactivation (tau) was calculated by fitting a single exponential function to the inactivation phase of $I_{Ca\text{-}L}$. Figure 15-A illustrates representative recordings of $I_{Ca\text{-}L}$ from young adult and aged myocytes. The rate of inactivation appeared slower in the aged cell. Figure 15-B shows that the mean time constant of inactivation (tau) was significantly increased in aged myocytes compared to young adult myocytes. Thus, it appeared the rate of $I_{Ca\text{-}L}$ inactivation was reduced in aged myocytes.

Figure 13: Cell shortening and peak $I_{Ca\text{-}L}$ density were significantly reduced in aged myocytes compared to young adult myocytes.

A) Mean cell shortening was significantly decreased in aged myocytes compared to young adult myocytes. Cell shortening is expressed as percent of maximum cell length. B) Peak $I_{Ca\text{-}L}$ density was significantly decreased in aged myocytes compared to young adult myocytes. * Significantly different from young adult (n = 24 young adult myocytes and 34 aged myocytes).

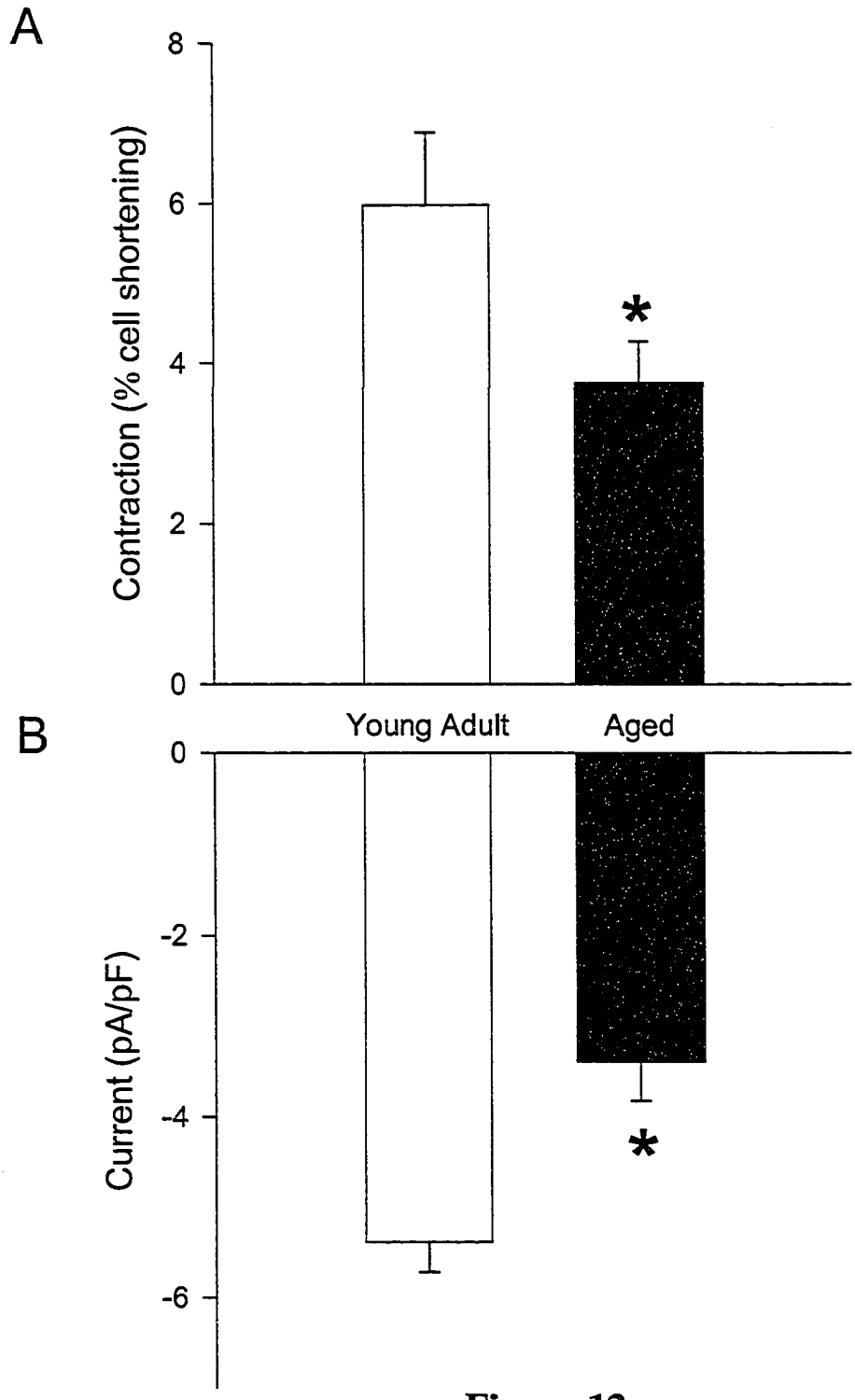
A
8
6
4
2
0
Contraction (% cell shortening)
*
B
0
-2
-4
-6
Current (pA/pF)
Young Adult
Aged
*

Figure 13

Figure 14: Time-to-peak contraction was significantly prolonged in aged myocytes compared to young adult myocytes.

A) Mean time-to-peak contraction was significantly prolonged in aged myocytes compared to young adult myocytes. B) Half-relaxation times were similar in young adult and aged myocytes. * Significantly different from young adult (n = 19 young adult myocytes and 23 aged myocytes).

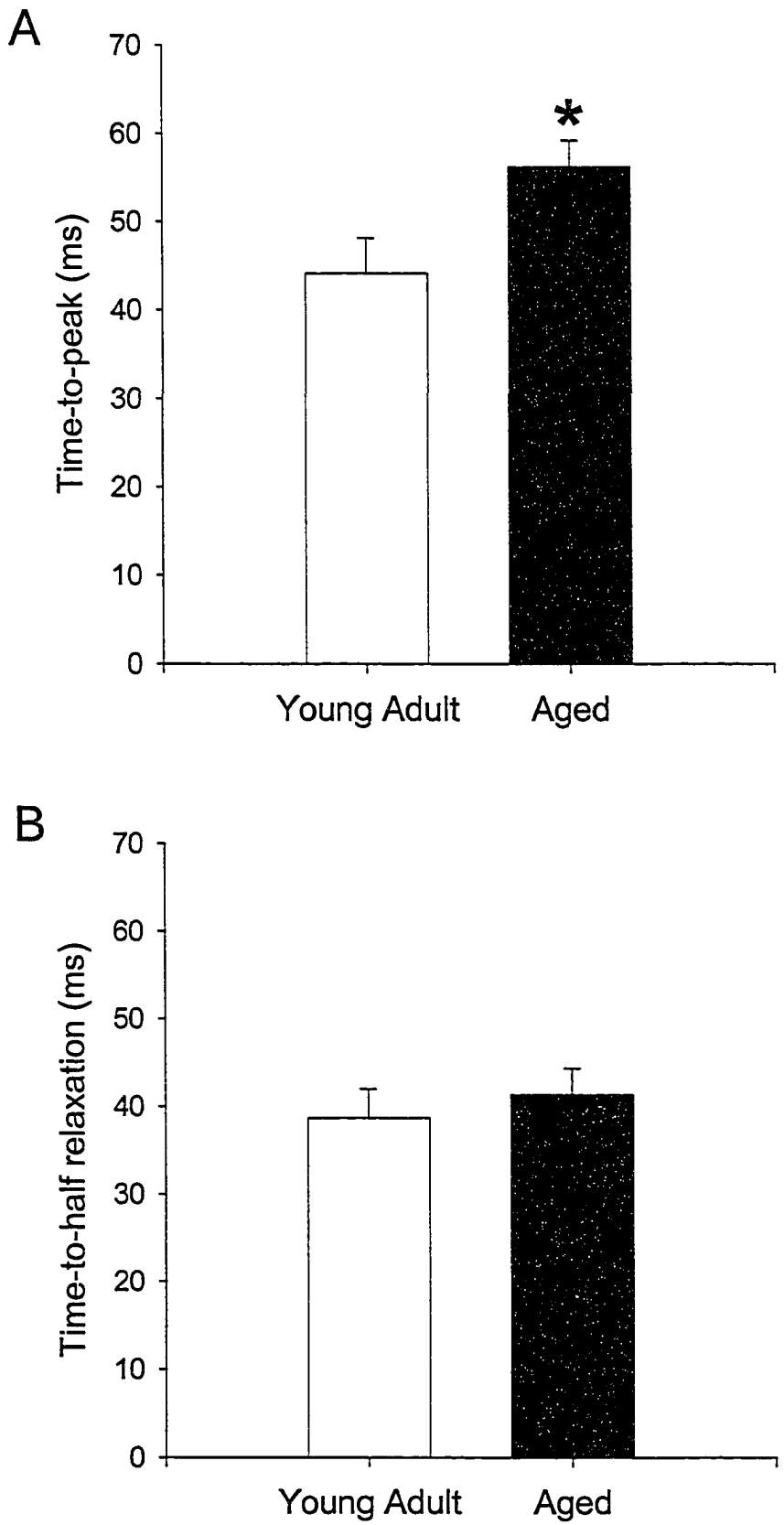
A
70
60
50
40
30
20
10
0
Time-to-peak (ms)
*
Young Adult
Aged
B
70
60
50
40
30
20
10
0
Time-to-half relaxation (ms)
Young Adult
Aged

Figure 14

Figure 15: The rate of inactivation of $I_{Ca\text{-}L}$ was significantly slower in aged myocytes compared to young adult myocytes.

A) Representative traces from a young adult myocyte and an aged myocyte show that $I_{Ca\text{-}L}$ inactivation is slowed in the aging cell. B) Mean time required for $I_{Ca\text{-}L}$ inactivation (tau) was significantly prolonged in aged myocytes compared to young adult myocytes. * Significantly different from young adult (n = 24 young adult myocytes and 34 aged myocytes).

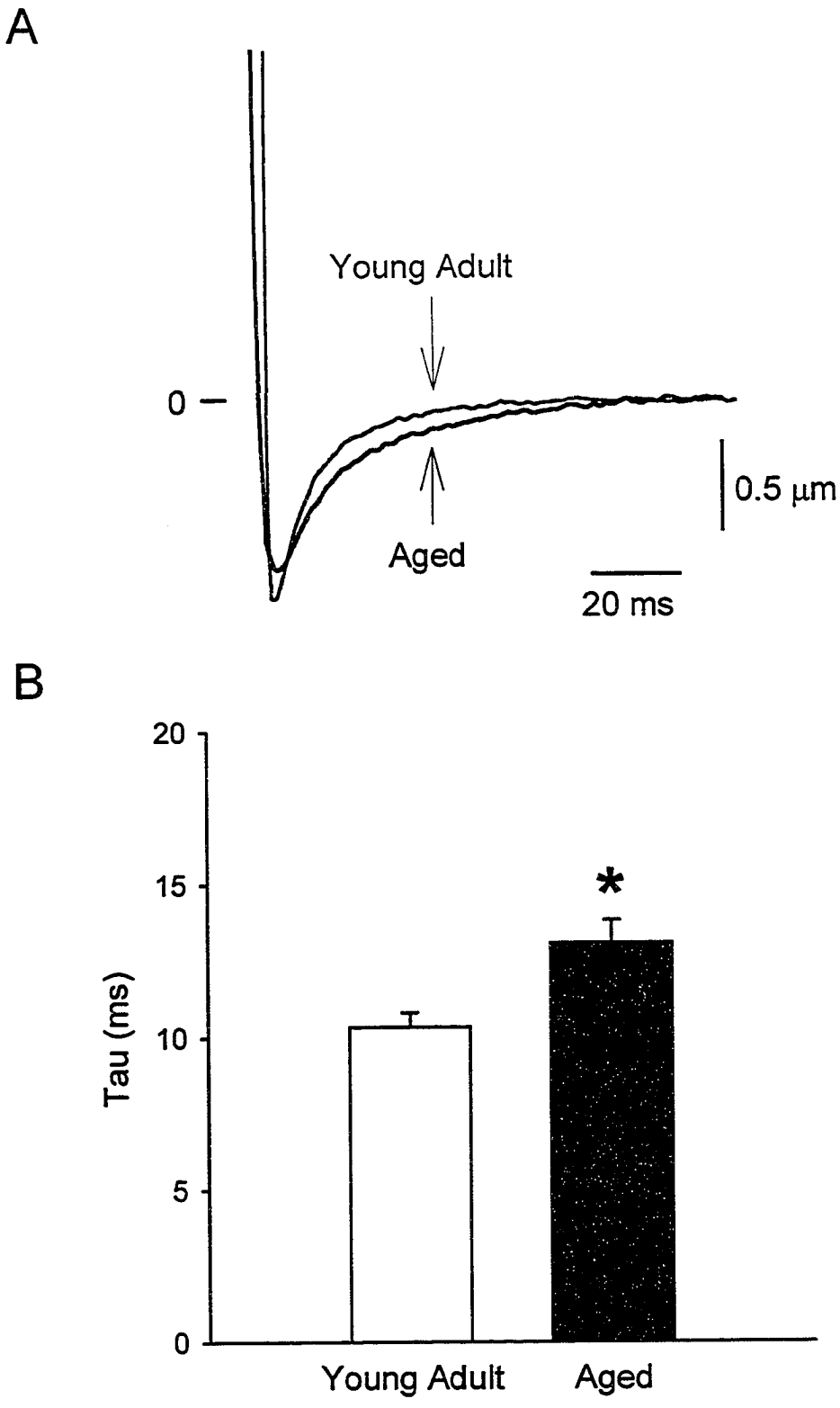
A
Young Adult
0
0.5 µm
Aged
20 ms
B
20
15
10
5
0
Tau (ms)
*
Young Adult
Aged

Figure 15

Ca^{2+} transients and SR Ca^{2+} load in young adult and aged ventricular myocytes.

Cardiac contraction is initiated by a transient rise in intracellular Ca^{2+}. Therefore, the next series of experiments determined whether Ca^{2+} transient amplitudes were altered in ventricular myocytes from aged mice. Figure 16 shows representative original recordings of Ca^{2+} transients from young adult and aged myocytes. Ca^{2+} transients were activated by depolarizing cells from a postconditioning potential of –40 mV to 0 mV (Figure 16-A). Test steps were preceded by five 50 ms conditioning pulses delivered at a frequency of 2 Hz. Figure 16-B shows representative Ca^{2+} transients from young adult and aged myocytes. These recordings also show the diastolic Ca^{2+} concentration, which is the Ca^{2+} concentration that precedes the Ca^{2+} transient. The representative recordings show that diastolic Ca^{2+} concentration was approximately 350 nM in young adult myocytes compared to approximately 300 nM in the aged myocytes. Systolic Ca^{2+} concentrations were approximately 600 nM and 425 nM for young adult and aged myocytes, respectively. Ca^{2+} transient amplitude, calculated as the difference between systolic and diastolic Ca^{2+} concentrations, appeared smaller in the aged myocyte compared to the young adult myocyte. Mean Ca^{2+} transient data are shown in figure 17. Figure 17-A shows mean diastolic and mean systolic Ca^{2+} concentrations were significantly decreased in aged myocytes compared to young adult myocytes. Figure 17-B shows that mean Ca^{2+} transient amplitudes also were significantly smaller in aged myocytes compared to young adult myocytes.

The gain of CICR is the amount of SR Ca^{2+} release per nA of $I_{Ca\text{-}L}$. To determine whether the gain of CICR was altered in aging, gain was calculated and compared in young adult and aged myocytes. Gain was calculated for each cell by dividing SR Ca^{2+}

Figure 16: Ca^{2+} transient amplitudes were smaller in aged myocytes compared to young adult myocytes.

A) Following 5 conditioning pulses delivered at a frequency of 2 Hz, cells were depolarized from –40 to 0 mV. B) Representative Ca^{2+} transients from a young adult (left panel) and an aged myocyte (right panel).

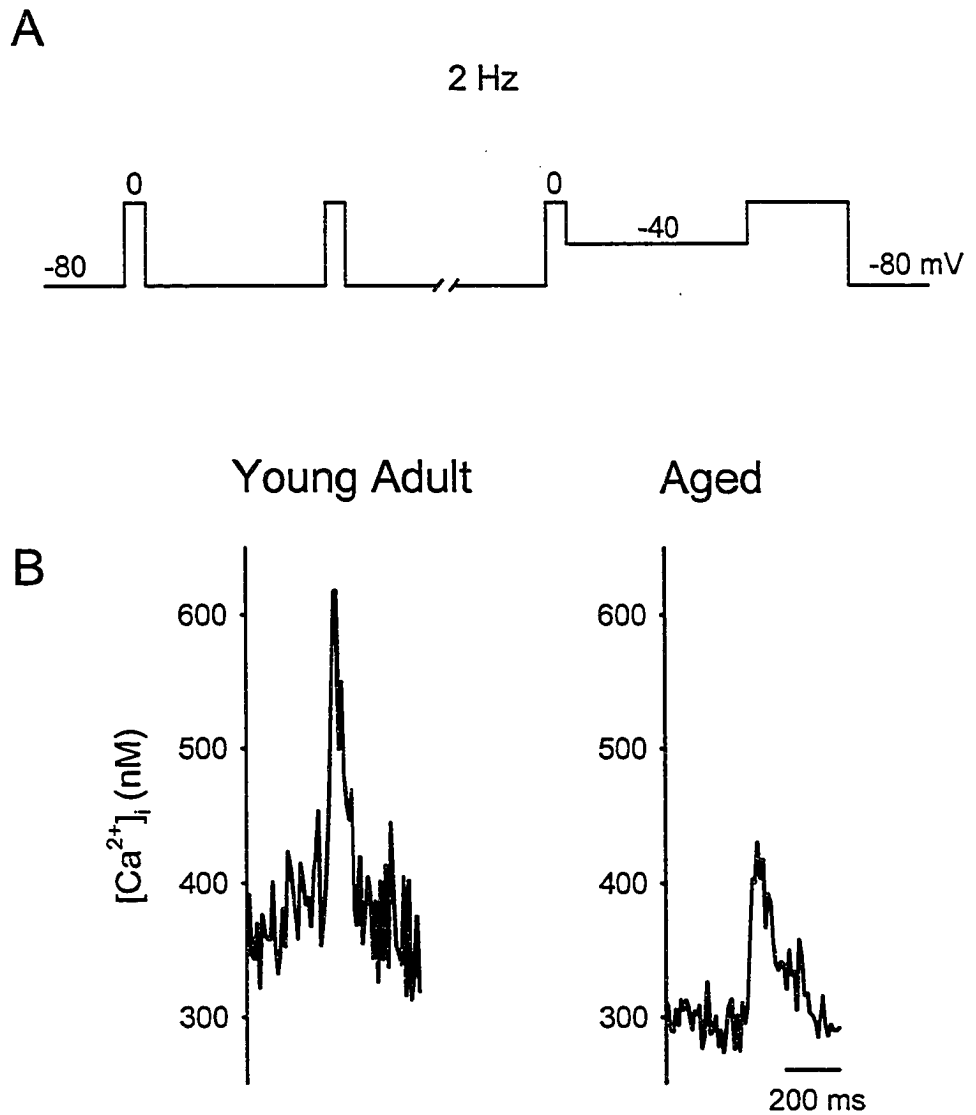
A
2 Hz
0
0
-40
-80
-80 mV
Young Adult
Aged
B
600
500
400
300
[Ca2+]i (nM)
600
500
400
300
200 ms

Figure 16

Figure 17: Diastolic and systolic intracellular Ca^{2+} concentrations and Ca^{2+} transient amplitudes were significantly reduced in aged myocytes compared to young adult myocytes.

A) Diastolic and systolic Ca^{2+} concentrations were significantly decreased in aged myocytes. B) Mean Ca^{2+} transient amplitudes were significantly reduced in myocytes from aged mice. * Significantly different from young adult (n = 19 young adult myocytes and 28 aged myocytes).

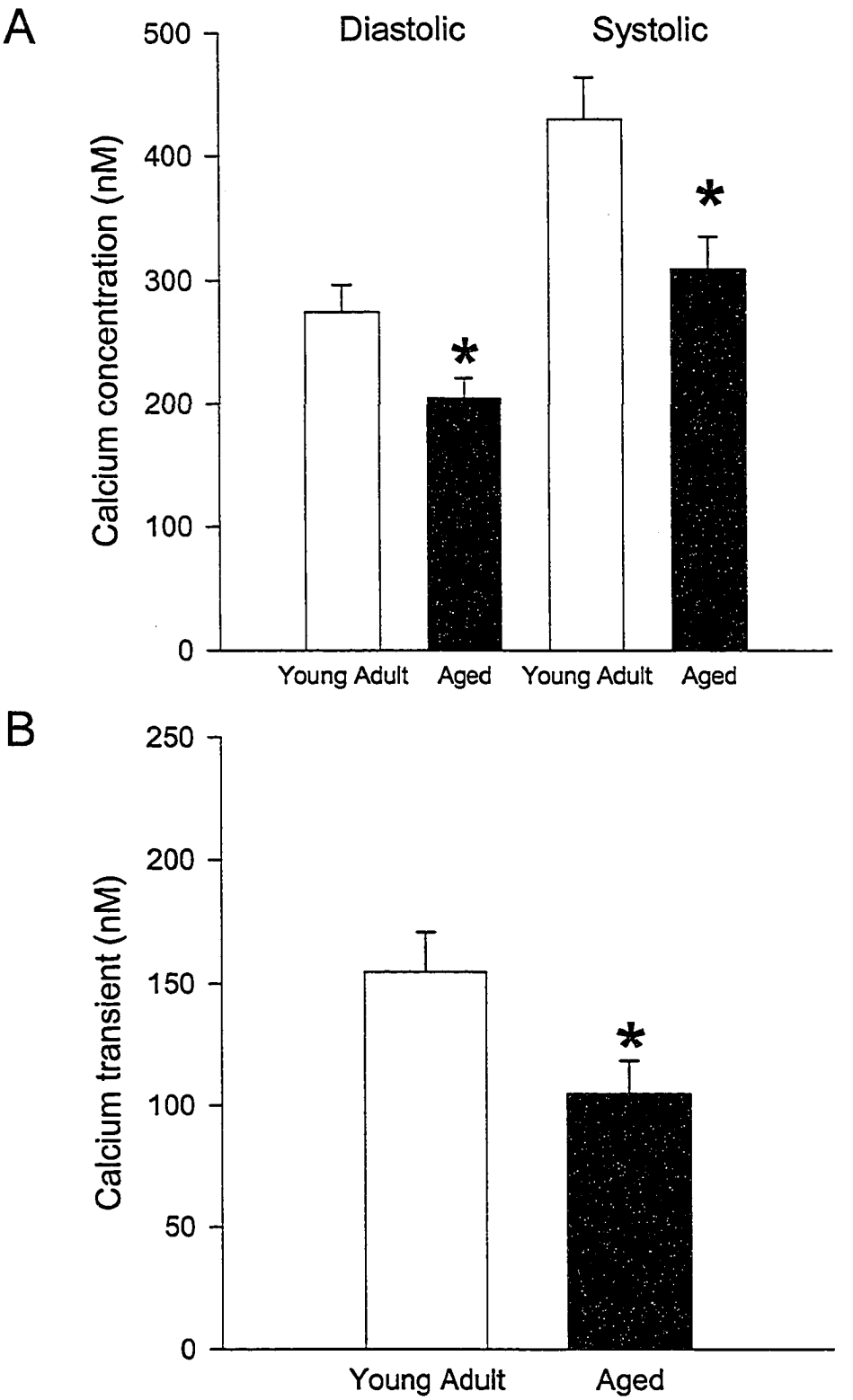
A
Diastolic
Systolic
Calcium concentration (nM)
500
400
300
200
100
0
*
*
Young Adult
Aged
Young Adult
Aged
B
Calcium transient (nM)
250
200
150
100
50
0
*
Young Adult
Aged

Figure 17

release (Ca^{2+} transient) by the trigger Ca^{2+} ($I_{Ca\text{-}L}$). Figure 18 shows that the mean gain of CICR was similar in young adult and aged myocytes. Thus, it was unlikely that decreased SR Ca^{2+} release in aged myocytes was attributable to changes in the gain of CICR.

As Ca^{2+} transients are derived primarily from Ca^{2+} released from the SR, decreased SR Ca^{2+} release could be at least partially attributable to changes in SR Ca^{2+} load. Therefore, the final set of experiments in this series determined whether SR Ca^{2+} load differed between young adult and aged myocytes. The Ca^{2+} sensitive dye fura-2 was used to measure SR Ca^{2+} load as described in the methods. The voltage protocol used for this series of experiments is illustrated in figure 19-A. Cells were stimulated with a train of conditioning pulses delivered at a frequency of 2 Hz. Following the last conditioning pulse, cells were held at –60 mV and caffeine was applied for 1 second with a rapid solution switcher. Caffeine was applied in a 0 mM Na^{+}, 0 mM Ca^{2+} solution to minimize the loss of Ca^{2+} through the NCX. Figure 19-B shows representative caffeine-induced Ca^{2+} transients from young adult and aged myocytes. Caffeine-induced Ca^{2+} transients are preceded by Ca^{2+} transients corresponding to the train of conditioning pulses. Amplitudes of caffeine-induced Ca^{2+} transients appeared similar in the young adult and the aged myocyte. Mean amplitudes of caffeine-induced Ca^{2+} transients are shown in Figure 20. Interestingly, amplitudes of caffeine-induced Ca^{2+} transients were similar in young adult and aged cells. This suggests that SR Ca^{2+} load was similar in young adult and aged myocytes. Thus, decreased SR Ca^{2+} release in aging is not likely attributable to reduced SR Ca^{2+} load.

Figure 18: The gain of CICR was similar in young adult and aged myocytes stimulated at 2 Hz.

Gain was calculated as SR Ca^{2+} release divided by peak $I_{Ca\text{-}L}$. (n = 18 young adult myocytes and 28 aged myocytes).

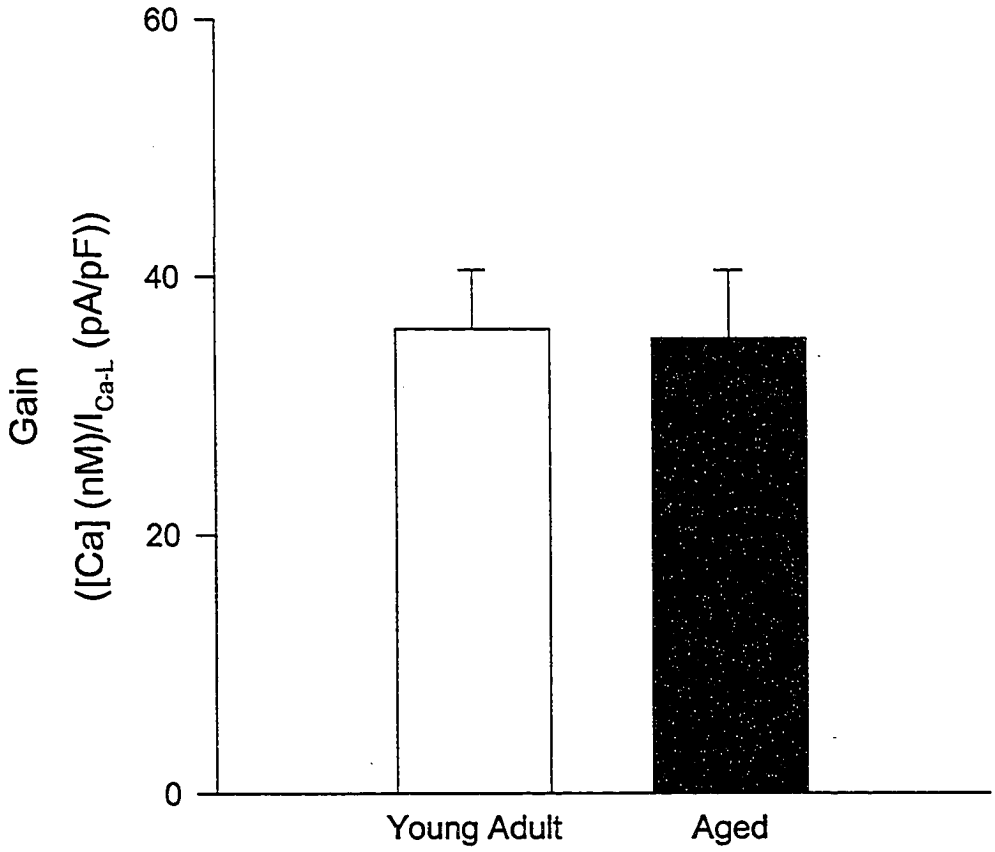

Figure 18

Figure 19: Amplitudes of caffeine-induced Ca^{2+} transients were similar in young adult and aged myocytes.

A) Cells were stimulated at a frequency of 2 Hz with 11 conditioning pulses. Following the last conditioning pulse, cells were held at –60 mV and caffeine was applied for 1 second to release SR Ca^{2+} stores. B) Representative traces show the amplitudes caffeine-induced Ca^{2+} transients were similar in young adult (top panel) and aged (bottom panel) myocytes.

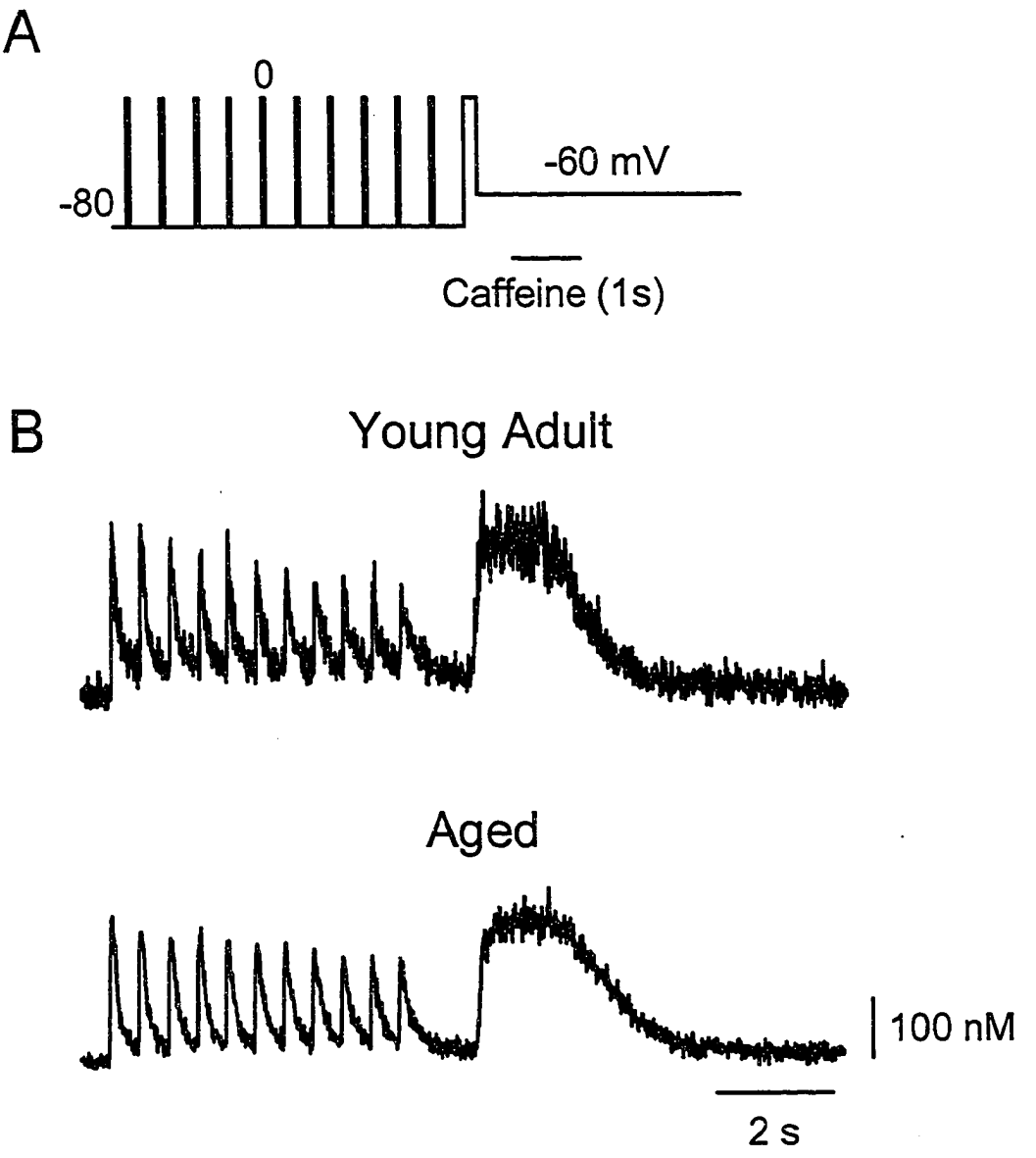

Figure 19

Figure 20: Amplitudes of caffeine-induced Ca^{2+} transients were not significantly different in young adult and aged myocytes.

(n = 22 young adult myocytes and 30 aged myocytes)

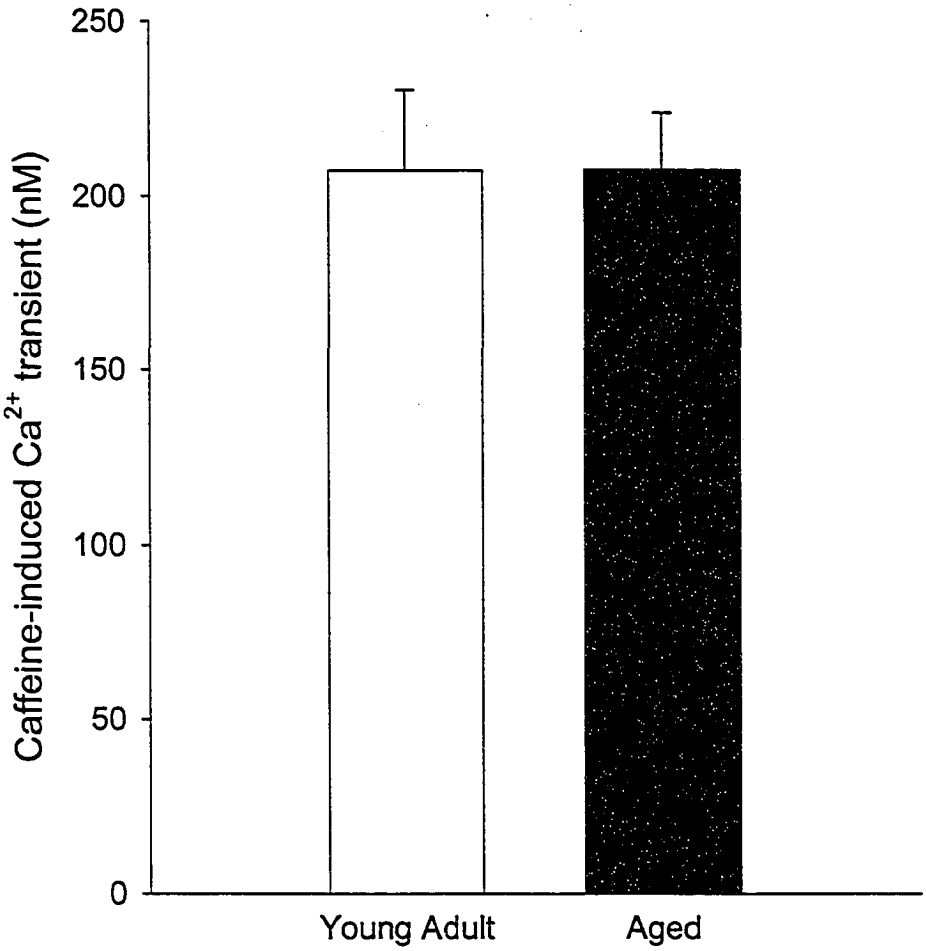
250
200
150
100
50
0
Caffeine-induced Ca^{2+} transient (nM)
Young Adult
Aged

Figure 20

In summary, peak $I_{Ca\text{-}L}$ and peak contraction amplitudes were significantly depressed in aged myocytes compared to young adult myocytes stimulated at 2 Hz. Ca^{2+} transient amplitudes also were significantly decreased in aged myocytes. This study also found that the gain of CICR was similar in young adult and aged myocytes. As well, SR Ca^{2+} load was similar in both groups. These results suggest that decreased Ca^{2+} transient amplitudes in aged myocytes were not the result of a change in gain of CICR or SR Ca^{2+} load. Therefore, the reduction in SR Ca^{2+} release was most likely attributable to a reduction in trigger $I_{Ca\text{-}L}$.

The effects of stimulation frequency on $I_{Ca\text{-}L}$ and contraction amplitudes in young adult and aged myocytes.

Previous work has shown that stimulation frequencies greater than 4 Hz augment the reduction in contraction amplitude in aged myocytes in field-stimulated cells (Lim et al., 2000). Interestingly, a separate study showed amplitudes of peak $I_{Ca\text{-}L}$ are similar in young adult and aged myocytes paced at 4 Hz or higher (Isenberg et al., 2003). However, $I_{Ca\text{-}L}$ and contraction have not been measured in cells stimulated at rapid rates in the same cells under the same experimental conditions. Therefore, the next set of experiments simultaneously measured $I_{Ca\text{-}L}$ and contraction in voltage clamped cells to determine whether increasing stimulation frequency alters the relationship between $I_{Ca\text{-}L}$ and contraction in young adult and aged myocytes. Figure 21 shows representative contraction and $I_{Ca\text{-}L}$ recordings from a young adult myocyte paced at 2 and 6 Hz. The 2 Hz and 6 Hz voltage protocols are illustrated in figure 21-A. For both protocols, cells were held at a postconditioning potential of –40 mV and test steps were made to 0 mV to

Figure 21: Contraction amplitude and $I_{Ca\text{-}L}$ were decreased in voltage clamped young adult myocytes stimulated at 6 Hz compared to young adult myocytes stimulated at 2 Hz.

A) Following 5 conditioning pulses administered at either 2 Hz (left panel) or 6 Hz (right panel), cells were depolarized from –40 to 0 mV. B) Representative examples of contractions from a young adult myocyte stimulated at 2 Hz (left panel) or 6 Hz (right panel). C) Representative examples of $I_{Ca\text{-}L}$ from young adult myocytes stimulated at 2 Hz (left panel) and 6 Hz (right panel).

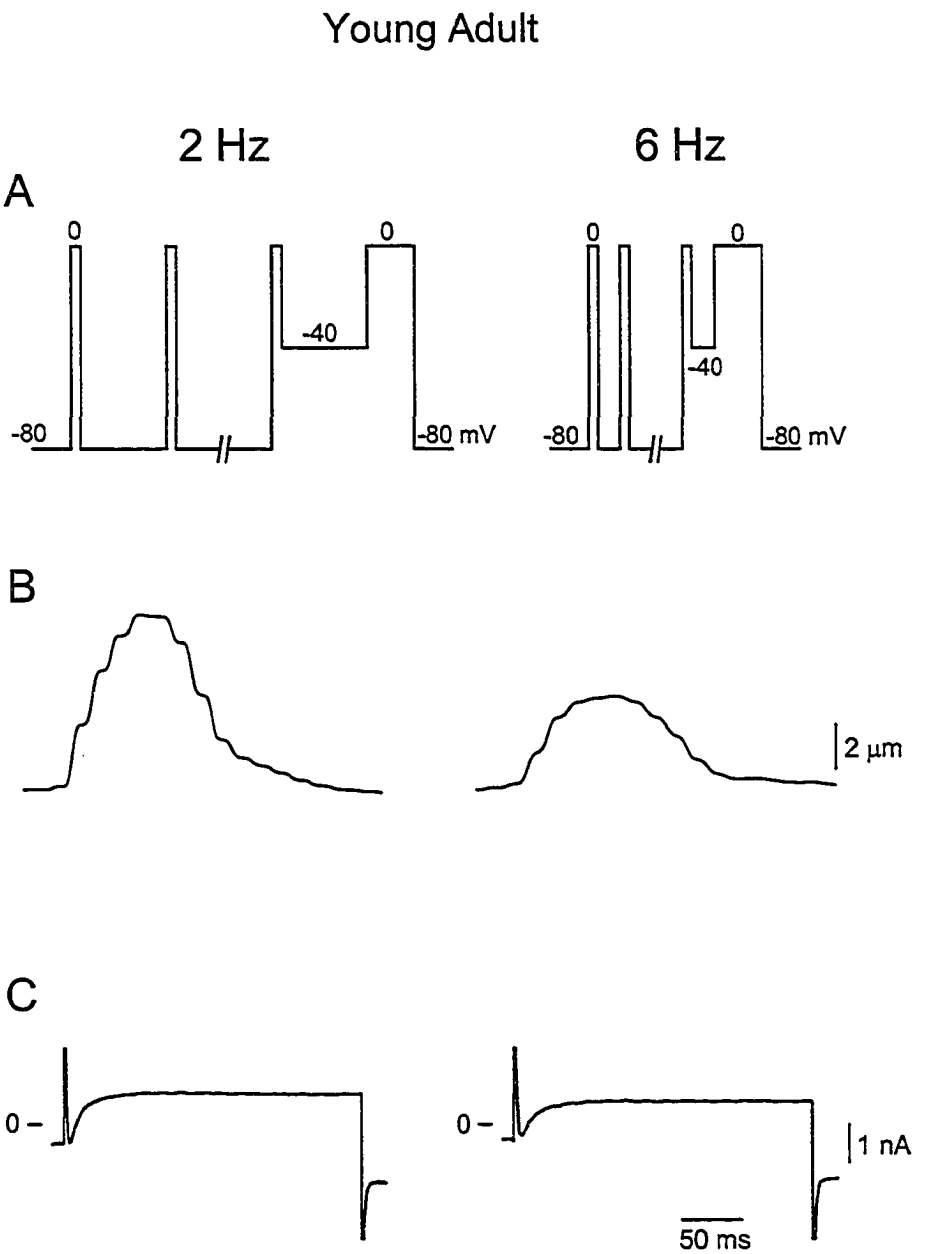
Young Adult
2 Hz
6 Hz
A
0
0
-40
-80
-80 mV
0
0
-40
-80
-80 mV
B
2 µm
C
0 –
0 –
1 nA
50 ms

Figure 21

activate transmembrane currents and contraction. Test steps were preceded by five 50 ms conditioning pulses delivered at 2 Hz (left panel) or 6 Hz (right panel). Figure 21-B shows that contraction amplitude decreased in the young adult myocyte when stimulation frequency was increased from 2 to 6 Hz. Similarly, peak $I_{Ca\text{-}L}$ also decreased in the young adult myocyte when stimulation frequency was increased (Figure 21-C). Mean contraction and current data are shown in figure 22. Figure 22-A shows contraction amplitude was significantly reduced when young adult myocytes were stimulated at 6 Hz compared to when young adult myocytes were stimulated at 2 Hz. Peak $I_{Ca\text{-}L}$ density also decreased when stimulation frequency was increased from 2 Hz to 6 Hz in the young adult myocytes (Figure 22-B).

The next series of experiments determined the effects of stimulation frequency on contraction and $I_{Ca\text{-}L}$ in aged myocytes. Figure 23 shows representative examples of contractions and $I_{Ca\text{-}L}$ from an aged myocyte stimulated at 2 Hz and 6 Hz. The voltage protocols used for these experiments are illustrated in figure 23-A and are described above. In brief, the left panel depicts the 2 Hz voltage protocol and the right panel depicts the 6 Hz voltage protocol. Figure 23-B shows that contraction amplitude is decreased in the aged myocyte when stimulation frequency is increased from 2 Hz to 6 Hz. Figure 23-C shows peak $I_{Ca\text{-}L}$ is depressed when the aged myocyte was stimulated at 6 Hz compared to 2 Hz. Mean normalized contraction and current data are shown in figure 24. In aged myocytes stimulated at 6 Hz, contraction amplitudes were significantly reduced compared to aged myocytes stimulated at 2 Hz (Figure 24-A). Interestingly, $I_{Ca\text{-}L}$ density was reduced at 6 Hz compared to 2 Hz in aged myocytes, but this reduction was not statistically significant (Figure 24-B). Thus, in voltage clamped

Figure 22: Mean contraction amplitude and peak $I_{Ca\text{-}L}$ were significantly reduced in young adult myocytes stimulated at 6 Hz compared to young adult myocytes stimulated at 2 Hz.

A) Mean contraction amplitude was significantly reduced in young adult myocytes stimulated at 6 Hz compared to young adult myocytes stimulated at 2 Hz. B) Peak $I_{Ca\text{-}L}$ density was significantly decreased in young adult myocytes stimulated at 6 Hz compared to young adult myocytes stimulated at 2 Hz. * Significantly different from young adult myocytes paced at 2 Hz (n = 24 young adult myocytes stimulated at 2 Hz and 18 young adult myocytes stimulated at 6 Hz).

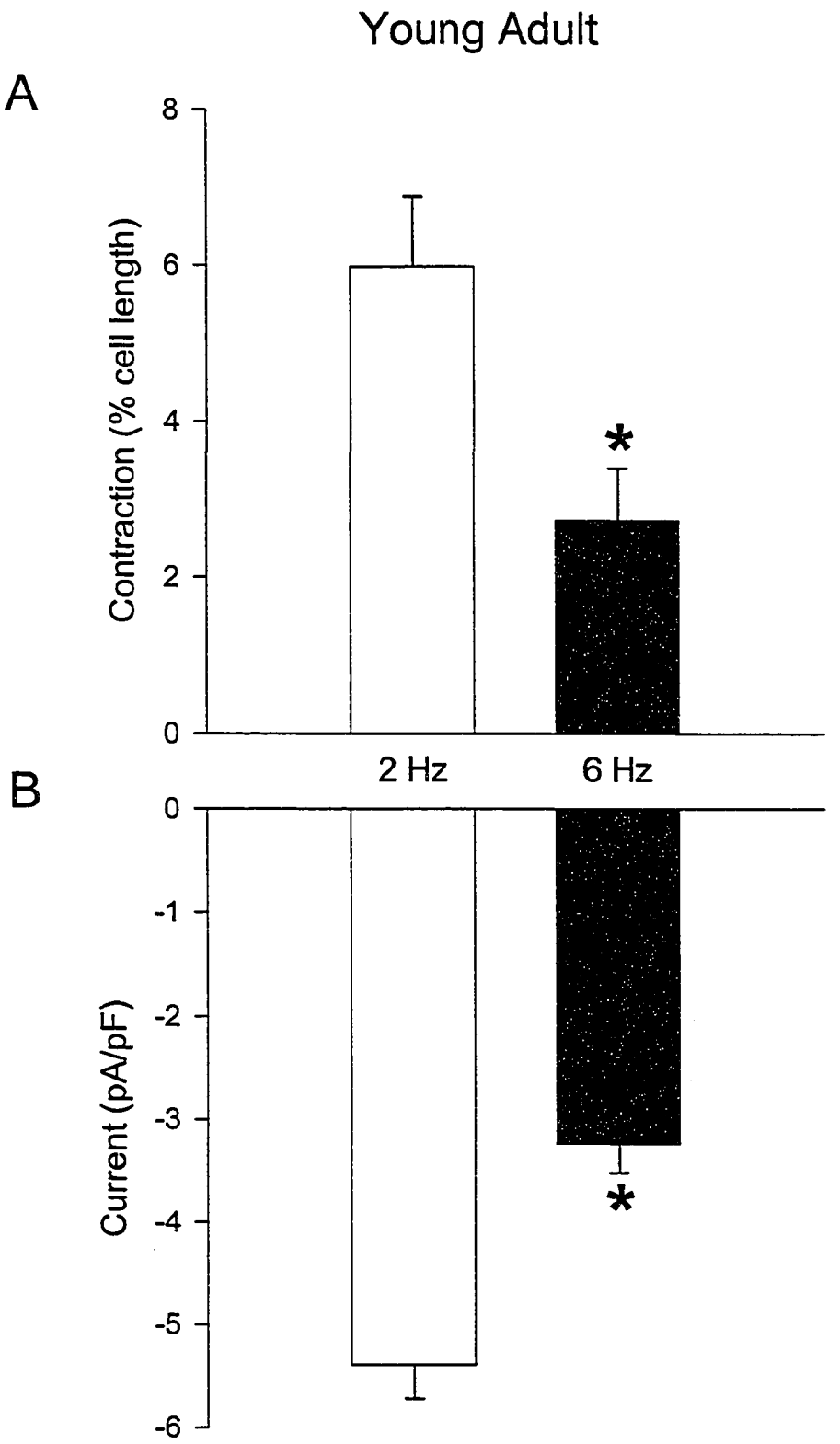
Young Adult
A
Contraction (% cell length)
8
6
4
2
0
*
2 Hz
6 Hz
B
Current (pA/pF)
0
-1
-2
-3
-4
-5
-6
*

Figure 22

Figure 23: Contraction amplitude and $I_{Ca\text{-}L}$ were decreased in voltage clamped aged myocytes stimulated at 6 Hz compared to aged myocytes stimulated at 2 Hz.

A) Following 5 conditioning pulses administered at either 2 Hz (left panel) or 6 Hz (right panel), cells were depolarized from –40 to 0 mV. (B) and (C) Representative examples of contractions and $I_{Ca\text{-}L}$ from aged myocytes stimulated at 2 Hz (left panel) or 6 Hz (right panel).

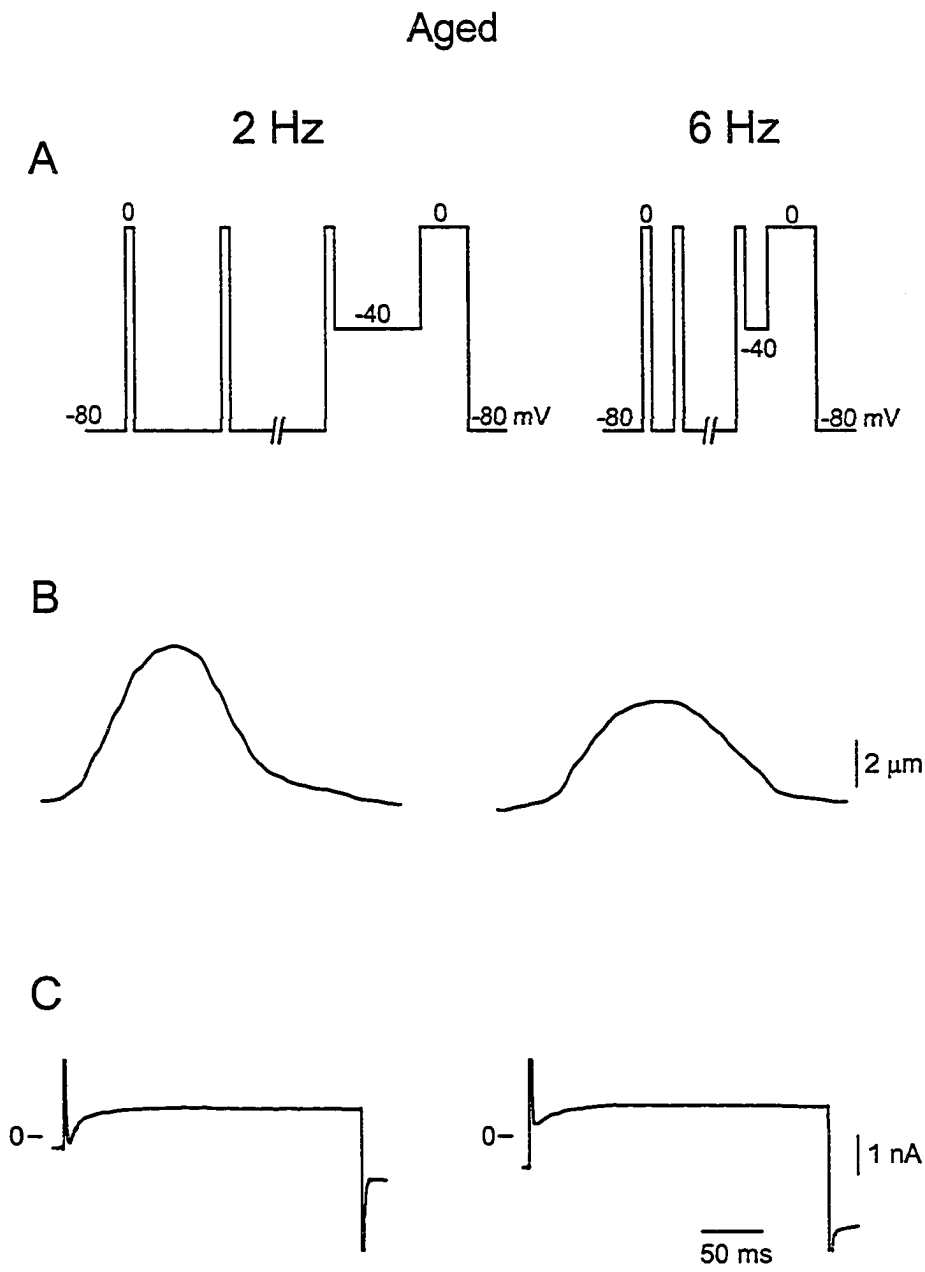

Figure 23

Figure 24: In aged myocytes paced at 6 Hz, contraction amplitudes were significantly reduced compared to aged myocytes paced at 2 Hz.

A) Mean data shows that contraction amplitude was significantly reduced in aged myocytes stimulated at 6 Hz compared to aged myocytes stimulated at 2 Hz. B) Peak $I_{Ca\text{-}L}$ density was reduced in aged myocytes stimulated at 6 Hz compared to aged myocytes stimulated at 2 Hz. * Significantly different from aged myocytes stimulated at 2 Hz (n = 34 aged myocytes stimulated at 2 Hz and 23 aged myocytes stimulated at 6 Hz).

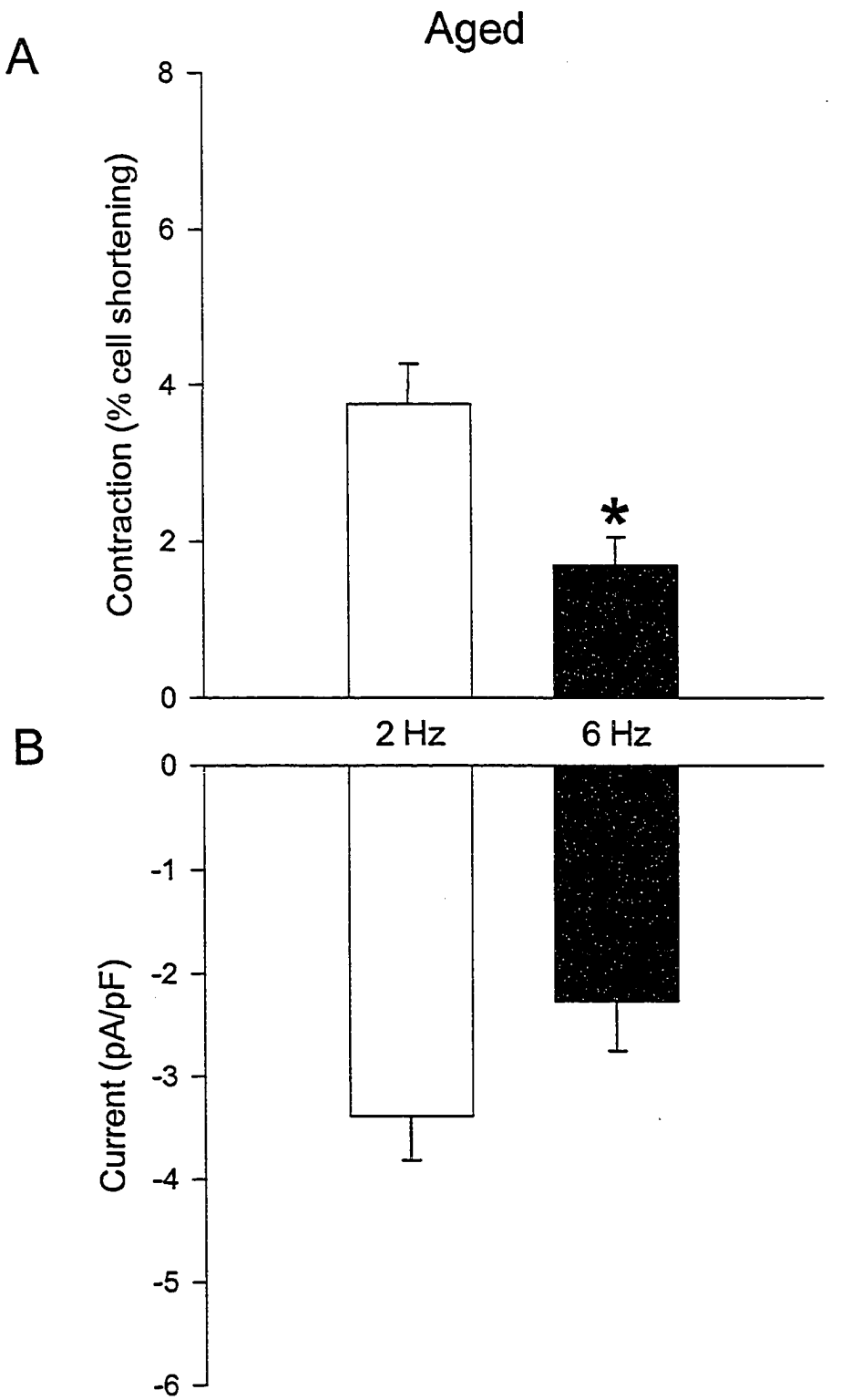
Aged
A
Contraction (% cell shortening)
8
6
4
2
0
*
2 Hz
6 Hz
B
Current (pA/pF)
0
-1
-2
-3
-4
-5
-6

Figure 24

cells, it appears that increasing stimulation frequency decreases contraction amplitude in young adult and aged myocytes. However, increasing stimulation frequency decreased $I_{Ca\text{-}L}$ only in young myocytes.

This study previously showed that contraction and $I_{Ca\text{-}L}$ were significantly reduced in aged myocytes stimulated at 2 Hz compared to young adult myocytes stimulated at 2 Hz. Therefore, contractions and Ca^{2+} currents from young adult and aged myocytes stimulated at 6 Hz were compared to determine whether these differences would be exacerbated at rapid pacing rates. Figure 25 shows mean normalized contraction and current data from young adult and aged myocytes stimulated at 6 Hz. Interestingly, contraction amplitudes (Figure 25-A) and peak $I_{Ca\text{-}L}$ densities (Figure 25-B) were only slightly smaller in aged myocytes when compared to young adult cells, and this difference was no longer statistically significant. Thus, differences in peak amplitudes of contraction and $I_{Ca\text{-}L}$ between young adult and aged myocytes at 2 Hz were abolished at higher stimulation frequencies.

The effects of stimulation frequency on Ca^{2+}transient amplitude and SR Ca^{2+} load in young adult and aged myocytes.

Increasing stimulation frequency was shown to eliminate the differences in contraction amplitudes between young adult and aged myocytes. Therefore, the next series of experiments was designed to determine if differences in Ca^{2+} transients observed between young adult and aged myocytes persisted at rapid pacing frequencies (6 Hz). Figure 26 shows mean Ca^{2+} transient data from young adult and aged myocytes stimulated at 6 Hz. Figure 26-A shows that diastolic Ca^{2+} concentrations were

Figure 25: Amplitudes of contraction and $I_{Ca\text{-}L}$ were similar in young adult and aged myocytes stimulated at 6 Hz.

A) Mean contraction amplitudes were similar in young adult and aged myocytes stimulated at 6 Hz. B) Peak $I_{Ca\text{-}L}$ density was similar in young adult and aged myocytes stimulated at 6 Hz. (n = 18 young adult myocytes and 23 aged myocytes)

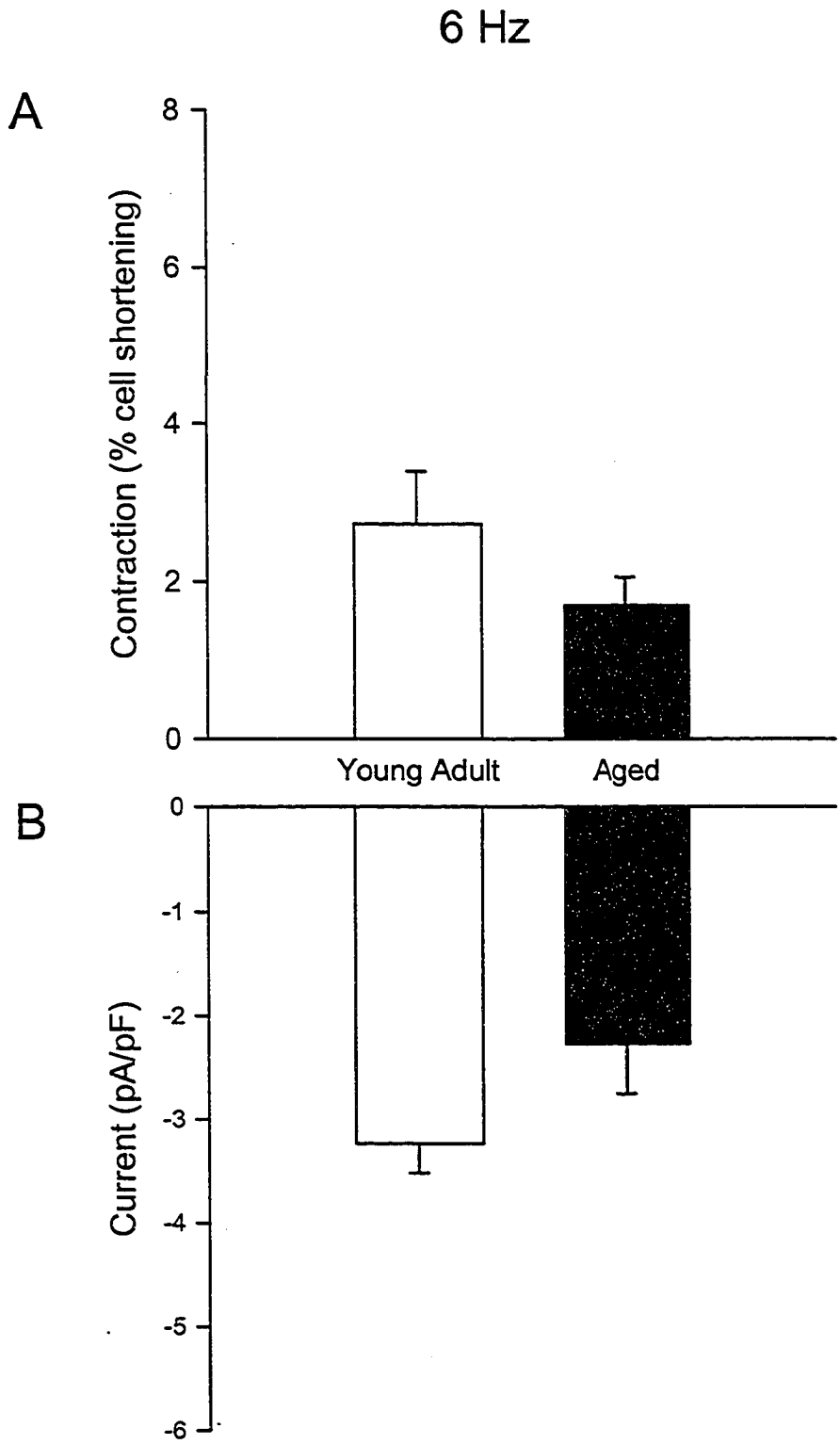
6 Hz
A
Contraction (% cell shortening)
8
6
4
2
0
Young Adult
Aged
B
Current (pA/pF)
0
-1
-2
-3
-4
-5
-6

Figure 25

Figure 26: Diastolic Ca^{2+} concentration was significantly reduced in aged myocytes stimulated at 6 Hz compared to young adult myocytes stimulated at 6 Hz.

A) Mean diastolic Ca^{2+} concentration was significantly decreased in aged myocytes compared to young adult cells, whereas mean systolic Ca^{2+} concentrations were similar in young adult and aged myocytes. B) Mean Ca^{2+} transient amplitudes were similar in young adult and aged myocytes. * Significantly different from young adult (n = 13 young adult myocytes and 16 aged myocytes).

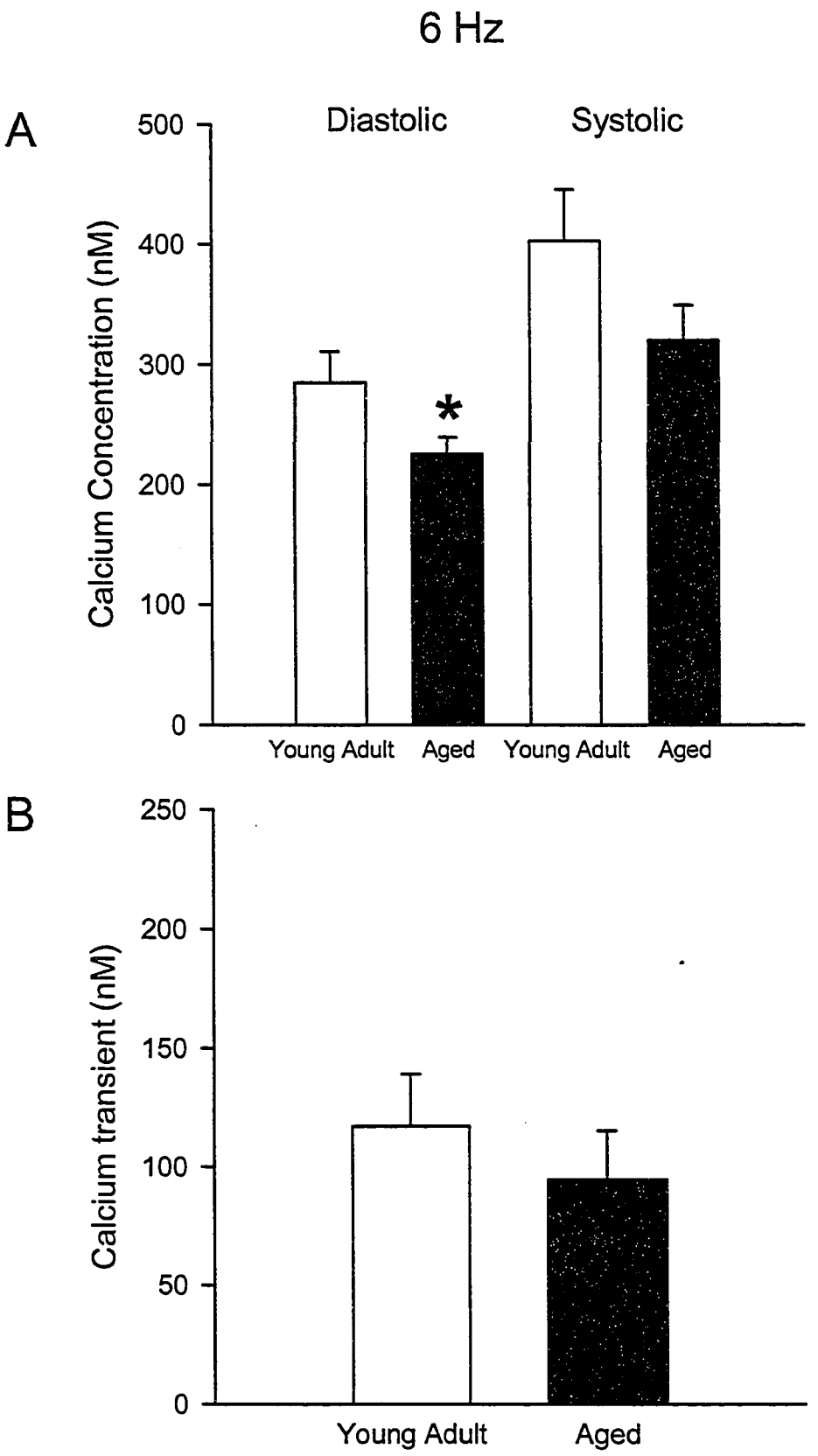
6 Hz
A
Diastolic
Systolic
Calcium Concentration (nM)
500
400
300
200
100
0
*
Young Adult
Aged
Young Adult
Aged
B
Calcium transient (nM)
250
200
150
100
50
0
Young Adult
Aged

Figure 26

significantly reduced in aged myocytes stimulated at 6 Hz compared to young adult myocytes stimulated at 6 Hz, whereas systolic Ca^{2+} concentrations were similar in both groups. Figure 26-B shows that mean Ca^{2+} transient amplitudes were similar in young adult and aged myocytes stimulated at 6 Hz. Thus, diastolic Ca^{2+} concentration was reduced in aged myocytes compared to younger cells at both 6 Hz and 2 Hz stimulation frequencies. However, differences in systolic Ca^{2+} and Ca^{2+} transient amplitudes between young adult and aged myocytes stimulated at 2 Hz were abolished at higher stimulation frequencies.

Ca^{2+} transient amplitude is modulated in part by SR Ca^{2+} load (Bers, 2001). Therefore, the final set of experiments in this series compared SR Ca^{2+} load in young adult and aged myocytes to determine whether SR Ca^{2+} load was altered in aged myocytes stimulated at higher frequencies. Figure 27 shows that mean caffeine-induced Ca^{2+} transients were similar in young adult and aged myocytes stimulated at 6 Hz. This suggests that age had no effect on SR Ca^{2+} load at higher stimulation frequencies.

In summary, when stimulation frequency was increased from 2 Hz to 6 Hz, peak contraction amplitudes and peak $I_{Ca\text{-}L}$ amplitudes were reduced in both young adult and aged myocytes. However, stimulation at 6 Hz abolished the differences in amplitudes of contraction, $I_{Ca\text{-}L}$ and Ca^{2+} transients between young adult and aged myocytes stimulated at 2 Hz.

Figure 27: SR Ca^{2+} load was similar in young adult and aged myocytes stimulated at 6 Hz.

(n = 13 young adult myocytes and 18 aged myocytes)

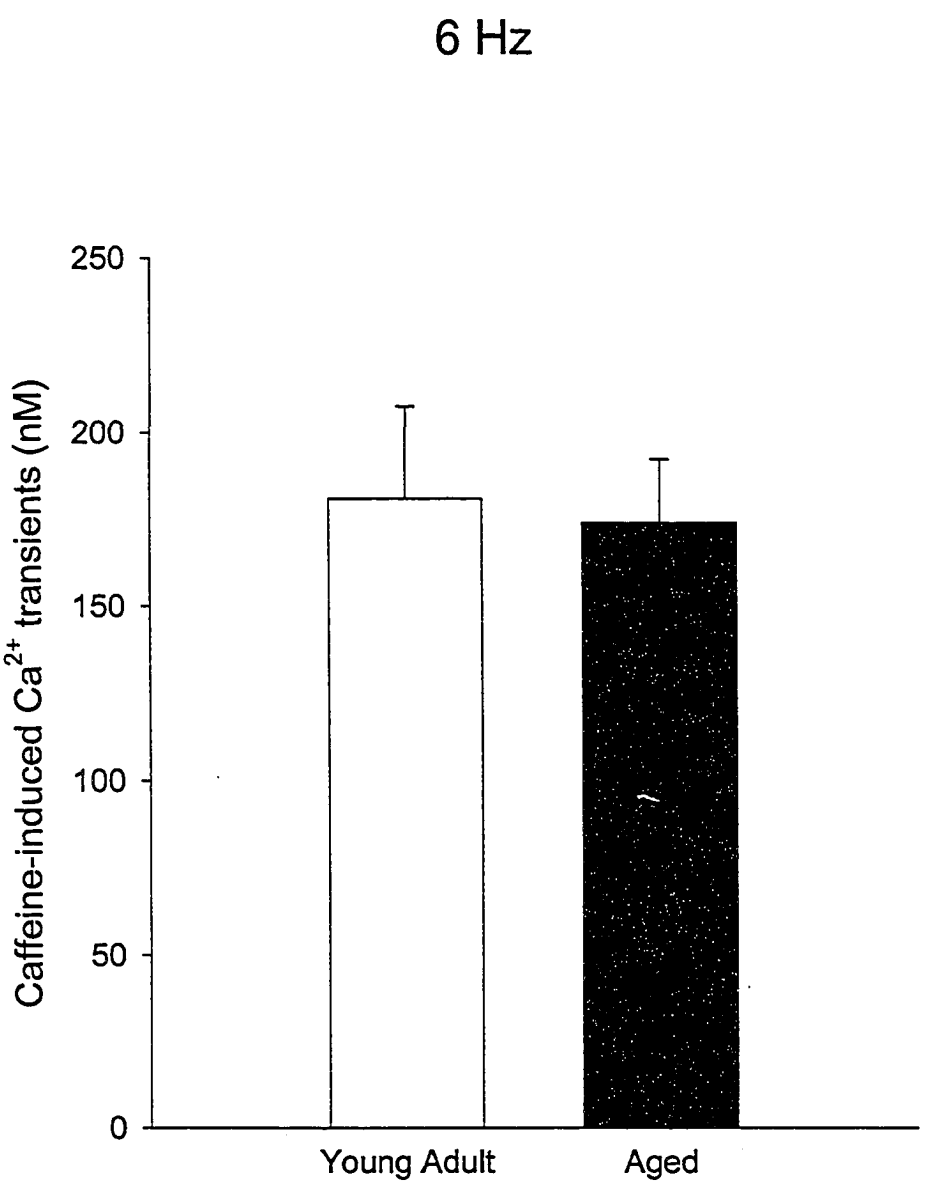
6 Hz
250
200
150
100
50
0
Caffeine-induced Ca^{2+} transients (nM)
Young Adult
Aged

Figure 27

2. The effects of cardiac β_2AR overexpression on EC coupling in ventricular myocytes

TG4 ventricular myocytes overexpress β_2ARs (Milano et al., 1994). Several studies have reported that contraction amplitudes and Ca^{2+} transient amplitudes are significantly increased in field-stimulated TG4 myocytes in experiments conducted at 22°C (Zhou et al., 1999a; Zhou et al., 1999b). Since cardiac contraction is graded by the magnitude of $I_{Ca\text{-}L}$, it would be expected that increases in the amplitude of contraction would be accompanied by an increase in $I_{Ca\text{-}L}$. However, the magnitude of $I_{Ca\text{-}L}$ measured in voltage clamped TG4 cells was found to be unchanged (Zhou et al., 1999a; Zhou et al., 1999b) or decreased (Heubach et al., 1999; Liggett et al., 2000) when compared to WT myocytes. An increase in contraction amplitude without a corresponding increase in $I_{Ca\text{-}L}$ in TG4 myocytes could be explained by an increase in gain of CICR, although this has not been investigated. To determine whether CICR gain is increased in TG4 myocytes, it is necessary to simultaneously measure $I_{Ca\text{-}L}$, Ca^{2+} transients and contraction in the same cell under the same experimental conditions. Therefore, this study measured $I_{Ca\text{-}L}$ and contraction simultaneously to determine if the relationship between $I_{Ca\text{-}L}$ and contraction was altered in TG4 myocytes. Ca^{2+} transients and SR Ca^{2+} load also were investigated under conditions comparable to those used to measure current and contraction. In addition, myocyte size was compared in WT and TG4 myocytes to determine if overexpression of β_2ARs altered resting cell length or cell membrane area.

Myocyte morphology

Freshly isolated ventricular myocytes from WT and TG4 mice were used for the experiments described in the following sections. Figure 28 shows a representative example of a WT myocyte (panel A) and a TG4 myocyte (panel B). Cells were visualized using differential interference contrast microscopy at 60X power and then photographed. In additional experiments, cell length was measured with the edge detector and cell capacitance was measured as described in the methods. Figure 29 shows that mean cell length (A) and mean cell capacitance (B) were similar in WT and TG4 myocytes. These results suggest that cell size and cell membrane area were similar in the two groups.

Contraction amplitude in field-stimulated WT and TG4 ventricular myocytes.

The first series of experiments was designed to compare the amplitudes of contraction in WT and TG4 myocytes at 37°C in cells that were field stimulated at 2 Hz. Representative contraction recordings of unloaded cell shortening from WT and TG4 myocytes are shown in Figure 30, panels A and B, respectively. Contraction amplitude was markedly increased in the TG4 myocyte compared to the WT myocyte, while time courses of contraction appeared similar in both groups. Figure 30-C shows that the mean amplitudes of contraction were significantly greater in TG4 myocytes compared to WT controls. Figure 31 shows the mean data for the time courses of contraction in WT and TG4 cells. The mean time-to-peak contraction (panel A) and the mean time-to-half relaxation (panel B) were similar in WT and TG4 myocytes. Thus, although contraction

Figure 28: WT (A) and TG4 (B) mouse ventricular myocytes visualized using differential interference contrast microscopy at 60X power.

A)

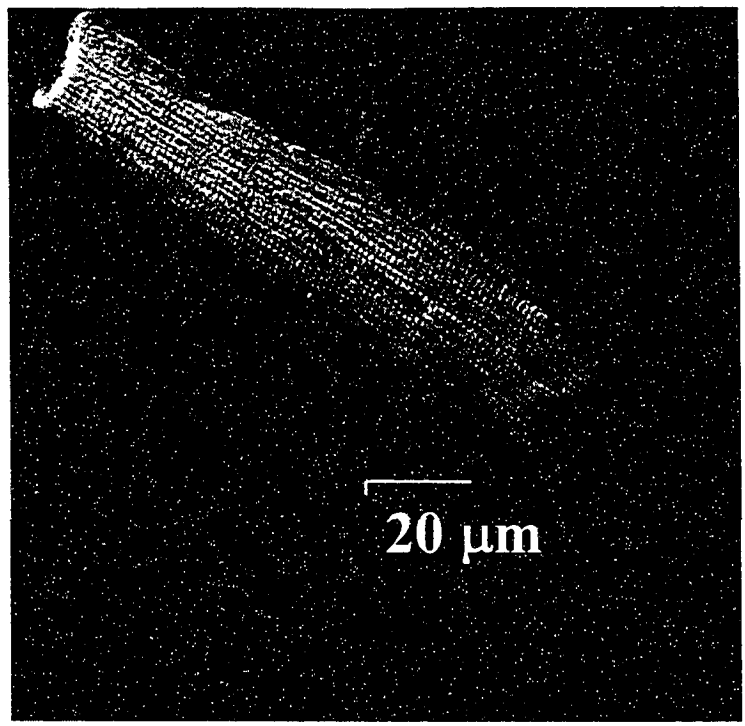

B)

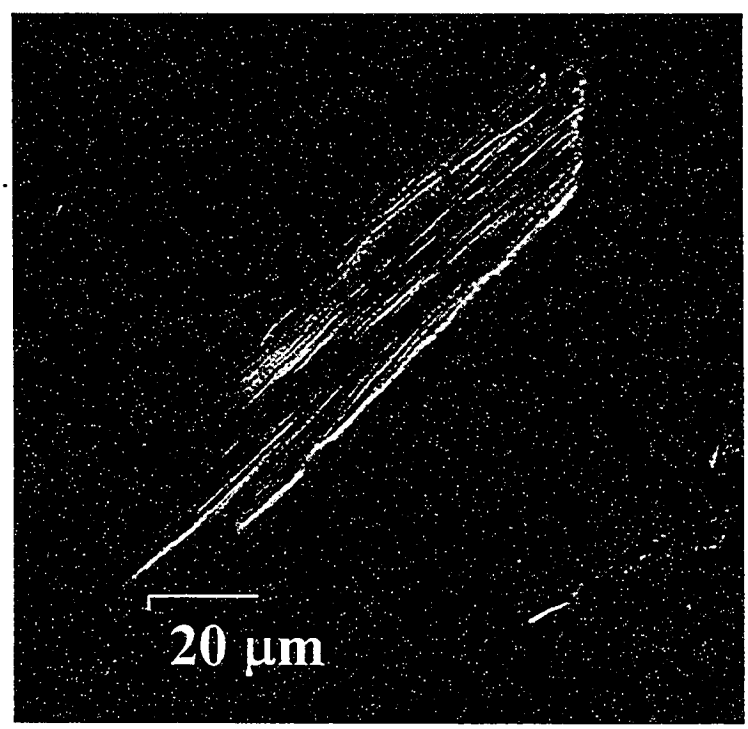

Figure 28

Figure 29: Ventricular myocytes isolated from WT and TG4 hearts were similar in size.

A) Resting cell length was similar in WT and TG4 myocytes. B) Cell capacitance was similar in WT and TG4 myocytes. (n = 9-11 WT myocytes and 5-8 TG4 myocytes)

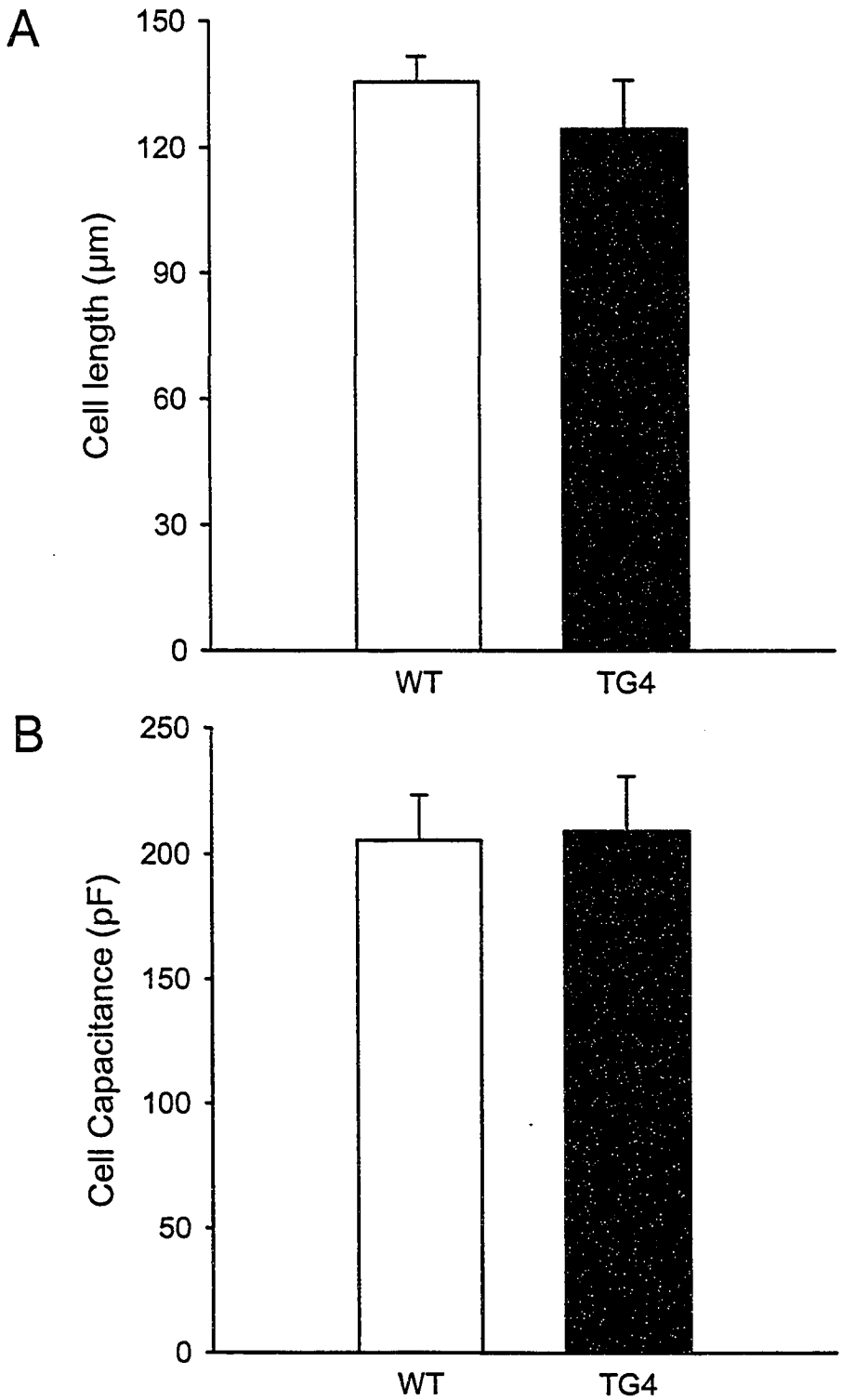
A
150
120
90
60
30
0
Cell length (µm)
WT
TG4
B
250
200
150
100
50
0
Cell Capacitance (pF)
WT
TG4

Figure 29

Figure 30: Contraction amplitude was significantly greater in field-stimulated TG4 myocytes in comparison to WT cells.

Representative contractions from WT (A) and TG4 (B) myocytes. C) Mean contraction amplitudes were significantly greater in TG4 myocytes compared to WT myocytes. Cell shortening was expressed as percent of maximum cell length. Cells were stimulated at 2 Hz at 37°C. * Significantly different from WT (n = 4 WT myocytes and n = 5 TG4 myocytes)

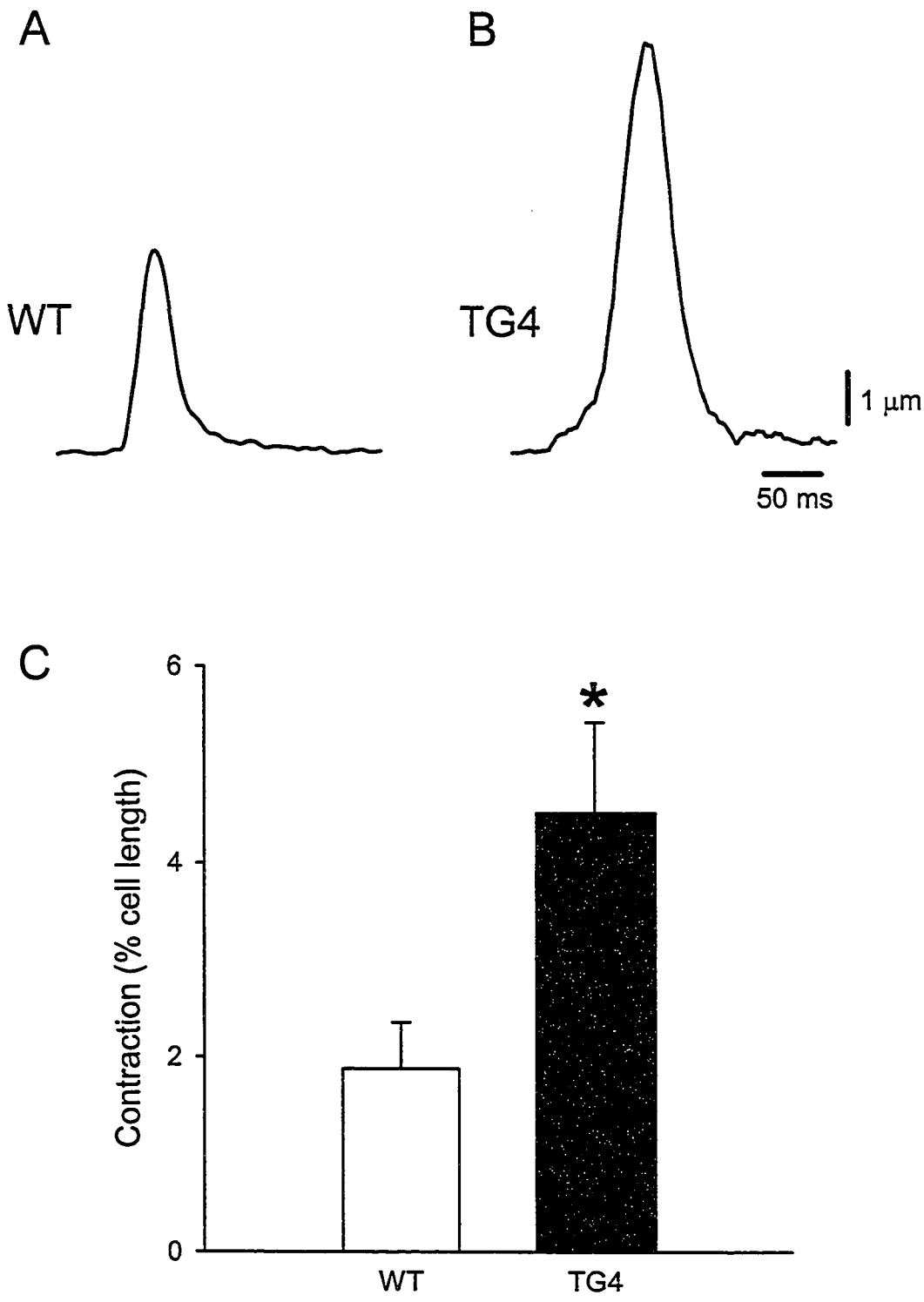

Figure 30

Figure 31: Time courses of contraction were similar in field-stimulated WT and TG4 myocytes.

There was no significant difference in time-to-peak contraction (A) or time to half-relaxation (B) between TG4 and WT myocytes. WT and TG4 cells were stimulated at 2 Hz at 37°C. (n = 7-9 WT myocytes and n = 5 TG4 myocytes)

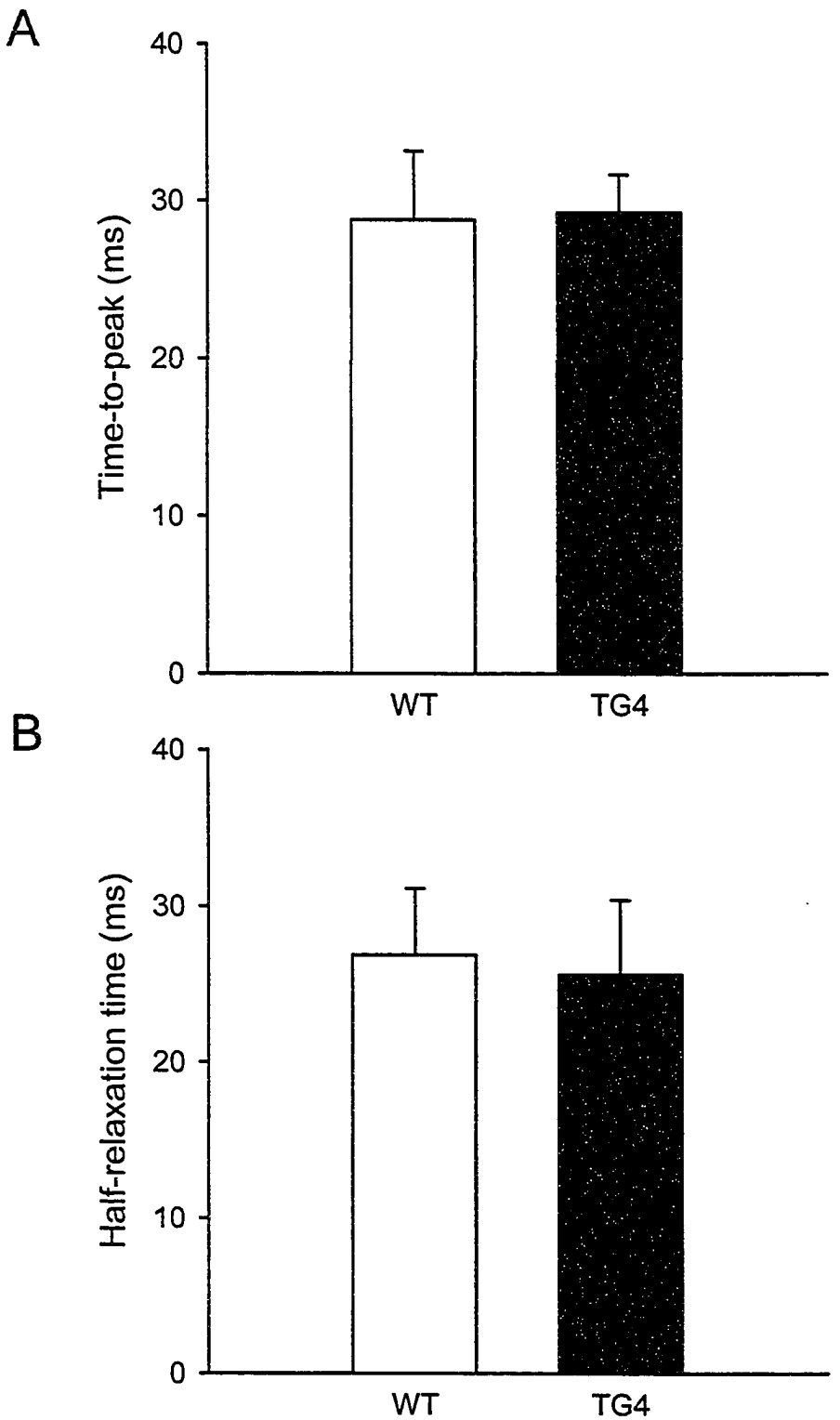
A
40
30
20
10
0
Time-to-peak (ms)
WT
TG4
B
40
30
20
10
0
Half-relaxation time (ms)
WT
TG4

Figure 31

amplitude was significantly increased in field-stimulated TG4 myocytes when compared to WT cells, there was no alteration in the time course of contraction between the two groups.

The next set of experiments assessed the effect of stimulation frequency on amplitudes of contraction in field-stimulated WT and TG4 myocytes. Figure 32 illustrates representative contraction recordings in WT and TG4 myocytes for stimulation frequencies of 2, 4, 6, 8 and 10 Hz. In both WT (A) and TG4 (B) myocytes, a positive inotropic effect was observed when cells were stimulated at 2, 4 and 6 Hz. In WT cells, contraction amplitude also was increased at 8 Hz, but declined at 10 Hz. In contrast, contraction amplitude appeared to plateau at 8 Hz in field-stimulated TG4 myocytes and declined at 10 Hz. In addition, it appeared that the amplitudes of contraction were greater in TG4 myocytes than in WT cells at all stimulation frequencies (Figure 32). Mean contraction-frequency data are shown in Figure 33. At all stimulation frequencies, amplitudes of contraction were greater in TG4 myocytes compared to WT cells. However, the difference between WT and TG4 myocytes was only significant at 2 Hz. In addition, peak amplitudes of contraction occurred at 6 Hz in TG4 myocytes, compared to 8 Hz in WT myocytes. Thus, it appears the contraction-frequency curve is shifted upwards and to the left in TG4 myocytes.

Contraction amplitude in voltage-clamped WT and TG4 ventricular myocytes.

In field-stimulation experiments contractions are activated by action potentials, whereas in voltage-clamp experiments rectangular voltage clamp steps activate

Figure 32: Contraction amplitudes increased with increasing stimulation frequency in WT and TG4 myocytes.

Representative examples of contractions from WT myocytes (A) and TG4 myocytes (B) paced at frequencies from 2 to 10 Hz.

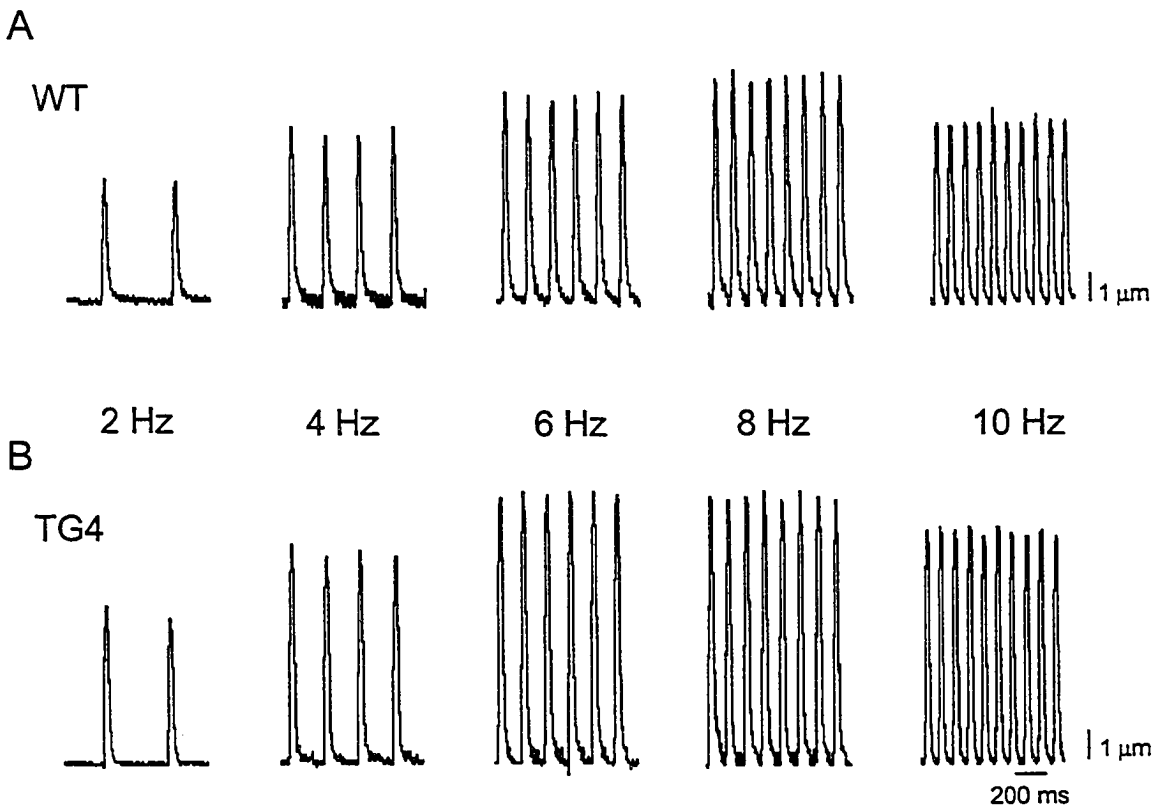

Figure 32

Figure 33: The contraction-frequency curve in WT and TG4 myocytes.

Contraction amplitude was significantly increased in TG4 myocytes compared to WT myocytes at 2 Hz. * Significantly different from WT (n = 4 WT myocytes and n = 5 TG4 myocytes)

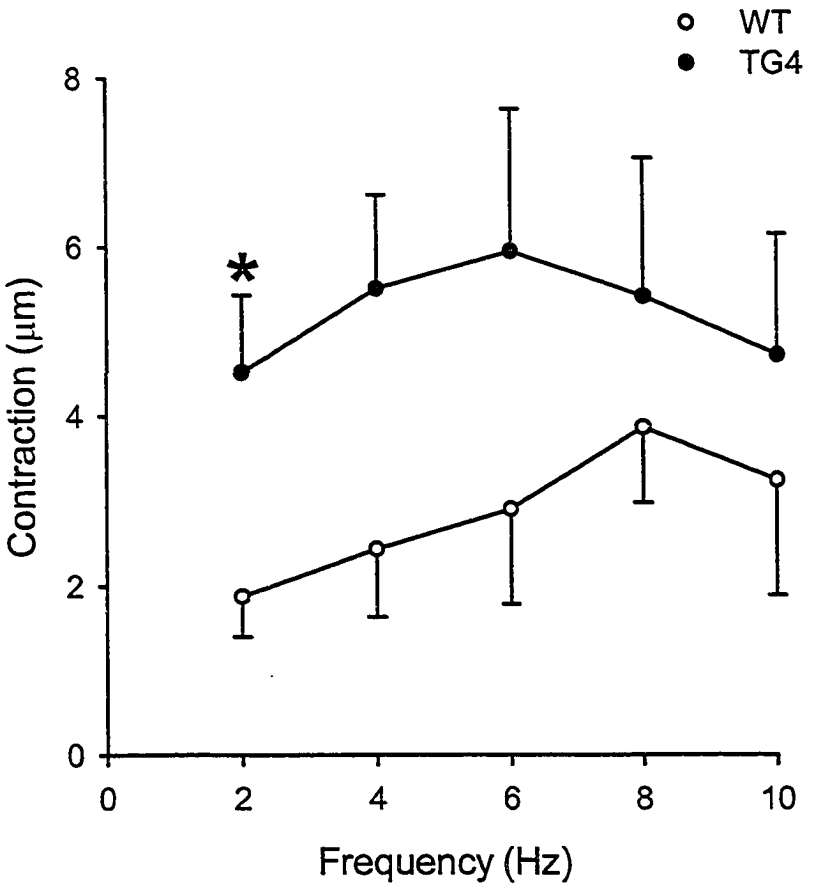

Figure 33

contractions. Therefore, the next series of experiments was designed to determine if increases in contraction amplitude persisted when the duration of depolarization was controlled by voltage clamp. Figure 34 shows representative contraction and Ca^{2+} current recordings from voltage clamped WT and TG4 myocytes. A sample voltage clamp protocol is illustrated in figure 34-A. Test steps were preceded by five 200 ms conditioning pulses to provide comparable activation histories in each cell. Trains of conditioning pulses were administered at a frequency of 2 Hz and followed by repolarization to a postconditioning potential of either –65 mV or –40 mV. Cells were depolarized by a step to 0 mV from the postconditioning potential to activate transmembrane currents and contractions. Since many previous studies of $I_{Ca\text{-}L}$ have used a postconditioning potential of –40 mV, the current study also used this potential. However, in other experiments, the more physiological postconditioning potential of -65 mV was used.

Figure 34 illustrates representative contractions and Ca^{2+} currents initiated by depolarizations from –65 mV to 0 mV in WT (B) and TG4 myocytes (C). Interestingly, in voltage clamped cells where the duration of depolarization was controlled, contraction amplitudes were similar in WT (panel B) and TG4 (panel C) myocytes. However, Ca^{2+} current was reduced in the TG4 myocyte (panel C) compared to the WT myocyte (panel B). Similar findings were observed when WT and TG4 myocytes were depolarized from –40 mV (data not shown). Mean amplitudes of contraction and current for WT and TG4 cells depolarized to 0 mV from either –65 or –40 mV are shown in figure 35, panels A and B, respectively. The top panel of figure 35-A, shows that amplitudes of contraction

Figure 34: Contraction amplitudes were similar in voltage-clamped TG4 and WT myocytes.

A) Following trains of 5 conditioning pulses, cells were depolarized from –65 mV to 0 mV. Representative traces illustrate that contraction amplitudes were similar in voltage clamped WT (B) and TG4 myocytes (C). Interestingly, $I_{Ca\text{-}L}$ was reduced in TG4 (C) myocytes in comparison to WT (B) myocytes.

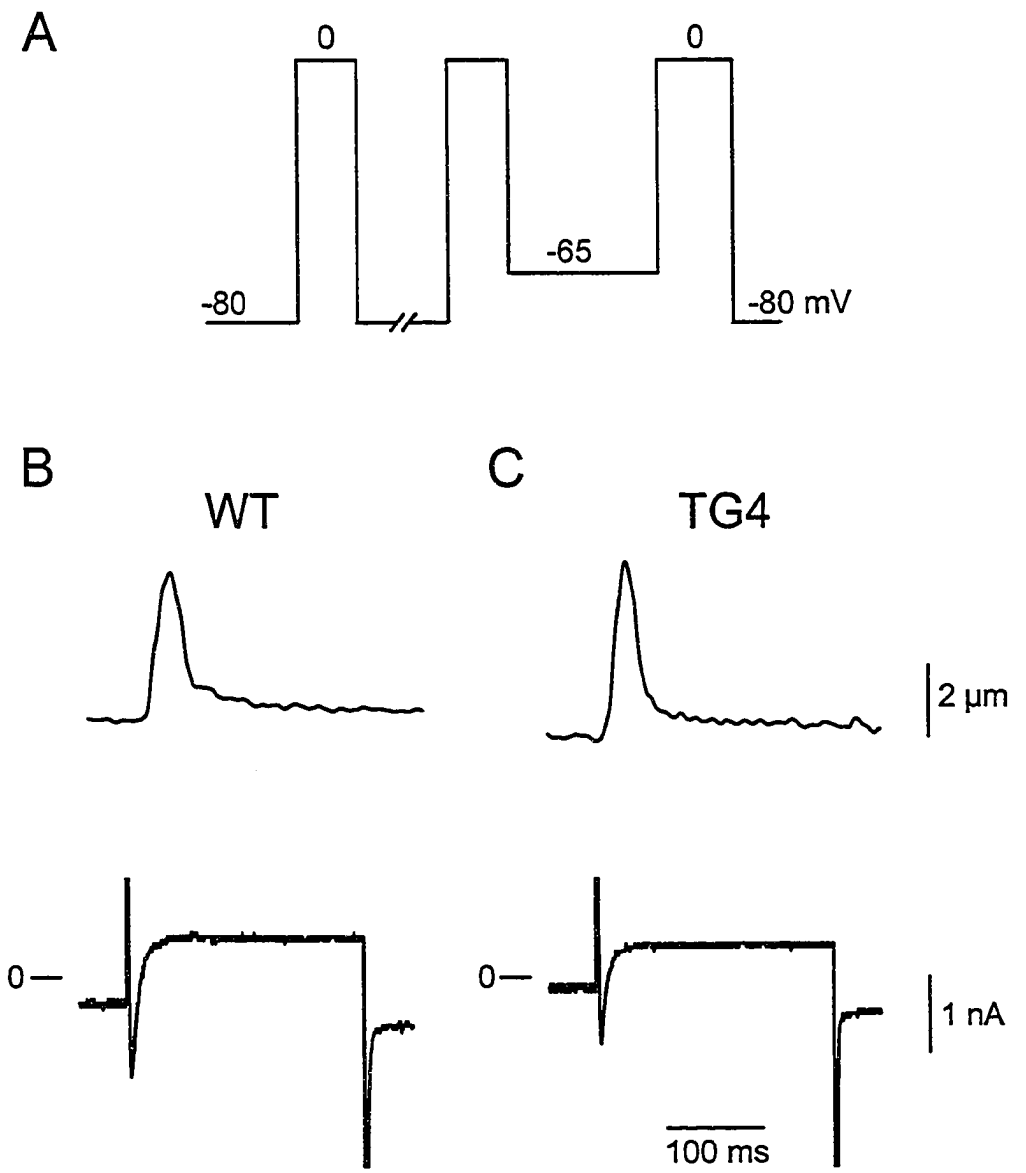

Figure 34

Figure 35: In voltage clamped cells, contraction amplitudes were similar in TG4 and WT myocytes, despite a significant reduction in $I_{Ca\text{-}L}$ in TG4 myocytes.

A) When cells were depolarized from -65 mV, contraction amplitudes (top panel) were similar in TG4 and WT myocytes. In contrast, mean peak $I_{Ca\text{-}L}$ density was significantly reduced in TG4 myocytes compared to WT cells (bottom panel). B) Similar results were obtained when cells were depolarized from -40 mV. * Significantly different from WT (n = 12-13 WT myocytes and n = 6-8 TG4 myocytes)

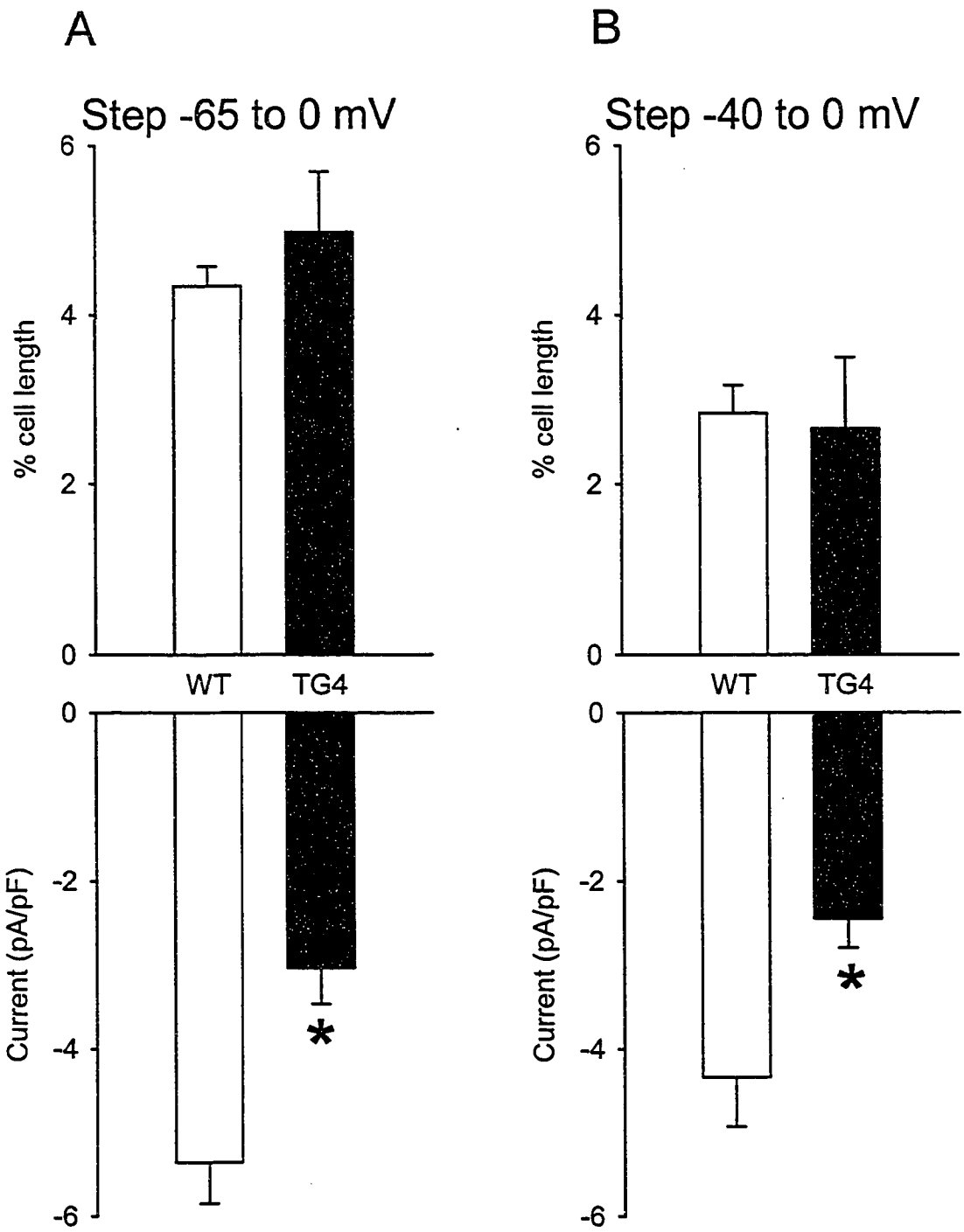
A
Step -65 to 0 mV
% cell length
6
4
2
0
WT
TG4
0
-2
-4
-6
Current (pA/pF)
*
B
Step -40 to 0 mV
% cell length
6
4
2
0
WT
TG4
0
-2
-4
-6
Current (pA/pF)
*

Figure 35

were not significantly different between WT and TG4 myocytes when cells were depolarized from –65 mV to 0 mV. However, peak $I_{Ca\text{-}L}$ density was significantly reduced in TG4 myocytes compared to WT myocytes (Figure 35-A, bottom). Figure 35-B shows that, when cells were depolarized from –40 mV, contraction amplitudes were similar in WT and TG4 myocytes (top panel), whereas peak $I_{Ca\text{-}L}$ density was significantly decreased in TG4 myocytes (bottom panel). Next, experiments determined if time courses of contraction differed in voltage clamped WT and TG4 myocytes. The mean time courses for contractions in WT and TG4 myocytes activated by test steps from either –65 mV or –40 mV are shown in figure 36. When cells were depolarized from –65 mV, times-to-peak contraction (panel A) and times-to-half relaxation (panel B) were similar between WT and TG4 myocytes. Similarly, when WT and TG4 cells were depolarized from –40 mV, no differences were observed in either times-to-peak contraction or times-to-half relaxation (Figure 36, panels C and D). Thus, in voltage clamped cells where the duration of depolarization is controlled, the amplitudes and time courses of contraction were similar in WT and TG4 myocytes. However, peak $I_{Ca\text{-}L}$ was significantly reduced in TG4 myocytes.

The effects of action potential duration on contraction amplitude.

Differences in the amplitudes of contraction in field-stimulated WT and TG4 myocytes were abolished when cells were voltage clamped. In field-stimulated myocytes, contractions were initiated by action potentials, whereas contractions were initiated by 250 ms rectangular test steps in voltage clamp experiments. Since action potential duration is prolonged in TG4 myocytes compared to WT cells (Zhou et al., 1999b), it was hypothesized that differences in amplitudes of contraction in WT and TG4

Figure 36: Time courses of contraction were similar in voltage clamped TG4 and WT myocytes.

When cells were depolarized from –65 mV, mean time-to-peak contraction (A) and mean time-to-half (B) relaxation were similar in TG4 and WT myocytes. Mean time courses of contraction were also similar when TG4 and WT cells were depolarized from –40 mV, panels (C) and (D). (n = 12-13 WT myocytes and n = 6-8 TG4 myocytes)

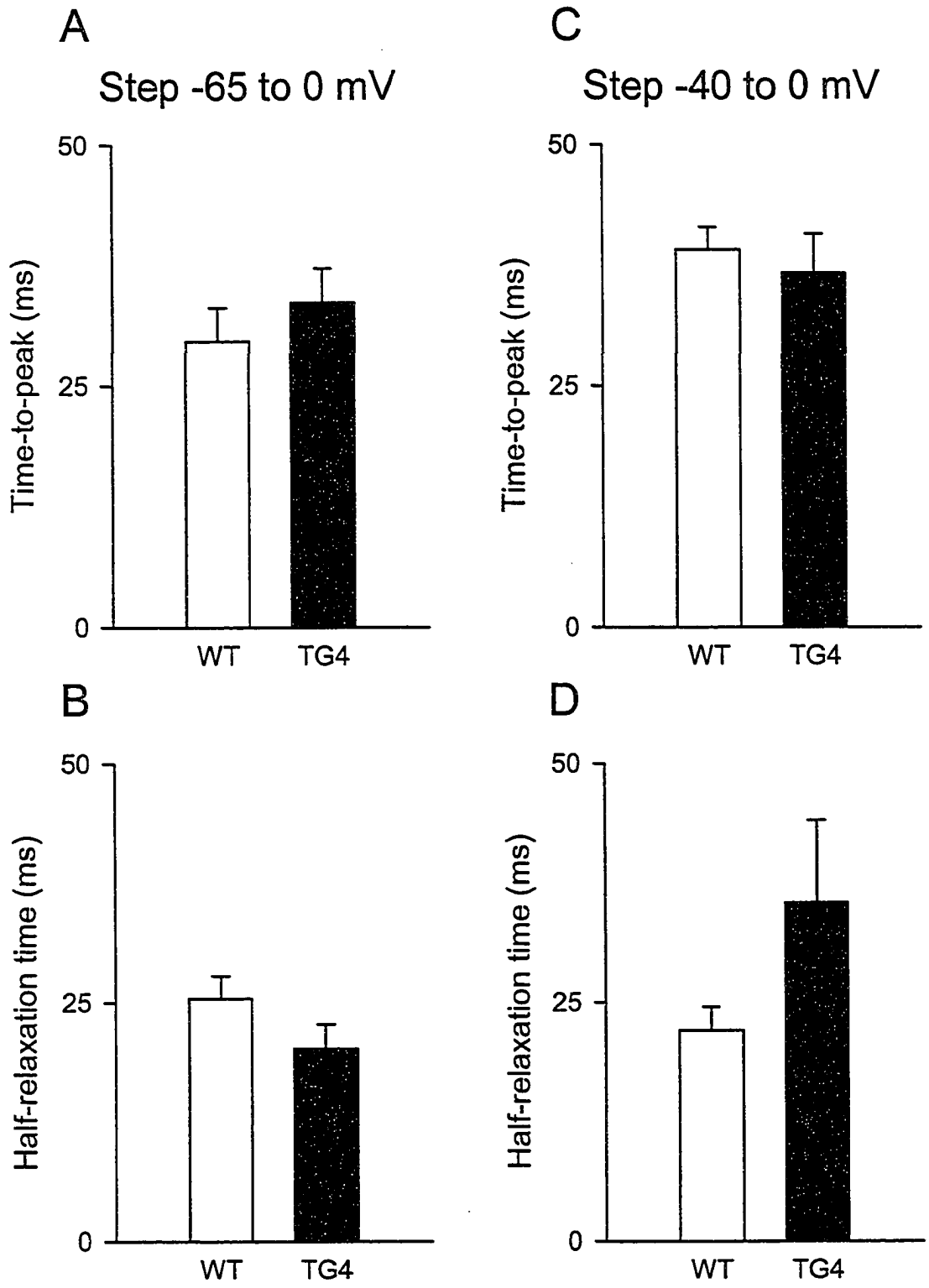
A
Step -65 to 0 mV
Time-to-peak (ms)
50
25
0
WT
TG4
C
Step -40 to 0 mV
Time-to-peak (ms)
50
25
0
WT
TG4
B
Half-relaxation time (ms)
50
25
0
WT
TG4
D
Half-relaxation time (ms)
50
25
0
WT
TG4

Figure 36

myocytes might reflect differences in action potential duration. To test this hypothesis, ventricular myocytes were voltage clamped and activated with simulated WT and TG4 action potential waveforms. The waveforms were created with previously published values for WT and TG4 resting potentials, action potential amplitudes and action potential durations at 50% and 90% repolarization (Zhou et al., 1999b). All values were similar in WT and TG4 myocytes with the exception of action potential duration at 90% repolarization, which was 48 ms in WT cells and 104 ms in TG4 cells. Figure 37 illustrates the effects of action potential duration on the amplitude of contraction. The waveforms for the simulated WT and TG4 action potentials are shown in panels A and panel B, respectively. Cells were held at –70 mV, stimulated with trains of either WT or TG4 action potentials and contractions were recorded. Figure 37-C, shows a representative recording of contraction from a WT myocyte activated by a simulated WT action potential (left panel). When the same cell was activated with a simulated TG4 action potential (right panel), contraction amplitude was noticeably greater. Mean contraction data are shown in figure 37-D. Mean contraction amplitude was significantly greater when cells were activated with a simulated TG4 action potential than when the cells were activated with a simulated WT action potential. Thus, the increase in action potential duration could contribute to the increased amplitudes of contraction in field-stimulated TG4 myocytes.

Contraction-voltage and current voltage relationships in WT and TG4 myocytes.

The decrease in peak $I_{Ca\text{-}L}$ in TG4 myocytes (Figure 35) could be caused by a reduction in maximum Ca^{2+} current or a shift in the current voltage relationship. To

Figure 37: Contraction amplitudes were greater when cells were voltage clamped with action potentials designed to mimic the prolonged duration of TG4 action potentials.

A representative WT myocyte was voltage clamped with a simulated action potential waveform designed to mimic the WT action potential (A). C) The simulated action potential triggered a contraction (left panel). Resting potential (-70 mV), peak action potential amplitude (118 mV) and time to 50% repolarization (8.7 ms) were the same for the simulated WT and TG4 action potentials (Zhou et al., 1999b). The time to 90% repolarization of the simulated action potential was increased from 48 ms to 104 ms to mimic a TG4 action potential (B). C) The amplitude of contraction of the same myocyte was increased when action potential duration was increased (right panel). D) Mean amplitudes of contraction were increased when myocytes were voltage clamped with simulated TG4 action potentials compared to when cells were voltage clamped with simulated WT action potentials.

* Significantly different from WT (n = 13 myocytes)

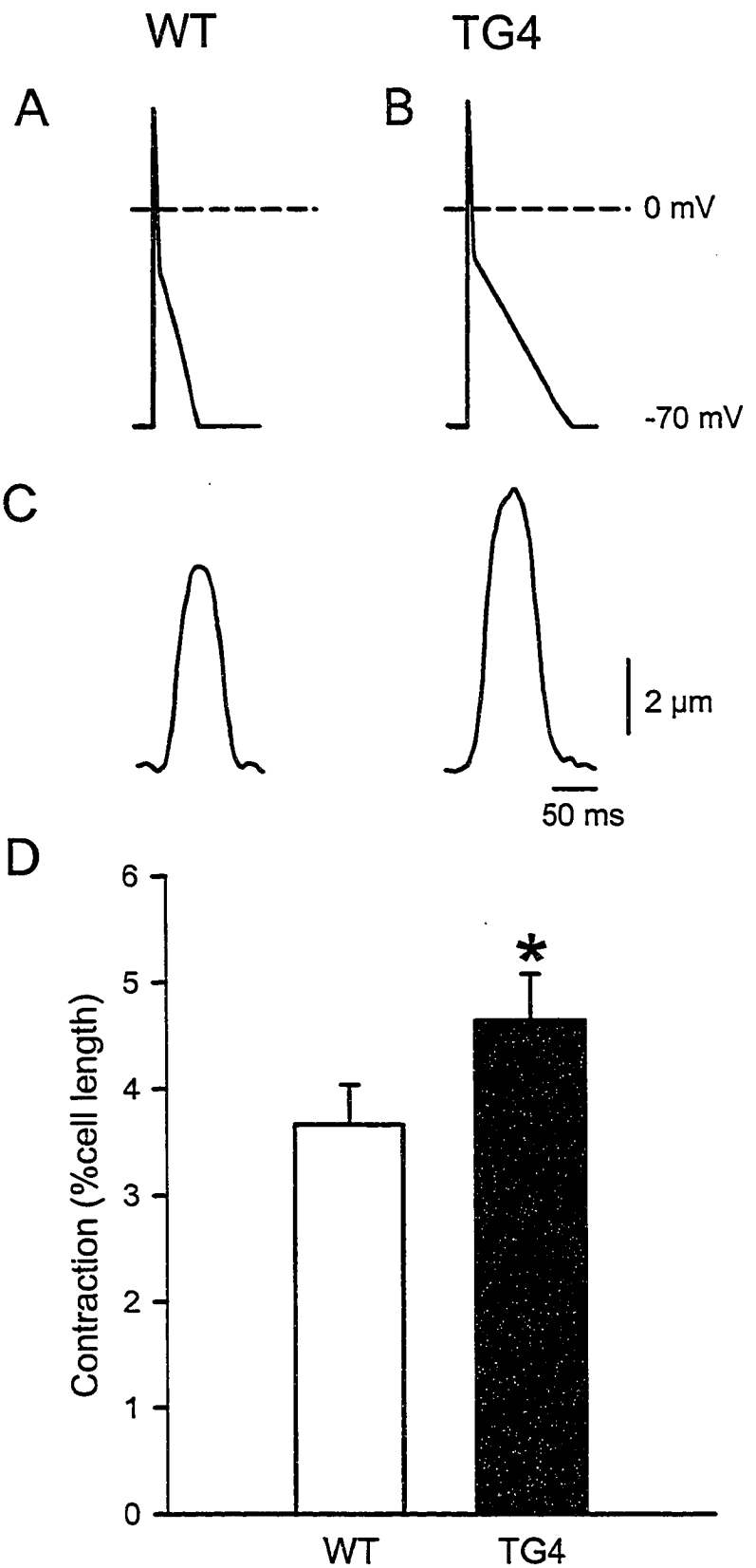
WT
TG4
A
B
0 mV
-70 mV
C
2 µm
50 ms
D
Contraction (%cell length)
0
1
2
3
4
5
6
*
WT
TG4

Figure 37

differentiate between these possibilities the voltage dependencies of contraction and Ca^{2+}current were determined. Figure 38 shows the mean contraction-voltage and mean current-voltage relationships for WT and TG4 myocytes. The voltage clamp protocol used in this set of experiments is illustrated in figure 38-A. Following a train of five conditioning pulses, administered at a frequency of 2 Hz, test steps were initiated from a postconditioning potential of –40 mV. With each repetition of the protocol, the test step was increased by 10 mV up to +60 mV. Contraction and current amplitudes were then plotted against voltage to construct contraction-voltage and current-voltage curves for WT and TG4 myocytes (Figure 38, panels B and C). Figure 35-B shows that contraction-voltage relationships for WT and TG4 myocytes were bell-shaped and peaked near 0 mV. Likewise, current-voltage relationships were bell-shaped and peaked at 0 mV (Figure 38-C). This indicated that the contraction-voltage and current-voltage relationships were not shifted in TG4 myocytes compared to WT myocytes. Interestingly, although contraction amplitudes were virtually identical in WT and TG4 myocytes (Figure 38-B), $I_{Ca\text{-}L}$ was significantly reduced between –10 and +20 mV in TG4 myocytes (Figure 38-C). Thus, contraction amplitude was maintained in TG4 myocytes, despite a significant reduction in $I_{Ca\text{-}L}$. This suggested that the relationship between $I_{Ca\text{-}L}$ and contraction was altered in TG4 myocytes.

Ca^{2+} transients and SR Ca^{2+} load in WT and TG4 myocytes.

An increase in the gain of EC coupling could account, at least in part, for the observation that contraction amplitude is maintained in TG4 myocytes, despite a reduction in $I_{Ca\text{-}L}$. Therefore, the next series of experiments examined and compared SR

Figure 38: Contraction amplitude is maintained despite a significant reduction in the magnitude of $I_{Ca\text{-}L}$.

A) Following 5 conditioning pulses, cells were depolarized from –40 to +60 mV in 10 mV increments. B) Mean contraction-voltage relationships were similar in TG4 and WT myocytes. C) Mean current-voltage relationships were depressed in TG4 myocytes compared to WT cells. This difference was statistically significant at membrane potentials from –10 to +20 mV. * Significantly different from WT (n = 12 WT myocytes and n = 6 TG4 myocytes)

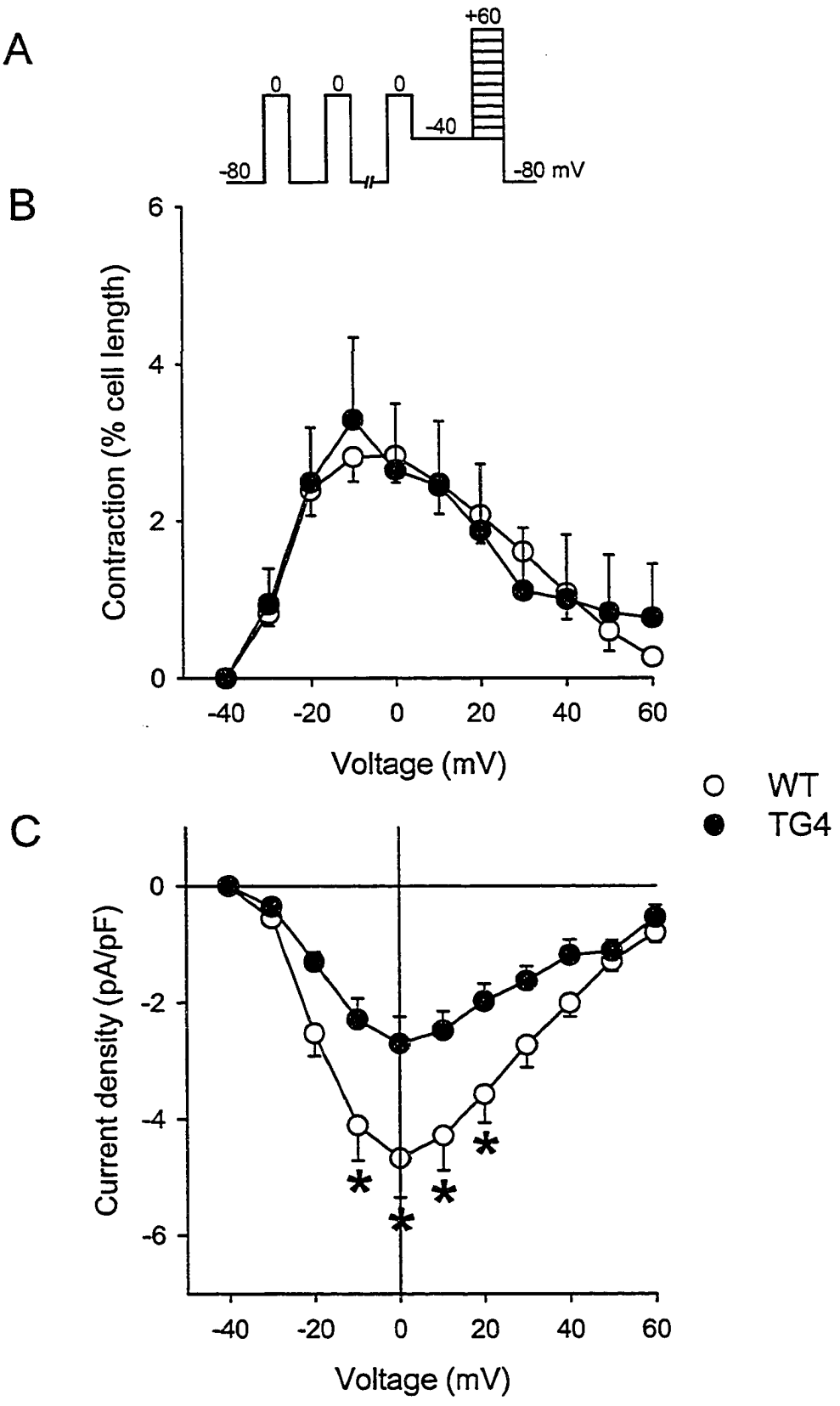
A
+60
0
0
0
-40
-80
-80 mV
B
Contraction (% cell length)
6
4
2
0
-40
-20
0
20
40
60
Voltage (mV)
WT
TG4
C
Current density (pA/pF)
0
-2
-4
-6
*
*
*
*
-40
-20
0
20
40
60
Voltage (mV)

Figure 38

Ca^{2+} release and SR Ca^{2+} content in WT and TG4 myocytes. The first set of studies compared and characterized diastolic Ca^{2+} concentrations and Ca^{2+} transient amplitudes in WT and TG4 mice. The ratiometric dye fura-2 was used to measure Ca^{2+} concentrations. Cells were held at –80 mV and depolarized by trains of voltage clamp steps to 0 mV at a frequency of 2 Hz. Representative Ca^{2+} transients from WT and TG4 myocytes and mean Ca^{2+} transient data are shown in Figure 39. Panel A illustrates a train of 5 Ca^{2+} transients from a WT myocyte and panel B illustrates a train of 5 Ca^{2+} transients from a TG4 myocyte. Diastolic Ca^{2+} concentrations and peak Ca^{2+} concentrations appeared similar in WT and TG4 myocytes. Figure 39-C shows that mean diastolic Ca^{2+} concentrations were not significantly different between WT and TG4 myocytes. Furthermore, mean amplitudes of Ca^{2+} transients elicited by steps from –80 to 0 mV were similar in WT and TG4 myocytes (Figure 39-D). These data demonstrate that, like contractions, Ca^{2+} transient amplitudes were similar in voltage clamped WT and TG4 myocytes.

Studies have shown that the sensitivity of CICR is increased when SR Ca^{2+} load is elevated (Bassani et al., 1995; Lukyanenko et al., 1996; Viatchenko-Karpinski & Gyorke, 2001). Therefore, the next series of experiments investigated the possibility that increased CICR gain was accompanied by an increase in SR Ca^{2+} stores in TG4 myocytes. Fura-2 was used to measure Ca^{2+} concentrations in voltage clamped WT and TG4 myocytes. Figure 40 shows representative examples of caffeine-induced Ca^{2+} transients from WT and TG4 myocytes. The voltage protocol used for this series of experiments is illustrated in figure 40 (*inset*). Cells were held at -80 mV and then

Figure 39: Diastolic Ca^{2+} levels and Ca^{2+} transient amplitudes were similar in WT and TG4 myocytes.

Ca^{2+} transients were elicited by voltage clamp steps from –80 to 0 mV. Representative Ca^{2+} transients from WT (A) and TG4 (B) myocytes. C) Mean diastolic Ca^{2+} levels were similar in WT and TG4 myocytes. D) Ca^{2+} transient amplitudes were not significantly different between TG4 and WT myocytes. (n = 10 WT myocytes and n = 6 TG4 myocytes)

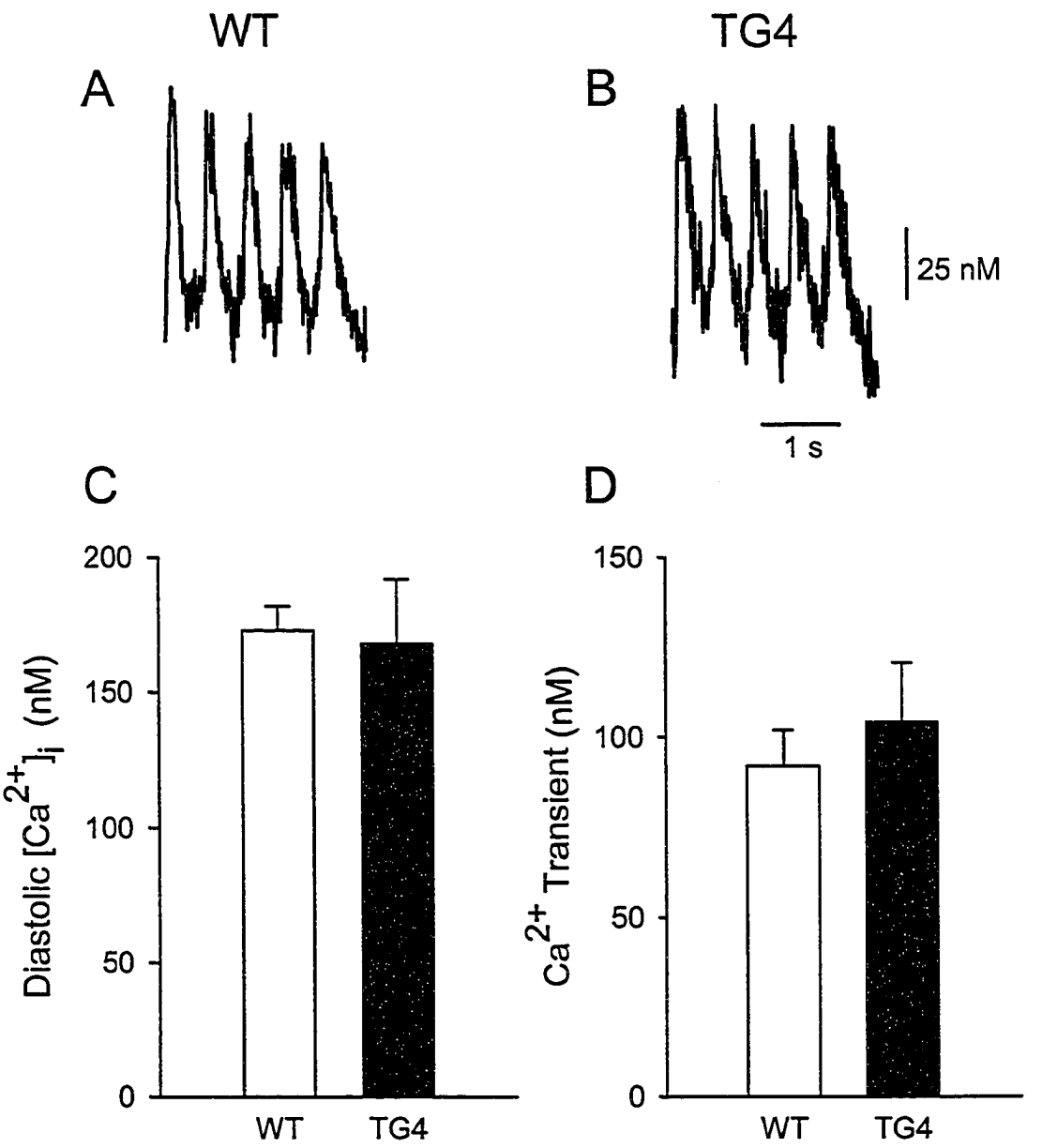
WT
TG4
A
B
25 nM
1 s
C
D
200
150
100
50
0
Diastolic [Ca2+]i (nM)
WT
TG4
150
100
50
0
Ca2+ Transient (nM)
WT
TG4

Figure 39

Figure 40: SR Ca^{2+} load, assessed by the rapid application of 10 mM caffeine, was greater in TG4 myocytes compared to WT cells.

The voltage-clamp protocol used in these experiments is shown in the top panel. Representative Ca^{2+} transients induced by caffeine show that SR Ca^{2+} load is greater in TG4 myocytes (A) compared to WT myocytes (B).

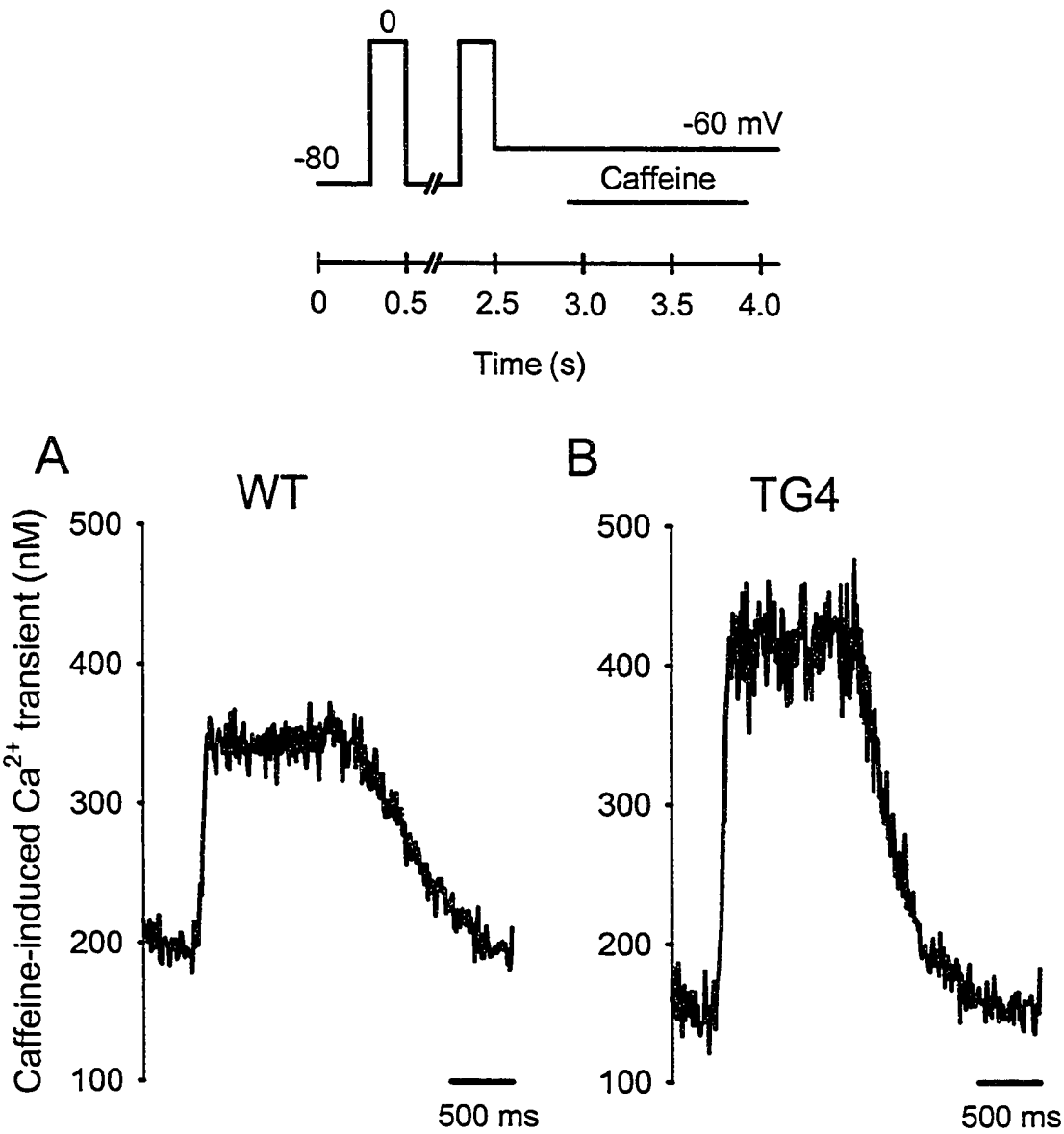
0
-60 mV
-80
Caffeine
0
0.5
2.5
3.0
3.5
4.0
Time (s)
A
WT
B
TG4
Caffeine-induced Ca2+ transient (nM)
500
400
300
200
100
500 ms
500 ms

Figure 40

stimulated with a train of five conditioning pulses delivered at a frequency of 2 Hz. Following the last conditioning pulse, cells were held at –60 mV and caffeine was applied for 1 second with a rapid solution switcher. Caffeine was applied in a 0 mM Na^+, 0 mM Ca^{2+} solution to minimize the loss of Ca^{2+} through the NCX. Figure 40-A illustrates a caffeine-induced Ca^{2+} transient from a WT myocyte and panel B illustrates a caffeine-induced Ca^{2+} transient from a TG4 myocyte. The amplitude of the caffeine-induced Ca^{2+} transient was markedly greater in the TG4 myocyte than in the WT myocyte. Mean data for caffeine-induced Ca^{2+} transients are shown in figure 41. Mean amplitudes of caffeine-induced Ca^{2+} transients were significantly greater in TG4 myocytes compared to WT myocytes. Thus, increased SR Ca^{2+} load likely contributes to the increased gain of CICR observed in TG4 myocytes.

The effects of β_2AR blockade on Ca^{2+} handling in WT and TG4 myocytes.

Increased SR Ca^{2+} stores in TG4 myocytes may be at least partially attributable to constitutive β_2AR activity. Therefore, the next series of experiments compared SR Ca^{2+} stores in WT and TG4 myocytes in the presence of the β_2AR inverse agonist ICI. Initial experiments characterized diastolic Ca^{2+} concentrations and Ca^{2+} transient amplitudes in WT and TG4 myocytes in the absence and presence of the β_2AR inverse agonist ICI. Briefly, cells were superfused with a HEPES-buffered solution that contained 0 or 0.5 μM ICI. Cells were held at –80 mV and depolarized by trains of voltage clamp steps to 0 mV at a frequency of 2 Hz. Figure 42 shows the effects of ICI on diastolic Ca^{2+} concentration and Ca^{2+} transient amplitudes in WT myocytes. Figure 42-A shows representative trains of Ca^{2+} transients from WT myocytes in the absence (left panel) and

Figure 41: SR Ca^{2+} load was significantly greater in TG4 myocytes compared to WT myocytes.

Mean amplitudes of caffeine-induced transients were greater in TG4 myocytes compared to WT myocytes. * Significantly different from WT (n = 10 WT myocytes and n = 7 TG4 myocytes)

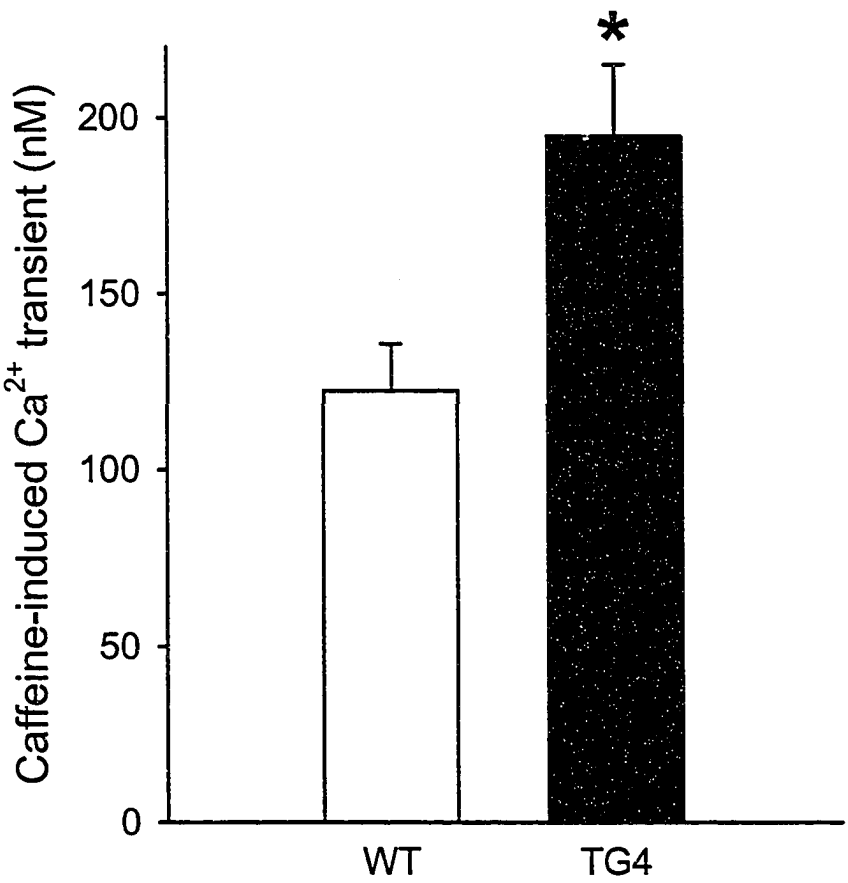

Figure 41

Figure 42: The β_2AR inverse agonist ICI 118, 151 had no effect on diastolic Ca^{2+} levels or Ca^{2+} transient amplitudes in WT myocytes.

Voltage clamp steps from –80 to 0 mV were used to trigger Ca^{2+} transients. A) Representative Ca^{2+} transients from WT myocytes in the absence (control) and presence (ICI) of the β_2AR inverse agonist ICI. Mean diastolic Ca^{2+} levels (B) and Ca^{2+} transient amplitudes (C) were similar in the presence and absence of ICI in WT myocytes. (n = 10 control myocytes and n = 5 myocytes treated with ICI)

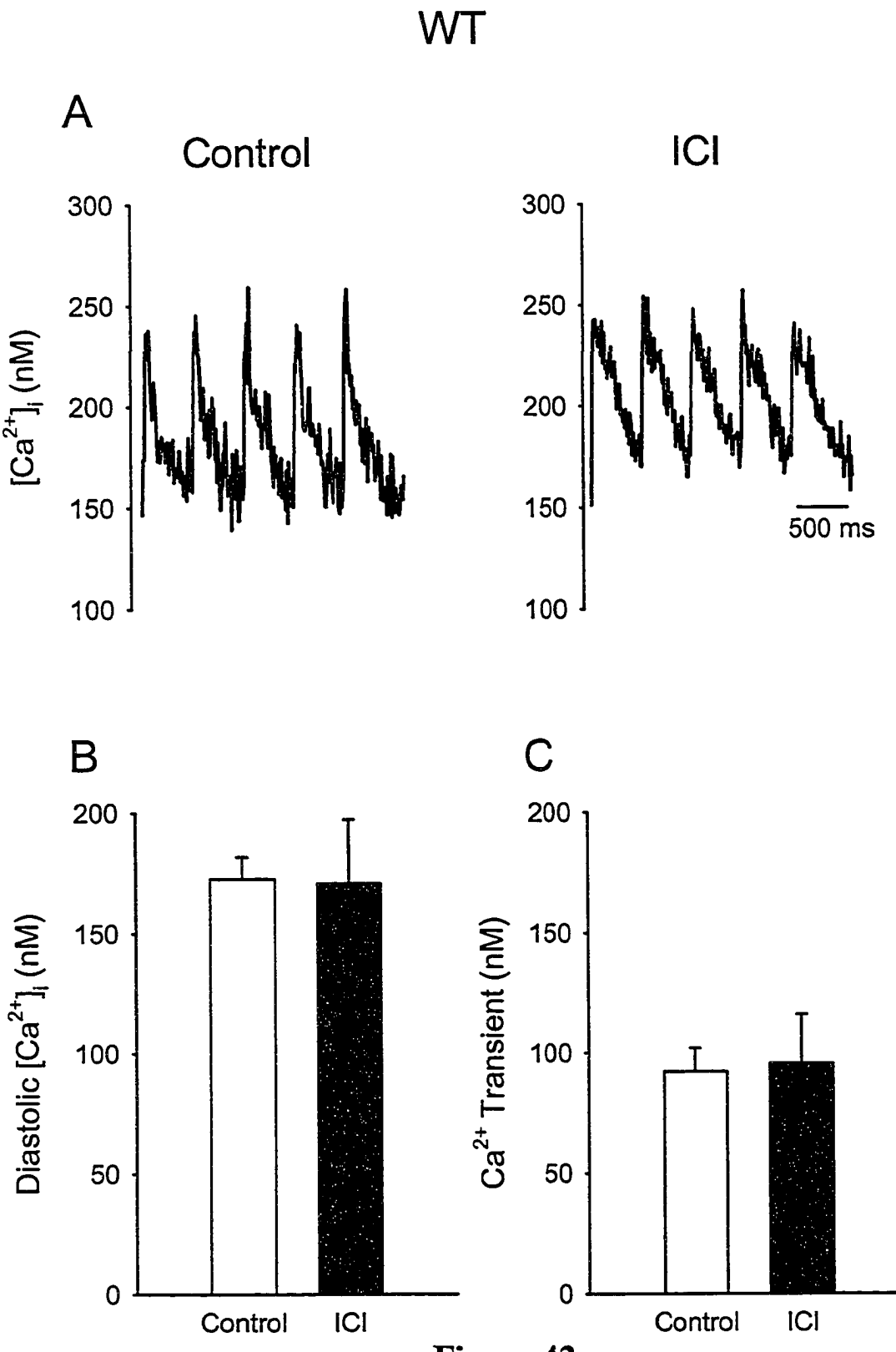
WT
A
Control
ICl
300
250
200
150
100
[Ca2+]i (nM)
500 ms
B
C
Diastolic [Ca2+]i (nM)
Ca2+ Transient (nM)
200
150
100
50
0
Control
ICl

Figure 42

presence (right panel) of ICI. It appeared that ICI had no effect on either diastolic Ca^{2+} concentrations or peak systolic Ca^{2+} concentrations in WT myocytes. Figure 42-C and D shows that mean diastolic Ca^{2+} concentrations and mean Ca^{2+} transient amplitudes were not altered in WT myocytes treated with ICI compared to control WT myocytes. Figure 43 shows the effects of ICI on diastolic Ca^{2+} concentrations and Ca^{2+} transient amplitudes in TG4 myocytes. Representative example trains of Ca^{2+} transients from control TG4 myocytes (left panel) and TG4 myocytes treated with ICI (right panel) are shown in Figure 43-A. Resting and peak Ca^{2+} concentrations appeared similar in TG4 myocytes treated with ICI and control TG4 myocytes. Figure 43-B shows mean data which demonstrates that diastolic Ca^{2+} concentrations were not significantly different in TG4 myocytes treated with ICI compared to control TG4 myocytes. Figure 43-C shows that mean Ca^{2+} transient amplitudes were similar in TG4 myocytes treated with ICI and control TG4 myocytes. Thus, it appeared that constitutive β_2AR activity had no effect on diastolic Ca^{2+} concentrations or Ca^{2+} transient amplitudes in TG4 myocytes in cells activated by voltage clamp steps.

The final set of experiments determined if increased SR Ca^{2+} stores in TG4 myocytes were the result of constitutive β_2AR activity. Figure 44 shows the effects of ICI on caffeine-induced Ca^{2+} transients in WT myocytes. Cells were superfused with a HEPES-buffered solution containing 0 or 0.5 μM ICI. Cells were voltage clamped at –80 mV and stimulated with the voltage protocol illustrated in figure 44-A. Figure 44-B shows a representative caffeine-induced Ca^{2+} transient in a control WT myocyte (left panel), whereas the right panel illustrates a caffeine-induced Ca^{2+} transient from a WT

Figure 43: The β_2AR inverse agonist ICI 118, 151 had no significant effect on diastolic Ca^{2+} levels or Ca^{2+} transient amplitudes in TG4 myocytes.

Voltage clamp steps from –80 to 0 mV were used to trigger Ca^{2+} transients. A) Representative Ca^{2+} transients from TG4 myocytes in the absence (control) and presence (ICI) of the β_2AR inverse agonist ICI. Mean diastolic Ca^{2+} levels (B) and Ca^{2+} transient amplitudes (C) were not significantly different in TG4 myocytes treated with ICI compared to control TG4 myocytes. (n = 6 control myocytes and n = 3 myocytes treated with ICI)

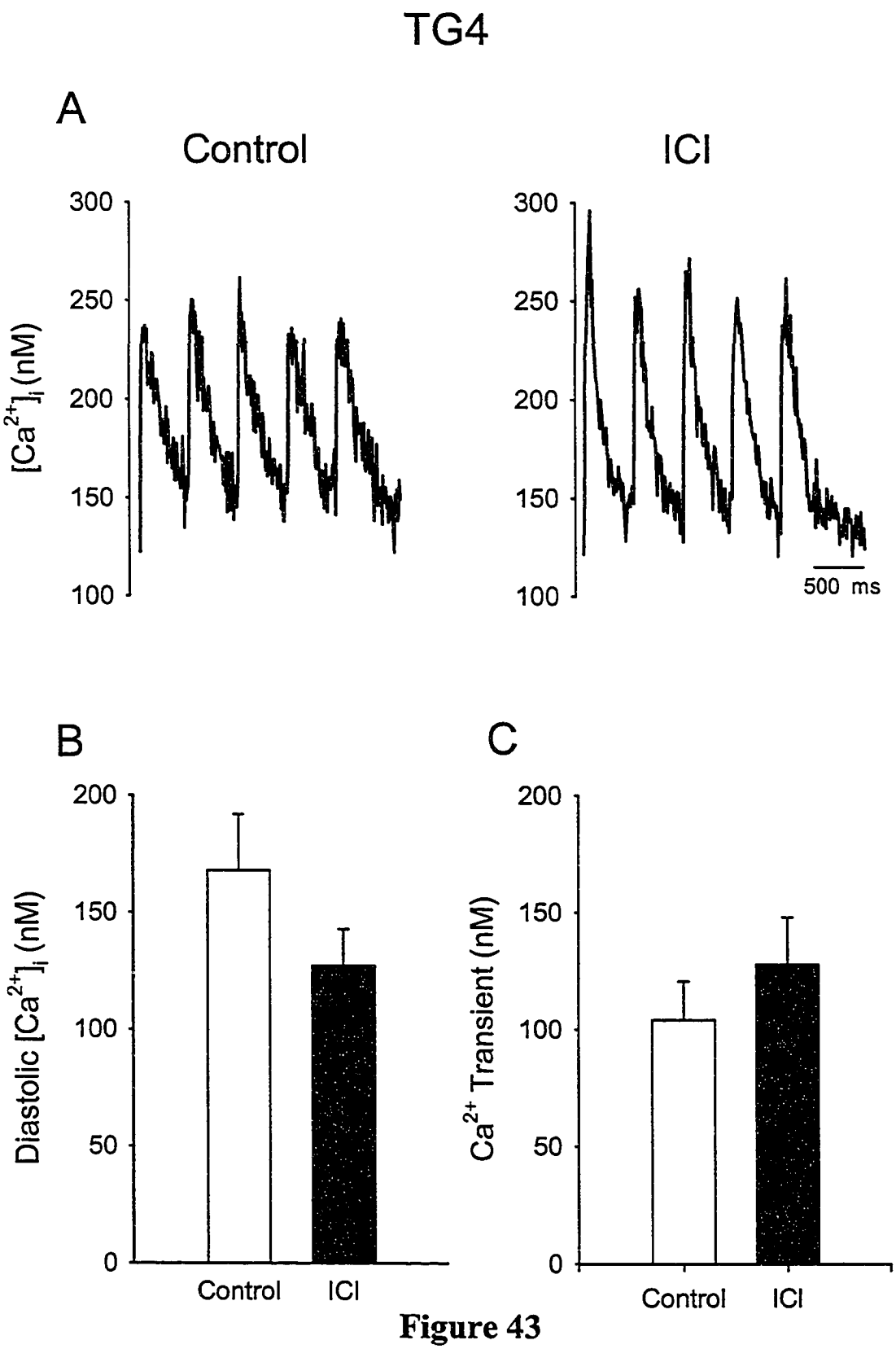
TG4
A
Control
ICl
300
250
200
150
100
[Ca2+]i (nM)
500 ms
B
C
Diastolic [Ca2+]i (nM)
Ca2+ Transient (nM)
200
150
100
50
0
Control
ICl

Figure 43

Figure 44: The β_2AR inverse agonist ICI 118, 151 had no significant effect on SR Ca^{2+} load in WT myocytes.

The voltage-clamp protocol used in these experiments is shown in panel (A). B) Representative caffeine-induced Ca^{2+} transients from WT myocytes in the absence and presence of ICI. C) The mean amplitude of caffeine-induced transients was similar in WT myocytes treated with ICI compared to control WT myocytes. (n = 10 control myocytes and n = 5 myocytes treated with ICI)

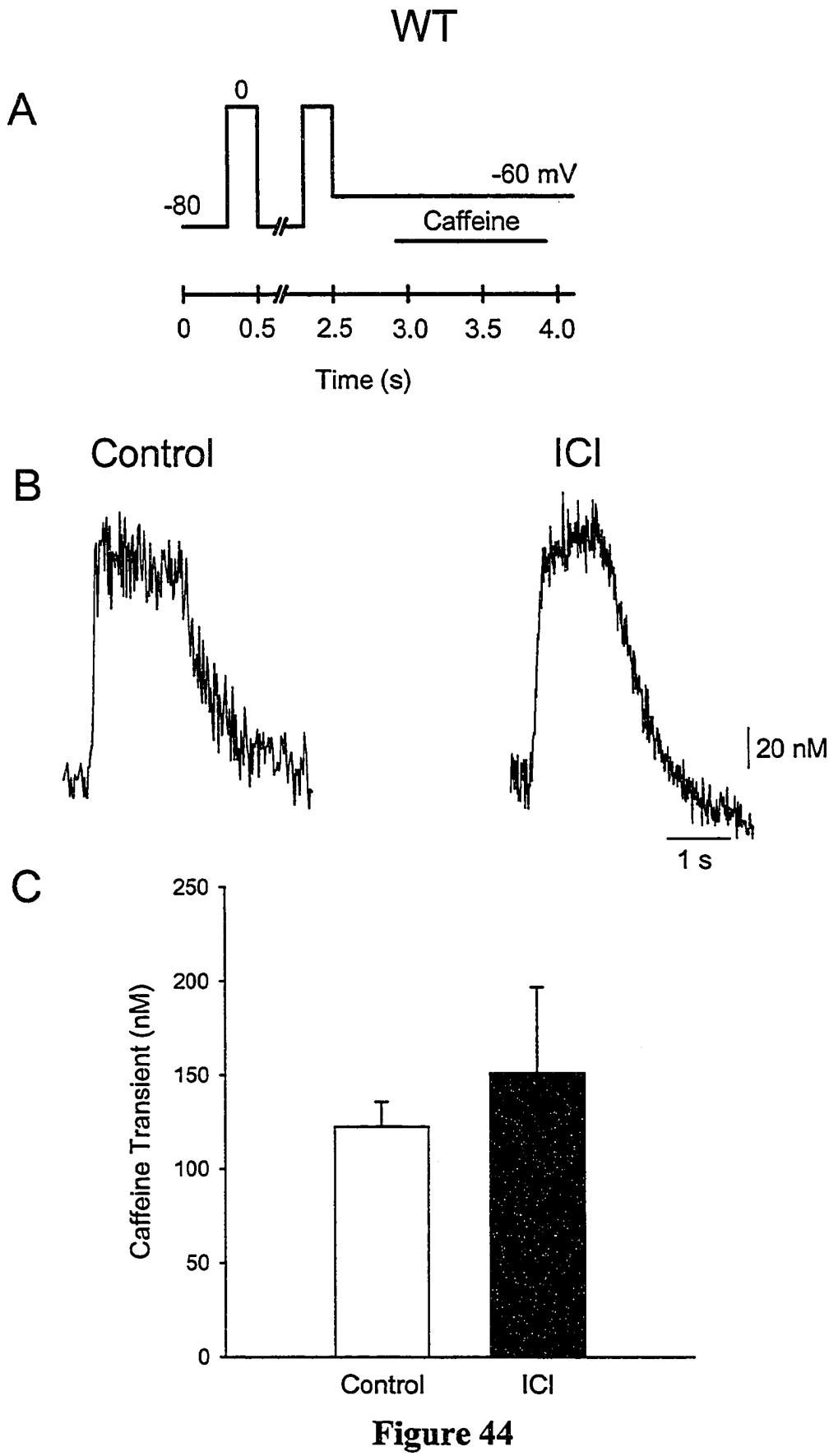
WT
A
0
-80
-60 mV
Caffeine
0
0.5
2.5
3.0
3.5
4.0
Time (s)
B
Control
ICl
20 nM
1 s
C
Caffeine Transient (nM)
250
200
150
100
50
0
Control
ICl

Figure 44

myocyte treated with ICI. The amplitudes of the caffeine-induced Ca^{2+} transients appeared similar in both groups. Figure 44-C shows the mean amplitudes of caffeine-induced Ca^{2+} transients were similar in WT myocytes in the absence and presence of ICI. Figure 45 shows the effect of ICI on caffeine-induced Ca^{2+} transients in TG4 myocytes. Representative caffeine-induced Ca^{2+} transients from TG4 myocytes in the absence and presence of ICI are depicted in Figure 45-B. In the TG4 cell treated with ICI, the amplitude of the caffeine-induced Ca^{2+} transient was reduced compared to control. Figure 45-C shows that the mean amplitudes of caffeine-induced Ca^{2+} transients were significantly reduced in TG4 myocytes exposed to ICI in comparison to control TG4 myocytes. These data suggest that the increased SR Ca^{2+} stores in TG4 myocytes were at least partially dependent on β_2AR constitutive activity.

In summary, results from part II of this study showed that contraction amplitude was increased in field-stimulated TG4 myocytes compared to WT cells. In voltage clamp experiments, differences in contraction amplitudes between WT and TG4 myocytes were abolished. However, a previous study has shown that action potential duration is prolonged in TG4 myocytes (Zhou et al., 1999b). When myocytes were activated with simulated TG4 action potentials, contraction amplitude was greater than when the same cell was activated with the shorter simulated WT action potential. Although contraction amplitudes were similar in WT and TG4 myocytes, peak $I_{Ca\text{-}L}$ was significantly reduced in TG4 myocytes. This decrease in $I_{Ca\text{-}L}$ in TG4 cells was not the result of a shift in the voltage dependence of the Ca^{2+} current. Diastolic Ca^{2+} concentrations and peak Ca^{2+}

Figure 45: The β_2AR inverse agonist ICI 118, 151 significantly reduced SR Ca^{2+} load in TG4 myocytes.

The voltage-clamp protocol used in these experiments is shown in panel (A). B) In TG4 myocytes, the representative caffeine-induced transient was smaller in the presence of ICI compared to the control caffeine-induced transient. C) The mean amplitude of caffeine-induced transients was significantly reduced in the presence of ICI compared to control in TG4 myocytes. * Significantly different from control (n = 7 control myocytes and n = 3 myocytes treated with ICI)

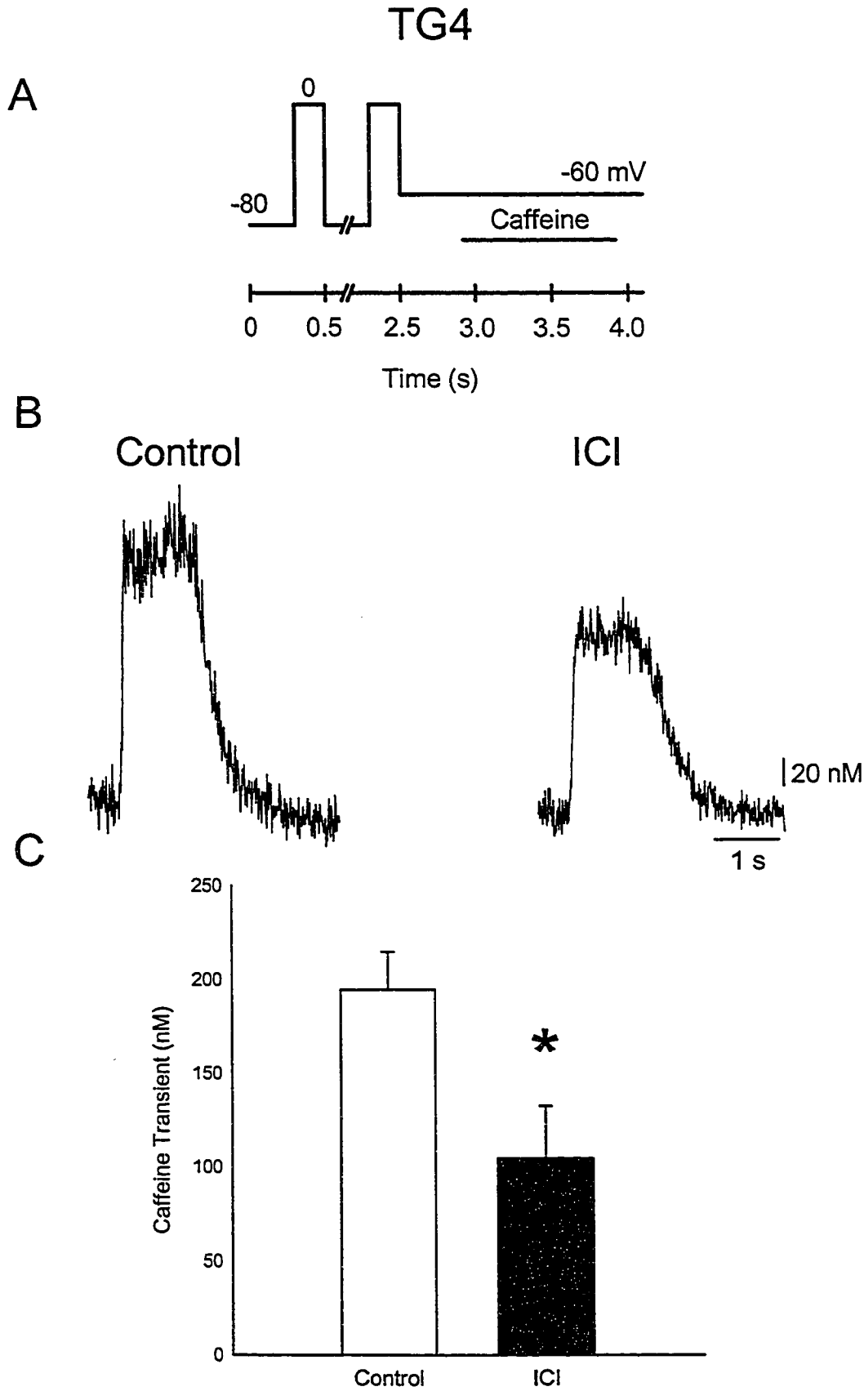
TG4
A
0
-80
-60 mV
Caffeine
0
0.5
2.5
3.0
3.5
4.0
Time (s)
B
Control
ICI
20 nM
1 s
C
250
200
150
100
50
0
Caffeine Transient (nM)
*
Control
ICI

Figure 45

transient amplitudes were similar in WT and TG4 myocytes. However, SR Ca^{2+} load was increased in TG4 myocytes. Experiments with the β_2AR inverse agonist ICI suggested that increased SR Ca^{2+} load was at least partially attributable to constitutive activity of β_2ARs.

DISCUSSION

Alterations in EC coupling in aged ventricular myocytes

The major hypothesis for part I of this thesis was that age-related abnormalities in cardiac EC coupling disrupt cardiac contractile function. Unlike previous studies, this study examined $I_{Ca\text{-}L}$, SR Ca^{2+} release and contraction simultaneously at physiological temperature. Results showed that contraction amplitudes, $I_{Ca\text{-}L}$ amplitudes and Ca^{2+} transient amplitudes were significantly reduced in aged myocytes paced at 2 Hz. However, the gain of CICR was similar in both young adult and aged myocytes. The current study also found that SR Ca^{2+} loads were similar in young adult and aged myocytes. Therefore, it is unlikely that the reduction in SR Ca^{2+} release observed in aged myocytes was the result of a reduction in SR Ca^{2+} load. Decreased SR Ca^{2+} release in aged myocytes is likely attributable to the reduction in trigger Ca^{2+}. Thus, the reduced magnitudes of $I_{Ca\text{-}L}$ and SR Ca^{2+} release result in a reduction in contraction amplitudes in aged ventricular myocytes. It was also hypothesized that these differences in cardiac EC coupling would be exacerbated when cells were paced at higher frequencies. However, this study found that when cells were paced at 6 Hz, contraction amplitudes, $I_{Ca\text{-}L}$ amplitudes and Ca^{2+} transient amplitudes were no longer different between young adult and aged myocytes. Thus, it appears that increasing stimulation frequency abolishes differences in EC coupling between young adult and aged myocytes.

The mice used in this study were between 21 and 26 months of age. The mortality rate of mice in this age range is between 10 to 20% (Turturro et al., 1999). In addition to increased mortality, changes in physical characteristics have been associated with advancing age (de Boer et al., 2002; Gerhard & Kasales, 2003; Shore, 1985;

Trifunovic et al., 2004). Indeed, this study found that the incidence of palpebral closure was significantly higher in aged mice than in young adult mice. Previous work has shown that eyelid laxity increases with advancing age (Shore, 1985). Thus, the increase in palpebral closure in aged mice might be attributable to an increase in eyelid laxity. In addition, more than 50% of aged animals used in this study were classified as ungroomed. Ungroomed mice were characterized as having erected and/or scruffy fur and/or had patches of fur missing. Aged animals also displayed a significant increase in closed posture (e.g. hunched or curved spine). Both closed posture and ungroomed fur are physical characteristics that have been observed in some animal models of aging (de Boer et al., 2002; Trifunovic et al., 2004). Kyphosis, an increase in the curvature of the spine, has been identified as a characteristic of advancing age (Gerhard & Kasales, 2003). Thus, the increase in hunched posture may be attributable to kyphosis, which is characteristic of advanced age. Overall, these findings show that 21 to 26 month old mice display several physical characteristics that are associated with aging.

This study also found that body weight was significantly increased in aged mice. It has been established that weight control is dependent on energy balance. The number of calories taken in must equal the number of calories burned to maintain a set weight (Tou & Wade, 2002). Thus, an increase in body weight suggests that the aged animals were consuming more calories than they were expending. It is possible that energy expenditure is decreased through a reduction in physical activity in aging (Tou & Wade, 2002). Several studies have previously shown that physical activity declines with advancing age (Ingram, 2000; Tou & Wade, 2002). This study found that exploratory activity was slightly decreased in aged animals, although the decrease was not

statistically significant. One earlier study showed that exploratory activity was decreased by 50% in senescent mice (Ingram, 2000). However, Ingram et al. (2000) used older mice than were used in the present study and it is likely that activity levels decline with age. Overall, these findings suggest that the activity levels of mice used in this study are similar in young adult and aged animals.

The incidence of heart failure has been shown to increase during senescence (Lye & Donnellan, 2000). Both cardiac hypertrophy and pulmonary edema are characteristic of heart failure (Kitzman, 2000; Kitzman, 2002). This study found that lung fluid was significantly increased in aged animals. Thus, the increase in lung fluid in aged mice could indicate pulmonary edema and the onset of heart failure (Kitzman, 2000; Kitzman, 2002). However, this study also found that dry lung weight was significantly increased in the aged mice. This indicates that the amount of lung tissue was greater in aged mice. Furthermore, lung weight to body weight ratios were similar in young adult and aged animals. Therefore, the increase in lung fluid likely represents an increase in lung tissue, and is not indicative of pulmonary edema and cardiac disease.

The ventricles from young adult and aged animals were compared to determine whether there was any evidence of cardiac hypertrophy in aged mice. This study showed that ventricle wet weight was significantly increased in aged animals. This suggests that ventricular hypertrophy had occurred in the aged animals. Body weight also was significantly increased in aged animals. When ventricular weight was normalized to body weight, ventricle weight to body weight ratios were similar in young adult and aged mice. Thus, the increase in ventricular weights in aged mice was proportional to the increase in animal weights.

The current study showed that contraction and Ca^{2+} transient amplitudes were significantly reduced in aged myocytes stimulated at 2 Hz. This finding conflicts with the results of previous studies which found that contraction and Ca^{2+} transient amplitudes are similar in young adult and aged rodent myocytes paced at the same stimulation frequency (Fraticelli et al., 1989; Isenberg et al., 2003; C. Lim et al., 2000). However, the present study examined contraction in voltage clamped myocytes where contractions were activated with rectangular voltage clamp pulses. Earlier studies were conducted in field-stimulated myocytes where contractions were initiated by action potentials (Fraticelli et al., 1989; Isenberg et al., 2003; C. Lim et al., 2000). Thus, the differences in contraction and Ca^{2+} transient amplitudes observed between studies may reflect differences in the duration of depolarization between cells activated with action potentials and those activated with voltage clamp pulses. Interestingly, several previous studies have shown that action potential duration is prolonged in aged myocytes (Capasso et al., 1983; Dibb et al., 2004; Liu et al., 2000; Walker et al., 1993; Wei et al., 1984). Furthermore, one study has shown that Ca^{2+} transient amplitudes are larger in aged cells stimulated with long duration action potentials compared to the same cells stimulated with short duration action potentials (Janczewski, Spurgeon, & Lakatta, 2002). Therefore, it has been suggested the increase in action potential duration maintains contractile function in aged myocytes by increasing SR Ca^{2+} release. However, in the present study the duration of depolarization was controlled by rectangular voltage clamp steps. In these experiments Ca^{2+} transient and contraction amplitudes were decreased in aged myocytes. This demonstrates that, when the duration of depolarization is controlled with voltage clamp, contractions and Ca^{2+} transients are decreased in aged cells.

This study also showed that time-to-peak contraction was prolonged in aged myocytes. Other studies have also found that time-to-peak contraction is prolonged in aged cells (Fraticelli et al., 1989; Orchard & Lakatta, 1985; Wahr et al., 2000; Wei et al., 1984). It has been suggested that the increased action potential duration in aged myocytes may contribute to increases in time-to-peak contraction by altering the rate at which intracellular Ca^{2+} increases (Wei et al., 1984). However, the present study was conducted in voltage clamped cells where the duration of depolarization was controlled. Therefore, changes in action potential duration in aged myocytes cannot account for the increase in time-to-peak contraction observed in this study. Another possible explanation is that age-related alterations in the myofilaments could be responsible for the increase in time-to-peak contraction. Several previous studies have shown that a shift in the myosin heavy chain (MHC) isoform from α-MHC to the slower β-MHC isoform decreases the rate at which contractions develop in aged heart (Fitzsimons et al., 1998; Wahr et al., 2000). There is increased expression of β-MHC and a downregulation of α-MHC expression in aged hearts (Carnes et al., 2004; Fitzsimons et al., 1999; Wahr et al., 2000). This shift in MHC isoforms has been shown to alter the Ca^{2+} sensitivity of the myofilaments (Metzger et al., 1999; Wahr et al., 2000), which results in an increase in the time-to peak contraction in the aging heart (Wahr et al., 2000). Thus, it is possible that the increase in time-to-peak contraction in aged myocytes is attributable to an increase in expression of β-MHC coupled with a reduction in the expression of α-MHC.

The present study showed that times-to-half relaxation are unchanged in aged myocytes. This is in agreement with studies by Wahr et al. (2000) that also showed times-to-half relaxation are unchanged in aged myocytes. However, some previous

studies have shown that the times-to-half relaxation are increased in aged myocytes (Orchard & Lakatta, 1985; Wei et al., 1984). It has been suggested that increased time-to-half relaxation is attributable to the increased action potential duration observed in aged myocytes (Wei et al., 1984). However, in the present study the duration of depolarization was controlled by voltage clamp, which eliminated the effect of increased action potential duration in aged myocytes. Therefore, age appears to have little effect on time-to-half relaxation in aged myocytes when the duration of depolarization is controlled.

There are several explanations that could account for the reduction in Ca^{2+} transient amplitudes observed in aged myocytes in this study. One explanation is that a reduction in SR Ca^{2+} load could result in decreased SR Ca^{2+} release (Bassani, 1995). However, this study found that SR Ca^{2+} stores were similar in young adult and aged myocytes. This suggests that decreased SR Ca^{2+} release in aged myocytes is not attributable to a reduction in SR Ca^{2+} load. SR Ca^{2+} release also is graded by $I_{Ca\text{-}L}$ (Cannell et al., 1994; Lopez-Lopez et al., 1994), so a reduction in trigger Ca^{2+} could account for a reduction in SR Ca^{2+} release in aging cells. The present study found that $I_{Ca\text{-}L}$ was decreased in aged myocytes. Thus, the reduction in trigger Ca^{2+} is likely responsible for decreased SR Ca^{2+} release in aged myocytes.

The present study found that the amplitude of $I_{Ca\text{-}L}$ was significantly depressed in aged myocytes compared to young adult cells. These results are in agreement with the results of other studies that have found that the magnitude of $I_{Ca\text{-}L}$ is depressed in aging mouse and rat myocytes (Isenberg et al., 2003; Liu et al., 2000). In contrast, in other studies the amplitude of $I_{Ca\text{-}L}$ has been found to be unchanged (Walker et al., 1993) or

even increased (Dibb et al., 2004) in aged myocytes. Studies that found amplitudes of $I_{Ca\text{-}L}$ were unchanged or increased with age utilized ventricular myocytes from rats (Walker et al., 1993) and sheep (Dibb et al., 2004). Therefore, it is possible that the disparity in results between studies is attributable to species differences. However, it seems clear from the results of the present study and one previous study (Isenberg et al., 2003) that $I_{Ca\text{-}L}$ density is decreased in aging mouse ventricular myocytes.

The reduction in the magnitude of $I_{Ca\text{-}L}$ in aged murine myocytes could be attributable to a number of factors. The inactivation of $I_{Ca\text{-}L}$ is partially dependent on intracellular Ca^{2+} concentration (Bers, 2001; Eisner et al., 1998). Thus, increased Ca^{2+}-induced inactivation of $I_{Ca\text{-}L}$ related to increased SR Ca^{2+} stores could be responsible for the reduction in $I_{Ca\text{-}L}$ in aged myocytes. However, this study showed that SR load was not changed in aged myocytes and that SR Ca^{2+} release was decreased. Thus, it is unlikely that the amplitudes of $I_{Ca\text{-}L}$ were reduced in aged myocytes as a result of an increase in Ca^{2+} induced-inactivation. The reduction in the magnitude of $I_{Ca\text{-}L}$ in aged myocytes also might be the result of a decrease in the open probability of L-type Ca^{2+} channels in aging cells. Previous work has shown that a decrease in the open probability of L-type Ca^{2+} channels reduces Ca^{2+} influx (Niimi et al., 2003). However, one study has shown that the open probability and availability of L-type Ca^{2+} channels is actually increased in aged ventricular myocytes (Josephson et al., 2002). Thus, it is unlikely that a reduction in open probability is responsible for the reduction in the magnitude of $I_{Ca\text{-}L}$ in aged myocytes.

It also is possible that a decrease in the density of L-type Ca^{2+} channels is responsible for the decrease in the magnitude of $I_{Ca\text{-}L}$ in aged myocytes. Previous work

has shown that L-type Ca^{2+} channel mRNA is reduced in the aged heart (Yue et al., 1999). Thus, a reduction in L-type Ca^{2+} channel expression could explain the reduction in the magnitude of $I_{Ca\text{-}L}$ in aged myocytes. In fact, it has been shown that the density of L-type Ca^{2+} channels is reduced in aging ventricular myocytes (Howlett & Nicholl, 1992). Therefore, the reduction in the magnitude of $I_{Ca\text{-}L}$ observed in this study may be attributable to an age-related reduction in the density of L-type Ca^{2+} channels.

This study also found that the rate of inactivation of $I_{Ca\text{-}L}$ was decreased in aged myocytes. This is in agreement with previous studies that showed that the rate of inactivation of $I_{Ca\text{-}L}$ is slowed in aged myocytes (Liu et al., 2000; Walker et al., 1993). Walker et al (1993) also showed that the rates of inactivation of $I_{Ca\text{-}L}$ are slower in young adult and aged myocytes dialyzed with a solution containing the Ca^{2+} chelator EGTA compared to control cells. This suggests that a reduction in intracellular Ca^{2+} concentration reduces Ca^{2+} dependent inactivation of $I_{Ca\text{-}L}$ (Walker et al., 1993). Interestingly, the present study showed that diastolic Ca^{2+} concentration and SR Ca^{2+} release were decreased in aged myocytes. Thus, intracellular Ca^{2+} concentrations were lower in aged myocytes than in young adult myocytes. This decrease in intracellular Ca^{2+} concentration could alter Ca^{2+} dependent inactivation of $I_{Ca\text{-}L}$ and thereby decrease the rate of inactivation of $I_{Ca\text{-}L}$ in aged myocytes.

A decrease in the rate of inactivation of $I_{Ca\text{-}L}$ has been shown to increase net Ca^{2+} influx (Sah et al., 2001), which would be predicted to result in an increase in cytosolic Ca^{2+} concentration (Eisner et al., 1998). Therefore, if diastolic Ca^{2+} is decreased in aged cells, a larger proportion of cytosolic Ca^{2+} would have to be removed via the NCX and/or SR Ca^{2+}ATPase in aged cells in comparison to young adult cells (Eisner et al., 1998).

The reduction in diastolic Ca^{2+} concentration in aged myocytes suggests that NCX and/or SR Ca^{2+}ATPase activity is increased. If SR Ca^{2+} ATPase activity is increased, then SR Ca^{2+} content should also be increased. However, this study showed that SR Ca^{2+} content was unchanged in aged myocytes, which suggests that there was no change in SR Ca^{2+}ATPase activity. In addition, previous work has shown that SR Ca^{2+}ATPase activity actually is decreased in aging myocytes (Schmidt et al., 2000). Therefore, it is unlikely that decreased diastolic Ca^{2+} concentration in aged myocytes is attributable to increased SR Ca^{2+}ATPase activity. Interestingly, one previous study has shown that forward NCX activity is increased in aged myocytes (Mace et al., 2003), which could result in increased Ca^{2+} removal from the cytosol. Thus, the reduction in diastolic Ca^{2+} concentration in aged myocytes could be attributable, at least in part, to an age-related increase in NCX activity.

Ca^{2+} transient amplitudes and contraction amplitudes were significantly smaller in aged myocytes paced at 2 Hz compared to young adult myocytes. It was hypothesized that increasing stimulation frequency to 6 Hz would exacerbate the differences in contraction amplitudes and Ca^{2+} transient amplitudes between young adult and aged myocytes. Surprisingly, the present study found that Ca^{2+} transient amplitudes and contraction amplitudes were similar in young adult and aged myocytes paced at 6 Hz with voltage clamp pulses. This is in contrast to previous studies that have shown that contraction and Ca^{2+} transient amplitudes are depressed in aged myocytes compared to younger cells when myocytes are paced at frequencies of 4 Hz or greater with field stimulation (Isenberg et al., 2003; Lim et al., 2000). In voltage clamp experiments, contractions and Ca^{2+} transients are activated by voltage clamp pulses where the duration

of depolarization does not vary. However, in field-stimulated myocytes, contractions and Ca^{2+} transients are activated by actions potentials. Therefore, it is possible that differences in the duration of depolarization account for the disparity in results between the present study and studies conducted by Lim et al. (2000) and Isenberg et al. (2003).

This study also showed that contraction amplitudes were depressed in young adult myocytes paced at 6 Hz in comparison young adult cells paced at 2 Hz. Similarly, increasing stimulation frequency from 2 Hz to 6 Hz resulted in a further reduction in contraction amplitudes in aged myocytes. In fact, contraction amplitudes were reduced by more than 50% at 6 Hz in both young adult and aged myocytes. The reduction in contraction amplitudes in both young adult and aged myocytes at 6 Hz also reduced the difference in contraction amplitudes between groups. Thus, this study found that contraction amplitudes were similar in young adult and aged myocytes paced at 6 Hz. Therefore, it appears that increasing stimulation frequency abolishes the differences in contraction amplitudes between young adult and aged myocytes observed at lower stimulation frequencies.

The reduction in contraction and Ca^{2+} transient amplitudes with increasing stimulation frequency can be explained by a number of factors. One possibility is that that SR Ca^{2+} release is reduced at higher stimulation frequencies as a result of a reduction in SR Ca^{2+} content (Bassani et al., 1995). However, this is unlikely since the present study found that increasing stimulation frequency from 2 Hz and 6 Hz did not affect SR Ca^{2+} loads in either young adult and aged myocytes (comparison not shown). Another possibility is that increasing stimulation frequency from 2 Hz to 6 Hz decreases the magnitude of trigger Ca^{2+}. Previous work has shown that SR Ca^{2+} release is graded by

the magnitude of $I_{Ca\text{-}L}$ (Cannell et al., 1994; Lopez-Lopez et al., 1994). Therefore, if the magnitude $I_{Ca\text{-}L}$ is reduced as a result of increasing stimulation frequency, a reduction in SR Ca^{2+} release would be expected. Evidence from this study supports this idea, as $I_{Ca\text{-}L}$ was depressed in both young adult and aged myocytes stimulated at 6 Hz compared to myocytes stimulated at 2 Hz. Thus, a frequency-induced reduction in trigger Ca^{2+} in young adult and aged myocytes ultimately leads to a reduction in amplitudes of contractions and Ca^{2+} transients.

The present study found that the magnitudes of $I_{Ca\text{-}L}$ were significantly reduced in young adult myocytes paced at 6 Hz compared to young adult myocytes paced at 2 Hz. This study also found that the amplitudes of $I_{Ca\text{-}L}$ were decreased in aged myocytes paced at 6 Hz compared to aged cells paced at 2 Hz, but not to the same extent as observed in young adult myocytes. These findings agree with the results of previous studies that showed the magnitudes of $I_{Ca\text{-}L}$ are reduced at higher stimulation frequencies in both young adult and aged myocytes (Isenberg et al., 2003; Kaspar & Pelzer, 1995). Furthermore, the present study showed that magnitudes of $I_{Ca\text{-}L}$ were similar in young adult and aged myocytes paced at 6 Hz. Thus, increasing stimulation frequency reduced the magnitude of $I_{Ca\text{-}L}$ in both young adult and aged myocytes and abolished the differences in the magnitudes of $I_{Ca\text{-}L}$ between young adult and aged myocytes observed at 2 Hz. The reduction in $I_{Ca\text{-}L}$ at higher stimulation frequencies is most likely attributable to an ultraslow, voltage dependent inactivation (Bates & Gurney, 1999; Kaspar & Pelzer, 1995). As stimulation frequency increases, more time is spent at positive potentials during a given period of time and voltage dependent inactivation

accumulates (Kaspar & Pelzer, 1995). Thus, the reduction in $I_{Ca\text{-}L}$ in young adult and aged myocytes at 6 Hz may be attributable to frequency dependent inactivation.

When myocytes were stimulated at 2 Hz, the magnitudes of $I_{Ca\text{-}L}$, Ca^{2+} transient amplitudes and contraction amplitudes were significantly reduced in aged myocytes. However, $I_{Ca\text{-}L}$ amplitudes, Ca^{2+} transient amplitudes and contraction amplitudes were similar in young adult and aged myocytes paced at 6 Hz. Thus, increasing stimulation frequency abolishes age-related differences in EC coupling between young adult and aged myocytes. However, it is not clear why the effects of aging on EC coupling were abolished at higher frequencies. One explanation is that the frequency-induced reduction in the magnitude of trigger Ca^{2+} was greater in young adult myocytes than in aged myocytes. The current study shows that increasing stimulation frequency from 2 Hz to 6 Hz decreased the magnitude of $I_{Ca\text{-}L}$ by approximately 40% in young adult myocytes, whereas the reduction in $I_{Ca\text{-}L}$ was closer to 30% in aged myocytes. Thus, the frequency-induced reduction in the amplitude of $I_{Ca\text{-}L}$ was greater in young adult myocytes than in aged myocytes. Since both SR Ca^{2+} release and contraction amplitude are graded by the magnitude of $I_{Ca\text{-}L}$ (Bers, 2001), the reduction in contraction and Ca^{2+} transient amplitudes would also be larger in young adult myocytes than in aged cells. Thus, reductions in $I_{Ca\text{-}L}$ amplitudes, SR Ca^{2+} release and contraction amplitudes were greater in young adult myocytes than in aged myocytes. This, in turn, abolished the differences in $I_{Ca\text{-}L}$ amplitudes, Ca^{2+} transient amplitudes and contraction amplitudes between young adult and aged myocytes observed at 2 Hz.

In summary, this study showed that $I_{Ca\text{-}L}$ was decreased in voltage clamped aged myocytes paced at 2 Hz. Since $I_{Ca\text{-}L}$ is the primary trigger for CICR, SR Ca^{2+} release also

was reduced in aged cells. This, in turn, decreased the magnitude of contraction in aged cells. Interestingly, advanced age had no effect on SR Ca^{2+} stores or the gain of CICR. In addition, when stimulation rate was increased, contraction amplitudes decreased in both young adult and aged myocytes. Furthermore, the magnitude of $I_{Ca\text{-}L}$ was reduced in young adult and aged myocytes at higher stimulation frequencies, but the reduction was greater in young adult myocytes than in aged cells. As a result, amplitudes of Ca^{2+} transients and contractions were similar in both groups when stimulation frequency was higher. Overall, these results demonstrate that alterations in EC coupling occur with aging and that these alterations may disrupt cardiac contractile function in the aging heart.

The effects of cardiac β_2AR overexpression on EC coupling in ventricular myocytes

The major hypothesis for part II of this thesis was that the overexpression of β_2ARs increases the gain of CICR in TG4 myocytes, which results in increased contraction amplitude. Therefore, this study was designed to characterize the relationship between magnitudes of $I_{Ca\text{-}L}$, SR Ca^{2+} release and contraction in TG4 myocytes under comparable experimental conditions at 37°C. Results showed that amplitudes of contraction were significantly greater in field-stimulated TG4 myocytes compared to WT myocytes. However, when contractions were initiated with rectangular voltage clamp steps, contraction amplitudes were similar in TG4 and WT myocytes. The difference between contractions in field-stimulated and voltage clamped TG4 cells is likely the result of prolongation of the action potential, which is characteristic in TG4 cells. When voltage clamped cells were activated with a simulated TG4 action potential, contraction amplitudes were significantly greater than when the same cell was activated with a simulated WT action potential. In voltage clamp experiments, measurement of Ca^{2+} current and contractions in the same cells revealed that peak amplitudes of $I_{Ca\text{-}L}$ were significantly reduced in TG4 myocytes while contraction amplitudes were unchanged. Interestingly, peak Ca^{2+} transient amplitudes were similar in TG4 and WT myocytes. Since peak amplitudes of contraction and Ca^{2+} transients were maintained despite a reduction in $I_{Ca\text{-}L}$, this suggests that the gain of CICR was increased in TG4 myocytes. Furthermore, SR Ca^{2+} load was significantly increased in TG4 myocytes, which could account for the increase in gain of CICR.

This study compared amplitudes of contraction in field-stimulated TG4 and WT myocytes at physiological temperature. The current study found that the amplitudes of contraction were significantly larger in field-stimulated TG4 myocytes paced at 2 Hz compared to WT myocytes. These results are in agreement with the results of earlier studies that reported that contractions are larger in field-stimulated TG4 myocytes than in WT myocytes (Xiao et al., 1999; Zhang et al., 2000; Zhou et al., 1999a; Zhou et al., 1999b). In contrast, other studies have shown that contraction amplitudes are similar in field-stimulated WT and TG4 myocytes (Gong et al., 2000; Heubach et al., 1999). It is not clear why some studies did not observe an increase in contraction amplitudes in TG4 mice. However, the transgenic mouse model used by Heubach et al. (1999) has a 400-fold increase in cardiac β_2AR density, whereas the TG4 mice used in this study have a 195-fold increase in cardiac β_2AR density (Milano et al., 1994). Interestingly, Liggett et al. (2000) showed that high levels of cardiac β_2AR overexpression have a smaller positive inotropic effect than low levels of β_2AR overexpression. Thus, differences in contraction amplitudes between the present study and the study by Heubach et al (1999) are likely attributable to differences in cardiac β_2AR density. It is not clear why contraction amplitudes in WT and TG4 myocytes were similar in the study by Gong et al. (2000). However, the animals used by Gong et al. (2000) were much older than those used in this study and experiments were conducted at 32° C. Thus, the disparity in results between studies could be attributable to differences in the ages of the experimental animals and/or differences in experimental procedures.

The current study also demonstrated that the amplitudes of contraction increased with increasing stimulation frequency up to 6 Hz and 8 Hz for TG4 and WT myocytes,

respectively. This is in agreement with previous studies that have shown contractile force increases with increasing stimulation frequencies in mouse ventricular myocytes (Antoons et al., 2002; Palakodeti et al., 1997). However, previous studies have only compared contraction amplitudes in TG4 and WT myocytes at low stimulation frequencies (e.g. 0.5 Hz to 1 Hz) (Gong et al., 2000; Heubach et al., 1999; Xiao et al., 1999; Zhang et al., 2000; Zhou et al., 1999a; Zhou et al., 1999b). Therefore, it was not known whether differences in contraction amplitudes between WT and TG4 myocytes would persist at higher stimulation frequencies. The present study showed that contraction amplitudes were greater in TG4 myocytes than in WT myocytes at all stimulation frequencies (2 to 10 Hz). Thus, the results of this study suggest that contraction amplitude is increased in TG4 myocytes over a wide range of frequencies.

There are several possible explanations for the increase in amplitudes of contraction in TG4 myocytes. It is possible that contraction amplitude was increased as a result of an increase in TG4 myocyte size. However, this is unlikely since the current study found that resting cell length and cell membrane area were similar in WT and TG4 myocytes. This is in agreement with previous studies that have shown resting cell length is not altered TG4 myocytes (Heubach et al., 1999; Xiao et al., 1999). In contrast, one study found that cell membrane area was significantly increased in transgenic mice overexpressing cardiac β_2ARs (Liggett et al., 2000). However, the degree of β_2AR overexpression differed markedly between the mice utilized in this study and those used by Liggett et al. (2000). In the present study, myocytes were isolated from hearts where cardiac β_2AR overexpression was approximately 195 times greater than native β_2ARs (Milano et al., 1994). In contrast, the mice utilized in studies by Liggett et al. (2000)

overexpress β_2ARs approximately 350 times greater than native β_2ARs. Thus, it appears that changes in myocyte size only occur at high levels of β_2AR overexpression. Therefore, it is unlikely that increased contraction amplitudes in TG4 myocytes are attributable to an increase in cell size.

One possibility is that alterations in action potential configuration may contribute to the increase in contraction in field-stimulated TG4 myocytes. Indeed, an earlier study showed that the action potential configuration is altered in TG4 myocytes (Zhou et al., 1999b). Specifically, Zhou et al. (1999b) showed that resting membrane potential, action potential amplitude and time to 50% repolarization were similar in WT and TG4 myocytes. However, the time to 90% repolarization was markedly prolonged in TG4 myocytes (e.g. 48.3 ms and 104 ms for WT and TG4 myocytes, respectively) (Zhou et al., 1999b). Therefore, it was hypothesized that prolongation of the action potential duration contributes to increased contraction amplitudes in TG4 myocytes. This hypothesis was supported by the results of this study which showed that contraction amplitudes were greater when myocytes were activated with simulated TG4 action potentials than when cells were activated with simulated WT action potentials. Thus, it appears that increased contraction amplitudes in field-stimulated TG4 myocytes can be, at least, partially attributed to increased action potential duration.

Interestingly, this study found that the differences in amplitudes of contraction between WT and TG4 myocytes disappeared when cells were voltage clamped to control the duration of depolarization. This contrasts with the increased contraction amplitudes in field-stimulated TG4 myocytes observed both in this study and in earlier studies (Xiao et al., 1999; Zhang et al., 2000; Zhou et al., 1999a; Zhou et al., 1999b). In field-

stimulated myocytes, contractions are initiated by action potentials. However, in voltage clamped myocytes, contractions are initiated by rectangular voltage pulses and thus the duration of depolarization is the same for both WT and TG4 myocytes. As the increased contraction amplitudes in TG4 myocytes are likely attributable to increased action potential duration, it was not surprising that contraction amplitudes were similar in WT and TG4 myocytes when the duration of depolarization was controlled with voltage clamp.

This study also found that the magnitude of $I_{Ca\text{-}L}$ was significantly smaller in TG4 myocytes than in WT myocytes. This is in agreement with the results of several previous studies that compared the magnitude of $I_{Ca\text{-}L}$ in WT and TG4 myocytes (Heubach et al., 2001; Heubach et al., 1999; Liggett et al., 2000). In contrast, other studies have found that there is no difference in the magnitude of $I_{Ca\text{-}L}$ between WT and TG4 myocytes (Zhou et al., 1999a; Zhou et al., 1999b). Studies that found the magnitude of $I_{Ca\text{-}L}$ was decreased in TG4 myocytes used cells from 3 to 12 month old mice (Heubach et al., 2001; Heubach et al., 1999; Liggett et al., 2000). These animals are similar in age to the mice used in the present study. However, studies where the magnitude of $I_{Ca\text{-}L}$ was similar in WT and TG4 myocytes, used cells from 2 to 3 month old mice (Zhou et al., 1999a; Zhou et al., 1999b). It has been suggested previously that the reduction in $I_{Ca\text{-}L}$ may develop with age in TG4 myocytes (Heubach et al., 2001). The results of the present study support this idea that the magnitude of $I_{Ca\text{-}L}$ decreases with age in TG4 myocytes, but not in WT cells.

There are several possible explanations for a reduction in the magnitude of $I_{Ca\text{-}L}$ in TG4 myocytes. One explanation is that there is increased Ca^{2+}-induced inactivation of

$I_{Ca\text{-}L}$ related to the increase in SR Ca^{2+} stores in TG4 cells. Inactivation of $I_{Ca\text{-}L}$ is partially dependent on intracellular Ca^{2+} concentration in cardiac myocytes (Bers, 2001; Eisner et al., 1998). It is believed that Ca^{2+}-dependent inactivation of $I_{Ca\text{-}L}$ provides a feedback mechanism to limit further entry of extracellular Ca^{2+} (Bers, 2001). Normal SR Ca^{2+} release has been shown to reduce $I_{Ca\text{-}L}$ by approximately 50% in ventricular myocytes (Puglisi et al., 1999). Furthermore, elevation of SR Ca^{2+} stores increases SR Ca^{2+} release, which augments the reduction in $I_{Ca\text{-}L}$ (Eisner et al., 1998). Thus, an increase in SR Ca^{2+} release in TG4 myocytes could explain the reduction in $I_{Ca\text{-}L}$ observed in this study. However, the present study showed that the amplitudes of Ca^{2+} transients were similar in WT and TG4 myocytes. Therefore, it is not likely that increased SR Ca^{2+} release contributes to the decreased magnitude of $I_{Ca\text{-}L}$ in TG4 myocytes.

It also is possible that the magnitude of $I_{Ca\text{-}L}$ is reduced in TG4 myocytes as a result of a decrease in the open probability of L-type Ca^{2+} channels. A previous patch clamp study has shown that open times for L-type Ca^{2+} channels are shorter whereas closed times for the channels are increased in TG4 myocytes (Heubach et al., 2001). This leads to a reduction in the open probability for L-type Ca^{2+} channels (Heubach et al., 2001). In addition, Heubach et al. (2001) showed that the availability of L-type Ca^{2+} channels is reduced in TG4 myocytes. Together, the reduction in L-type Ca^{2+} channel availability and the reduction in open probability result in a decrease in maximum ensemble Ca^{2+} current in TG4 myocytes (Heubach et al., 2001). Interestingly, the peak magnitude of $I_{Ca\text{-}L}$ is restored when TG4 myocytes are treated with pertussis toxin to disrupt inhibitory G-protein function (Heubach et al., 2001). Since β_2ARs are known to

couple to inhibitory G-proteins, this finding suggests that constitutive β_2AR activity may be responsible for the decrease in the amplitude of $I_{Ca\text{-}L}$ in TG4 myocytes (Heubach et al., 2001). Thus, a reduction in the open probability of L-type Ca^{2+} channels and/or β_2AR signaling via inhibitory G-proteins may account for the reduction in $I_{Ca\text{-}L}$ in TG4 myocytes.

Finally, a reduction the expression of L-type Ca^{2+} channels also could account for the reduction in the magnitude of $I_{Ca\text{-}L}$ observed in TG4 myocytes. However, Heubach et al. (2001) showed that the magnitude of $I_{Ca\text{-}L}$ was similar in WT myocytes and pertussis toxin-treated TG4 myocytes. This suggests that the density of L-type Ca^{2+} channels is similar in WT and TG4 myocytes. Thus, it is unlikely that the reduction in $I_{Ca\text{-}L}$ in TG4 myocytes is attributable to a reduction in L-type Ca^{2+} channel density.

Interestingly, contraction amplitudes were maintained in TG4 myocytes, despite a reduction in $I_{Ca\text{-}L}$. If SR Ca^{2+} release were maintained in TG4 myocytes, it could explain why a reduction in the magnitude of $I_{Ca\text{-}L}$ does not result in a decrease in contraction amplitude. Indeed, this study found that Ca^{2+} transient amplitudes were similar in TG4 and WT myocytes. In contrast, Zhou et al. (1999b) found that Ca^{2+} transient amplitudes were increased in TG4 myocytes compared to WT cells. However, the study by Zhou et al. (1999b) activated Ca^{2+} transients by action potentials, whereas Ca^{2+} transients were activated by rectangular voltage clamp pulses in the present study. Thus, the difference between the results of this study and previous work (Zhou et al., 1999b) might be due to the differences in the duration of depolarization.

Since SR Ca^{2+} release is graded by the magnitude of $I_{Ca\text{-}L}$ (Cannell et al., 1994; Lopez-Lopez et al., 1994), a reduction in $I_{Ca\text{-}L}$ should result in decreased SR Ca^{2+} release

in TG4 cells. However, this study found that SR Ca^{2+} release was maintained despite a reduction in the magnitude of $I_{Ca\text{-}L}$ in TG4 myocytes. If $I_{Ca\text{-}L}$ is decreased, how are Ca^{2+} transient amplitudes maintained in TG4 myocytes? Previous work has shown that phosphorylation of SR Ca^{2+} release channels increases their open probability (Bers, 2001). Therefore, it is possible that the constitutive activity of β_2ARs in TG4 cells phosphorylates SR Ca^{2+} release channels and increases their sensitivity to trigger Ca^{2+}. Thus, a small L-type Ca^{2+} current should trigger a large SR Ca^{2+} release (Bers, 2001). If constitutive activity of β_2ARs is responsible for the maintenance of Ca^{2+} transient amplitudes in TG4 myocytes, then inhibition of constitutive activity with ICI should result in a decrease in Ca^{2+} transient amplitude. However, this study found that Ca^{2+} transient amplitudes were similar in TG4 myocytes treated with ICI and control TG4 myocytes. Thus, it is unlikely that constitutive activity of β_2ARs is responsible for the maintenance of Ca^{2+} transient amplitudes in TG4 myocytes.

SR Ca^{2+} load also is known to affect SR Ca^{2+} release (Bers, 2001; Eisner et al., 1998). For instance, it is well documented that an increase in SR Ca^{2+} content results in an increase in SR Ca^{2+} release (Bers, 2001; Eisner et al., 1998). This study found that SR Ca^{2+} load was significantly greater in TG4 myocytes. Therefore, the increase in SR Ca^{2+} content in TG4 myocytes would be predicted to lead to an increase in SR Ca^{2+} release. However, this study found that SR Ca^{2+} release was similar in WT and TG4 myocytes, despite the increase in SR Ca^{2+} content in TG4 myocytes. An explanation for these observations can be found in the work of Eisner and colleagues (Eisner et al., 1998). These investigations have shown that alterations in CICR, such as changes in trigger Ca^{2+} or SR Ca^{2+} stores, have only a transient effect on SR Ca^{2+} release (Trafford, Diaz, &

Eisner, 1998). For example, an increase in SR Ca^{2+} load would initially increase the size of the Ca^{2+} transient (Eisner et al., 1998). This, in turn, decreases the magnitude of Ca^{2+} current and increases Ca^{2+} efflux until a new steady-state is achieved (Eisner et al., 1998). Thus, the myocyte compensates for an increase in SR Ca^{2+} release to bring Ca^{2+} cycling back into equilibrium. Increased, SR Ca^{2+} content can only maintain increased SR Ca^{2+} release if Ca^{2+} removal from the cell has been altered (Trafford et al., 1998). Otherwise, Ca^{2+} cycling will return to a state of equilibrium. Therefore, it appears that Ca^{2+} efflux mechanisms are not altered in TG4 myocytes. Thus, after an initial increase in SR Ca^{2+} stores, Ca^{2+} efflux returns Ca^{2+} cycling back to a state of equilibrium and prevents a continual increase in SR Ca^{2+} release.

In contrast to the results of the present study, one previous study has shown that SR Ca^{2+} loads are similar in WT and TG4 myocytes (Zhou et al., 1999b). The difference between results of the present study and the study by Zhou et al. (1999b) can be explained by a number of factors. First, the present study used fura-2 to measure Ca^{2+} concentration, whereas Zhou et al. (1999b) used fluo-3, which does not directly measure Ca^{2+} concentration. Zhou et al. (1999b) reported SR Ca^{2+} stores as the ratio of peak fluorescence to background fluorescence and did not calculate the actual Ca^{2+} concentration in WT and TG4 myocytes. Second, studies described in this thesis were conducted at 37°C, whereas in the latter study (Zhou et al., 1999b) experiments were performed at room temperature. Temperature has been shown to have marked effects on SR Ca^{2+} load and EC coupling (Bers, 2001; Ferrier et al., 2003; Ferrier & Howlett, 2001). Thus, differences in experimental techniques may account for the disparity in results between studies.

The present study found that SR Ca^{2+} load was significantly increased in TG4 myocytes. One explanation for the increase in SR Ca^{2+} content is that Ca^{2+} reuptake is increased in TG4 myocytes. A previous study has shown that levels of PLB protein are reduced in TG4 myocytes (Rockman et al., 1996). Since PLB inhibits the SR Ca^{2+} pump (Frank et al., 2003), a reduction in PLB levels would be expected to increase SR Ca^{2+} uptake. This could account for the increase in SR Ca^{2+} content in TG4 cells. In addition, the non-selective βAR agonist isoproterenol has been shown to increase PLB phosphorylation (Reiken et al., 2003). Therefore, it also is possible that constitutively active β_2ARs could phosphorylate PLB and increase SR Ca^{2+} reuptake. This study showed that when constitutive β_2AR activity was blocked with ICI, differences in SR Ca^{2+} load between TG4 and WT myocytes were abolished. ICI prevents the constitutive activity of β_2AR because it stabilizes the inactive state of the receptor (Bond et al., 1995). Thus, constitutive activity of β_2ARs may be responsible, in part, for increased SR Ca^{2+} content in TG4 myocytes. Additionally, if a reduction in PLB protein levels had been responsible for the increase in SR Ca^{2+} content in TG4 cells, then SR Ca^{2+} content should have remained elevated in the presence of ICI. However, SR Ca^{2+} content was decreased in the presence of ICI. Thus, alterations in PLB protein levels in TG4 myocytes are not likely to be responsible for increased SR Ca^{2+} content. Therefore, it appears that constitutively active β_2ARs are primarily responsible for the increase in SR Ca^{2+} load in TG4 myocytes.

It is possible that the increase in SR Ca^{2+} stores in TG4 myocytes compensates for the decreased magnitude of trigger $I_{Ca\text{-}L}$. Several studies have shown that increased SR Ca^{2+} content can increase the sensitivity of SR Ca^{2+} release channels (Bassani et al.,

1995; Lukyanenko et al., 1996; Viatchenko-Karpinski & Gyorke, 2001). Specifically, increased SR Ca^{2+} load increases the open probability of RyRs (Lukyanenko et al., 1996), which increases the ability of $I_{Ca\text{-}L}$ to trigger SR Ca^{2+} release (Viatchenko-Karpinski & Gyorke, 2001). Thus, a small influx of trigger Ca^{2+} should be able trigger a large release of SR Ca^{2+} in cells where SR Ca^{2+} load is high. Since more SR Ca^{2+} is released for a given amount of trigger Ca^{2+}, it can be said that the gain of CICR is increased when SR Ca^{2+} load increases. The present study found that Ca^{2+} transient amplitudes were similar in WT and TG4 myocytes, despite a reduction in the magnitude of $I_{Ca\text{-}L}$ in TG4 myocytes. This suggests that more SR Ca^{2+} is released in TG4 myocytes for a given amount of trigger Ca^{2+}. This may indicate that the sensitivity of RyRs to Ca^{2+} in TG4 myocytes is increased, which results in an increase in gain of CICR. Further evidence for an increase in RyR sensitivity in TG4 myocytes comes from studies which have examined Ca^{2+} sparks in WT and TG4 myocytes. Previous work has shown that an increase in the sensitivity of SR Ca^{2+} release channels is associated with an increase in the frequency of spontaneous Ca^{2+} sparks (Viatchenko-Karpinski & Gyorke, 2001). Indeed, several studies have shown that the frequency of Ca^{2+} sparks is increased in TG4 myocytes (Grandy et al., 2004; Zhou et al., 1999b). This also suggests that the sensitivity of RyRs may be increased in TG4 myocytes. Overall, these findings support the idea that the sensitivity of CICR is increased in TG4 myocytes. Therefore, an increase in SR Ca^{2+} load, which results in an increase in the sensitivity of CICR, may explain the maintenance of normal contractions and Ca^{2+} transients despite a reduction in $I_{Ca\text{-}L}$ in voltage clamped TG4 myocytes.

The preceding considerations explain how contraction amplitude is maintained in voltage clamped TG4 myocytes despite a reduction in the magnitude of $I_{Ca\text{-}L}$. However, they do not entirely explain the increase in contraction amplitudes observed in field-stimulated TG4 myocytes. One possible explanation for the increase in contraction amplitudes in field-stimulated cells is the increase in action potential duration in TG4 myocytes (Janczewski et al., 2002; Zhou et al., 1999b). The present study has shown that when voltage clamped cells were activated with simulated TG4 action potentials, contractions were larger than when the cells were activated with simulated WT action potentials. This finding suggests that action potential duration is involved in the modulation of contraction amplitude in TG4 myocytes. Several studies have shown that increasing action potential duration decreases the rate of inactivation of $I_{Ca\text{-}L}$ (Sah et al., 2001). Thus, it is possible that the decreased rate of repolarization in TG4 myocytes decreases the rate of inactivation of $I_{Ca\text{-}L}$. This would result in a greater influx of extracellular Ca^{2+} even though peak $I_{Ca\text{-}L}$ is decreased (Sah et al., 2001). Ca^{2+} also can enter the cell via reverse mode NCX during the late phase of the action potential (Weisser-Thomas et al., 2003). Prolongation of action potential duration increases Ca^{2+} influx via reverse mode NCX (Weber et al., 2003; Weisser-Thomas et al., 2003). Thus, an increase in action potential duration in TG4 myocytes could increase cytosolic Ca^{2+} concentration, which would augment contraction. In addition, this study showed that SR Ca^{2+} stores are elevated in TG4 mice. An increase in SR Ca^{2+} stores can increase the sensitivity of SR Ca^{2+} release channels (Bassani et al., 1995; Lukyanenko et al., 1996; Viatchenko-Karpinski & Gyorke, 2001) and improve the ability of $I_{Ca\text{-}L}$ to trigger SR Ca^{2+} release (Viatchenko-Karpinski & Gyorke, 2001). Thus, a small $I_{Ca\text{-}L}$ can trigger a

large SR Ca^{2+} release. Therefore, increased SR Ca^{2+} stores also may contribute to the maintenance of contraction amplitudes in field-stimulated TG4 myocytes.

In summary, the present study demonstrates the magnitude of contraction is increased in field-stimulated TG4 myocytes that overexpress β_2ARs. In addition, this study shows that the increase in contraction amplitudes disappears in voltage clamped myocytes. Furthermore, the magnitude of $I_{Ca\text{-}L}$ is reduced in TG4 myocytes compared to WT myocytes. However, the gain of CICR is increased in TG4 myocytes and likely is related to increased SR Ca^{2+} stores. Overall, the results from this study show that the overexpression of β_2ARs alters EC coupling and increases the gain of CICR. Increased CICR gain likely compensates for the reduction in $I_{Ca\text{-}L}$ in voltage clamped myocytes and also may contribute to increased amplitudes of contraction in field-stimulated TG4 myocytes.

Global Conclusions

The results of this study demonstrate that EC coupling is dramatically altered in aged cardiac myocytes. These findings have shown that an age-related reduction in the magnitude of $I_{Ca\text{-}L}$ is partially responsible for significant reductions in contraction amplitudes at low stimulation frequencies (2 Hz). These changes at the cellular level would be predicted to negatively affect the overall performance of the heart. Thus, it appears that advancing age has a negative inotropic effect on cardiac function. This study also examined the possible beneficial effects of β_2AR overexpression on cardiac contractile function. The results showed that β_2AR ovexpression augmented contraction amplitude in murine ventricular myocytes by increasing the gain of CICR. Therefore, in

theory, it is possible that overexpression of β_2ARs in the aged heart also could increase the gain of CICR. This could result in the augmentation of contraction and improvement of cardiac function in the aging heart. However, whether the overexpression of β_2ARs would have similar effects on EC coupling in human ventricular myocytes or in aged myocytes is not yet clear and requires further investigation.

REFERENCES

Adamson DL, Money-Kyrle AR, & Harding SE. (2000). Functional evidence for a cyclic-AMP related mechanism of action of the β_2-adrenoceptor in human ventricular myocytes. *J Mol Cell Cardiol, 32*(7), 1353-1360.

Antoons G, Mubagwa K, Nevelsteen I, & Sipido KR. (2002). Mechanisms underlying the frequency dependence of contraction and $[Ca^{2+}]_i$ transients in mouse ventricular myocytes. *J Physiol (Lond), 543*(3), 889-898.

AstraZeneca. (2000). *The quiet heartbeat: A historical review of heart failure.* Molndal, Sweden: AstraZeneca.

Baartscheer A, Schumacher C, Opthof T, & Fiolet J. (1996). The origin of increased cytoplasmic calcium upon reversal of the Na^+/Ca^{2+}-exchanger in isolated rat ventricular myocytes. *J Mol Cell Cardiol, 28*(1), 1963-1973.

Bartel S, Krause EG, Wallukat G, & Karczewski P. (2003). New insights into β_2-adrenoceptor signaling in the adult rat heart. *Cardiovasc Res, 57*(3), 694-703.

Bassani J, Yuan W, & Bers D. (1995). Fractional SR Ca release is regulated by trigger Ca and SR Ca content in cardiac myocytes. *Am J Physiol, 268*, C1313-1319.

Bates S, & Gurney A. (1999). Use-dependent facilitation and depression of L-type Ca^{2+} current in guinea-pig ventricular myocytes: modulation by Ca^{2+} and isoprenaline. *Cardiovasc Res, 44*(2), 381-389.

Bean, B. (1985). Two kinds of calcium channels in canine atrial cells. *J Gen Physiol, 86*(1), 1-30.

Bers, D. (2001). *Excitation-contraction coupling and cardiac contractile force* (Second ed.). Boston: Kluwer Academic Publishers.

Bers D, Christensen D, & Nguyen T. (1988). Can Ca entry via Na-Ca exchange directly activate cardiac muscle contraction? *J Mol Cell Cardiol, 20*(5), 405-414.

Bers D, & Perez-Reyes E. (1999). Ca channels in cardiac myocytes: structure and function in Ca influx and intracellular Ca release. *Cardiovasc Res, 42*(2), 339-360.

Bers D, & Stiffel V. (1993). Ratio of ryanodine to dihydropyridine receptors in cardiac and skeletal muscle and implications for E-C coupling. *Am J Physiol: Cell Physiol, 264*(33), C1587-1593.

Bers DM. (2002). Cardiac excitation-contraction coupling. *Nature, 415*(6868), 198-205.

Besse S, Assayag P, Delcayre C, Carre F, Cheav SL, Lecarpentier Y, et al. (1993). Normal and hypertrophied senescent rat heart: mechanical and molecular characteristics. *Am J Physiol Heart Circ Physiol, 265*(1), H183-190.

Beuckelmann D, & Wier W. (1988). Mechanism of release of calcium from sarcoplasmic reticulum of guinea-pig cardiac cells. *J Physiol (Lond), 405*, 233-255.

Boluyt MO, Converso K, Hwang HS, Mikkor A, & Russell MW. (2004). Echocardiographic assessment of age-associated changes in systolic and diastolic function of the female F344 rat heart. *J Appl Physiol, 96*(2), 822-828.

Bond R, Johnson TD, Milano CA, Rockman HA, McMinn TR, Apparsundaram S, Hyek MF, Kenakin TP, Allen LF, & Lefkowitz RJ. (1995). Physiological effects of inverse agonists in transgenic mice with myocardial overexpression of the β_2-adrenoceptor. *Nature, 374*(6519), 272-276.

Brandl C, de Leon, S., Martin D, & MacLennan D. (1987). Adult forms of the Ca^{2+}ATPase of sarcoplasmic reticulum. Expression in developing skeletal muscle. *J Bio Chem, 262*(8), 3768-3774.

Brandl C, Green N, Korczak B, & MacLennan D. (1986). Two Ca^{2+} ATPase genes: homologies and mechanistic implications of deduced amino acid sequences. *Cell, 44*(4), 597-607.

Brette F, & Orchard C. (2003). T-tubule function in mammalian cardiac myocytes. *Circ Res, 92*(11), 1182-1192.

Bristow M, Hershberger RE, Port JD, Gilbert EM, Sandoval A, Rasmussen R, Cates A, & Feldman A. (1990). β-adrenergic pathways in nonfailing and failing human ventricular myocardium. *Circ, 82*(Suppl I), I-12-I-25.

Brittsan A, & Kranias E. (2000). Phospholamban and cardiac contractile function. *J Mol Cell Cardiol, 32*(12), 2131-2139.

Brodde O, Karad K, Zerkowski HR, Rohm N, & Reidemeister JC. (1983). Coexistance of β_1- and β_2-adrenoceptors in human right atrium. Direct identification by (+/–)-^{125}idocyanopindolol binding. *Circ Res, 53*(6), 752-758.

Callewaert G, Cleemann L, & Morad M. (1988). Epinephrine enhances Ca^{2+} current-regulated Ca^{2+} release and Ca^{2+} reuptake in rat ventricular myocytes. *PNAS, 85*(6), 2009-2013.

Canada. (2002). *Canada's Aging Population*. Ottawa, ON: Government of Canada.

Cannell M, Berlin J, & Lederer W. (1987). Effect of membrane potential changes on the calcium transient in single rat cardiac muscle cells. *Science, 238*(4832), 1419-1423.

Cannell M, Cheng H, & Lederer W. (1994). Spatial non-uniformities in $[Ca^{2+}]_i$ during excitation-contraction coupling in cardiac myocytes. *Biophys J, 67*(5), 1942-1956.

Cannell M, Cheng H, & Lederer W. (1995). The control of calcium release in heart muscle. *Science, 268*(5213), 1045-1049.

Capasso JM, Malhotra A, Remily RM, Scheuer J, & Sonnenblick EH. (1983). Effects of age on mechanical and electrical performance of rat myocardium. *Am J Physiol Heart Circ Physiol, 245*(1), H72-81.

Carnes CA, Geisbuhler TP, & Reiser PJ. (2004). Age-dependent changes in contraction and regional myocardial myosin heavy chain isoform expression in rats. *J Appl Physiol, 97*(1), 446-453.

Chen C, Nakayama M, Nevo E, Fetics B, Maughan W, & Kass D. (1998). Coupled systolic-ventricular and vascular stiffening with age: implications for pressure regulation and cardiac reserve in the elderly. *J Am Coll Cardiol, 32*(5), 1221-1227.

Cheng H, Lederer W, & Cannell M. (1993). Calcium sparks: elementry events underlying excitation-contraction coupling in heart muscle. *Science, 262*(5134), 740-744.

Chen-Izu Y, Xiao RP, Izu LT, Cheng H, Kuschel M, Spurgeon H, et al. (2000). G_i-dependent localization of beta 2-adrenergic receptor signaling to L-type Ca^{2+} channels. *Biophys J, 79*(5), 2547-2556.

Cribbs LL, Lee JH, Yang J, Satin J, Zhang Y, Daud A, et al. (1998). Cloning and characterization of α_{1H} from human heart, a member of the T-type Ca^{2+} channel gene family. *Circ Res, 83*(1), 103-109.

Daaka Y, Luttrell L, & Lefkowitz R. (1997). Switching of the coupling of β_2-adrenergic receptor to different G proteins by protein kinase A. *Nature, 300*(6655), 88-91.

Dannenberg A, Levy D, & Garrison R. (1989). Impact of age on echocardiographic left ventricular mass in a healthy population (the Framingham study). *Am J Cardiol, 64*(16), 1066-1068.

de Boer J, Andressoo JO, de Wit J, Huijmans J, Beems RB, van Steeg H, et al. (2002). Premature aging in mice deficient in DNA repair and transcription. *Science, 296*(5571), 1276-1279.

Devic E, Xiang Y, Gould D, & Kobilka B. (2001). Beta-adrenergic receptor subtype-specific signaling in cardiac myocytes from beta 1 and beta 2 adrenoceptor knockout mice. *Mol Pharmacol, 60*(3), 577-583.

Dibb K, Rueckschloss U, Eisner D, Insberg G, & Trafford A. (2004). Mechanisms underlying enhanced excitation contraction coupling observed in the senescent sheep myocardium. *J Mol Cell Cardiol, 37*(6), 1171-1181.

Dorn GW, Tepe NM, Lorenz JN, Kock WJ and Liggett SB. (1999). Low and high-level transgenic expression of β_2-adrenergic receptors differentially affect cardiac hypertrophy and function in Gαq-overexpressing mice. *Proc Natl Acad Sci, 96*(11), 6400-6405.

Dzimiri N. (1999). Regulation of β-adrenoceptor signaling in cardiac function and disease. *Pharmacol Rev, 51*(3), 465-502.

Eisner D, Trafford AW, Diaz ME, Overend CL, & O'Neill SC. (1998). The control of Ca release from the cardiac sarcoplasmic reticulum: regulation versus autoregulation. *Cardiovasc Res, 38*(3), 589-604.

Endo M, Tanaka M, & Ogawa Y. (1970). Calcium induced release of calcium from the sarcoplasmic reticulum of skinned skeletal muscle fibers. *Nature, 228*(5266), 34-36.

Engelhardt S, Hein L, Wiesmann F, & Lohse MJ. (1999). Progressive hypertrophy and heart failure in beta 1-adrenergic receptor transgenic mice. *PNAS, 96*(12), 7059-7064.

Fabiato A. (1983). Calcium-induced release of calcium from the cardiac sarcoplasmic reticulum. *Am J Physiol Cell Physiol, 245*(1), C1-14.

Fabiato A. (1985a). Rapid ionic modifications during the aequorin-detected calcium transient in a skinned canine cardiac Purkinje cell. *J Gen Physiol, 85*(2), 189-246.

Fabiato A. (1985b). Simulated calcium current can both cause calcium loading in and trigger calcium release from the sarcoplasmic reticulum of a skinned canine cardiac Purkinje cell. *J Gen Physiol, 85*(2), 291-320.

Fabiato A. (1985c). Time and calcium dependence of activation and inactivation of calcium- induced release of calcium from the sarcoplasmic reticulum of a skinned canine cardiac Purkinje cell. *J Gen Physiol, 85*(2), 247-289.

Fabiato A, & Fabiato F. (1973). Activation of skinned cardiac cells. Subcellular effects of cardioactive drugs. *Eur J Cardiol, 1*(2), 143-155.

Fabiato A, & Fabiato F. (1975). Contractions induced by a calcium-triggered release of calcium from the sarcoplasmic reticulum of single skinned cardiac cells. *J Physiol(Lond), 249*(3), 469-495.

Fabiato A, & Fabiato F. (1977). Calcium release from the sarcoplasmic reticulum. *Circ Res, 40*(2), 119-129.

Fabiato A, & Fabiato F. (1978). Calcium-induced release of calcium from the sarcoplasmic reticulum of skinned cells from adult human, dog, cat, rabbit, rat, and frog hearts and from fetal new-born rat ventricles. *Ann N Y Acad Sci, 307*, 491-522.

Fabiato A, & Fabiato F. (1979). Use of chlorotetracycline fluorescence to demonstrate Ca^{2+}-induced release of Ca^{2+} from the sarcoplasmic reticulum of skinned cardiac cells. *Nature, 281*(5727), 146-148.

Ferrier G, & Howlett S. (1995). Contractions in guinea-pig ventricular myocytes triggered by a calcium-release mechanism separate from Na^{+} and L-currents. *J Physiol (Lond), 484 (Pt 1)*, 107-122.

Ferrier G, Richard M, Shutt R, & Howlett SE. (2004). A separate ultra-high gain CICR mechanism accounts for sigmoidal contraction-voltage relations in cardiac ventricular myocytes when phosphorylation pathways are preserved at physiologic temperature. *Biophys J, 86*(1), 65a.

Ferrier G, Smith RH, & Howlett SE. (2003). Calcium sparks in mouse ventricular myocytes at physiological temperature. *Am J Physiol: Heart Circ Physiol, 285(4)*, H1495-1505.

Ferrier GR, & Howlett SE. (2001). Cardiac excitation-contraction coupling: role of membrane potential in regulation of contraction. *Am J Physiol: Heart Circ Physiol, 280*(5), H1928-1944.

Ferrier GR, Redondo IM, Mason CA, Mapplebeck C, & Howlett SE. (2000). Regulation of contraction and relaxation by membrane potential in cardiac ventricular myocytes. *Am J Physiol Heart Circ Physiol, 278*(5), H1618-1626.

Ferrier GR, Zhu J, Redondo IM, & Howlett SE. (1998). Role of cAMP-dependent protein kinase A in activation of a voltage-sensitive release mechanism for cardiac contraction in guinea-pig myocytes. *J Physiol (Lond), 513*(1), 185-201.

Fitchett D, & Rockwood K. (2002). *Heart disease in an elderly population.* Paper presented at the Consensus Conference 2002: Management of Heart Disease in the Elderly Patient.

Fitzsimons DP, Patel JR, & Moss RL. (1998). Role of myosin heavy chain composition in kinetics of force development and relaxation in rat myocardium. *J Physiol (Lond), 513*(1), 171-183.

Fitzsimons DP, Patel JR, & Moss RL. (1999). Aging-dependent depression in the kinetics of force development in rat skinned myocardium. *Am J Physiol Heart Circ Physiol, 276*(5), H1511-1519.

Fleg JL, O'Connor F, Gerstenblith G, Becker LC, Clulow J, Schulman SP., et al. (1995). Impact of age on the cardiovascular response to dynamic upright exercise in healthy men and women. *J Appl Physiol, 78*(3), 890-900.

Ford L, & Podolsky R. (1970). Regenerative calcium release within muscle cells. *Science, 167*(914), 58-59.

Frank K, Bolck B, Erdmann E, & Schwinger R. (2003). Sarcoplasmic reticulum Ca^{2+}-ATPase modulates cardiac contraction and relaxation. *Cardiovasc Res, 57*(1), 20-27.

Franzini-Armstrong C. (1970). Studies of the triad. I. Structure of the junction in frog twitch fibers. *J Cell Biol, 47*(2), 488-499.

Fraticelli A, Josephson R, Danziger R, Lakatta E, & Spurgeon H. (1989). Morphological and contractile characteristics of rat cardiac myocytes from maturation to senescence. *Am J Physiol Heart Circ Physiol, 257*(26), H259-265.

Ganau A, Saba P, Roman M, de Simone G, Realdi G, & Devereux R. (1995). Aging induces left ventricular concentric remodeling in normotensive patients. *J Hypertens, 13*(12 Pt 2), 1818-1822.

Gardin J, Arnold A, Bild D, Smith V, Lima J, Klopfenstein H, et al. (1998). Left ventricular diastolic filling in the elderly: The Cardiovascular Health Study. *Am J Cardiol, 82*(3), 345-351.

Gerhard G, & Kasales C. (2003). Aging and kyphosis. *J Gerontol: Biol Sci, 58A*(11), 968.

Gille E, Lemoine H, Ehle B, & Kaumann AJ. (1985). The affinity of (-)-propranolol for β_1- and β_2-adrenoceptors of human heart. Differential antagonism of the positive inotropic effects and adenylate cyclase stimulation by (-)-noradrenaline and (-)-adrenaline. *Naunyn-Schmiedeberg's Arch Pharmacol, 331*(1), 60-70.

Gong H, Adamson DL, Ranu HK, Koch WJ, Heubach JF, Ravens U, Zolk O, & Harding SE. (2000). The effect of G_i-protein inactivation on basal, and β_1- and β_2AR-stimulated contraction of myocytes from transgenic mice overexpressing the β_2-adrenoceptor. *Br J Pharmacol, 131*(3), 594-600.

Grandy S, Denovan-Wright EM, Ferrier GR, & Howlett SE. (2004). Overexpression of human β_2-adrenergic receptors increases gain of excitation-contraction coupling in mouse ventricular myocytes. *Am J Physiol Heart Circ Physiol, 287*, H1029-1038.

Grynkiewicz G, Poenie M, & Tsien R. (1985). A new generation of Ca^{2+} indicators with greatly improved fluorescence properties. *J Biol Chem, 260*(6), 3440-3450.

Gurdal H, Bond RA, Johnson MD, Friedman E, & Onaran HO. (1997). An efficacy-dependent effect of cardiac overexpression of β_2-adrenoceptor on ligand affinity in transgenic mice. *Mol Pharmacol, 52*(2), 187-194.

Hadley R, & Hume J. (1987). An intrinsic potential-dependent inactivation mechanism associated with calcium channels in guinea-pig myocytes. *J Physiol (Lond), 389*, 205-222.

Hagiwara N, Irisawa H, & Kameyama M. (1988). Contribution of two types of calcium currents to the pacemaker potentials of rabbit sino-atrial node cells. *J Physiol (Lond), 395*, 233-253.

Hees PS, Fleg JL, Dong SJ, & Shapiro EP. (2004). MRI and echocardiographic assessment of the diastolic dysfunction of normal aging: altered LV pressure decline or load? *Am J Physiol Heart Circ Physiol, 286*(2), H782-788.

Heitz A, Schwartz J, & Velly J. (1983). β-adrenoceptors of human myocardium - determination of β_1 and β_2 subtypes by radioligand binding. *Br J Pharmacol, 80*(4), 711-717.

Heubach J, Graf E, Molenaar P, Jager A, Schroder F, Herzig S, et al. (2001). Murine ventricular L-type Ca^{2+} current is enhanced by zinterol via β_1-adrenoceptors, and is reduced in TG4 mice overexpressing the human β_2-adrenoceptor. *Br J Pharmacol, 133*(1), 73-82.

Heubach J, Trebess I, Wettwer E, Himmel H, Michel M, Kaumann A, et al. (1999). L-type calcium current and contractility in ventricular myocytes from mice overexpressing the cardiac β_2-adrenoceptor. *Cardiovasc Res, 42*(1), 173-182.

Hicks M, Shigekawa M, & Katz A. (1979). Mechanism by which cyclic adenosine 3':5'-monophosphate-dependent protein kinase stimulates calcium transport in cardiac sarcoplasmic reticulum. *Circ Res, 44*(3), 384-391.

Hirano Y, Fozzard HA, & January CT. (1989). Characteristics of L- and T-type Ca^{2+} currents in canine cardiac Purkinje cells. *Am J Physiol Heart Circ Physiol, 256*(5), H1478-1492.

Hobai I, Howarth FC, Pabbathi VK, Dalton GR, Hancox JC, Zhu JQ, Howlett SE, Ferrier GR, & Levi AJ. (1997). "Voltage-activated Ca release" in rabbit, rat, guinea-pig cardiac myocytes, and modulation by internal cAMP. *Pflugers Archive, 435*(1), 164-173.

Howlett S, & Nicholl P. (1992). Density of 1,4-dihydropyridine receptors decreases in the hearts of aging hamsters. *J Mol Cell Cardiol, 24*(8), 885-894.

Howlett S, Zhu JQ, & Ferrier GR. (1998). Contribution of a voltage-sensitive calcium release mechanism to contraction in cardiac ventricular myocytes. *Am J Physiol: Heart Circ Physiol, 274*(1 Pt 2), H155-170.

Heart and Stroke Foundation of Canada. (2003). *The Growing Burden of Heart Disease and Stroke.* Ottawa: Heart and Stroke Foundation of Canada.

Ingram D. (2000). Age-related decline in physical activity: generalization to nonhumans. *Med Sci Sports Exerc, 32*(9), 1623-1629.

Inui M, Chamberlain B, Saito A, & Fleischer S. (1986). The nature of the modulation of Ca2+ transport as studied by reconstitution of cardiac sarcoplasmic reticulum. *J Biol Chem, 261*(4), 1794-1800.

Inui M, Saito A, & Fleischer S. (1987a). Isolation of the ryanodine receptor from cardiac sarcoplasmic reticulum and identity with the feet structures. *J Biol Chem, 262*(32), 15637-15642.

Inui M, Saito A, & Fleischer S. (1987b). Purification of the ryanodine receptor and identity with feet structures of junctional terminal cisternae of sarcoplasmic reticulum from fast skeletal muscle. *J Biol Chem, 262*(4), 1740-1747.

Isenberg G, Borschke B, & Rueckschloss U. (2003). Ca^{2+} transients in cardiomyocytes from senescent mice peak late and decay slowly. *Cell Calcium, 34*(3), 271-280.

Janczewski A, Spurgeon H, & Lakatta E. (2002). Action potential prolongation in cardiac myocytes of old rats is an adaptation to sustain youthful intracellular Ca^{2+} regulation. *J Mol Cell Cardiol, 34*(6), 641-648.

Josephson I, Guia A, Stern M, & Lakatta E. (2002). Alterations in properties of L-type Ca channels in aging rat heart. *J Mol Cell Cardiol, 34*(3), 297-308.

Jurevicius J, & Fischmeister R. (1996). cAMP compartmentation is responsible for a local activation of cardiac Ca^{2+} channels by beta -adrenergic agonists. *PNAS, 93*(1), 295-299.

Kaftan E, Marks AR, & Ehrlich BE. (1996). Effects of Rapamycin on Ryanodine Receptor/Ca^{2+}-Release Channels From Cardiac Muscle. *Circ Res, 78*(6), 990-997.

Kaspar S, & Pelzer D. (1995). Modulation of stimulation rate of basal cAMP-elevated Ca^{2+} channel current in guinea pig ventricular cardiomyocytes. *J Gen Physiol, 106*(2), 175-201.

Kaumann A, & Lemoine H. (1987). β_2-adrenoceptor-mediated positive inotropic effect of adrenaline in human ventricular myocradium. *Naunyn-Schmiedeberg's Arch Pharmacol, 335*(4), 403-411.

Kaumann A, Lemoine H, & Ehle B. (1985). Differential involvement of β_1- and β_2-adrenoceptors in the effects of (-)-noradrenaline and (-)-adrenaline in several heart regions of cat, guinea pig and man. *Pflugers Archive, 403*, R27.

Kaumann A, Lemoine H, Morris T, & Schwederski U. (1982). An initial characterization of human β-adrenoceptors and their mediation of the positive inotropic effects of catecholamines. *Naunyn-Schmiedeberg's Arch Pharmacol, 319*(3), 216-221.

Kaumann A, & Lobnig BM. (1986). Mode of action of (-)-pindolol on feline and human myocardium. *Br J Pharmacol, 89*(1), 207-218.

Kirchberger MA, Tada M, & Katz AM. (1974). Adenosine 3':5'-monophosphate-dependent protein kinase-catalyzed phosphorylation reaction and its relationship to calcium transport in cardiac sarcoplasmic reticulum. *J Biol Chem, 249*(19), 6166-6173.

Kitzman D. (2000). Heart failure with normal systolic function. *Clin Geriatr Med, 16*(3), 489-512.

Kitzman D. (2002). Diastolic heart failure in the elderly. *Heart Fail Rev, 7*(1), 17-27.

Kitzman D, Scholz D, Hagen P, Ilstrup D, & Edwards W. (1988). Age-related changes in normal human hearts during the first 10 decades of life. Part II (Maturity): A quantitative anatomic study of 765 specimens from subjects 20-99 years old. *Mayo Clin Proc, 63*(2), 137-146.

Kitzman D, Sheikh K, Beere P, Philips J, & Higginbotham M. (1991). Age-related Doppler left ventricular filling indexes in normal subjects are independent of left ventricular mass, heart rate, contractility and loading conditions. *J Am Coll Cardiol, 18*(5), 1243-1250.

Koss KL, & Kranias EG. (1996). Phospholamban: A prominent regulator of myocardial contractility. *Circ Res, 79*(6), 1059-1063.

Kranias E. (1985). Regulation of Ca^{2+} transport by cyclic 3',5'-AMP-dependent and calcium calmodulin-dependent phosphorylation of cardiac sarcoplasmic reticulum. *Biochim Biophys Acta, 844*(2), 193-199.

Kukushkin N, Gainullin R, & Sosunov E. (1983). Transient ouward current and rate dependence of action potential duration in rabbit cardiac ventricular muscle. *Pflugers Arch, 399*(2), 87-92.

Kuschel M, Zhou YY, Cheng H, Zhang SJ, Chen Y, Lakatta EG, et al. (1999). G_i protein-mediated functional compartmentalization of cardiac beta 2-adrenergic signaling. *J Biol Chem, 274*(31), 22048-22052.

Kuschel M, Zhou YY, Spurgeon HA, Bartel S, Karczewski P, Zhang SJ, et al. (1999). $ß_2$-adrenergic cAMP signaling is uncoupled from phosphorylation of cytoplasmic proteins in canine heart. *Circ, 99*(18), 2458-2465.

Lai F, Erickson H, Rousseau E, Liu Q, & Meissner G. (1988). Purification and reconstitution of the calcium release channel from skeletal muscle. *Nature, 331*(6154), 315-319.

Lakatta E, & Sollot S. (2002). Perspectives on mammalian cardiovascular aging: humans to molecules. *Comp Biochem Physiol, 132*(Part A), 699-721.

Lakatta E, & Yin F. (1982). Myocardial aging: functional alterations and related cellular mechanisms. *Am J Physiol Heart Circ Physiol, 242*(11), H927-941.

Langer G. (1997). *The Myocardium* (2 ed.). Boston: Academic Press.

Langer G, & Peskoff A. (1996). Calcium concentration movement in the diadic cleft space of the cardiac ventricular cell. *Biophys J, 70*(3), 1169-1182.

Leblanc N, & Hume J. (1990). Sodium current-induced release of calcium from cardiac sarcoplasmic reticulum. *Science, 248*(4953), 372-376.

Lederer W, Niggli E, & Hadley R. (1990). Sodium-calcium exchange in excitable cells: fuzzy space. *Science,* 24(4953)8, 283.

Lee K, Marban E, & Tsien R. (1985). Inactivation of calcium channels in mammalian heart cells: joint dependence on membrane potential and intracellular calcium. *J Physiol (Lond), 364*, 395-411.

Levi AJ, Spitzer KW, Kohmoto O, & Bridge JH. (1994). Depolarization-induced Ca entry via Na-Ca exchange triggers SR release in guinea pig cardiac myocytes. *Am J Physiol Heart Circ Physiol, 266*(4), H1422-1433.

Levin K, & Page E. (1980). Quantitative studies on plasmalemmal folds and caveolae of rabbit ventricular myocardial cells. *Circ Res, 46*(2), 244-255.

Levy W, Cerqueira M, Abrass I, Schwartz R, & Stratton J. (1993). Endurance exercise training augments diastolic filling at rest and during exercise in healthy young and older men. *Circ, 88*(1), 116-126.

Liggett S, Tepe NM, Lorenz JN, Canning AM, Jantz TD, Mitarai S, Yatani A, & Dorn GW. (2000). Early and delayed consequences of β_2-adrenergic receptor overexpression in mouse hearts : critical role for expression level. *Circ, 101*(14), 1707-1714.

Lim C, Apstein C, Colucci W, & Liao R. (2000). Impaired cell shortening and relengthening with increased pacing frequency are intrinsic to the senescent mouse cardiomyocyte. *J Mol Cell Cardiol, 32*(11), 2075-2082.

Lim CC, Liao R, Varma N, & Apstein CS. (1999). Impaired lusitropy-frequency in the aging mouse: role of Ca^{2+}-handling proteins and effects of isoproterenol. *Am J Physiol Heart Circ Physiol, 277*(5), H2083-2090.

Liu SJ, Wyeth RP, Melchert RB, & Kennedy RH. (2000). Aging-associated changes in whole cell K^+ and L-type Ca^{2+} currents in rat ventricular myocytes. *Am J Physiol Heart Circ Physiol, 279*(3), H889-900.

Lohn M, Furstenau M, Sagach V, Elger M, Schulze W, Luft FC., et al. (2000). Ignition of calcium sparks in arterial and cardiac muscle through caveolae. *Circ Res, 87*(11), 1034-1039.

London B, & Krueger J. (1986). Contraction in voltage-clamped, internally perfused single heart cells. *J Gen Physiol, 88*(4), 475-505.

Lopez-Lopez J, Shacklock P, Balke C, & Wier, W. (1994). Local, stochastic release of Ca^{2+} in voltage-clamped rat heart cells: visualization with confocal microscopy. *J Physiol (Lond), 480*(1), 21-29.

Lopez-Lopez J, Shacklock P, Balke C, & Wier W. (1995). Local calcium transients triggered by single L-type calcium channel currents in cardiac cells. *Science, 268*(5213), 1042-1045.

Lukyanenko V, Gyorke I, & Gyorke E. (1996). Regulation of calcium release by calcium inside the sarcoplasmic reticulum in ventricular myocytes. *Pflugers Archive, 432*(6), 1047-1054.

Lutz J. (1988). A XII century description of heart failure. *Am J Cardiol, 61*(6), 494-495.

Lye M, & Donnellan C. (2000). Heart disease in the elderly. *Heart, 84*, 560-566.

Mace LC, Palmer BM, Brown DA., Jew KN, Lynch JM, Glunt JM, et al. (2003). Influence of age and run training on cardiac Na^{+}/Ca^{2+} exchange. *J Appl Physiol, 95*(5), 1994-2003.

Marx SO, Ondrias K, & Marks AR. (1998). Coupled sating between individual skeletal muscle Ca^{2+} release channels (Ryanodine Receptors). *Science, 281*(5378), 818-821.

Maurice JP, Hata JA, Shah AS, White DC, McDonald PH, Dolber PC, et al. (1999). Enhancement of cardiac function after adenoviral-mediated in vivo intracoronary β_2-adrenergic receptor gene delivery. *J Clin Invest, 104*(1), 21-29.

Meissner G. (1975). Isolation and characterization of two types of sarcoplasmic reticulum vesicles. *Biochim Biophys Acta, 389*(1), 51-68.

Meissner G. (2004). Molecular regulation of the cardiac ryanodine receptor ion channel. *Cell Calcium, 35*(6), 621-628.

Meissner G, & Henderson J. (1987). Rapid calcium release from cardiac sarcoplasmic reticulum vesicles is dependent on Ca^{2+} and is modulated by Mg^{2+}, adenine nucleotide, and calmodulin. *J Biol Chem, 262*(7), 3065-3073.

Melzer W, Schneider MF, Simon BJ, & Szues G. (1986). Intramembrane charge movement and calcium release in frog skeletal muscle. *J Physiol (Lond), 373*, 481-511.

Metzger J, Wahr P, Michele D, Albayya F, & Westfall M. (1999). Effects of myosin heavy chain isoform switching on Ca^{2+}-activated tension in single adult cardiac myocytes. *Circ Res, 84*(11), 1310-1317.

Mikami A, Imoto K, Tanabe T, Niidome T, Mori Y, Takeshima H, et al. (1989). Primary structure and functional expression of cardiac dihydropyridine sensitive calcium channel. *Nature, 340*(6230), 230-233.

Milano C, Allen LF, Rockman HA, Dobler PC, McMinn TR, Chien KR, Johnson TD, Bond RA, & Lefkowitz RJ. (1994). Enhanced myocardial function in transgenic mice overexpressing the β_2-adrenergic receptor. *Science, 264*(5158), 582-586.

Mitra R, & Morad M. (1986). Two types of calcium channels in guinea pig ventricular myocytes. *PNAS, 83*(14), 5340-5344.

Morley J, & Reese S. (1989). Clinical implications of the aging heart. *Am J Med, 86*(1), 77-86.

Nabauer M, Callewaert G, Cleemann L, & Morad M. (1989). Regulation of calcium release is gated by calcium current, not gating charge, in cardiac myocytes. *Science, 244*(4906), 800-803.

Nabauer M, & Morad M. (1990). Ca^{2+}-induced Ca^{2+} release as examined by photolysis of caged Ca^{2+} in single ventricular myocytes. *Am J Physiol Cell Physiol, 258*(1), C189-193.

Najjar S, Schulman S, Gerstenblith G, Fleg J, Kass D, O'Connor F, et al. (2004). Age and gender affect ventricular-vascular coupling during aerobic exercise. *J Am Coll Cardiol, 44*(3), 611-617.

Niggli E, & Lederer W. (1990). Voltage-independent calcium release in heart muscle. *Science, 250*(4980), 565-568.

Niimi Y, Hino N, & Ochi R. (2003). Diltiazem facilitates inactivation of single L-type calcium channels in guinea pig ventricular myocytes. *Jpn Heart J, 44*(6), 1005-1014.

Okamoto T, Schlegel A, Scherer PE, & Lisanti MP. (1998). Caveolins, a family of scaffolding proteins for organizing "preassembled signaling complexes" at the plasma membrane. *J Biol Chem, 273*(10), 5419-5422.

Olivetti G, Melissari M, Capasso J, & Anversa P. (1991). Cardiomyopathy of the aging human heart. Myocyte loss and reactive cellular hypertrophy. *Circ Res, 68*(6), 1560-1568.

Orchard C, & Lakatta E. (1985). Intracellular calcium transients and developed tension in rat heart muscle. *J Gen Physiol, 86*(5), 637-651.

Ostrom RS, Post SR, & Insel PA. (2000). Stoichiometry and compartmentation in G protein-coupled receptor signaling: implications for therapeutic interventions involving G_s. *J Pharmacol Exp Ther, 294*(2), 407-412.

Oxenham H, & Sharpe N. (2003). Cardiovascular aging and heart failure. *Eur J Heart Fail, 5*(4), 427-434.

Pacher P, Mabley J, Liaudet L, Evgenov O, Marton A, Hasko G, et al. (2004). Left ventricular pressure-volume relationship in a rat model of aging-associated heart failure. *Am J Physiol Heart Circ Physiol, 287*(5), H2132-2137.

Page E, Fozzard H, & Solaro R. (2002). *The Heart* (Vol. 1). Toronto, ON: Oxford University Press.

Palakodeti V, Oh S, Oh BH, Mao L, Hongo M, Peterson KL, et al. (1997). Force-frequency effect is a powerful determinant of myocardial contractility in the mouse. *Am J Physiol Heart Circ Physiol, 273*(3), H1283-1290.

Peeters A, Mamun A, Willekens F, & Bonneux L. (2002). A cardiovascular life history. A life course analysis of the original Framingham Heart Study cohort. *Eur Heart J, 23*(6), 458-466.

Perez-Reyes E, Castellano A, Kim H, Bertrand P, Baggstrom E, Lacerda A, et al. (1992). Cloning and expression of a cardiac/brain beta subunit of the L-type calcium channel. *J Biol Chem, 267*(3), 1792-1797.

Perez-Reyes E, Cribbs L, Daud A, Lacerda A, Barclay J, Williamson M, et al. (1998). Molecular characterization of a neuronal low-voltage activated T-type Ca channel. *Nature, 39*(6670), 896-900.

Perez-Reyes E, Kim H, Lacerda A, Horne W, Wei X, Rampe D, et al. (1989). Induction of calcium currents by the expression of α_1-subunit of the dihydropyridine receptor from skeletal muscle. *Nature, 340*(6230), 233-236.

Post SR, Hammond HK, & Insel PA. (1999). Beta-adrenergic receptors and receptor signaling in heart failure. *Annu Rev Pharmacol Toxicol, 39*(1), 343-360.

Puglisi J, Bassani RA, Bassani JW, Amin JN, & Bers DM. (1996). Temperature and relative contributions of Ca transport systems in cardiac myocyte relaxation. *Am J Physiol: Heart Circ Physiol, 270*(5), H1772-1778.

Puglisi JL, Yuan W, Bassani JWM, & Bers DM. (1999). Ca^{2+} influx through Ca^{2+} channels in rabbit ventricular myocytes during action potential clamp: Influence of temperature. *Circ Res, 85*(6), 7-16.

Rapundalo S. (1998). Cardiac protein phosphorylation: functional and pathophysiological correlates. *Cardiovasc Res, 38*(3), 559-588.

Reddy LG, Jones LR, Pace RC, & Stokes DL. (1996). Purified, reconstituted cardiac Ca^{2+}-ATPase is regulated by phospholamban but not by direct phosphorylation with Ca^{2+}/calmodulin-dependent protein kinase. *J Biol Chem, 271*(25), 14964-14970.

Reiken S, Gaburjakova M, Guatimosim S, Gomez AM, D'Armiento J, Burkhoff D, et al. (2003). Protein kinase A phosphorylation of the cardiac calcium release channel (ryanodine receptor) in normal and failing hearts. Role of phosphatases and response to isoproterenol. *J Biol Chem, 278*(1), 444-453.

Robberecht P, Delhaye M, Tanton G, De Neef P, Waelbrock M, De Smet JM, Leclerc JL, Chatelain P, & Christophe J. (1983). The human heart β-adrenergic receptors. I. Heterogenity of the binding sites: Presence of 50% β_1-adrenergic receptors. *Mol Pharmacol, 24*(2), 169-173.

Rockman H, Hamilton R, Jones LR, Milano CA, Mao L, & Lefkowitz RJ. (1996). Enhanced myocardial relaxation in vivo in transgenic mice overexpressing the β_2-adrenergic receptor is associated with reduced phospholamban protein. *J Clinical Invest, 97*(7), 1618-1623.

Rothschuh K. (1973). *History of Physiology* (G. Risse, Trans.). Huntington, New York: Robert E. Krieger Publishing Company.

Rousseau E, & Meissner G. (1989). Single cardiac sarcoplasmic reticulum Ca^{2+}-release channel: activation by caffeine. *Am J Physiol Heart Circ Physiol, 256*(2), H328-333.

Rybin VO, Xu X, Lisanti MP, & Steinberg SF. (2000). Differential targeting of beta -adrenergic receptor subtypes and adenylyl cyclase to cardiomyocyte caveolae. A mechanism to functionally regulate the cAMP signaling pathway. *J Biol Chem, 275*(52), 41447-41457.

Sah R, Ramirez RJ, Kaprielian R, & Backx PH. (2001). Alterations in action potential profile enhance excitation-contraction coupling in rat cardiac myocytes. *J Physiol (Lond), 533*(1), 201-214.

Samama P, Bond RA, Rockman HA, Milano CA, & Lefkowitz RJ. (1997). Ligand-induced overexpression of a constitutively active β_2-adrenergic receptor: Pharmacological creation of a phenotype in transgenic mice. *PNAS, 94*(1), 137-141.

Santana L, Cheng H, Gomez A, Cannell M, & Lederer W. (1996). Relation between sarcolemmal Ca^{2+} current and Ca^{2+} sparks and local control theories for cardiac excitation-contraction coupling. *Circ Res, 78*(1), 166-171.

Sathyamangla V, Prasad N, Nienaber J, & Rockman H. (2001). β-adrenergic axis and heart disease. *Trends in Genetics, 17*(10), S44-S49.

Saxon M, & Safronova V. (1982). The rest-dependent depression of action potential duration in rabbit myocardium and the possible role of the transient outward current. A pharmacological analysis. *J Physiol (Paris), 78*(5), 461-466.

Schmidt U, del Monte F, Miyamoto MI, Matsui T, Gwathmey JK, Rosenzweig A, et al. (2000). Restoration of diastolic function in senescent rat hearts through adenoviral gene transfer of sarcoplasmic reticulum Ca^{2+}-ATPase. *Circ, 101*(7), 790-796.

Schulman SP, Lakatta EG, Fleg JL, Lakatta L, Becker LC, & Gerstenblith G. (1992). Age-related decline in left ventricular filling at rest and exercise. *Am J Physiol Heart Circ Physiol, 263*(6), H1932-1938.

Schwencke C, Yamamoto M, Okumura S, Toya Y, Kim SJ, & Ishikawa Y. (1999). Compartmentation of cyclic adenosine 3',5'-monophosphate signaling in caveolae. *Mol Endocrinol, 13*(7), 1061-1070.

Shah AS, Lilly RE, Kypson AP, Tai O, Hata JA, Pippen A, et al. (2000). Intracoronary adenovirus-mediated delivery and overexpression of the β_2-adrenergic receptor in the heart: prospects for molecular ventricular assistance. *Circ, 101*(4), 408-414.

Sham J, Cleemann L, & Morad M. (1992). Gating of cardiac Ca^{2+} release channel: The role of Na^+ and Na^+-Ca^{2+} exchange. *Science, 255*(5046), 850-853.

Sham J, Cleemann L, & Morad M. (1995). Functional coupling of Ca^{2+} channels and ryanodine receptors in cardiac myocytes. *PNAS, 92*(1), 121-125.

Shannon TR, Ginsburg KS, & Bers DM. (2000). Potentiation of fractional sarcoplasmic reticulum calcium release by total and free intra-sarcoplasmic reticulum calcium concentration. *Biophys J, 78*(1), 334-343.

Shaul PW, & Anderson RGW. (1998). Role of plasmalemmal caveolae in signal transduction. *Am J Physiol Lung Cell Mol Physiol, 275*(5), L843-851.

Shore J. (1985). Changes in lower eyelid resting position, movement and tone with age. *Am J Ophthalmol, 99*(4), 415-423.

Simmerman H, Collins J, Theibert J, Wegener A, & Jones L. (1986). Sequence analysis of phospholamban. Identification of phosphorylation sites and two major structural domains. *J Biol Chem, 261*(28), 13333-13341.

Sipido K Carmeliet E, & Pappano A. (1995). Na^+ current and Ca^{2+} release from the sarcoplasmic reticulum during action potentials in guinea-pig ventricular myocytes. *J Physiol (Lond), 489*(1), 1-17.

Sipido K, Carmeliet E, & Van de Werf F. (1998). T-type Ca^{2+} current as a trigger for Ca^{2+} release from the sarcoplasmic reticulum in guinea-pig ventricular myocytes. *J Physiol, 508.2*, 439-451.

Sipido KR, Maes M, & Van de Werf, F. (1997). Low efficiency of Ca^{2+} entry through the Na^+-Ca^{2+} exchanger as trigger for Ca^{2+} release from the sarcoplasmic reticulum : A comparison between L-Type Ca^{2+} current and reverse-mode Na^+-Ca^{2+} Exchange. *Circ Res, 81*(6), 1034-1044.

Sjaastad I, Wasserstrom J, & Sejersted O. (2003). Heart Failure - a challenge to our current concepts of excitation-contraction coupling. *J Physiol, 546.1*, 33-47.

Skeberdis VA, & Fischmeister AR. (1997). Beta-2 adrenergic activation of L-type Ca^{++} current in cardiac myocytes. *J Pharmacol Exp Ther, 283*(2), 452-461.

Steinberg SF. (2000). The cellular actions of β-adrenergic receptor agonists: looking beyond cAMP. *Circ Res, 87*(12), 1079-1082.

Steinberg SF, & Brunton LL. (2001). Compartmentation of G protein-coupled signaling pathways in cardiac myocytes. *Annu Rev Pharmacol Toxicol, 41*(1), 751-773.

Stern M. (1992). Theory of excitation-contraction coupling in cardiac muscle. *Biophys J, 63*(2), 497-517.

Stern M, & Lakatta E. (1992). Excitation-contraction coupling in the heart: the state of the question. *FASEB J., 6*(12), 3092-3100.

Stiles G, Taylor S, & Lefkowitz RJ. (1983). Human cardiac β-adrenergic receptors: subtype heterogenity delineated by direct radiologand binding. *Life Sciences, 33*(5), 467-473.

Tada M, Kirchberger MA, Repke DI, & Katz AM. (1974). The stimulation of calcium transport in cardiac sarcoplasmic reticulum by adenosine 3':5'-monophosphate-dependent protein kinase. *J Biol Chem, 249*(19), 6174-6180.

Tada M, Yamada M, Kadoma M, Inui M, & Ohmori F. (1982). Calcium transport by cardiac sarcoplasmic reticulum and phosphorylation of phospholamban. *Mol Cell Biochem, 46*(2), 73-95.

Tou J, & Wade C. (2002). Determinants affecting physical activity levels in animal models. *Exp Biol Med, 227*(8), 587-600.

Trafford A, Diaz M, & Eisner D. (1998). Stimulation of Ca-induced Ca release only transiently increases the systolic Ca transient: measurements of Ca fluxes and sarcoplasmic reticulum Ca. *Cardiovasc Res, 37*(3), 710-717.

Trafford A, Diaz ME, & Eisner DA. (2001). Coordinated control of cell Ca^{2+} loading and triggered release from the sarcoplasmic reticulum underlies the rapid inotropic response to increased L-type Ca^{2+} current. *Circ Res, 88*(2), 195-201.

Trifunovic A, Wredenberg A, Falkenberg M, Spelbrink J, Rovio A, Bruder C, et al. (2004). Premature aging in mice expressing defective mitochondrial DNA polymerase. *Nature, 429*(6990), 417-423.

Turturro A, Witt W, Lewis S, Hass B, Lipman R, & Hart R. (1999). Growth curves and survival characteristics of the animals used in the biomarkers of aging program. *J Gerentol: Biol Sci, 54A*(11), B492-B501.

Valdeolmillos M, O'Neill S, Smith G, & Eisner D. (1989). Calcium-induced calcium release activates contraction in intact cardiac cells. *Pflugers Archive, 413*(6), 676-678.

Van Praagh R. (1983). Aristotle's "Triventricular " heart and the relevant early history of the cardiovascular system. *Chest, 84*(4), 462-468.

Vanoverschelde JJ, Essamri B, Vanbutsele R, d'Hondt A, Cosyns JR, Detry JR, et al. (1993). Contribution of left ventricular diastolic function to exercise capacity in normal subjects. *J Appl Physiol, 74*(5), 2225-2233.

Viatchenko-Karpinski S, & Gyorke S. (2001). Modulation of the Ca^{2+}-induced Ca^{2+} release cascade by β-adrenergic stimulation in rat ventricular myocytes. *J Physiol (Lond), 533*(3), 837-848.

Vildivia H, Kaplan J, Ellis-Davies G, & Lederer W. (1997). Rapid adaptation of cardiac ryanodine receptors: Modulation by Mg^{2+} and phosphorylation. *Science, 267*(5206), 1997-2000.

Wahr PA, Michele DE, & Metzger JM. (2000). Effects of aging on single cardiac myocyte function in Fischer 344 x Brown Norway rats. *Am J Physiol Heart Circ Physiol, 279*(2), H559-565.

Walker K, Lakatta E, & Houser S. (1993). Age associated changes in membrane currents in rat ventricular myocytes. *Cardiovasc Res, 27*(11), 1968-1977.

Wasserstrom J, & Vites A. (1996). The role of Na^{+}-Ca^{2+} exchange in activation of excitation-contraction coupling in rat ventricular myocytes. *J Physiol (Lond), 493*(2), 529-542.

Weber A, & Herz R. (1968). The relationship between caffeine contracture of intact muscle and the effect of caffeine on reticulum. *J Gen Physiol, 52*(5), 750-759.

Weber CR, Piacentino V, Houser SR, & Bers DM. (2003). Dynamic regulation of sodium/calcium exchange function in human heart failure. *Circ, 108*(18), 2224-2229.

Wehrens X, & Marks A. (2004). Molecular determinants of altered contractility in heart failure. *Ann Med, 36 (Suppl 1)*, 70-80.

Wei JY, Spurgeon HA, & Lakatta EG. (1984). Excitation-contraction in rat myocardium: alterations with adult aging. *Am J Physiol Heart Circ Physiol, 246*(6), H784-791.

Weisser-Thomas J, Piacentino V, Gaughan J, Margulies K, & Houser, S. (2003). Calcium entry via Na/Ca exchange during the action potential directly contributes to contraction of failing human ventricular myocytes. *Cardiovasc Res, 57*(4), 974-985.

Wier W, Egan T, Lopez-Lopez J, & Balke C. (1994). Local control of excitation-contraction coupling in rat heart cells. *J Physiol, 474*(3), 463-471.

Wilson C, & Lincoln C. (1984). β-adrenoceptor subtypes in human, rat, guinea pig, and rabbit atria. *J Cardiovasc Pharmacol, 6*(6), 1216-1221.

Winegrad S. (1965). Autoradiographic studies of intracellular calcium in frog skeletal muscle. *J Gen Physiol, 48*(3), 455-479.

Witcher D, Kovacs R, Schulman H, Cefali D, & Jones L. (1991). Unique phosphorylation site on the cardiac ryanodine receptor regulates calcium channel activity. *J Biol Chem, 266*(17), 11144-11152.

Wu JY, & Lipsius SL. (1990). Effects of extracellular Mg^{2+} on T- and L-type Ca^{2+} currents in single atrial myocytes. *Am J Physiol Heart Circ Physiol, 259*(6), H1842-1850.

Xiang Y, Rybin VO, Steinberg SF, & Kobilka B. (2002). Caveolar localization dictates physiologic signaling of beta 2-adrenoceptors in neonatal cardiac myocytes. *J Biol Chem, 277*(37), 34280-34286.

Xiao R, Avdonin P, Zhou Y, Cheng H, Akhter SA, Eschenhagen T, Lefkowitz RJ, Koch WJ, & Lakatta EG. (1999). Coupling of β_2-adrenoceptor to G_i proteins and its physiological relevance in murine cardiac myocytes. *Circ Res, 84*(1), 43-52.

Xiao R, Cheng H, Zhou Y, Kuschel M, & Lakatta EG. (1999). Recent advances in cardiac β_2-adrenergic signal transduction. *Circ Res, 85*(11), 1092-1100.

Xiao R, Hohl C, Altschuld R, Jones L, Livingston B, Ziman B, Tantini B, & Lakatta E. (1994). β_2-adrenergic receptor stimulated increases in cAMP in rat heart cells is not coupled to changes in Ca^{2+} dynamics, contractility, or phospholamban phosphorylation. *J Biol Chem, 269*(29), 19151-19156.

Xiao R, Ji X, & Lakatta, E. (1995). Functional coupling of the beta 2-adrenoceptor to a pertussis toxin-sensitive G protein in cardiac myocytes. *Mol Pharmacol, 47*(2), 322-329.

Xiao R, & Lakatta E. (1993). Beta 1-adrenoceptor stimulation and beta 2-adrenoceptor stimulation differ in their effects on contraction, cytosolic Ca^{2+}, and Ca^{2+} current in single rat ventricular cells. *Circ Res, 73*(2), 286-300.

Xiao RP. (2001). β-adrenergic signaling in the heart: Dual coupling of the β_2-adrenergic receptor to G_s and G_i proteins. *Science STKE, 104*, RE15.

Xiong W, Ferrier GR, & Howlett SE. (2004). Diminished inotropic response to amrinone in ventricular myocytes from myopathic hamsters is linked to depression of high-gain Ca^{2+}-Induced Ca^{2+} release. *J Pharmacol Exp Ther, 310*(2), 761-773.

Xu A, & Narayanan N. (1998). Effects of aging on sarcoplasmic reticulum Ca^{2+}-cycling proteins and their phosphorylation in rat myocardium. *Am J Physiol Heart Circ Physiol, 275*(44), H2087-2094.

Yang B, Larson D, & Watson R. (1999). Age-related left ventricular function in the mouse: analysis based on in vivo pressure-volume relationships. *Am J Physiol Heart Circ Physiol, 277*(46), H1906-1913.

Yuan W, Ginsburg K, & Bers D. (1996). Comparison of sarcolemmal calcium channel current in rabbit and rat ventricular myocytes. *J Physiol (Lond), 493*(3), 733-746.

Yue L, Melnyk P, Gaspo R, Wang Z, & Nattel S. (1999). Molecular mechanisms underlying ionic remodeling in a dog model of atrial fibrillation. *Circ Res, 84*(7), 776-784.

Zhang S, Cheng H, Zhou Y, Wang D, Zhu W, Ziman B, et al. (2000). Inhibition of spontaneous β_2-adrenergic activation rescues β_1-adrenergic contractile response in cardiomyocytes overexpressing β_2-adrenoceptor. *J Biol Chem, 275*(28), 21773-21779.

Zhou Y, Cheng H, Song L, Wang D, Lakatta E, & Xiao R. (1999a). Spontaneous β_2-adrenergic signaling fails to modulate L-type Ca^{2+} current in mouse ventricular myocytes. *Mol Pharmacol, 56*(3), 485-493.

Zhou Y, Song L, Lakatta E, Xiao R, & Cheng H. (1999b). Constitutive β_2-adrenergic signaling enhances sarcoplasmic reticulum Ca^{2+} cycling to augment contraction in mouse heart. *J Physiol (Lond), 521*(2), 351-361.

Zhou Y, Yang D, Zhu W, Zhang S, Wang D, Rohrer D, et al. (2000). Spontaneous activation of β_2- but not β_1-adrenoceptors expressed in cardiac myocytes from $\beta_1\beta_2$ double knockout mice. *Mol Pharmacol, 58*(5), 887-894.

Zhou YY, Cheng H, Bogdanov KY, Hohl C, Altschuld R, Lakatta EG, et al. (1997). Localized cAMP-dependent signaling mediates β_2-adrenergic modulation of cardiac excitation-contraction coupling. *Am J Physiol Heart Circ Physiol, 273*(3), H1611-1618.

Zhou Z, & January C. (1998). Both T- and L-type Ca^{2+} channels contribute to excitation contraction coupling in cardiac Purkinje cells. *Biophys J, 74*(4), 1830-1839.

Zhu J, & Ferrier GR. (2000). Regulation of a voltage-sensitive release mechanism by Ca^{2+}-calmodulin-dependent kinase in cardiac myocytes. *Am J Physiol Heart Circ Physiol, 279*(5), H2104-2115.

APPENDIX A